Advancing Lignocellulosic Biorefineries through Co-Production of Hemicellulosic Biopolymers and Bioenergy

By

Gezahegn Teklu Mihiretu

Dissertation presented for the Degree

of

DOCTOR OF PHILOSOPHY
(CHEMICAL ENGINEERING)

in the Faculty of Engineering
at Stellenbosch University

The financial assistance of the National Research Foundation (NRF) and The Research Council of Norway (RCN) towards this research is hereby acknowledged. Opinions expressed and conclusions arrived at, are those of the author and are not necessarily to be attributed to the NRF and RCN.

Supervisor

Prof. J.F. Görgens

Co-Supervisor

Prof. A.F.A. Chimphango

April 2022

DECLARATION

By submitting this thesis electronically, I declare that the entirety of the work contained therein is my own, original work, that I am the sole author thereof (save to the extent explicitly otherwise stated), that reproduction and publication thereof by Stellenbosch University will not infringe any third party rights and that I have not previously in its entirety or in part submitted it for obtaining any qualification.

This dissertation includes two original papers published in peer-reviewed journals and one unpublished publication. The development and writing of the papers (published and unpublished) were the principal responsibility of myself and, for each of the cases where this is not the case, a declaration is included in the dissertation indicating the nature and extent of the contributions of co-authors.

Date: April 2022

PLAGIARISM DECLARATION

1. Plagiarism is the use of ideas, material and other intellectual property of another's work and to present it as my own.
2. I agree that plagiarism is a punishable offense because it constitutes theft.
3. I also understand that direct translations are plagiarism.
4. Accordingly, all quotations and contributions from any source whatsoever (including the internet) have been cited fully. I understand that the reproduction of text without quotation marks (even when the source is cited) is plagiarism.
5. I declare that the work contained in this assignment, except where otherwise stated, is my original work and that I have not previously (in its entirety or in part) submitted it for grading in this module/assignment or another module/assignment.

Initials and Surname: **Gezahegn Teklu Mihiretu**

Signature: _____

Date: April 2022

THESIS ABSTRACT

This research project was conceived in the context of advancing a lignocellulosic biorefinery for co-production of xylan biopolymers, bioethanol and electricity from two agro-industrial materials, namely sugarcane residues (SCT) and aspen wood (AW). The research was primarily designed to include two full-fledged experimental studies and one techno-economic case study. Accordingly, two biomass pretreatment approaches, namely: microwave-assisted pressurised hot water (MWA-PHW) and alkalinised steam explosion pretreatment (ASEPT) methods were experimentally investigated for their effect on the extraction of xylan from SCT and AW. Extraction experiments (via MWA-PHW and ASEPT) were conducted by varying temperatures between 165 – 205 ℃ and retention times 3 - 22 min at test points identified using Central Composite Design (CCD) as response surface methodology (RSM). Pretreatment conditions were intended for a dual purpose: maximizing xylan extraction yield while simultaneously enhancing cellulose digestibility.

Experimental results on xylan yield and cellulose digestibility were analysed using ANOVA method to establish optimal conditions for significantly enhanced values. Accordingly, under the MWA-PHW method, maximum xylan yields of 66 and 50%, and highest cellulose digestibility of 78 and 74%, were respectively attained for AW at (195℃, 20 min) and SCT at (195 ℃, 15 min). Whereas maximum xylan yields of 51 and 24%, and highest cellulose digestibility of 92 and 81%, were attained for SCT and AW respectively, following their pretreatment under ASEPT at (204 ℃, 10 min). Under both methods, the xylan extracts were predominantly non-monomeric with insignificant formation of degradation products. This strongly suggested both MWA-PHW and ASEPT were viable approaches for xylan extraction purposes. ANOVA results also revealed that temperature was the dominant factor influencing the xylan yield and cellulose digestibility.

The techno-economic case study was aimed at evaluating the economic viability of the biorefinery for co-production of xylan biopolymers, bioethanol and electricity (i.e. main-case scenario, MCS) against two benchmark processes, i.e. Base-case (BCS) and Intermediate-case (ICS) scenarios, where only bioethanol and electricity are produced from sugarcane residues (Basis: daily capacity of 1000 tons of dry biomass subjected to ASEPT condition of 204 °C and 10 min). The study results showed that co-production of xylan biopolymers substantially improved the economic performance of the main biorefinery case (i.e. MCS) by lowering the selling price of ethanol against higher values under the benchmark processes. A minimum hemicellulose selling price (MHSP) of 809 USD/ton of xylan co-product was determined by fixing ethanol selling price at 0.70 USD/L (market price of ethanol in 2019); higher MHSP values certainly lead to further lower prices. Minimum ethanol selling prices (MESP) under the MCS, BCS and ICS were respectively estimated at 0.61, 0.95 and 0.81 USD/L, where the xylan price was assumed at 1000 USD/ton (=> MCS). Even though the economic viability of the main biorefinery case was significantly enhanced with co-production of xylan than without, this multi-product biorefinery complex was rendered rather energy-intensive as a result of such co-production scheme where the recovery of xylan biopolymers necessitated substantial thermal and electrical energy demands. From environmental point of view, the co-production of xylan biopolymers along with bioethanol and electricity was shown to have a positive contribution towards mitigating GHG emissions from fossil sources. The GHG emissions savings under the MCS, BCS and ICS were estimated around 69, 64 and 65% against gasoline as fossil baseline of 90 gCO_2eq/MJ (RSB-Global), but there was only marginal difference between the savings under the main biorefinery case and that under the benchmark processes.

TESISOPSOMMING

Hierdie navorsingsprojek is ontwikkel in die konteks van die bevordering van ’n lignosellulosiese bioraffinadery vir ko-produksie van xilaanbiopolimere, bio-etanol en elektrisiteit uit twee agri-industriële materiale, naamlik suikerrietresidu’s (SCT) en espenhout (AW). Die navorsing is ontwerp rondom twee volledige eksperimentele studies en een tegno-ekonomiese gevallestudie. Dienooreenkomstig, is twee biomassa voorbehandelingbenaderings, naamlik mikrogolf-geassisteerde warm water onder druk (MWA-PHW) en gealkaliseerde stoomontploffing voorbehandeling (ASEPT) metodes eksperimenteel ondersoek vir hul effek op die ekstrahering van xilaan uit SCT en AW. Ekstraksie-ekperimente (via MWA-PHW en ASEPT) is uitgevoer deur temperature te varieer tussen 165 – 205 °C en retensietye tussen 3 – 22 min by toetspunte geïdentifiseer deur Sentrale Samestelling Ontwerp (CCD) as responsoppervlakmetodologie (RSM) te gebruik. Voorbehandelingskondisies is bedoel vir ’n tweeledige doel: maksimering van xilaanekstraksie-opbrengs terwyl sellulose verteerbaarheid gelyktydig verbeter word.

Eksperimentele resultate op xilaanopbrengs en selluloseverteerbaarheid is geanaliseer deur ANOVA-metode te gebruik om optimale kondisie/s vir beduidende verbeteringswaardes te bepaal. Dienooreenkomstig, onder die MWA-PHW-metode, is maksimum xilaanopbrengs van 66 en 50%, en hoogste selluloseverteerbaarheid van 78 en 74%, onderskeidelik, verkry vir AW by (195 °C, 20 min) en SCT by (195 °C, 15 min). Maksimum xilaanopbrengste van 51 en 24%, en hoogste selluloseverteerbaarheid van 92 en 81%, is verkry vir SCT en AW onderskeidelik, na hul voorbehandeling onder ASEPT by (204 °C, 10 min). Onder beide metodes, was die xilaanekstraksies oorwegend nie-monomeries met onbeduidende formasie van degradasie produkte daarvan. Hierdie stel sterk voor dat beide MWA-PHW en ASEPT lewensvatbare benaderings vir

xilaanekstraksie doeleindes is. ANOVA-resultate het ook gewys dat temperatuur die hooffaktor is wat xilaanopbrengs en sellulose verteerbaarheid beïnvloed.

Die tegno-ekonomiese gevallestudie het beoog om die ekonomiese lewensvatbaarheid van die bioraffinadery vir ko-produksie van xilaanbiopolimere, bio-etanol en elektrisiteit (i.e. hoofgeval scenario, MCS) te evalueer teenoor twee standaardprosesse, i.e. Basis-geval (BCS) en Intermediêre-geval (ICS) scenario's, waar slegs bio-etanol en elektrisiteit geproduseer word uit suikerrietresidu's (Basis: daaglikse kapasiteit van 1000 ton droë biomassa onderwerp aan ASEPT-kondisie van 204 °C en 10 min). Die studie se resultate het getoon dat ko-produksie van xilaanbiopolimere die ekonomiese prestasie van die hoof-bioraffinaderygeval (i.e. MCS) substansieel verbeter, deur die verkoopsprys van etanol (teenoor hoër waardes onder die standaardprosesse) te verlaag. 'n Minimum hemisellulose-verkoopsprys (MHSP) van 809 USD/ton xilaan ko-produk is vasgestel deur etanol se verkoopsprys teen 0.70 USD/L (markprys van etanol in 2019) vas te maak; hoër MHSP-waardes het verseker tot verdere laer pryse gelei. Minimum etanol verkoopspryse (MESP) onder die MCS, BCS en ICS is onderskeidelik beraam teen 0.61, 0.95 en 0.81 USD/L, waar die xilaanprys aangeneem is teen 1000 USD/ton (=> MCS). Selfs al is die ekonomiese lewensvatbaarheid van die hoofbioraffinadery beduidend verbeter met ko-produksie van xilaan as daarsonder, is hierdie multi-produk bioraffinaderykompleks bewys om energie-intensief te wees as 'n resultaat van so 'n ko-produksieskema waar die herwinning van xilaanbiopolimere substansiële termiese en elektriese energievereistes genoodsaak het. Uit omgewingsoogpunt, het die ko-produksie van xilaanbiopolimere saam met bio-etanol en elektrisiteit 'n positiewe bydrae gelewer tot die versagting van GHG-emissies uit fossielhulpbronne. Die GHG-emissiebesparing onder die MCS, BCS en ICS is beraam rondom 69, 64 en 65% teenoor petrol as fossielbasislyn van 90 gCO_2eq/MJ (RSB-Global),

maar daar was slegs ’n marginale verskil tussen die besparing onder die hoofbioraffinaderygeval en die onder die standaard prosesse.

Dedicated to my Family,

&

To my little shining star, Heluwaa!

ACKNOWLEDGEMENTS

Delving into the world of unknowns with keen sense of purpose and a legitimate cause to serve is perhaps the key ingredient of any research undertaking of this sort. As much captivating that can be, finding oneself therein can also be full of challenges. This piece of research work would not have become possible without the help, support and encouragement I have had from diverse set of people whom – mentioned herein or not – I generally owe my heartfelt gratitude. I hereby acknowledge those who have left their indelible mark all along the way or at some point in the course of doing this research.

First and most of all, I would like to express my earnest gratitude to my supervisors Prof. J.F. Görgens and Prof. A.F.A. Chimphango not only for offering me the opportunity to join the vibrant biorefinery research group they are spearheading within the Process Engineering Department of Stellenbosch University, but also for their unwavering support, academic guidance, constructive critique, patience and understanding towards the completion of this research work. My sincere thanks also goes to Dr. Abdul M. Petersen, Dr. Luvuyo Tyhoda and Dr. Maria Garcia-Aparicio, all from the same research group, for their academic assistance and kindly sharing resourceful information where in need. I would also like to gratefully acknowledge Mrs. Levine Simmers and Mr. Jaco van Rooyen, both from the analytical labs, for their invaluable analytical services. My heartfelt gratitude also goes to senior staffs like Mr. Jos Weerdenburg and his colleagues at the main workshop, as well as Mr. Henry Solomon and his colleagues at the wood science lab, for their contagious personality, cooperativeness and willingness to render technical assistance where in need. I would also like to take this opportunity to thank Mrs. Frances Layman, Mrs. Anita Kleinschmidt and Mrs. Mieke De Jager for their kind cooperation in offering administrative services as and when required by this research project.

I would like to extend my earnest gratitude to Dr. Philip A. Reme, Dr. Karin Øyaas and Dr. Malin Brodin for making all necessary arrangements for my research visit at RISE-PFI AS in Trondheim, Norway. It was a privilege to have undertaken a full-fledged experimental work with family-like technical and scientific staffs at this Nordic research institute. My deep sense of gratitude also goes to Mrs. Ingebjørg Leirset, Mrs. Mirjana Filipovic, Mrs. Anne M. Reitan and other PFI staffs for their technical assistance and cordial approach which I had enjoyed immensely throughout my stay there. I gratefully acknowledge Mrs. Elin Bremseth for her supportive roles and administrative assistance kindly rendered as and when required. I also extend my sincere thanks to Prof. Bård H. Hoff and Prof. Eiric Sundby, both from NTNU, for their kind cooperation in making necessary arrangements for the experimental study which was partly carried out within their chemical lab.

I gratefully acknowledge the grant allocated by the National Research Foundation (NRF) of South Africa and the Research Council of Norway (RCN) for this research project. I would also like to acknowledge the departmental bursary granted towards completion of this research.

Last but not least, I owe deep sense of gratitude to my entire family back Home for their unconditional support, love and encouragement which I immensely enjoyed throughout my academic endeavours. No words of thanks can sum up the gratitude I owe to my wife, Attiwaa, for her love, moral support and keen understanding which kept me moving on. And, my little darling, Heluwaa, the least thing I can owe you is myself!

Table of Contents

LIST OF FIGURES

LIST OF TABLES

List of abbreviations

- AIL – Acid-insoluble lignin
- AOC – Annual Operating Costs
- APT – Alkaline Pretreatment
- ASEPT – Alkalinised steam explosion pretreatment
- ASL – Acid-soluble lignin
- ASP – Anti-Solvent Precipitation
- AW – Aspen wood
- BBF – Biomass-based fuels
- CCD – Central Composite Design
- CEPCI – Chemical Engineering Plant Cost Index
- DMC – Dry matter content
- DP – Degree of Polymerization
- DWB – Dry Weight Basis
- FBF – Fossil-based Fuels
- FPU – Filter Paper Unit
- 2G – Second generation
- GHG-ERP – Greenhouse Gas Emission Reduction Potential
- GPC – Gel Permeation Chromatography
- HMF – Hydroxymethylfurfural
- HPLC – High-performance Liquid Chromatography
- ISBL – Inside Battery Limit
- LCBRY – Lignocellulosic biorefinery
- LF – Liquid Fraction
- LTVD – Low temperature vacuum drying
- MF - Microfiltration
- MESP – Minimum Ethanol Selling Price
- MHSP – Minimum Hemicelluloses Selling Price
- MSP – Minimum Selling Price
- NREL – National Renewable Energy Laboratory
- OD – Optical Density
- ODW – Oven-dry weight

- ODW – Oven-dry weight
- OSBL – Outside Battery Limit
- PLHW – Pressurized Liquid Hot Water
- RSM – Response Surface Methodology
- SCT – Sugarcane Trash aka Sugarcane harvesting residues
- SEC – Size Exclusion Chromatography
- SEPT – Steam Explosion Pretreatment
- SF – Solid Fraction
- SHF – Separate Hydrolysis and Fermentation
- SLS – Solid liquid separation
- SSF – Simultaneous Saccharification and Fermentation
- TCI – Total capital investment
- UF - Ultrafiltration
- WIS – Water Insoluble Solids

CHAPTER ONE: INTRODUCTION

1.1. BACKGROUND AND RATIONALE

Lignocellulosic materials represent largely untapped bio-renewable resource base having real potential in advancing low-carbon bioeconomy whereby a range of bio-based products intended for energy and material end-purposes are co-produced in an environmentally sustainable manner (Schroeder et al., 2019; Mohan et al., 2016). In this context, second generation (2G) biorefineries may have to aim not just at decarbonizing existing fossil-intensive economic systems, but more essentially, at creating enabling technological platforms for future-oriented bio-based products including advanced biofuels, biomaterials and speciality chemicals which are capable of serving versatile applications (Dragone et al., 2020; Liguori and Faraco, 2016; Chantal et al., 2012). Such biorefinery-centred approaches have indeed been highly regarded for their strategic importance and transformative role in making a paradigm shift from traditional fossil-based to an emerging bio-based economic realm (Ubando et al., 2020; Bennich et al., 2018; IEA Bioenergy, 2017). That to happen, it is vital to explore and tackle those technological challenges encountered in the course of advancing lignocellulosic biorefinery systems to the point where they can become a commercial and environmental success.

Advanced biofuels, in general, and cellulosic ethanol, in particular, perhaps represent one notable area towards which lignocellulosic materials have been researched extensively thus paving the way for their commercial scale production (Saini et al., 2020; Brown et al., 2013; Clark et al., 2012). Despite the remarkable technological developments and bioindustrial ventures made therein, cellulosic ethanol production apparently remains far from commercial success (Franck et al., 2019; Brown et al., 2013). One strategic approach in overcoming the integral challenge of making them commercially

more competitive is to look at the real potential of lignocellulosic biomass beyond bioethanol production and, through the application of the biorefinery concept, expand its use for the co-production of more valuable bio-based products for non-fuel applications (Dragone et al., 2020; Rosales-Calderon & Arantes, 2019; Ragauskas et al., 2006). Advancing second-generation biorefineries to the next level should consequentially imply the need to embrace the very idea of co-producing other value-added products along with biofuels and systematically deal with the challenges encountered.

The development of multi-product biorefineries is inevitably expected to lead to increased economic interest in non-cellulosic biomass components such as hemicelluloses and lignin (Serna-loaiza et al., 2019; Rosales-Calderon & Arantes, 2019; Silveira et al., 2015). Hemicelluloses are the second most abundant polysaccharide sugars, after cellulose, found in lignocellulosic materials. Unlike cellulose, which is probably the most utilized lignocellulosic component, hemicelluloses may have not been given sufficient attention from economic point of view (Banerjee et al., 2017; Zhang et al., 2014; Girio et al., 2010). One approach to enhance the economic use of hemicelluloses is to convert them, along with cellulose, into bioethanol thereby increasing the overall ethanol yield per unit of initial biomass. However, bioconversion of hemicellulosic sugars into ethanol via co-fermentation along with cellulose-derived glucose has been a challenge (Valinhas et al., 2018; Torres et al., 2016; Zhang and Geng, 2012). Despite any improvements that can be made on the co-fermentability of hemicellulosic C5 sugars, this approach may not add any more value to hemicelluloses than ethanol itself, as the latter still remains a low-value bulk product. Monomeric sugars of hemicellulosic origin (i.e. hexoses and pentoses) can also serve as starting material for the production of xylitol, furfural, 5-hydroxymethylfurfural, formic acid, levulinic acid and other fermentation products (Canilha et al., 2013; Christopher L., 2012).

On the other end of the value spectrum, an alternative biorefinery approach for enhanced economic utilization of lignocelluloses is to target hemicelluloses for high-value biomaterial applications while the cellulosic portion is primarily geared towards ethanol production. A number of studies have shown that hemicellulosic biopolymers can find applications in the food, agricultural, biopharmaceutical, biomedical, healthcare and cosmetic industries (Hu et al., 2018; Azelee et al., 2014; Chimphango et al., 2012; Ebringerova, 2006). Owing to their distinctive structural and functional properties, xylan-rich hemicelluloses have been identified as an indispensable precursor material intended for emerging applications. For instance, xylan-based hydrogels represent a unique opportunity towards the synthesis of smart biomaterials functionalized for advanced biomedical applications such as wound-dressing, nanomedicine, encapsulation and controlled drug release, and tissue engineering (Hu et al., 2018; Zhang et al., 2014; Venugopal et al., 2014; Ebringerova and Heinze, 2000). Owing to their substantial water absorbing and swelling capability, hemicellulosic hydrogels can also applied in modern agricultural practices in arid and water-scarce areas (Hu et al., 2018, Narjary et al., 2013; Zhang et al., 2014). Owing to their unique ability to form film coatings having oxygen barrier effect, xylan biopolymers have also been identified for their application in the packaging industry where there is an increasing demand for biodegradable packaging materials for food and pharmaceutical products (da Silva et al, 2012; Ebringerova A., 2006). Xylo-oligosaccharides (XOS) are commercially established hemicellulose-derived product applied as dietary supplement for improved health effects through their nutritional and functional properties (Aachary and Prapulla, 2011; Yang et al., 2015; Cano et al., 2020). Whichever potential application they are intended for, the basic question here is how and to what extent the extraction of xylan from lignocellulosic biomass can take place while rendering the cellulosic portion sufficiently digestible for bioethanol production, thus allowing lignocelluloses conversion into multiple products.

Xylans are the third most abundant natural biopolymers representing the major hemicellulosic constituent in hardwoods and agricultural residues generally comprising 20 to 30% (w/w) the dry biomass (Egito et al., 2012; Ebringerova and Heinze, 2000). Sugarcane harvesting residues and aspen wood sawdust (a hardwood by-product) belong to such xylan-rich lignocelluloses which can be sourced from biomass-intensive sectors (i.e. sugarcane and forestry industries). These agro-industrial materials may have traditionally been deemed of low economic value and wasted as such. Nonetheless, given their rich content in xylan, cellulose and other biopolymeric entities, these residual biomass should represent an attractive source of biorefinable carbon (Gomez et al., 2014; Baruah et al., 2018). Realizing the economic potential of such lignocellulosic feedstocks, however, requires that those technical challenges which inherently arise from the complex structure and properties of lignocellulosic materials be dealt with both thoroughly and systematically. In this respect, pretreatment technologies represent a crucial step in fractionating the lignocellulosic biomass into fractions that can ultimately be biorefined into targeted end-products. In cases where multiple end-products are intended from the same initial biomass, even more pronounced challenges can be expected to prevail at the pretreatment stage, as multiple biorefinery products essentially imply multi-purpose biomass valorisation needs demanding a trade-off between pretreatment conditions as required by competing biorefining pathways each leading to a specific end-product.

The present research was conceived with the aim of developing a lignocellulosic biorefinery system whereby the co-production of xylan biopolymers can take place with bioethanol and electricity from two agro-industrial materials: namely, sugarcane harvesting residues, aka sugarcane trash (SCT) and aspen wood sawdust (AW). The goal was (1) to explore the technical feasibility of selected biomass pretreatment methods for

the co-production of hemicellulosic biopolymers along with bioethanol and bio-power in a biorefinery setup; and, (2) to demonstrate whether such multi-product biorefinery would enhance the economic benefits gained from the lignocellulosic feedstock. Accordingly, the research was designed to have both experimental and modelling parts, the former being aimed at investigating the effects of selected pretreatment techniques on the extraction of biopolymeric hemicelluloses as well as on the enzymatic digestibility of cellulose; whereas the latter was aimed at evaluating the techno-economic viability of the most promising pretreatment approach having reasonable chance of being scaled up to an industrial level, that is depending on how enhanced xylan extraction yield and cellulose digestibility become, the technological readiness and prior industrial applicability of the pretreatment method. A simplified block diagram depicting the major steps involved in an integrated production of xylan biopolymers, bioethanol and electricity is shown under Fig 1.1 below.

Furthermore, advancing modern biorefineries should take due consideration of the environmental implication their development entails; in fact, environmental sustainability is one critical requirement for their advancement (Wellisch et al., 2010; Junqueira et al., 2017; Mandegari et al., 2017; Hassan et al., 2019). In this context, the present study attempts to evaluate the envisaged biorefinery from climate change mitigation points of view in general, and in terms of its potential towards greenhouse gases (GHG) emissions reduction, in particular. The GHG Emissions Reduction Potential (GHG-ERP), aka GHG emissions savings, resulting from the lignocellulosic biorefinery (producing bioethanol, xylan biopolymers and electricity) shall be estimated based on the apparent (indirect) reduction of GHG emissions that can result from it in comparison to fossil-fuel baseline (Falano et al., 2014; Junqueira et al., 2017).

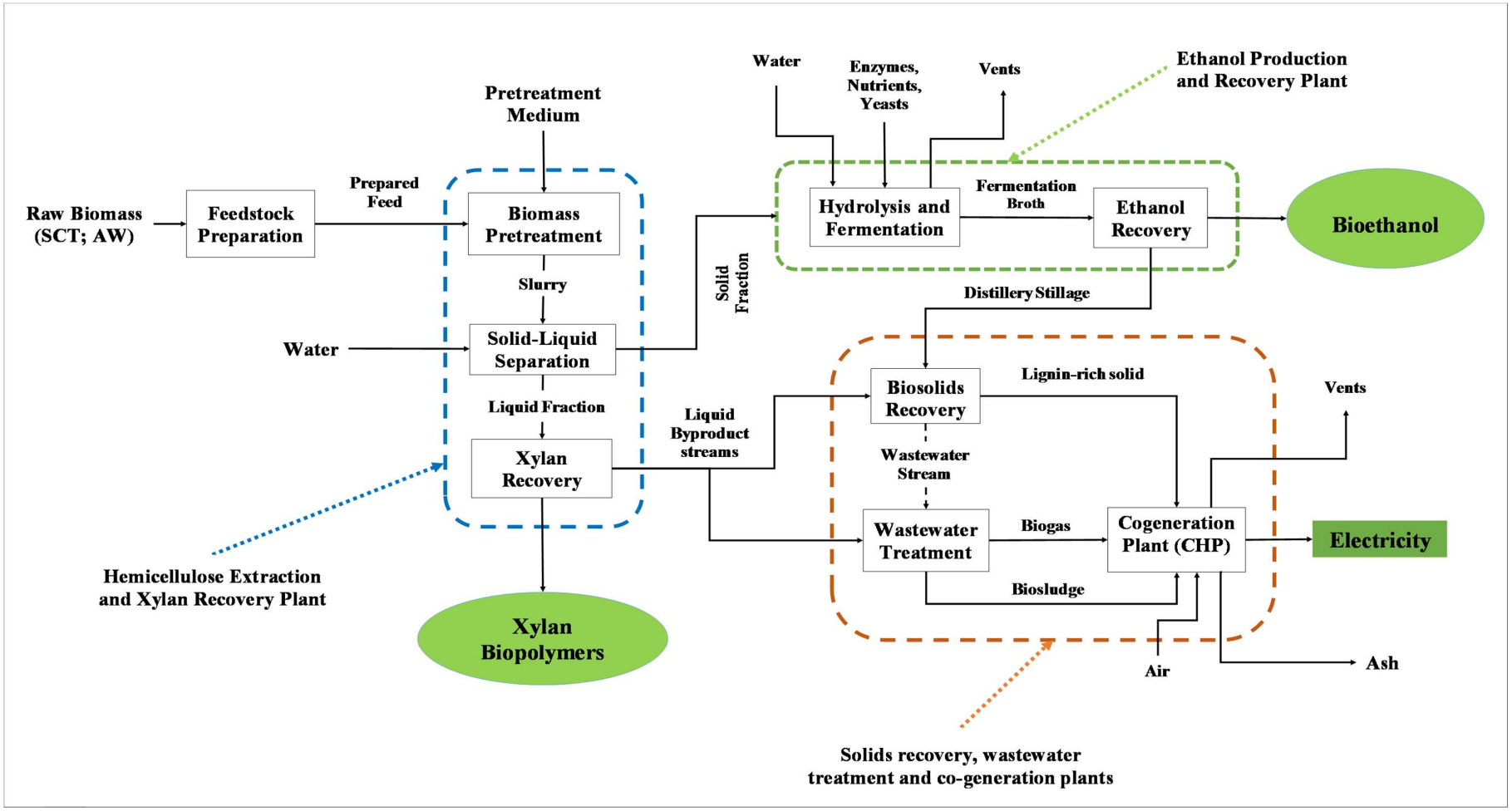

Fig. 1.1 Simplified process flow diagram for the envisaged biorefinery intended for an integrated production of xylan biopolymers, bioethanol and electricity from selected lignocellulosic feedstock types (Sugarcane trash and aspen wood sawdust)

1.2. THE RESEARCH PROBLEM

Central to the present biorefinery research was the biomass pretreatment step which is intended to fulfil a dual purpose: to enable the extraction of hemicelluloses in their least possible degraded form while simultaneously rendering the cellulosic portion sufficiently amenable for enzymatic digestion (see process schema in Fig 1.1). Existing biomass pretreatment techniques may have largely been investigated and deployed for the purpose of lignocellulosic ethanol production, very often involving an integrated co-generation plant to meet their thermal and electrical energy requirements (Baruah et al., 2018; Silveira et al., 2015; Toma´s-Pejo et al., 2011). Under such conventional production setup, bioethanol and electricity constitute the two outputs derived from the initial raw biomass. Integrating a new line of production for a third output to be co-produced from the same initial biomass, i.e. introducing the very idea of co-producing hemicellulosic biopolymers along with ethanol and electricity in a multi-product biorefinery setup, certainly gives rise to a set of technical and process optimization challenges which must be approached and dealt with in their own respects (Ajao et al., 2018; Rosales-Calderon and Avantes, 2019). These challenges, discussed herein below, can be caused by a number of interconnected factors which deserve a closer contextual look.

The complex and recalcitrant nature of lignocellulosic materials coupled with the labile nature of hemicelluloses is one main reason behind those technical and process optimization challenges expected to prevail at the pretreatment stage – which, in the study context here, has an intended dual purpose of enhancing hemicellulose extraction while leading to increased cellulose digestibility (Zhao et al., 2012; Chen, 2014; Wang et al., 2018). Besides such inherent feedstock characteristics, the pretreatment method employed for biomass fractionation and process conditions selected thereof certainly play a key role in determining not just the extent of hemicellulose extraction from the

lignocellulosic matrix, but also the enzymatic digestibility of cellulose for subsequent ethanol production (Sun et al., 2016; Carvalheiro et al., 2008). Pretreatment conditions that are favoured for enhanced cellulose digestibility (=> increased ethanol yield) may not necessarily lead to enhanced extraction of biopolymeric hemicelluloses, and vice versa. The two may rather emerge as "competing processes", especially in terms of their requirement for pretreatment conditions. Consequently, how the overall biorefinery system as envisaged here (see Fig 1.1) behaves upon any changes made at the interface of pretreatment conditions intended for enhanced hemicellulose extraction yield and/or enzymatic cellulose digestibility is far from clear. This is one key problem area which the present research intends to resolve based on experimental as well as process modelling and simulation studies aimed at exploring and gaining insight on the dynamic behaviour and techno-economic viability of the biorefinery intended for co-production of bioethanol, xylan biopolymers and electricity from the selected lignocellulosic materials.

The other challenge prevailing at the pretreatment stage is how the hemicelluloses extraction yield can be enhanced while minimizing the extent of degradation of extracts thereof. The extraction of hemicelluloses from lignocellulosic materials may generally require relatively mild pretreatment conditions so as to minimize degradation as well as de-polymerization of the hemicellulosic extracts (Popa and Spiridon, 2008; Carvalheiro et al., 2008; Sun et al., 2013). With increased severity of pretreatment conditions, not only will the extent of hemicelluloses removal increases, but also the extent of degradation of extracts thereof. In other words, increasing the severity of conditions can lead to increased extraction yield, but at the expense of increased depolymerisation and further degradation of the hemicellulose extracts, which would mean direct loss of biopolymeric extracts (Popa and Spiridon, 2008; Longue Junior et al., 2013). Therefore, striking the right balance between conditions for enhanced extraction yields and those for minimized

degradation of hemicellulose extracts poses an optimization problem. Extracting hemicelluloses while maintaining their natural biopolymeric characteristics is desired for high-value end-product.

From ethanol production point of view, increased removal of hemicelluloses from the lignocellulosic matrix, through more severe pretreatment conditions, is generally desirable for enhanced cellulose digestibility during subsequent enzymatic hydrolysis yielding fermentable sugars for ethanol production (Yang et al., 2011; Zhang et al., 2009). However, as stated earlier, milder conditions are generally required to ensure biopolymeric hemicelluloses are extracted with minimal degradation. As a result, getting optimal pretreatment conditions that simultaneously lead to maximized yields for xylan biopolymers and cellulosic ethanol is hardly feasible, thus requiring a compromise between conditions for hemicellulose extraction and cellulose digestibility. Achieving maximum yields of both products under one set of pretreatment conditions, therefore, poses a real biorefinery challenge. A range of process parameters will have to be investigated to characterize a solution space for enhanced xylan extraction and ethanol yields. Depending on the severity of pretreatment condition, simultaneous removal of lignin can take place during hemicelluloses extraction (Li et al; 2016; Humpert et al., 2016) While increased removal of lignin from the lignocellulosic matrix is generally desired for enhanced cellulose digestibility, its presence with the hemicellulose extracts would impair the quality of the biopolymeric end-product.

Another challenge that arises with increased severity of conditions is the formation of degradation products – mainly of hemicellulosic origin – having inhibitory effect on the biocatalytic action of enzymes and yeasts during the downstream bioprocessing of pretreated lignocelluloses (Kim, 2018; Jönsson and Martin, 2016). Even though cellulose can be rendered more digestible under severe conditions, the possible

formation of inhibitors can pose a counter-effect on enzymatic digestibility by obstructing the action of enzymes on cellulose. Should such effect of inhibitors be minimized or avoided, then an integrated detoxification step would be required – which means cost, so brings with it economic questions. Therefore, how biomass pretreatment conditions need to be optimized for minimal inhibitors' formation while enhancing the enzymatic cellulose digestibility is an actual biorefining problem.

Furthermore, in the research context here, any portion of the lignocellulosic biomass which is not converted into hemicellulosic biopolymers and cellulosic ethanol shall represent a residue to fuel up the co-generation plant. This solid residue primarily comprises of the majority of lignin present in the initial lignocellulose as well as undigested cellulose and hemicelluloses that remained intact therein. This means the amount of lignin-rich residue that can be availed as fuel to the CHP plant will increase (or decrease) with decreased (or increased) yields of biopolymeric xylan and bioethanol. Depending on the value of the three biorefinery products (xylan biopolymers, bioethanol and electricity), the combined economic output of the biorefinery is thus dependent on the process conditions upon which the amount of each final product is determined. The actual optimization problem here is under what set of pretreatment conditions the initial lignocellulosic material needs to be fractionated so that it can lead to best economic performance of the envisaged biorefinery. Considering environmental sustainability as one driving force behind their development, the present research shall also attempt to assess the performance of the envisaged biorefinery in terms of its potential for GHG emissions reduction thus its contribution towards climate change mitigation efforts.

1.3 RESEARCH OBJECTIVES

1.3.1. Overall research objective:

To investigate the dynamic behaviour of a lignocellulosic biorefinery system for co-production of hemicellulosic (xylan) biopolymers, cellulosic ethanol and electricity across the interface of hemicellulose extraction conditions (lignocelluloses fractionation/pretreatment) and select the conditions that enhance digestibility of cellulose-enriched solid residue. The aim is to explore combinations of process conditions and establish optimal extraction/pretreatment conditions at which the economic and environmental performance shall be assessed as the main benefits of the biorefinery system. Two feedstock types, namely: Sugarcane trash (SCT) and aspen wood sawdust (AW); and two different biomass pretreatment approaches, namely: Microwave-assisted Pressurized Hot Water (MAPHW) method and Alkalinised Steam Explosion Pretreatment (ASEPT) methods were selected for the study purpose here.

1.3.2. Specific research objectives:

1. To assess the effects of selected biomass pretreatment techniques (MAPHW and ASEPT) on the extraction of hemicelluloses from selected lignocellulosic materials (SCT and AW) as well as on the enzymatic digestibility of cellulose for ethanol production.

2. Under each selected pretreatment approach (MAPHW and ASEPT methods) and for each selected feedstock type (SCT and AW), to determine the effect of pretreatment parameters (mainly temperature and retention time) on xylan extraction yield, enzymatic cellulose digestibility and to establish optimal conditions thereof.

3. To establish a range of process parameters (temperature, retention time, loading ratios) over which extraction of xylan biopolymers from selected lignocellulosic materials and enzymatic digestibility of the solid residue can acceptably occur.

4. "To determine the amount of bioethanol produced per unit mass of raw biomass based on fermentation test results on pretreated solids obtained at optimal pretreatment condition"

5. To assess the techno-economic viability and environmental performance (expressed in greenhouse gases (GHG) emission reduction potential) of a biorefinery for co-production of cellulosic ethanol, xylan biopolymers and electricity under different scenarios. The aim is primarily to determine the best economic performance of the envisaged biorefinery.

1.4. THESIS ORGANIZATION

In line with the research objectives stated hereinabove, the present thesis was structured into seven chapters. It starts with an introductory chapter (Chapter One) wherein general background of this biorefinery-oriented research, the rationale behind it as well as salient aspects of the research problem that necessitated its undertaking are covered. The overall as well as specific objectives of the research are also clearly stated up front here. The second chapter (Chapter Two), which intends to provide a comprehensive review of literature, covers different aspects of a lignocellulosic biorefinery system including feedstock characteristics and major conversion processes leading to targeted end-products (xylan biopolymers, bioethanol and electricity). Accordingly, this chapter starts with a brief review on the compositional nature of lignocellulosic biomass as well as basic characteristics of its major constituents: cellulose, hemicelluloses and lignin. Besides the identification of potential application areas for

hemicellulosic biopolymers, assessment and selection of pretreatment methods for hemicelluloses extraction, as well as methods for recovering the biopolymeric extracts as a targeted co-product have also been covered. Furthermore, the literature review also covers those salient aspects of bioethanol production from lignocellulosic biomass with a focus on biomass pretreatment (especially those methods considered for hemicellulose extraction purpose) as well as the downstream bioprocessing steps (enzymatic hydrolysis and fermentation) where ethanol production takes place.

Chapter Three is on the research approach followed and the methodologies employed towards carrying out this research. The present study was designed to have an experimental part where selected biomass fractionation technologies are investigated in the research context here as well as a modelling part where the techno-economic and environmental performance of the envisaged biorefinery are assessed. Discussed under the experimental part are procedural steps from the design of experiments to statistical analysis and interpretation of results obtained thereof. The modelling part starts with conceptual process development for the envisaged biorefinery, the identification of process scenarios, and the comparative economic assessment among identified biorefinery scenarios. The environmental performance was assessed in terms of the potential GHG emissions avoided under each biorefinery scenario.

The subsequent three chapters, i.e. Chapters 4, 5 and 6, consist of the main body of the research work. Chapter Four covers a full-fledged experimental study aimed at investigating the technical viability of one of the novel biomass fractionation approaches selected for the research purpose here. Investigated here was the application of microwave-induced pressurized hot water method for a dual purpose: to extract hemicelluloses from selected lignocellulosic materials (namely: sugarcane trash and aspenwood sawdust) while enhancing the enzymatic digestibility of the cellulose-

enriched solid fraction. Likewise, covered under Chapter Five was an experimental study carried out to investigate the technical viability and applicability of the second selected biomass fractionation method, namely: alkaline steam explosion pretreatment, both for hemicellulose extraction and enhanced cellulose digestibility purposes. Experimental results were statistically analysed and discussed in the biorefinery context here. The outcomes from these two experimental works have been published in Mihiretu et al., (2017) and Mihiretu et al., (2019) respectively.

Chapter Six is mainly aimed at demonstrating the techno-economic viability of large-scale production of xylan biopolymers, bioethanol and electricity in a biorefinery setup; and, to a lesser extent, on the environmental benefit expected from such biorefinery. For this purpose, a lignocellulosic biorefinery based on sugarcane harvesting residues (as the preferred feedstock type) and alkalinized steam explosion pretreatment (as the preferred biomass fractionation method) was considered for further techno-economic analysis. Three biorefinery scenarios were identified with the aim of assessing how the techno-economic viability of the envisaged biorefinery is impacted by the very introduction of the hemicellulose extraction step at the pretreatment stage. The economic analysis was performed to determine the feasibility of each biorefinery scenario based on mass and energy balance results generated using ASPENPLUS® simulation software coupled with methods established for estimation of capital investment requirement, annual operation costs and minimum selling prices for main products (bioethanol and hemicellulosic biopolymers). The environmental impact analysis was made in terms of the potential GHG emissions reductions under each scenario. Comparative assessment of economic and environmental performance was made among the three biorefinery scenarios and results thereof were discussed in the study context here.

The last chapter (Chapter Seven) concludes this thesis with reflection points on major findings of the present research and what that would mean in view of advancing lignocellulosic biorefineries for co-production of high-value biopolymeric products with bioethanol and electricity. Besides the practical implications of such research undertakings, potential areas and directions for further research have also been identified in view of advancing 2G biorefineries.

CHAPTER TWO: LITERATURE REVIEW

2.1. LIGNOCELLULOSIC BIOMASS

Lignocelluloses are fibrous plant biomass primarily made up of three major chemical constituents, namely cellulose, hemicelluloses and lignin. These three macromolecular components generally make up 70 to 90 % (w/w) of plant cell wall, dry weight lignocellulosic biomass (Betts et al., 1991; Kamm et al., 2006; Chen, 2014; Sun et al., 2016). Cellulose is the most abundant of all and, as polysaccharide, it is usually considered as a polymer of glucose, with high degree of polymerization that ranges from 800 to 10000 (Albersheim et al., 1994; Fengel & Wegener, 1989; Zhang et al., 2004). A number of cellulose chains are structurally closely associated via extensive hydrogen bonding networks to form microfibrils, which – owing to their reinforcing effect and crystalline nature – make the cellulosic component relatively unreactive and stable (Fengel & Wegener, 1989; Sun et al., 2016). Cellulose, as a result, is the main cell wall component that makes lignocelluloses rather recalcitrant to biological, chemical and/or thermal degradation (Zhang et al., 2007; Zhao et al., 2012; Sun et al., 2016). As is seen in Table 1.1, celluloses make up one-third to about half (%w/w) of lignocellulosic materials.

Hemicelluloses are the second most abundant natural polysaccharides in plant cell walls after cellulose and generally comprise 20 to 35% (w/w) of dry lignocellulosic biomass (Fengel & Wegener, 1989; Ebringerova and Heinze, 2000). Unlike cellulose, hemicelluloses are structurally less ordered and more amorphous by their nature. They also exhibit lower molecular weight than cellulose with a degree of polymerization in the range of 200-300 (Fengel & Wegener, 1989; Popa and Spiridon, 1998). Hemicelluloses are composed of various hexoses (e.g. glucose, mannose, and galactose), pentoses (xylose and arabinose), acetyl groups, uronic acids and other minor sugars. The various polysaccharide units that make up hemicelluloses can, however, vary depending on their

origin. Thus, by definition, hemicelluloses are short branched-chain heteropolysaccharides of mixed hexosans and pentosans (Michael et al., 1999; Kamm et al. 2006). As is seen in Table 1.1, hemicellulose content in selected lignocellulosic materials generally falls between 20 to 35 wt% for sugarcane biomass and 20-40% for hardwoods. Hemicelluloses in hardwoods such as aspen wood as well as sugarcane harvesting residues are mainly comprised of xylan (Popa and Spiridon, 1998, Michael et al., 1999; Kamm et al., 2006; Popa and Spiridon, 2008).

Within the lignocellulosic structural domain they are natural part of, hemicelluloses are believed to serve as interfacial coupling agents between the highly polar surface of cellulosic microfibrils and the much less polar lignin matrix; they do impart viscoelastic properties to the plant cell wall structure (Popa and Spiridon, 1998; Walker, 2006; Ebringerova, 2006). Because they contain the greatest proportion of accessible OH-groups of the cell wall, hemicelluloses are thermally and chemically less stable and react more readily than cellulose and lignin (Popa and Spiridon, 1998; Karaaslan et al., 2011). Another significant factor in the thermal degradation of hemicelluloses is the presence of acetyl groups associated with it. Given their thermally labile nature, these groups can easily lead to acetic acid formation, which can inherently cause acid-catalysed degradation of the hemi-polysaccharides upon pretreatment at elevated temperatures (Popa and Spiridon 1998; Ebringerova, 2006; Popa and Spiridon, 2008). Thermal degradation of polymeric components of hemicelluloses also increases with temperature and duration of exposure to heating. Owing to their heteropolymeric and complex nature, the structure and properties of hemicelluloses can indeed be highly influenced by the methods employed for their extraction and purification (Ebringerova, 2006; Popa and Spiridon, 2008; Karaaslan et al, 2011; Peng et al. 2012).

Table 1.1: Composition of Major components (cellulose, hemicellulose and lignin) in selected lignocellulosic biomass

	Feedstock Type	Percentage of major components per unit dry biomass			Reference
		Cellulose	Hemicellulose	Lignin	
SUGARCANE BIOMASS	Sugarcane bagasse (SCB)	40,0-45,0	30,0-35,0	20,0-30,0	Cardona et al., (2010)
		32,0-44,0	27,0-32,0	19,0-24,0	Karp et al., (2013)
		38,8-45,5	22,7-27	19,1-32,4	Canilha et al., (2013)
		32,0-48,0	19,0-24,0	23,0-32,0	Kumar et al., (2009)
		41,7-43,1	24,2-27,5	22,4-24,8	Mihiretu et al., (2017)
	Sugarcane Trash (SCT)***	36,1-45,0	25,0-32,7	18,0-26,2	Singh et al., (2008)
		33,3-36,1	18,4-28,9	26,1-30,7	Canilha et al., (2013)
		39,0	26,0	19,0	da Silva et al., (2012)
		39.2-41-6	28.7-32,0	21.5-23.3	Franco et al., 2013
		38,7-40,5	25,3-27,5	18,3-19,5	Mihiretu et al., (2017)
HARDWOOD BIOMASS	Hardwoods, general	45,0-47,0	25,0-40,0	20,0-25,0	Limayema et al., (2012)
		30,0-43,0	19,0-30,0	20,0-25,0	Kamm et al., (2006)
		40,0-55,0	24,0-35,0	18,0-25,0	Kumar et al., (2009)
	Aspen wood (AW)***	42,0-46,0	21,5-24,1	24,5-25,1	Z.Wang et al., (2018)
		44,5	21,2	21,1	Xu and Tschirner (2012)
		47.07	16.50*	21.47	W.Lie et al., (2012)
		46,7	23.1-28,3	19,3-22,5	A. von Schenck et al., (2013)
		49,6-51,0	18,0-19,4*	21,6-23,2	Mihiretu et al., (2017)
		51,6	24,2	20,6**	Chronet et al., (1991)

Note: * only xylan content ** Klason lignin only *** selected for the study purpose here

Lignin is another major constituent of lignocellulosic biomass. It is highly amorphous phenolic polymer with indeterminate molecular weight (Fengel & Wegener, 1989; Hatakeyama H., & Hatakeyama T., 2008; Ralph et al., 2019). It is also known for its insolubility in most solvents and it cannot be broken down to its monomeric form, even when hydrolysed; it is very much susceptible to oxidation and readily undergoes condensation reaction (Walker, 2006; Hatakeyama H., & Hatakeyama T., 2008; Li et al., 2016). The chemical linkage between some hemicellulosic components, especially arabinoxylans, with lignin and the interpenetration of lignin itself into hemicelluloses pose structural barrier for chemical isolation of pure hemicelluloses or lignin out from the lignocellulosic matrix (Popa & Spiridon, 1998; Walker, 2006; Azelee et al., 2014).

2.2. HEMICELLULOSIC BIOPOLYMERS AND THEIR APPLICATIONS

Natural biopolymers of hemicellulosic origin can potentially find a wide range of industrial applications, given that they are extracted from the lignocellulosic matrix in their polymeric and/or oligomeric form. The plain fact that hemicelluloses are the second most abundant carbohydrate biopolymers in nature can simply make them a resource worth considered in economic terms (Carvalheiro et al., 2008, Ebringerova and Heinze, 2000; Walker, 2006). Beyond their mere natural abundance, what makes biopolymeric hemicelluloses economically even more attractive is their remarkable structural and functional properties such as viscoelasticity, gel-like properties, film forming capability, ability to self-associate in a spatially networked manner (Ebringerova, 2006; Karaaslan et al., 2011; Lindblad et al., 2005; Liu et al., 2020). Such unique properties of hemicellulosic biopolymers have indeed made them potentially applicable as gels, films, coatings, adhesives, stabilizing and viscosity-enhancing additives in the food and pharmaceutical industries (Popa and Spiridon, 1998; Ebringerova A., 2006; da Silva et al., 2012; Canilha et al., 2013; Liu et al., 2020; Hu et al., 2020). Their ability to impart improved rheological properties and dermatological effect has also made hemicellulosic biopolymers worthwhile for their potential application in the cosmetics and skincare industry (Popa and Spiridon, 2008; Ebringerova, 2006; Lahtinen et al., 2019; Hu et al., 2020).

Furthermore, hemicellulosic biopolymers, notably xylan biopolymers, have also been identified as suitable candidates for advanced applications in the nanomedicine and biopharmaceutical areas. What makes them attractive towards such application areas is not just the unique combination of functional and structural properties they have, but also their biodegradability, biocompatibility and hydrosolubility (da Silva et al., 2012; Azelee et al., 2014; Liu et al., 2020; Lu et al., 2021). For instance, owing to their gel-forming ability, xylan-based hydrogels can be applied in wound-dressing, advanced healthcare

biomaterials with foreseeable applications for encapsulation and controlled release of medicinal drugs as well as in tissue engineering (Silva et al., 2010; Azelee et al., 2014; Zhang et al., 2014; Venugopal et al., 2014; Hinderer et al., 2015). The use and application of hemicellulosic hydrogels for agricultural purposes has also been mentioned in some papers (Hu et al., 2018, Narjary et al., 2013; Zhang et al., 2014). Such agricultural applications make use of the substantial water absorbing and swelling capability of xylan-based hydrogels – potential application for modern agricultural practices under water-scarce situations (Zhang et al., 2014; Klein and Poverenov, 2020).

Owing to their ability to form film coatings with a remarkable barrier effect to air (oxygen barrier effect), grease and aroma, biopolymers of hemicellulosic origin have also been identified as attractive candidates for potential application in the packaging industry, especially where long shelf life of packed items is highly desired (Ebringerova A., 2006; Canilha et al., 2013; Nechita et al., 2021; Huang et al., 2021; Zhao et al., 2020). A study by Sabiha-Hanim et al., (2012) demonstrated the possibility that polymeric hemicellulose extracts from sugarcane bagasse can serve as a starting material for the production of such biodegradable films. One interesting feature of products based on these biopolymers is their biodegradability, a property which makes them a target for their application in green and environmentally benign packaging materials for food and pharmaceutical products (Zhao et al., 2020; Nechita et al., 2021; da Silva et al, 2012; Ebringerova A., 2006). Xylo-oligosaccharides (XOS) are commercially well-established prebiotic product of hemicellulosic origin applied as dietary supplement for improved health effects through their nutritional and functional properties (Aachary and Prapulla, 2011; Yang et al., 2015; Wang et al., 2019; Cano et al., 2020; Chen et al., 2021). Xylan-rich lignocelluloses such as hardwoods and fibrous agro-industrial residues can serve as

bioresource for XOS production whereby xylan extract obtained thereof is subjected to chemical and/or enzymatic conversion pathways (Cano et al., 2020; Alvarez et al., 2017).

2.3. EXTRACTION OF HEMICELLULOSES FROM LIGNOCELLULOSIC BIOMASS

2.3.1. *Overview and selection of extraction methods*

Different biomass pretreatment techniques can generally be considered for the extraction of hemicelluloses from lignocellulosic materials. The choice of extraction method should, however, take into account the inherent characteristics of hemicelluloses, the purpose they are extracted for, and at what yield, form and purity they are to be extracted (Carvalheiro et al., 2008; Oriez et al., 2019). Cost competitiveness and environmental friendliness of the method need to be considered as well. With such factors in mind, and given the biorefinery context here, where hemicellulosic (xylan) biopolymers are to be co-produced with bioethanol, it is equally important that the chosen pretreatment method be suitable for enhanced enzymatic digestibility of the solid residue obtained after hemicellulose extraction. Based on relevant literature reviewed thereon (see Table A-1.1 in Appendix A), different pretreatment methods – chemical, physicochemical/hydrothermal or combinations thereof – were assessed in terms of their suitability for hemicellulose extraction and for enhanced cellulose digestibility. As extraction processes fundamentally involve mass transfer operations, physical methods applied for biomass size reduction result in mechanical de-construction of the lignocellulosic matrix, thus facilitating mass and heat transfer effects required for enhanced hemicellulose extraction (Tomas-Pejo et al., 2011; Yang and Wyman, 2008).

One main criterion in assessing the suitability of the pretreatment method for hemicellulose extraction was whether significant recovery of biopolymeric hemicelluloses can be achieved with minimal degradation/decomposition of extracts

thereof. The challenge here is though, hemicelluloses are both thermally and chemically so labile that, upon increased severity of pretreatment conditions, their extraction can only be enhanced at the expense of depolymerisation of the polymeric/oligomeric extracts and their further degradation into undesired side products (Popa and Spiridon, 1998; Walker, 2006; Ebringerova, 2006; Ajao et al., 2018). Increased formation of degradation products such as furfural, HMF and other organic complexes (mainly of hemicellulosic origin) not just indicate increased severity of conditions; when not minimized by the employed technique or conditions set thereof, the presence of such degradation products may necessitate detoxification and/or purification steps along the downstream biorefining steps – be it along bioethanol production line or recovery of xylan biopolymers (Parawira and Tekere, (2010); Joensson et al., 2013; Kim, 2018). The lower extent degradation products form, the more attractive the extraction method becomes. With respect to cellulosic ethanol production from solid residues obtained after hemicellulose extraction, degree of removal of hemicelluloses, enzymatic digestibility of the cellulosic portion, degree of formation of inhibitory products, degree of lignin removal and effectiveness of the method in causing structural changes in the components remaining in the solid residue are important factors (Baruah et al., 2018; Wang et al., 2018; Sun et al., 2016).

Based on the above-stated factors or criteria, different biomass pretreatment methods were assessed for the purpose of this research. Accordingly, the alkaline pretreatment (APT), pressurized liquid hot water (PLHW) and steam explosion pretreatment (SEPT) methods were considered. A summary of literature-reported results on xylan extraction yield and enzymatic hydrolysis sugar yields for different lignocellulosic materials (mainly agricultural residues including sugarcane trash and hardwoods including aspen wood) under these three pretreatment methods (APT, PLHW

and SEPT) is presented under Table A-1.2 and Table A-1.3 of Appendix A. The alkaline route has been well proven to be effective for extraction of hemicelluloses in their polymeric form (Gabrielii et al., 2000; Beckham et al., 2014; Kim et al., 2016). However, alkaline methods are also well known for their unique ability of removing lignin from the lignocellulosic matrix along with hemicellulose solubilisation, but with minor effects on the cellulosic component (Carvalheiro et al., 2008; Kim et al., 2016; Xu and Sun, 2016). Alkaline pretreatment routes generally lead to lower degradation of the structural sugars in lignocelluloses and so lower formation of inhibitory products than acid-based ones; they can also lead to improved cellulose digestibility following biomass pretreatment under relatively milder conditions (Harmsen et al., 2010; Kim et al., 2016). Pressurized liquid hot water and steam explosion pretreatment methods have also been found effective for extraction of hemicelluloses from lignocellulosic materials, the extracts being mainly in their oligomeric and/or monomeric form (Aachary and Prapulla, 2011; Teo et al., 2010). Unlike the alkaline methods, these two hydrothermal pretreatments often manifest higher degree of degradation products formed as a result of autohydrolytic action of weak organic acids that can form during biomass pretreatment under subcritical conditions (Ewanick and Bura, 2010; Duque et al., 2016; Joensson and Martin, 2016). From ethanol production point of view, these hydrothermal methods are not only well capable of producing digestible cellulose, but they can also be environmentally attractive, they primarily involve subcritical water as extraction medium (Sun et al., 2014; Teo et al., 2010). More details on selected methods follow in the next sections.

Although most of the pretreatment methods assessed here (see Tables A-1.1, A-1.2 and A-1.3 in Appendix A) can lead to sufficiently digestible cellulosic residues, not all of them are attractive enough in view of extracting hemicellulosic biopolymers. Among the reasons hereto are high capital requirement associated with the methods (e.g. wet

oxidation and ammonia-based methods); high degradation of hemicelluloses (especially acid-based methods), safety-related issues (e.g. ammonia-based and alkaline-peroxide methods) (Yang and Wyman, 2008; Harmsen et al., 2010; Baruah et al., 2018). Organosolv method, which uses organic or aqueous solvents to extract lignin, has been found to produce highly digestible substrate but with significant formation of degradation products (of hemicellulose and lignin origin) that have inhibitory effect (Tomas-Pejo et al., 2011; Baruah et al., 2018). Ammonia-based methods are known for their effect on enhanced sugar yields with minimal formation of inhibitors, but they are costly and may require considerable safety precautions as they are operated under pressurized condition (Carvalheiro et al, 2008; Yang and Wyman, 2008; Singh et al., 2015). Another method known for its selective removal of xylan from pulps is the nitren extraction method which makes use of nickel-based organometallic complex as an active agent, but its use at industrial level is restricted due to the cost of recovery of nickel (Santos et al., 2013).

2.3.2 *Alkaline extraction of hemicelluloses*

Owing to their hydroxide ions (OH^-), alkaline agents are chemically capable of disrupting the intermolecular linkage between lignin and the structural carbohydrates (hemicellulose and cellulose), a phenomenon that not only leads to hemicellulose solubilisation but also of lignin (Kim et al., 2017; Agbor et al., 2011; Zhang et al., 2009). Aqueous solutions of sodium, potassium, calcium, and ammonium hydroxides are generally applicable for hemicellulose extraction purpose, of which sodium and potassium hydroxides are more common extraction routes to take hemicelluloses out from the lignocellulosic matrix (Peng et al., 2012; Lawther et al., 1996). Sodium hydroxide is generally more capable of higher hemicelluloses extraction than potassium hydroxide, but hemicellulose extract via potassium hydroxide route is more pure (Peng et al., 2012; Sun et al. (2013)). Calcium hydroxide can also be used for hemicellulose extraction

purpose, but it can be less selective towards hemicelluloses and often requires rather long retention times (Kim et al., 2016; Peng et al., 2012; Kim and Holtzapple, 2005).

The extraction of hemicelluloses from different lignocellulosic materials has been shown to be influenced by a number of factors, of which alkaline loading/concentration, temperature and retention time are reportedly the majors ones (Kim et al., 2016; Chen et al., 2013; Krishnan et al., 2010; Dalton et al., 2010). Accordingly, increasing any of the these factors results in increased extraction yield but, with increased severity of conditions, the molecular distribution of hemicellulosic extracts may vary with increased formation of degradation products and decreased extraction yield for biopolymeric hemicelluloses (Chen et al., 2013, Dalton et al., 2010; Brienzo et al., 2009). Longue Junior et al., (2013) has investigated the effect of different alkali (NaOH) loadings on the degree of hemicellulose extraction per unit mass of woody materials (*Eucalyptus globulus* and Sweetgum – both hardwood types) subjected to pretreatments at 100°C and 60 minutes. The loadings compared were 10 and 50% NaOH on wood (oven dry weight basis, ODW) and the water-to-wood loading ratio was 10:1. The results showed that increasing the alkali charge from 10 to 50% led to higher extraction of hemicelluloses (mainly xylan), but with lower degree of polymerization (DP) as determined by GPC method. DP at 10% NaOH on wood were 250 and 274 for *Eucalyptus globulus* and Sweetgum respectively. DP's at 50% NaOH were 97 and 88 respectively. Ethanol precipitated hemicellulose extracts from eucalyptus wood samples were recovered at 39.3 & 58.6% at 10% and 50% alkali charge respectively. With increased alkali loading, increased extraction was possible but with decreased molecular weight and degree of polymerization for extracts.

Successive alkaline extraction steps for increased recovery of hemicelluloses from lignocelluloses have also been applied in some studies (Sun et al., 2004b; Sun et al., 2013; Peng et al., 2012). The rationale hereto is that under single-step alkaline pretreatment,

low alkali loadings often lead low extraction yields; and, at higher alkali loadings, the extraction yield can be increased, but with possible degradation of hemicellulose extracts (Chen et al., 2013; Kim et al, 2016). For instance, in Sun et al. (2004b), it was reported that two-step successive treatment of de-waxed bagasse with distilled water, mild concentration of NaOH and H_2O_2, and could release around 90% of the original hemicellulose. Also, in Sun et al. (2013), triple-stage sequential extraction of hemicellulose from sweet sorghum using first distilled water at 90°C; followed by alkaline extraction at different concentrations of KOH (0.3, 0.6, 1.0, 1.5 & 2.0% (w/v)) and at 75°C; and finally with KOH-EtOH solution (60% ethanol) at 75°C. The result was 76.3% (w/w) maximal recovery of the original hemicellulose which was achieved at 1.5% KOH loading. These studies have shown that sequential treatments were much more effective than single-step mild or severe alkaline concentrations. The studies have also indicated that the concentration level of the alkaline agent has significant influence on the chemical and structural features of hemicellulose extracts.

The effects of irradiation on the effectiveness of alkaline extraction via ultrasound and radio frequency heating modes have been studied and results showed that radiation-assisted alkaline extraction of hemicelluloses can be realized more effectively in a shorter time and milder condition than without them (Iroba et al., 2013). Microwave-assisted alkaline extraction of hemicellulose from lignocellulosic materials has been reported by some studies (Panthapulakkal S. et al., 2013). Tsubaki and Azuma (2011) discuss extensively the application of microwave irradiation technology towards pretreating different lignocellulosic biomasses (including woody and agricultural residues) and show its effectiveness in fractionating lignocelluloses into their components. For instance, Panthapulakkal et al., (2013) made comparison between microwave irradiated extractions of xylan with conventional alkaline extraction: microwave-assisted alkaline

extraction of xylan was carried out on 5-10 g biomass sample, with 1-4 % (w/w) NaOH Loading, 10:1 (v/w) solvent-to-biomass ratio, 10-600 seconds at room temp using 110-1100 W microwave power. The study found that microwave-based pretreatment of 10 g birch wood sample, 1:10 mL/g liquid-to-biomass-ratio, at 110MW and 10 minutes irradiation led to 60% xylan yield, which was the highest. The same xylan yield under conventional alkaline extraction route was obtained at 90 °C and 1.5 hrs extraction time.

Alkaline extraction of hemicelluloses is considered as suitable approach in view of its unique ability to retain the extracted hemicelluloses with minimal degradation. However, the extraction of xylans should take into account the costs associated with the use of the chemical and its recovery to avoid potential harm to the environment. In the study context here, it would thus be worthwhile to think of pretreatment approaches where such unique ability of the alkaline route can be exploited while minimizing the costs and environmental impact associated with its usage.

2.3.3. *Pressurized liquid hot water extraction of hemicelluloses*

Pressurized Liquid hot water (PLHW) method is a technique whereby a biomass sample, mixed with water, is subjected to a subcritical hot water condition whereby the extraction medium (i.e. water) is maintained in a pressurized liquid state during the extraction process (Mosier, 2013; Trajano & Wyman, 2013). Water under normal ambient conditions is generally considered unsuitable for the extraction of non-polar organic compounds. However, under sub-critical condition, i.e. temperature above its boiling point (100°C) and below its critical temperature (374.15°C) with pressure high enough to keep it in the liquid state, pure water can exhibit high concentrations of proton [H^+] and hydroxyls [OH^-] – a condition which enables it to catalyse acidic and/or basic reactions. As a result of this, water at subcritical conditions can behave both like polar and apolar solvents thereby allowing it to solubilize a wide range of biomass components which are

normally water-insoluble under normal ambient conditions (Mosier 2013; Chemat et al., 2012). An important property of water in this respect is its ionization constant which is a function of the concentration of [H^+] and [OH^-] in water (Mosier, 2013).

In the study context here, the phenomena of apparent ionization of water molecules at elevated temperature and pressure is thus potentially exploitable in the separation of biomass components, especially in the extraction of easily de-polymerisable lignocellulosic components such as hemicelluloses (Yang et al, 2005; Mosier, 2013). Although the concentration of protons (H^+) and hydroxyls (OH^-) increases with increased temperature of liquid water, acid-catalysed reactions become even more prevalent during biomass pretreatment under pressurized hot water conditions, (Mosier, 2013; Trajano & Wyman, 2013; Kapu et al., 2016). Reason hereto is that as the biomass is subjected to such high temperature and pressure conditions, organic acids such as acetic, uronic and phenolic acids that are originally associated with lignocellulosic components (mainly hemicellulose) are formed in the extraction medium (subcritical water) thereby making it more acidic (Al Dajani et al., 2009; Mosier, 2013). The hydronium ions that are released during severe pretreatment conditions lead to enhanced depolymerisation of hemicelluloses by the selective hydrolysis of glycoside linkages and this in turn would lead to the release and subsequent formation of acetic and uronic acids. The acids so released would catalyse not only the extraction of hemicelluloses from the lignocellulosic matrix, but they as well catalyse the decomposition of polymeric and oligomeric hemicellulose extracts. Such acid-catalysed extraction and depolymerisation effect generally increases with increased severity of extraction conditions, especially temperature, pH and extraction time (Sun et al., 2014; Mosier, 2013). Furthermore, such catalytic effect can also lead to degradation of monomeric sugars which eventually results in the formation of inhibitory products having undesired impacts on downstream

biocatalytic processes. However, by keeping the pH of the extraction medium between 4 and 7, formation of both monosaccharides as well as inhibitory products can be minimized (Hendriks and Zeeman, 2009), thus giving preference to oligomeric and polymeric hemicellulose products.

The main parameters that influence the hemicellulose extraction yield through pressurized LHW method are temperature, pressure, flow rate and loading of water and biomass retention time. Of all these, temperature is considered highly important factor in determining the efficiency and selectivity of this extraction method (Gulbrandsen et al., 2014; Teo et al., 2010). Pressurized water at elevated temperatures can exhibit high diffusion, low viscosity and low surface tension – properties which can enhance the solubility and extraction of hemicellulosic components (Teo et al., 2010). For extractible components that are labile by their nature (e.g. hemicelluloses), temperature is also that factor which needs to be closely controlled to avoid their degradation into undesired by-products. The degree of hemicellulose extraction as well as degradation of extracted ones generally increases with increased severity. So, there should be an optimal temperature up to which increase in temperature will lead to increased extraction of hemicellulose and further increases in temperature beyond this optimal point may still lead to increased extraction, but at the expense of degradation of hemicellulosic polymers and oligomers already extracted from the lignocellulosic material. Besides temperature, hemicellulose extraction yield can also be influenced by the particle size distribution of the biomass as size, from mass transfer point of view, does have significant role to play in the rate of diffusion of water into the lignocellulosic matrix thereby facilitating the extraction and solubilisation of components therein. A study by Li et al., (2013) investigated the effect of size of chipped Aspen wood on hemicelluloses extraction and found that the concentration of polymeric and oligomeric sugars in the extracted liquor increased with

decreased size of wood chip. This is expected as reduction in particle size of lignocellulosic material can, upon reduced diffusion distance and faster mass transfer, lead to enhanced extraction of leachable biomass components like hemicelluloses (Song et al., 2012).

Mode of biomass pretreatment, i.e. batch or flow-through /continuous, has been investigated as one factor that can influence the yield of hemicellulose extraction under pressurized hot water conditions (Kilpelainen et al., 2013; Liu and Wyman, 2004) . For instance, Liu and Wyman (2004) studied the effect of varying the flow rate of hot water (at 200 °C) on the extent of solubilisation of the solid biomass. In this study, the effect of liquid velocity on xylan extraction level from corn stover in a flowthrough reactor (25.4 mm OD x 10.7 mm length, internal volume of 37.8 mL; capable of handling 6.5 g biomass sample) was investigated at three different levels: 2.8, 5.2 and 10.7 cm/min and the corresponding removal of xylan were 60, 70 and 82 % (w/w) respectively. The results obtained thus showed that increased fluid velocity could lead to higher xylan removal. The same study also showed that similar trends were observed in lignin removal with increased velocity of the fluid, albeit at lower degrees, which means the extraction of hemicelluloses components was accompanied by partial delignification of the lignocellulosic matrix. Structural properties of the lignocellulosic biomass are not just a factor influencing the nature of hemicellulose extraction process, but these properties themselves are also altered as a result (Wang et al., 2012; Trajano & Wyman, 2013; Teo et al., 2010). Controlling the pH of the extraction medium by the addition of base or buffer solutions has been reported to enhance the extraction of oligo- and polysaccharides (Kilpelainen et al., 2013). In this liquid hot water method, pressure is usually kept high enough to maintain water in the liquid state at the required extraction temperatures, but reportedly has little effect on the extraction efficiency (Mosier et al., 2013).

2.3.4. *Steam explosion pretreatment for hemicellulose extraction*

Steam-explosion pretreatment is another extensively studied method for hydrothermal biomass fractionation; and, like that in pressurized LHW method, the auto-catalytic action of subcritical water with release of organic acids define the hemicellulose extraction process (Duque et al., 2016; Jönsson and Martin, 2016; Ewanick & Bura, 2010). Depending on the intended purpose of the steam explosion pretreatment (SEPT), the biomass feed is normally subjected to high-pressure saturated steam for short time (few minutes to many, but much shorter than an hour) at temperatures in the range of 160 to 260°C, after which the pretreated material is instantaneously discharged from the reactor through an explosion decompression effect (Duque et al., 2016). Un-catalysed SEPT, i.e. one with no addition of catalytic agent to biomass prior to its pretreatment, is an environmentally friendly method well known for its remarkable ability to selectively remove hemicelluloses from the lignocellulosic matrix. The hemicellulosic sugar extracts resulting from such auto-catalysed SEPT are typically in the form of oligomers and monomers, the latter being further degraded into other by-products with the extent of degradation being dependent on the severity of the employed conditions. A number of studies have shown that the extent of depolymerisation as well as formation of degradation products to be significant for SEPT temperatures beyond 195°C mainly catalysed by the increased release and presence of acidic entities such as acetic acid in the pretreatment medium (Tomas-Pejo et al., 2011; Romani et al., 2013; Alvarez et al., 2017; Manfredi et al., 2018). This is probably one major drawback of SEPT from the viewpoint of extracting hemicelluloses in their un-degraded form (Joensson and Martin, 2016; Pielhop et al., 2016). In the biorefinery study context here, where co-production of biopolymeric hemicelluloses is to take place with bioethanol production, un-catalysed (as well as acid-catalysed) SEPT may not be attractive enough to extract hemicelluloses in

their polymeric and/or oligomeric form. This, however, need not undermine the peculiar ability of SEPT in removing substantial amount hemicelluloses from lignocelluloses; a trade-off between pretreatment conditions for enhanced hemicellulose extraction and minimized degradation (depolymerisation) of polymeric extracts needs to be made.

2.3.5. *Separation and recovery hemicellulose extracts*

The slurry obtained after completion of the pretreatment-extraction process contains both a fibrous solid residue and a complex mix of solubilized biomass components (e.g. extracted hemicelluloses) in liquefied form. To recover the hemicellulose extracts from the fibrous pretreated biomass and to prepare the insoluble solid residue for subsequent hydrolysis-fermentation processes, the slurry needs to be separated into liquid and solid fractions using vacuum and/or press filtration techniques (Aden et al., 2002; Humbird et al., 2011). For lab-scale biomass fractionation experiments, the solid-liquid separation step may have to be accompanied with simultaneous and repeated washing of the pretreated solid residue until neutral pH is attained for the filtrate. Such washing step is an important step required for two reasons: firstly, to ensure any extracted hemicelluloses entrapped in the fibrous network of the pretreated biomass are washed out; and secondly, to remove degradation (side) products from the solid residue thereby avoiding their potential inhibitory effect on the downstream bioprocesses (Kim et al., 2018; Chen et al., 2012). However, projecting such lab-scale washing step to an industrial level should take into account the cost and energy consumption that can be associated with the recovery of this water from the process streams. The higher the washing water volume, the more dilute the product stream; which implies substantial energy requirement to remove water and get the targeted product in concentrated and/or dried form.

The 'solid' fraction, i.e. the pretreated and washed residue, contains as much of the original cellulose as in the raw biomass, large part of lignin, un-solubilized hemicellulosic and other minor components. This cellulose-rich solid shall serve as substrate for the subsequent bioconversion processes leading to bioethanol production. So, In the research context here, separation of the slurry into its water insoluble solids (WIS) and liquid fraction with soluble biomass components (such as hemicelluloses) forms an essential biorefining step at which the lignocellulosic biomass is fractionated into two product lines – one for hemicellulose biopolymers and the other for cellulosic ethanol production. The liquid fraction (LF) obtained after solid-liquid separation contains most of the solubilized hemicelluloses, degradation products, co-solubilized lignin, the extraction agent and medium. Further purification and product recovery steps employing different separation techniques, therefore, become crucial to achieve the desired quality of the biopolymeric end-product. Filtration and centrifugation can be employed as primary methods to separate the pretreated biomass into its solid and liquid fractions (Valoppi et al., 2019; Oriez et al., 2019; Iroba et al., 2013). A variety of methods have been reported for further separation and purification of hemicellulosic biopolymers to the required purity level: ethanol precipitation (Peng et al., 2010b; Longue Júnior et al., 2013); ammonium sulphate precipitation (Rao and Murali-Krishna, 2006); iodine-complex precipitation (Peng et al., 2012); column chromatography (Peng et al., 2010a; Oriez et al., 2019) and membrane fractionation technologies (Zeitoun et al., 2010; Oriez et al., 2019; Bokhary et al., 2018). Membrane-based fractionation, especially ultrafiltration and nanofiltration, have been noted as one promising separation technology for recovery of hemicelluloses (Persson et al., 2007; Huang et al., 2008; Oriez et al., 2019).

2.4. LIGNOCELLULOSIC BIOMASS FOR BIOETHANOL PRODUCTION

2.4.1. Pretreatment for cellulose digestibility

The primary purpose of biomass pretreatment from cellulosic ethanol production point of view is to break down the structurally rigid and complex lignocellulosic matrix, remove hemicellulosic components, make the cellulosic portion free from lignin shield, disrupt its crystalline structure and increase its relative surface area – effects which eventually lead to enhanced accessibility and so digestibility of the rather recalcitrant cellulose (Baruah et al., 2018; Karp et al., 2013; Zhang et al., 2009; Yang and Wyman, 2007). Pretreatment is probably the most critical step that determines not only the nature of subsequent biorefinery processing steps but also the overall economic utilization of lignocellulosic biomass for bioethanol production (Carvalheiro et al., 2008; Sun et al., 2016; Yang and Wyman, 2007). In this context, an effective pretreatment should thus be able to result in cellulose-rich solid residue with enhanced enzymatic digestibility with minimum cost and energy (Silveira et al., 2015; Baruah et al., 2018; Karp et al., 2013). Those biomass fractionation techniques, as selected for hemicellulose extraction purpose and discussed hereinabove, i.e. alkaline, pressurized liquid hot water and steam explosion pretreatments, are also widely applied to enhance cellulose digestibility for ethanol production (see Table A-1.3 in Appendix A).

Alkaline pretreatment methods lead to enhanced cellulose digestibility as a result of their unique ability to cause substantial hemicellulose solubilisation, structural changes in as well as removal of lignin to an extent that directly depends on the severity of the pretreatment condition (Carvalheiro et al., 2008; Harmsen et al., 2010). Alkaline routes can generally be considered as attractive not just for the extraction of hemicelluloses, but also for improved cellulose digestibility (Kim et al., 2016; Karp et al., 2014; Toma's-Pejo et al, 2011; Harmsen et al., 2010). This is mainly due to the ability of

this method to effectively remove hemicellulose from the lignocellulosic matrix with low degradation of the hemicellulose itself. Hemicellulose removal is largely related to higher accessibility of the cellulose polymers to hydrolytic enzymes: the higher its removal, the higher the hydrolytic digestion of cellulose (Kim et al., 2016; Yang et al., 2011). Furthermore, lower degradation of hemicellulosic polymers does mean that there is lower or minimized formation of inhibitory products which can hamper cellulosic digestibility as well as yeast fermentation processes (Yang et al., 2011). The presence (or formation) of inhibitors is thus one factor that determines the efficiency of the hydrolysis-fermentation process. Inhibitors can disrupt on the stability of the fermentation processes and thus become crucial factor in their successful development (Cardona et al., 2010; Joensson and Martin, 2016; Wang et al., 2018; Kim, 2018). Some studies showed that xylo-oligomers can have stronger inhibitory effect on enzymatic digestion of cellulose than do both xylan and xylose (Qing et al, 2010; Wang et al., 2018). This may, in the research context here, mean that partial de-polymerization of hemicellulose into oligomeric products need to be seen from the point of their possible inhibitory effect.

The digestibility of alkaline-pretreated lignocellulosic biomass can be influenced by a number of factors such as enzyme loading, hydrolysis time, lignin content, acetyl content, and crystallinity of the biomass as well as pretreatment conditions and methods (Tutt et al., 2012; Zhu et al., 2008; Yang & Wyman, 2007). Since digestibility itself directly affects the degree of cellulosic ethanol production, these factors need to be given due consideration in view of achieving enhanced bioethanol yield. The removal of the acetyl groups of hemicelluloses (de-acetylation) has been reported to significantly enhance the cellulosic digestibility (Yang et al., 2011; Kim and Holtzapple, 2005). Li et al. (2008) have investigated the effect of lignin content, acetyl content and crystallinity on the digestibility of alkaline pretreated poplar wood and concluded that there is inverse relationship

between these factors and enzymatic digestibility of the pretreated biomass. Enzymatic digestibility of a given lignocellulosic biomass can also be dependent on the method of pretreatment followed. Ioelovich & Morag (2012), for instance, investigated and compared the digestibility of four types of lignocellulosic feedstock (poplar, corn cobs, rice straw and switchgrass) under mild acid and alkaline pretreatment conditions and found that alkaline pretreated ones to have shown better digestibility than acid pretreated samples. Tutt et al., (2012) has compared the effect of acid (HCl) and alkaline (KOH) pretreated wheat straw and found that the alkaline-pretreatment could lead to higher ethanol yield (104.3 g/kg) than acid pretreatment (67.7 g/kg).

Pressurized Liquid Hot Water (LHW) biomass pretreatment often takes place at temperatures ranging from 150 to 220°C and pressures higher than that at saturation point (Carvalheiro et al, 2008). In view of ethanol production, this method is generally capable of producing digestible cellulose (Sun et al., 2014; Teo et al., 2010). Acidic components such as acetic, uronic and formic acids are believed to catalyse the auto-hydrolysis process through the formation of hydronium ions (Carvalheiro et al., 2008). LHW method is attractive for the removal of hemicelluloses, albeit in its oligomeric and monomeric forms; but under severe pretreatment conditions the proportion of monomeric, and so of fermentable sugars, can be substantially increased. A study by Franco et al., (2013) showed that hydrothermally pretreated sugarcane tops and leaves could lead to glucose yield of 60% within 48 hrs of enzymatic hydrolysis. Shuangliang et al., (2013) investigated the influence of hemicellulose and lignin removal on the enzymatic digestibility and sugar recovery from sugarcane bagasse treated with liquid water and aqueous ammonia. Their findings could reveal that the observed cellulose digestibility was largely attributed to the removal of hemicellulose and delignification played only a secondary role in enhancing the digestibility. Excessive lignin removal may,

contrary to what can initially be thought of, lead to reduced accessibility of cellulose for enzymatic attack; as substantial lignin removal can bring about collapse in the resulting porous structure of the lignocellulosic matrix (Zhu et al., 2008).

Steam explosion pretreatment (SEPT) is probably one of the most promising biomass fractionation method for cellulosic ethanol production. In this regard, SEPT has been shown technically viable mainly owing to its ability to remove hemicelluloses, cause structural disruption of the lignocellulosic matrix through its explosion decompression effect, reduce cellulose crystallinity while increasing its surface area and porosity – effects capable of leading to enhanced enzymatic digestibility of cellulose (Pielhop et al., 2016; Duque et al., 2016). Increased solubilisation of hemicelluloses under SEPT can indeed lead to enhanced cellulose recovery in the pretreated solid thus making it more accessible to enzymatic attack; however, thermal conditions required therefor (i.e. 190 to 220°C) often lead to increased formation of degradation products having inhibitory effect on subsequent bioconversion processes (Joensson and Martin, 2016; Duque et al., 2016). As a result, quite a number of studies have indicated that the recovery of fermentable sugars from lignocelluloses can be enhanced with the addition of acids (such as SO_2, H_2SO_4, CO_2) to the biomass prior to SEPT so as to allow increased removal of hemicelluloses at comparatively lower temperatures and shorter durations (J. Xu et al., 2017; Carrasco et al., 2010). Such acid-catalysed SEPT, however, not only leads to substantial formation of monomeric sugars but also degradation products thereof. Furthermore, both un-catalysed and acid-catalysed SEPT are, unlike for hemicelluloses, not good enough for lignin removal from lignocellulosic biomass. Lignin that remains intact within the lignocellulosic matrix can turn as a potential barrier to the bio-catalytic action of enzymes on cellulose thus impeding its digestibility (Rahikainen et al., 2013; Guo et al., 2014). For this reason, steam-exploded residues may subsequently be subjected to a second-step

conventional alkaline pretreatment to remove the lignin that otherwise remains therein (Rocha et al., 2012; Oliveira et al., 2013; Ratti et al., 2015). Such post-SEPT alkaline delignification step may, however, mean additional cost to an already cost-intensive biorefining step.

2.4.2. Ethanol production and recovery steps

Solid residues obtained after the pretreatment/fractionation of the lignocellulosic biomass serves as a substrate to the enzymatic hydrolysis step where biocatalytic conversion of polymeric sugars therein into the respective monomeric constituents takes place. The purpose of hydrolysis is basically to break down the natural polysaccharides (i.e. cellulose and/or hemicelluloses) into fermentable sugars for subsequent bioconversion by yeasts into ethanol (Yang et al., 2011; Silveira et al., 2015; Baruah et al., 2018). Hydrolysis is thus both important and crucial in cellulosic ethanol production with the liberation of fermentable sugars being achievable either through chemical or biological /enzymatic routes (Binod et al., 2011; Yang et al., 2011), of which the latter is of particular interest in the research context here. The biological route makes use of enzymes that are capable of digesting polysaccharide sugars to release the basic monomeric constituents thereof (Michael et al., 1999; Roehr, 2001). Enzymes are not only specific with respect to the macromolecular sugar type they can digest (e.g. cellulase for cellulose, xylanase for xylose), but – as biocatalytic agents – they are also run under milder conditions, generally exhibiting lower rate of hydrolysis but higher glucose yield (Roehr M., 2001; Saini et al., 2020). The effectiveness of this route is also highly dependent on the pretreatment method and conditions applied thereof as accessibility of cellulose to enzymes as well as the possible formation of inhibitory products that can impede the enzymatic hydrolysis process can very well be related to the pretreatment process (Yang et al., 2011; Yang and Wyman, 2008). Enzyme cost is the most significant factor that

determines large-scale application of the enzymatic hydrolysis route (Saini et al., 2020; Binod et al., 2011; Roehr, 2001). Despite its being the preferred route, enzymatic hydrolysis is considered to be the most complex step in the production of cellulosic ethanol owing to the complex nature of the interaction between the substrates and the enzymes (Yang et al., 2011; Roehr et al., 2001).

Fermentation of enzymatically released monomeric sugars takes place using appropriate yeast strains. The fermentation step is central for cellulosic ethanol production and its efficiency is highly dependent on the conditions under which the yeast can function optimally (Krishna et al., 2001; Fitzpatrick et al., 2010). The fermentation process is basically carried out under two usual modes: separate hydrolysis and fermentation (SHF) or simultaneous saccharification and fermentation (SSF). The biggest disadvantage of the SHF process is the accumulation of sugars which have inhibitory effect on the action of enzymes and thus require more enzymes loading. The SSF scheme is basically intended to avoid this end-product inhibition on enzymes by sugars by carrying out the hydrolysis and fermentation processes in one single unit, thus saving costs which otherwise would be spent on enzymes (Robak and Balcerek, 2018; Cardona et al., 2010; Dowe and McMillan, 2008; Krishna et al., 2000). Despite such an advantage, one major drawback of the SSF mode is the difficulty of striking at optimal conditions required for best hydrolytic performance and efficient fermentation, especially in terms of temperature (Krishna et al., 2001; Cardona et al., 2010; Balat et al., 2008).

Once the hydrolysis-fermentation process is over, the resulting broth needs to be subjected to a series of distillation, rectification and dehydration steps to recover the produced ethanol as the main biorefinery product. With the first two recovery steps around 92.4% ethanol concentration is achieved from the initial broth with low ethanol concentration (Huang et al., 2008; Aden et al., 2002; Ramaswamy et al., 2013). The

resulting azeotropic mixture of ethanol and water (azeotrope forms at 95.6% EtOH w/w; 78.15°C) cannot be separated any further using single distillation stage (Huang et al., 2008; Ramaswamy et al., 2013). Further dehydration technologies such as azeotropic distillation, extractive distillation, adsorption with molecular sieve and membrane pervaporation need to be employed to get anhydrous ethanol (Ramaswamy et al., 2013; Huang et al., 2008).

2.4.3. Biosolids (lignin) recovery and wastewater treatment

The distillery stillage – which is rich in lignin and other organic wastes – is separated into solid residue and liquid waste fraction by employing centrifugation and/or press filtration (Aden et al., 2001; Humbird et al., 2011; Ramaswamy et al., 2013). The recovered lignin-rich solid fraction would serve as direct fuel input to the integrated CHP plant, which provides steam and electricity to the lignocellulose conversion processes, while producing a net surplus of electricity for sale. Whereas the liquid part is subjected to evaporation to recover the water in condensed form which can then be recycled back for use as a process water; whereas the concentrated syrup resulting from the evaporation shall, together with the recovered solid fraction, serve as a fuel to the co-generation plant (Huang et al., 2008; Aden et al., 2001; Humbird et al., 2011). The fact that ethanol obtained from lignocellulosic material via biochemical conversions is at low concentration levels in the fermentation broth makes separation and recovery of ethanol an energy-intensive process thus driving production costs rather high (Ramaswamy et al., 2013; Huang et al, 2008). This may imply the need to develop efficient and low-cost separation and purification processes.

In the research context here, where cellulose and hemicelluloses from selected lignocellulosic feedstock (i.e. SCT and AW) are respectively targeted for their conversion into bioethanol and biopolymeric co-product, lignin is indeed that major biomass

component worth recovered from different biorefinery streams by deploying suitable technologies. A number of techniques for the recovery of lignin-rich solids have been reported: membrane based separation such as ultrafiltration and nanofiltration systems (Humpert et al., 2016; Bokhary et al., 2017; Kekana et al., 2016); multiple-effect evaporation system (Aden et al., 2002; Humbird et al., 2011; Rohde 2019); vacuum press filtration system (Davis et al., 2016; Schulze et al., 2019), the Lignoboost process (Li and Takkellapati, 2018; Per Tomani et al., 2010) and solvent-based recovery systems (Rohde et al., 2019; Tagami et al., 2019). These lignin recovery techniques can be applied either separately or in conjunction depending on the end-purpose of the biorefinery.

The process water containing organic wastes (bio-wastes) is concurrently recovered in its purer form to be recycled and reused, while having the organic contents therein are converted into less harmful and useable forms. The recovery of process water with minimal organic wastes necessitates the deployment of wastewater treatment technologies which are indispensable should biorefineries become ecologically sound. To this end, anaerobic biodigestion of the organic matter in wastewater streams followed by subsequent digestion of any anaerobically undigested organic matter under aerobic conditions has been identified as practical approach to treat wastewater streams emanating from 2G biorefineries (Aden et al., 2002; Humbird et al., 2011; Hagman et al., 2018). The methane-rich biogas generated from the anaerobic digestion unit can serve as additional fuel to the co-gen plant. The biosludge from the aerobic digester can either be used as solid fuel to the co-gen plant (in which case it has to be dewatered using press filters) or be disposed to the farm land where it can serve as fertilizer (Riya et al., 2020; Zhang et al., 2020). Whereas the clear water obtained after clarification can be safely recycled for reuse.

2.5. CURRENT TRENDS IN INDUSTRIAL-SCALE LIGNOCELLULOSIC BIOREFINERIES AND THE MOTIVATION BEHIND THEIR DEVELOPMENT

Recent developments in advanced biofuels industry reveal that there is indeed a revamped interest in the utilization of agro-industrial lignocellulosic biomass for the production of bioethanol. Consequentially, cellulosic ethanol production from harvesting residues and forest woods has already taken ground in the commercial scene (Padella et al., 2019; Rosales-Calderon and Avantes, 2019; Chandel et al., 2018; Winters, 2011). For instance, GranBio and Raizen Group's cellulosic ethanol projects (both in Brazil), Godavari Biorefineries of India can be noted for their use of sugarcane biomass as feedstock. Other projects which make use of agricultural residues for bioethanol production include the Crescentino Project (in Italy), 'Project Liberty' cellulosic ethanol project ventured by POET & DSM as well as similar industrial-scale projects by Abengoa Bioenergy and DuPont (in the USA). Mascoma Frontier's Biorefinery Project and ZeaChem commercial facilities base their cellulosic ethanol production on woody biomass.

Given the intensity of R&D undertakings in the bioindustrial arena, it can fairly be said that the time is ripe enough to think of the next higher level towards which the cellulosic industry needs to be pushed. The remarkable technological developments witnessed in the field are expected to continue over the decades ahead, but how that will unfold with time is very much dependant on strategies put forward and pursued along that direction. One such strategy could be the application of principles of "circular bio-economy" whereby existing lignocellulosic biomass will be used with minimized wastage of such (Ubando et al., 2020; Dragone et al., 2020; Bauer et al., 2017; Mohan et al., 2016). This may technically translate into the development of an integrated biorefinery system whereby as much of the lignocellulosic feedstock would be converted not only into advanced biofuels, but also into other non-fuel bio-based products having higher value.

The co-production of high-value bio-based products with biofuels apparently boosts more circular utilization of lignocellulosic biomass with enhanced economic value. Given that there is increasingly high demand for bioethanol, the industrial infrastructure laid for its large-scale production can serve as a shared facility for an integrated production of other high-value products from the same initial biomass. Such bioethanol-centred biorefinery developments can indeed be regarded as a cornerstone for sustainable bioeconomy future, albeit with more complex technical challenges.

Industrial-scale realization of biorefineries based on lignocellulosic biomass can largely be dictated by the current state of biomass conversion technologies, their high investment requirement, feedstock availability and cost, as well as the high cost that can be associated with biomass transportation (Kamm et al., 2006, King D., 2010). In view of this, existing biomass-intensive agro-industrial sectors, such as the sugarcane and forestry industries, have been identified as one way of advancing lignocellulosic biorefineries. Because of their first-generation biorefinery complexes and large amount of biomass at their disposal, the sugarcane as well as wood-based forestry industries (e.g. the pulp and paper industries) are suitably positioned for the realization of advanced biorefinery concept in their conventional manufacturing set-up (Chirat et al., 2010; Sousa, 2010; van Heiningen, 2006). While such first-generation bioindustrial setups are well established by their own, how these industries are making more economic use of the abundant residual biomass they have at their disposal remains questionable. For example, in the pulp and paper industry, significant portion of hemicelluloses is degraded during chemical pulping and simply dumped out (or burned with the lignin-rich residue) without any substantial economic gain from it (Fitzpatrick et al., 2010). Pre-extracting the hemicellulosic components from the raw material and turning it into value-added products has been put forward in the biorefinery context (Vena et al., 2013; Chimphango

et al, 2010; Sousa, 2010; van Heiningen, 2006). Similarly, in the sugarcane industry, sugarcane harvesting residues (which make up to 30% the cane biomass) remain largely underutilized – usually burned or simply left on the field with no economic value extracted from it (Manohar Rao, 1997). A study by Jeff Smithers (2014) reports that South African Sugar Industry has the potential for 2.7 Million tons of sugarcane trash but around 90% of this fibrous material is burnt out in the field. The same study also indicated that the possibility of turning this trash into electricity, which is of low value.

In view of such evident underutilization of potentially usable lignocellulosic components in abundant biomass, one perspective of research and development can be the co-production of high-value bio-products (such as hemicellulosic biopolymers) along with bulk chemicals like bioethanol and electricity production. The very idea of making more economical uses of the lignocellulosic components of sugarcane trash and woody raw materials is thus worth researching in view of demonstrating an integrated biorefinery concept thereby enabling the industries harness more economic opportunities from the same biomass they have had for long. By so doing, the industries would not only make economic gains from the rich biomass supply they have, but such move from the 'first-' to the 'second-generation' biorefineries would make them more competitive and dynamic sectors while bringing about substantial environmental and social benefits. This research project would address this problem of wastage or underutilization of lignocellulosic biomass (or, components thereof) at conventional sugarcane as well as wood-based industrial complexes and explore the techno-economic and environmental implication of advancing 2G biorefineries in the context of these sectors. Such industrial implications extend well to the South African sugar sector.

2.6. STATEMENTS OF NOVELTY

The utilization of non-edible plant biomass for energy generation purpose is comparatively well established field. From the literature survey made, it can be said that the production of second-generation bioethanol seems to have dominated the research and development landscape in the lignocellulosic biorefinery arena. There are even a number of cellulosic ethanol plants that are either at demonstration and/or industrial scale, albeit with little commercial success. It can generally be observed that many of the pretreatment-related studies in literature are focused on making the cellulose more accessible for hydrolytic agents and the effect of various factors is also investigated to this end. The prime objective, as can be expected from the very purpose of pretreatment, was inclined towards enhancing fermentable sugar yields from the structural sugars in lignocelluloses; however, making effective use of both celluloses and hemicelluloses towards bioethanol production is yet to be mastered.

What rather looks thinly covered in the literature is industrially-oriented approach where co-production of hemicellulosic biopolymers takes place from the same lignocellulosic biomass meant for energy generation and bioethanol production. Even though there are a number of studies which have been conducted with the aim of extracting hemicellulose-derived high value products from a variety of lignocellulosic materials, they are only at small/lab scale and, very often, separate from bioethanol production and/or electricity generation. There is as such no particular work which has been undertaken with the aim of establishing optimal set of pretreatment conditions intended both for hemicellulose biopolymers extraction and enhanced cellulosic ethanol production. Up to now the technologies for hemicellulose extraction and ethanol production from lignocellulose have progressed independently, each chasing commercialization on its own.

The novelty of the present research work lies in its biorefinery approach whereby the inclusion of a third product dimension to a bioethanol-centred use of lignocellulosic materials for co-production of hemicellulosic biopolymers along with bioethanol production and power generation. The combination of products selected is more specifically: xylan biopolymers, cellulosic ethanol and electricity. Novel biomass pretreatment/fractionation approaches, namely: microwave-assisted pressurized hot water method and alkalinized steam explosion pretreatment, have been proposed and experimentally investigated. As xylan is the major hemicellulosic sugar in hardwoods and agricultural residues, aspen wood (hardwood type) and sugarcane trash (an agro-industrial harvesting residue) were selected for the study purpose, to test the effects and suitability of proposed pretreatment approaches on the extraction of xylan biopolymers. One extension of this novelty is that based on this combination of product streams, mapping out of different biorefinery scenarios was carried out to assess the techno-economic viability of a lignocellulosic biorefinery system based on the experimental results that led to highest xylan extraction yield and enzymatic cellulose digestibility. Another extension of the present research can be seen in terms of the industrial context it is undertaken: that is, the techno-economic and environmental assessment of the envisaged multi-product biorefinery is approached in the context of sugarcane and/or forestry industries.

CHAPTER THREE: RESEARCH APPROACH AND METHODS

3.1. RESEARCH APPROACH

The present research was conceived with an overall aim of developing a lignocellulosic biorefinery system intended for an integrated production of bioethanol, hemicellulosic biopolymers and electricity from two feedstock types selected for this purpose. To this end, and in alignment with its stated objectives, this biorefinery-oriented research was designed to constitute both experimental and process modelling works. The experimental part was mainly meant to achieve three objectives:

(I) to investigate the technical viability of novel pretreatment approaches identified for hemicellulose extraction purpose;

(II) to establish optimal range of process conditions that will simultaneously achieve both hemicellulose extraction and cellulose digestibility; and,

(III) to determine what yields for targeted end-products, i.e. biopolymeric hemicelluloses and cellulosic ethanol, can be achieved per unit weight of dry biomass.

Whereas the modelling part was intended to assess the techno-economic behaviour as well as environmental performance of the envisaged biorefinery system at an industrial scale based on the most promising pretreatment technology and lignocellulosic biomass having a realistic chance of being scaled-up. The major steps involved in the technical, economic and environmental assessment of the biorefinery as envisaged by this study are depicted under Fig 3.1. Accordingly, the research shall have the following main components:

1. **Experimental works**: Here, the effects of varying combination of pretreatment parameters on the yields of hemicellulose extraction and cellulose digestibility (=> ethanol production) from selected lignocellulosic biomass samples shall be investigated in a statistically controlled manner. Aside from establishing how technically viable and promising the selected extraction method is, a set of process conditions as well as optimal yields for targeted end-products shall also be generated. Primary data obtained thereof would serve as input for subsequent process modelling purposes.

2. **Process synthesis and design:** Conceptual process development for different biorefinery scenarios and process configurations for an integrated production of xylan biopolymers, cellulosic ethanol and electricity from selected lignocellulosic materials.

3. **Process economics and environmental analysis**: Assessment of the techno-economic and environmental viability of synthesized lignocellulosic biorefinery processes through appropriate modelling and simulation approaches.

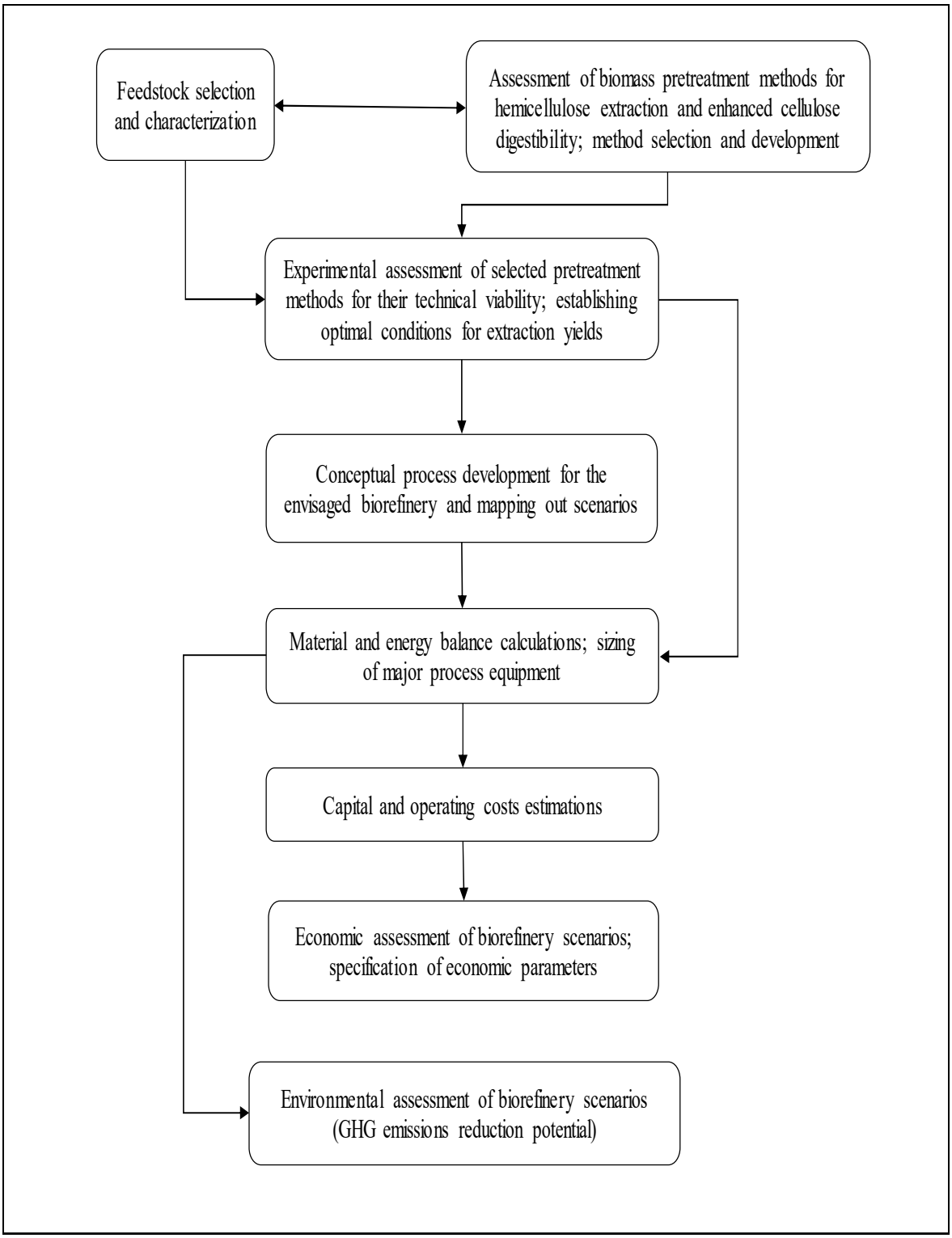

Fig 3.1. Flowchart for the overall approach and major steps followed in the technical, economic and environmental assessment of the envisaged biorefinery

3.2. EXPERIMENTAL METHODS

The present biorefinery-centred research basically intends to valorise selected lignocellulosic feedstock types (sugarcane trash, SCT and aspen wood sawdust, AW) into xylan biopolymers, bioethanol and electricity. This may, at experimental level, translate to finding out suitable biomass fractionation techniques as well as optimal conditions thereof to extract hemicellulosic biopolymers while simultaneously enhancing the cellulose enzymatic digestibility for ethanol production. To this end, novel biomass fractionation approaches shall be developed based on three existing pretreatment techniques, namely: pressurized liquid hot water, alkaline and steam explosion biomass pretreatment methods, which themselves were identified for their potential applicability for hemicellulose extraction purpose (see section 2.3, under Chapter II). Experiments were envisaged and planned in such a way that results generated therefrom shall serve as a starting point while evaluating the technical viability of the lignocellulosic biorefinery system for an integrated production of xylan biopolymers (the end-product resulting from hemicellulose extraction route), cellulosic ethanol (the end-product that necessitates enzymatic digestibility of polysaccharide sugars) and electricity (how much of the raw biomass, esp. lignin, can be recovered for heat and power generation purpose). In this respect, the scope of the experimental work shall encompass (1) full-fledged biomass pretreatment tests for the extraction of hemicelluloses from selected lignocellulosic materials; (2) enzymatic hydrolysis tests on raw as well as pretreated biomass samples to see how the cellulose digestibility is impacted by the pretreatment method and specific conditions applied; and (3) hydrolysis-fermentation tests on highly digestible pretreated solids to see how high the ethanol production yield is per unit weight of raw biomass. A conceptual framework to guide the approach and execution of experimental works is shown in Fig 3.2.

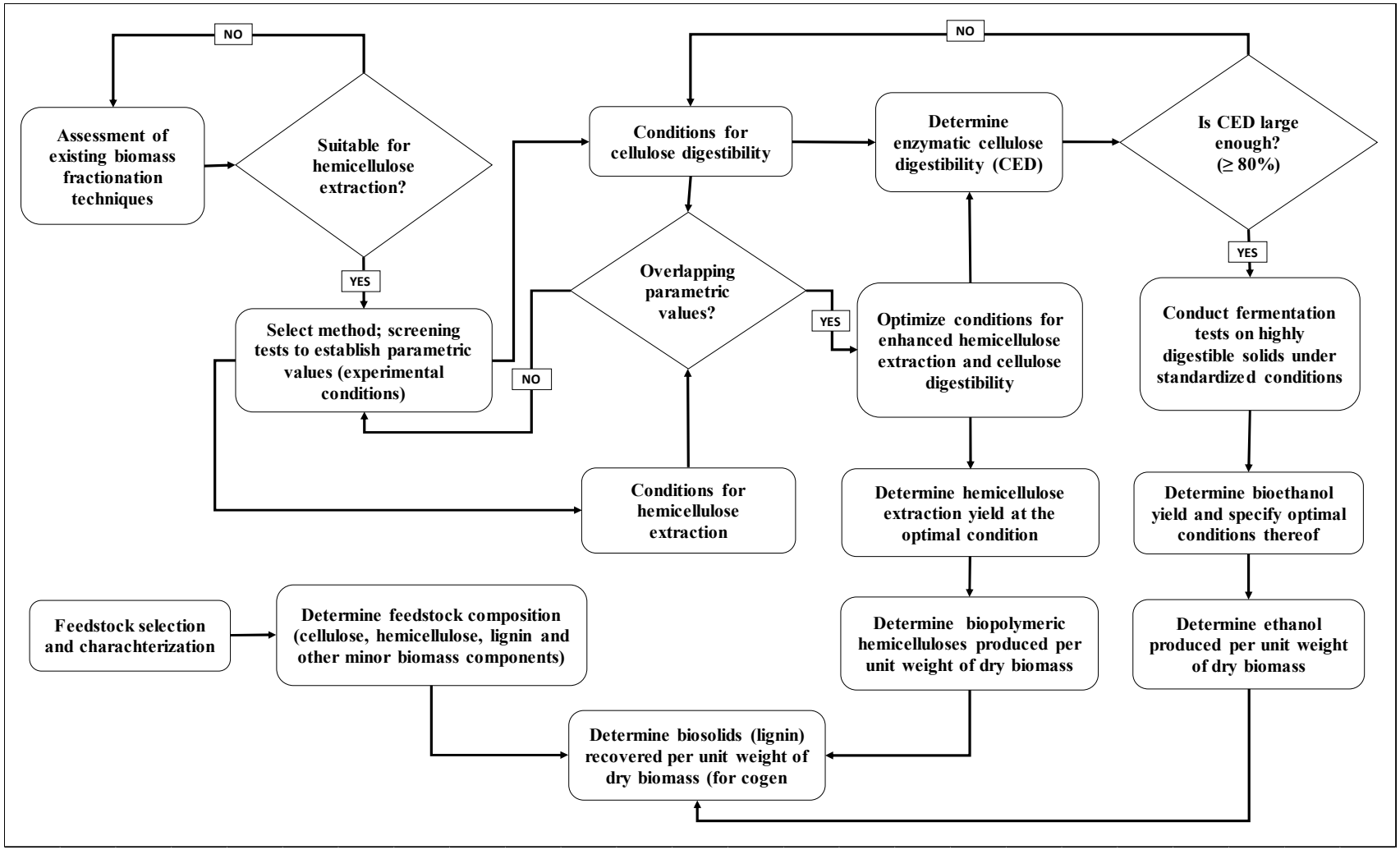

Fig 3.2. Conceptual framework outlining major logical steps guiding the experimental activities in the present research context

Experimental optimization of biomass pretreatment methods selected for the extraction of hemicellulosic biopolymers from sugarcane trash (SCT) and hardwood (aspen wood, AW) were conducted. In addition, solid residues obtained after hemicellulose extraction were concurrently tested for their enzymatic digestibility in accordance with established protocols and standardized procedures (Selig et al., 2008; Adney and Baker, 2008; Sluiter et al., 2008a; Sluiter et al., 2008b). A range of experimentally verified pretreatment conditions were developed for each selected feedstock, thus providing various possible combinations of acceptable yields for hemicellulose extraction as well as enzymatic cellulose digestibility high enough (80% w/w cellulose digestibility was aimed as minimum target) for ethanol production. Samples among pretreated residues exhibiting relatively high digestibility were to be subjected to subsequent hydrolysis-fermentation tests to determine ethanol production yield. These fermentation tests carried out were in accordance with standardized NREL protocols (Dowe and McMillan, 2008). The experimental work principally serves two main purposes: Firstly, as a way of investigating the separate and/or combined (interaction) effects of controlled input parameters (mainly temperature and retention time) on output parameters of interest (e.g. extraction yields, enzymatic digestibility, fermentation efficiency). Secondly, in establishing optimal values among tested input parameters (process conditions) for acceptable extraction, digestibility and fermentation results. Major steps encompassed by the planned experimental work are briefly discussed under the sub-sections herein below (see Fig. 3.3).

3.2.1. FEEDSTOCK PREPARATION AND CHARACTERIZATION

For the experimental purpose here, feedstock sample preparation as well as compositional analysis of representative samples thereof were carried out in accordance with established protocols (Hames et al., 2008; Sluiter et al., 2008c; Sluiter et al., 2008d; Sluiter et al., 2012). This is indeed the first essential step where the raw lignocellulosic material would be dried to about 90% dry matter content followed by milling and sieving to get samples within the required particle size distribution. Representative test samples shall be characterized in terms of their chemical composition (polysaccharides such as celluloses and hemicelluloses, lignin, ash and extractives) and results thereof shall serve as a basis in determining how much of the original biomass constituents (especially those major ones: cellulose, hemicelluloses and lignin) would have ended up to which intermediate and/or end-product while the raw biomass is being progressively biorefined. As a matter of fact, yields for targeted end-products (bioethanol, hemicellulosic biopolymers) are often expressed against original contents and/or amounts of such in the initial raw biomass.

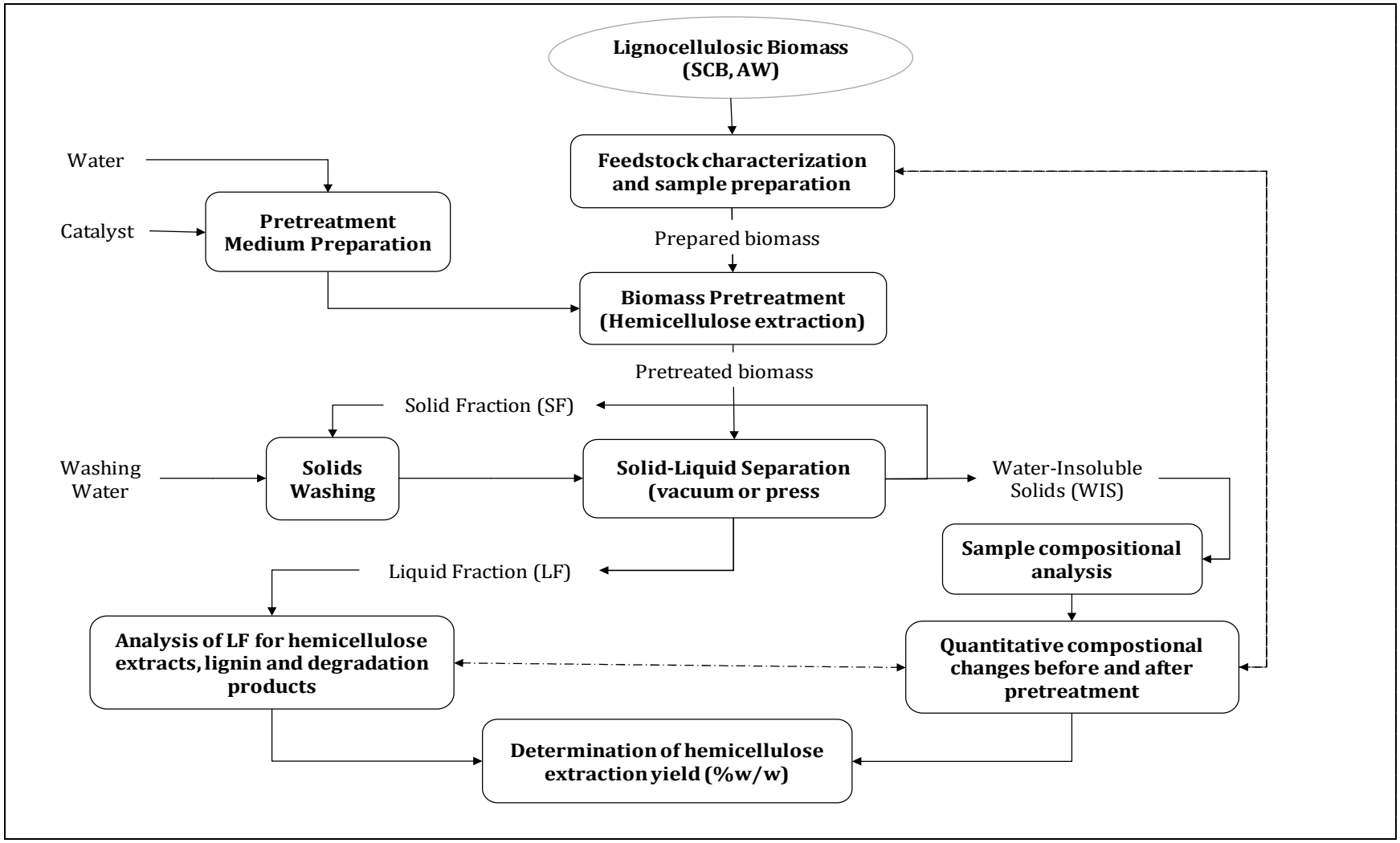

Fig 3.3 Experimental Steps for hemicellulose extraction and determination of extraction yield

3.2.2. HEMICELLULOSE EXTRACTION FROM LIGNOCELLULOSIC SAMPLES

Once biomass samples are prepared and characterized, measured amount thereof was taken for hemicellulose extraction tests which were conducted following the steps in Fig 3.3. The biomass pretreatment stage is certainly the central step where the actual extraction takes effect. In case of alkaline hemicellulose extraction, an alkaline medium required for the pretreatment would be prepared by dissolving specified amount of alkali in water at a proportion that would give the desired concentration level (Xu and Sun, 2016; Kim et al., 2016; Longue Junior et al., 2013; Peng et al., 2012). Prior to its pretreatment, the prepared biomass sample and alkaline medium were mixed at ambient conditions before placing the mixture in a reactor wherein the extraction takes place. The pretreatment unit shall have automatic temperature controller and, in case it should take place under pressurized conditions, a pressure sensor (Longue Junior et al., 2013; Trajano and Wyman, 2013). The alkali-to-biomass loading ratio [w/w], temperature [°C] and retention time [min] were the three factors considered for experimental investigation based on statistically selected test points (Sukhbaatar et al., 2014). Similarly, in the case of hemicellulose extraction via hydrothermal pretreatment approaches considered here (namely: pressurized liquid hot water or steam explosion methods), a specified amount of biomass sample was thoroughly mixed with water at a pre-determined water-to-biomass ratio; the prepared biomass was then subjected to subcritical water /saturated steam/ maintained under pressurized and high-temperature condition (Pielhop et al., 2016; Duque et al., 2016; Song et al., 2012; Li et al., 2013). Here again, pretreatment temperature, retention time, water-to-biomass loading ratio would be the factors considered for experimental investigation. Where catalysts (alkaline or acidic) are applied, the catalyst-to-biomass loading ratio were also specified.

After pretreatment, the pretreated biomass was collected and cooled down to ambient temperature. The fresh slurry was subsequently separated into its water-insoluble solid fraction and liquid fraction using vacuum or press filtration. To remove any solubilized biomass components (such as hemicelluloses) entrained therein, the solid fraction was washed with pure water repeatedly until the pH of the outgoing filtrate becomes neutral. The wet solid residue was dried until constant weight, after which its composition would be determined to examine the compositional changes that resulted from pretreatment. Compositional analysis of pretreated solid samples were done as per the respective NREL protocols (Sluiter et al., 2012; Hames et al., 2008). With respect to the liquid fraction (LF), it is important to determine which biomass components have ended up therein and how much. In the study context here, the most important parameter to be determined was oligomeric and/or polymeric sugars of hemicellulose origin. Solubilized lignin and degradation products such as acetic acid, furfural and HMF were also quantified. Analysis of samples from the liquid fraction was therefore carried out for sugars, by-products and degradation products in accordance with the respective NREL protocol, NREL/TP-510-42623 (Sluiter et al., 2008b) or methods of comparable applicability. With known weights and hemicellulose composition of the dried initial biomass as well as the dried solid residue, the degree of solubilisation of hemicellulose that resulted from the pretreatment was calculated. Equivalently, with quantified amount of hemicellulose extracts in the liquid fraction, the extraction yield can be estimated based on the original amount of hemicellulose in the initial raw biomass and the extent of solubilisation realized under specific set of extraction conditions. The extraction yield for hemicelluloses (HC) was determined using the following equation (3.1):

$$Extraction\ Yield\ [\%w/w] = \frac{\boldsymbol{amount\ of\ HC\ recovered\ in\ liquid\ fraction}}{\boldsymbol{amount\ of\ HC\ in\ initial\ feedstock}} \times 100 \quad \text{---- (3.1)}$$

3.2.3. ENZYMATIC DIGESTIBILITY AND HYDROLYSIS-FERMENTATION TESTS

In the context of the present research, which essentially is about bioethanol-centered lignocellulosic biorefinery development, the experimental study should, at least, aim at investigating the effects of pretreatment conditions on the enzymatic conversion of structural sugars (cellulose and xylan) into their respective monomeric and fermentable forms (glucose and xylose). The enzymatic digestibility tests on cellulose-enriched residue obtained after hemicellulose extraction were carried out as per the respective NREL protocols (Selig et al., 2008; Adney and Baker, 2008; Sluiter et al., 2008a; Sluiter et al., 2008b). Fig 3.4 shows the major steps followed in determining the enzymatic digestibility of biomass samples, mainly cellulose. The water insoluble solids (WIS) obtained under all tested pretreatment conditions was characterized for their composition; cellulose and xylan contents, in particular.

Duplicated enzymatic hydrolysis tests were conducted under the same experimental setups and following standardized procedures, all at 2% (w/v) substrate loading (Selig et al., 2008). The enzyme preparation was made to comprise of both cellulase and xylanase which are intended to convert cellulose and xylan into glucose and xylose respectively; cellulose, which is the most recalcitrant lignocellulosic component, was the main target of enzymatic digestion. However, given the nature and purpose of this study, the WIS substrates were expected to contain significant amounts of un-extracted hemicelluloses which would remain intact in the lignocellulosic matrix, thus representing potential sugar source for co-fermentation with glucose. In fact, supplementing cellulase with xylanase was intended to boost ethanol production yield, mainly for two underlying reasons: firstly, through the addition of monomeric sugars of hemicellulosic origin liberated via enzymatic digestion; and, secondly, further enzymatic removal of hemicelluloses from pretreated solids would render the cellulose-rich sample structurally

more open and so more accessible to enzymatic attacks (Shuangliang et al., 2013; Zhu et al., 2008). Meaning, any hemicellulose which would otherwise remain intact in the lignocellulosic matrix may represent potential barrier to enzymatic action on cellulose.

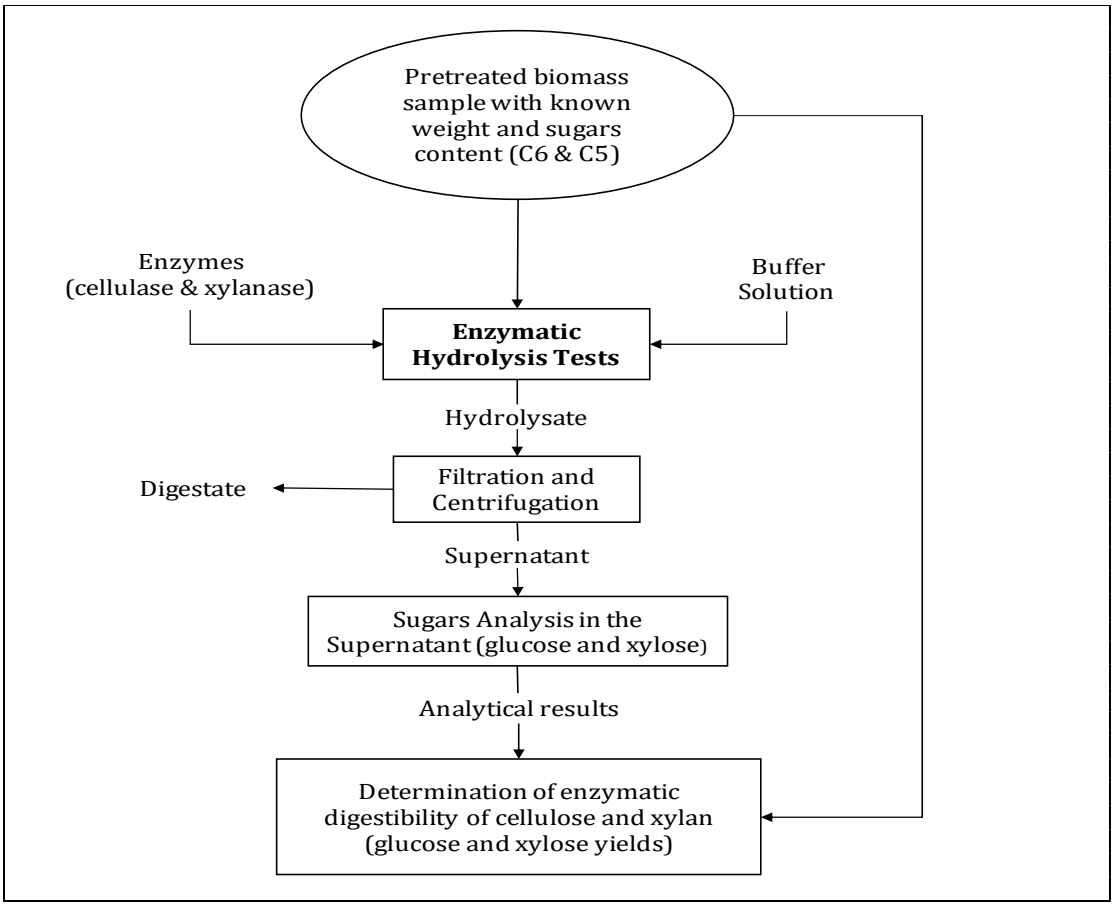

Fig 3.4 Experimental steps to determine enzymatic digestibility on pretreated solids

So, a combination of cellulase and hemicellulase/xylanase were applied uniformly for all hydrolysis tests. Once enzymatic hydrolysis tests were completed, the resulting hydrolysate was filtered centrifugal and/or vacuum filtration steps. The liquid fraction containing almost all enzymatically released sugars was filtered out as supernatant from which analytical samples were prepared. From analytical results, glucose and xylose contents were quantified to determine the enzymatic digestibility cellulose and xylan.

$$\%\ digestion = \frac{\boldsymbol{amount\ of\ digested\ cellulose}}{\boldsymbol{amount\ of\ cellulose\ input}} \text{ X } \mathbf{100} \text{ ----------}$$

While the enzymatic hydrolysis tests were conducted for all pretreated solids obtained after hemicellulose extraction, those solids having relatively higher extent of enzymatic digestibility were also subjected to fermentation tests. The aim was to determine how high the ethanol production yield achieved, apparently under those pretreatment conditions which led to the highest cellulose digestibility. Pretreated samples proven to have enhanced accessibility to enzymes were therefore chosen as a substrate for the fermentation tests conducted as per the NREL Protocol: SSF Experimental Protocols - Lignocellulosic Biomass Hydrolysis and Fermentation; Laboratory Analytical Procedure (Dowe and McMillan, 2008). While details hereon can be referred to this NREL protocol, the basic steps followed while carrying out the hydrolysis-fermentation experiments are as depicted in Fig 3.5.

Unlike that for enzymatic hydrolysis tests, the substrate loading for fermentation tests was taken at 10% [w/v]; other inputs to the SSF unit (such as enzymes, yeast and nutrients, water and the buffer solution) were loaded as per the respective NREL protocol for SSF experiments (Dowe and McMillan, 2008). While the fermentation tests are ongoing, liquid samples were taken within specified intervals (at least once a day), the last samples being taken right after the fermentation test is over. These liquid samples shall be analysed for ethanol content (as well as for unfermented monomeric sugars therein) to determine the extent of ethanol production resulting from the fermentation tests. Based on the analytical results, the ethanol yield shall be determined using the following equation (3.3):

$$\%\,Yield\ of\ Ethanol = 100 * \frac{\boldsymbol{EtOH\ Conc\ at\ the\ end\ of\ Fermentation}}{(\mathbf{0.51})*(\mathbf{1.111})*\boldsymbol{F}*\boldsymbol{CDB}} \quad \text{..... (3.3)}$$

where:

F = Cellulose fraction of dry biomass (g/g)

CDB = Dry biomass concentration at the beginning of the fermentation (g/L)

0.51 = Conversion factor for glucose to ethanol based on stoichiometric values

1.111 = Converts cellulose to equivalent glucose

EtOH Conc. = Ethanol concentration in the fermentation liquid sample

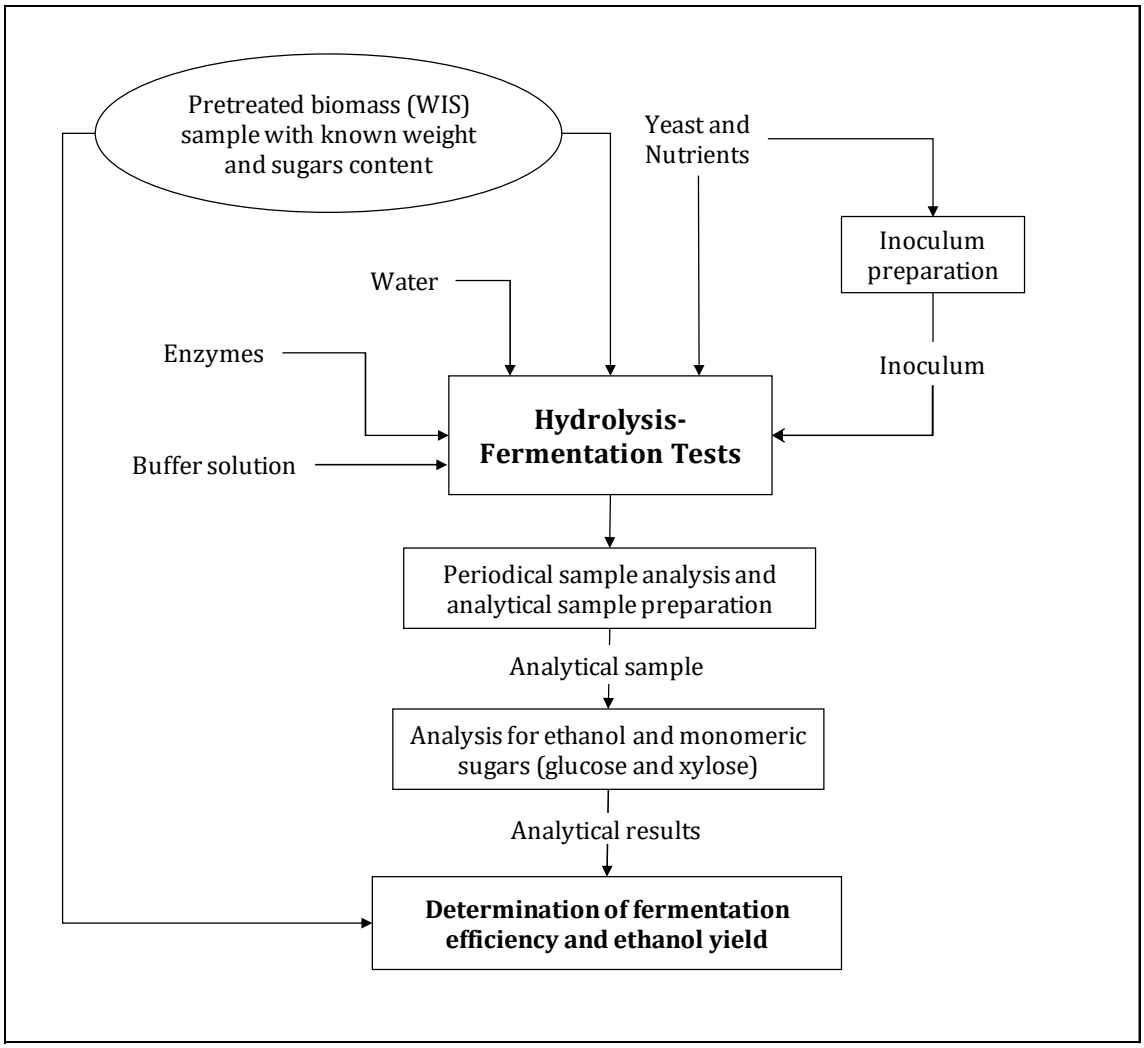

Fig 3.5. Flow diagram for hydrolysis-fermentation tests and steps towards determining ethanol production yield and fermentation efficiency

3.2.4 Materials and methods

Material and methods as required for the present experimental work were mainly adopted from the respective NREL protocols which were developed and fit enough for the intended experimental purpose. List of these NREL protocols which form the basis for the 'Material and Methods' sections of the experiments here are shown in Table 3.1. Unless otherwise mentioned, these protocols were adopted where found rightly applicable.

3.2.4.1 E*xperimental factors, levels and responses*

Factors influencing the extraction of hemicelluloses from lignocellulosic biomass, the enzymatic digestibility of pretreated solids as well as the potential cellulosic ethanol yield have been identified based on relevant extant works (see Sections 2.3 and 2.4 of the preceding chapter). Accordingly, biomass pretreatment approaches considered for hemicellulose extraction purpose (alkaline, pressurized liquid hot water and steam explosion methods), three factors, namely: pretreatment temperature, retention time and loading ratios (alkali-to-biomass and/or water-to-biomass) were taken into consideration for the experimental study. The response parameters influenced by these factors were primarily hemicellulose extraction yield, enzymatic cellulose digestibility and, to some extent, ethanol yield under selected pretreatment conditions. Experiments were statistically designed (using statistical softwares like DESIGN EXPERT and STATITICA) based on the Central Composite Design (CCD) method. Main experimental tests were accordingly carried out in five factorial levels, each test being run in duplicates. Optimization of extraction-pretreatment conditions for enhanced hemicellulose extraction yield and cellulose digestibility were also carried out using Response Surface Methodology, RSM (Bezerra et al., 2008; Silva et al., 2007; Myers et al., 2004).

Table 3.1 List of NREL protocols referred to in carrying out Experimental Works

No.	Description of NREL Laboratory Analytical Procedure (LAP)	Protocol referred to	Intended application of the experimental protocol	References
1	Preparation of Samples for Compositional Analysis	NREL/TP-510-42620	Characterization of feedstock and pretreated solid fractions	Hames et al., (2008)
2	Determination of Extractives in Biomass	NREL/TP-510-42619	Feedstock Characterization	Sluiter et al., (2008), (a)
3	Detemination of Structural Carbohydrates and Lingnin in Biomass	NREL/TP-510-42618	Characterization of raw feedstock and pretreated solids	Sluiter et al., (2012)
4	Determination of Total Solids in Biomass and Total Dissolved Solids in Liquid Process Samples	NREL/TP-510-42621	Characterization of biomass; pretreated solids and liquid fractions with biomass contents	Sluiter et al., (2008), (b)
5	Determination of Ash in Biomass	NREL/TP-510-42622	Characterization of feedstock and pretreated solid residues	Sluiter et al., (2008), (c)
6	Determination of Sugars, Byproducts, and Degradation Products in Liquid Fraction Process Samples	NREL/TP-510-42623	To characterize liquid fractions with hemicellulose extracts	Sluiter et al., (2008), (d)
7	Determination of Insoluble Solids in Pretreated Biomass Material	NREL/TP-510-42627	To characterize pretreated biomass	Sluiter et al., (2008), (e)
8	Measurement of Cellulase Activities	NREL/TP-510-42628	Enzymatic Digestibility tests on cellulose-rich pretreated residue	Adney and Baker (2008)
9	Enzymatic Saccharification of Lignocellulosic Material	NREL/TP-510-42629		Selig et al., (2008)
10	SSF Experimental Protocols — Lignocellulosic Biomass Hydrolysis and Fermentation	NREL/TP-510-42630	For the SSF tests on pretreated solid samples	Dowe and McMillan (2008)

3.2.4.2 Analysis and interpretation of experimental data

Analysis of experimental data were carried out using statistical software such as STATISTICA, DESIGN EXPERT and, of course, MICROSOFT EXCEL. Appropriate statistical tools were deployed in the design of experiments (DOE); optimization of input parameters towards acceptable values of responses (output parameters) through Response Surface Methodology, graphical presentation of results, and generating statistical parameters which bear important information on the cause-and-effect relationship between the factors (controlled variables being investigated for their effect) and response parameters (dependent variables on which the effect of the factors is studied). Statistical analysis of experimental data were also applied in establishing regressed mathematical model which depicts the quantitative relationship between the response and factorial variables under consideration. Furthermore, statistical methods such as ANOVA and Pareto chart analysis were carried out to determine the statistical significance of effects from each factor or combined effect from multiple factors thereby showing which factor has the most (or least) significant effect on the output parameter of interest (Zhong and Wang, 2010; Ye and Jiang, 2011).

3.3. PROCESS SYNTHESIS AND DESIGN BASIS

The process synthesis involves identification of different biorefinery scenarios which are mapped out in a way that facilitates the techno-economic assessment of a lignocellulosic biorefinery for an integrated production of biopolymeric hemicelluloses (xylan biopolymers), bioethanol and electricity from selected lignocellulosic feedstock (SCT and/or AW) via selected biomass fractionation approaches (MAPLHW and/or ASEPT). This would essentially entail appropriate sequencing of unit operations and/or processes for the co-production of xylan biopolymers and cellulosic ethanol. In other words, each biorefinery process needs to be clearly depicted by an appropriate process

flow-sheet where the required unit operations and processes are put together and interconnected by flow streams (Holm-Nielsen and Ehimen, 2014; Giuliano et al., 2015; Chaturvedi et al., 2020). The design basis for each synthesized biorefinery process shall be a well-defined scenario having its own distinguishing features, and aspects. This scenario-based process design shall be approached with the aim of pinpointing how the dynamic behaviour of the envisaged biorefinery system would be influenced by the very introduction of the hemicellulose extraction step. Process scenarios were, therefore, developed in such a way that comparative assessment among the respective process variations would provide a better insight as to how the envisaged biorefinery system would behave with and without the co-production of xylan biopolymers. Once biorefinery processes are synthesized in a conceptually sound manner, different process configurations may have to be developed depending on the specific purpose, design and operational requirements of the biorefinery envisaged at industrial level (Giuliano et al., 2015; Julio et al., 2017; Chaturvedi et al., 2020). To that end, primary and secondary technical data required for process specification purpose shall either be experimentally generated or collected from relevant sources. The nature of primary data required for the purpose of process modelling dictates what the experimental data should look like; or, vice versa. Secondary data shall be collected from relevant literature and other sources.

3.4. MATERIAL AND ENERGY BALANCES, EQUIPMENT SIZING AND COSTING

Material and energy balances closed around the overall biorefinery and/or major unit operations form the basis for any intended economic and environmental assessments of an industrial-scale project (Peters et al., 2003; Perry, 2008). In this respect, major process segments falling inside the battery limit (ISBL) of the envisaged biorefinery were first identified, namely: feedstock preparation, biomass pretreatment, hemicellulose extraction and recovery of xylan biopolymers, ethanol production and recovery, biosolids

recovery, wastewater treatment and co-generation plants (see Fig 1.1, Chapter 1). Detailed process flow diagrams encompassing major ISBL capital items were developed with identified process streams flowing in/out of the major unit operations therein. Rigorous mass balance calculations were carried out for the overall biorefinery as well as around major processing units therein; results thereof are presented in Table B-1.1 and Table-B-1.2 under Appendix B. Process parameters required for the purpose of closing mass balances were based on primary experimental data as generated in a previous study by Mihiretu et al., (2019) and secondary data from extant works (mainly NREL reports such as Aden et al., 2002; Humbird et al., 2011). A summary of process parameters are presented in Table B.1-3, Appendix B.

The immediate purpose of mass balance results was in the sizing and specification of major capital items within the ISBL boundary. Major process equipment are accordingly sized to appropriate capacity levels which, along with the respective (purchased/installed) equipment costs formed the basis for estimating the total capital investment (TCI) required for the envisaged biorefinery (Peters et al., 2003; Humbird et al., 2011; Perry, 2008; Chaturvedi et al., 2020). Equipment cost data required for capital items are collected from existing literature (e.g. relevant NREL technical reports such as NREL/TP-510-32438 and NREL/TP-5100-47764 (Humbird et al., 2011; Kazi et al., 2010; Aden et al., 2002) and/or other secondary sources (such as equipment suppliers/vendors – direct or indirect). Cost variations that may arise with different equipment sizes were adjusted using cost-capacity relationships, equation (3.4).

$$C2 = C1 * \left(\frac{S2}{S1}\right) \wedge n \quad \text{----------} \quad (3.4)$$

Where, C1 = cost of equipment at capacity S1; C2 = cost of equipment at capacity S2; and,
n = exponent varying from 0.4 to 0.9 depending on the equipment type

Equipment cost variations that may arise from different years, base year (=> Year-1) vs. actual year of interest (Year-2), shall be adjusted using cost indexes such as "Chemical Engineering Cost Index". All costs were adjusted to year 2019 following the equation 3.5.

$$Cost\ in\ Year2 = Cost\ in\ Year\ 1 * \left(\frac{Cost\ Index\ in\ Year\ 2}{Cost\ Index\ in\ year\ 1}\right) \quad \text{---------- (3.5)}$$

With respect to energy balances, the envisaged biorefinery shall be assumed self-sufficient in meeting its energy requirement (electricity and steam) without any need for fossil-derived fuels, but just biogenic carbon primarily derived from the lignocellulosic feedstock under consideration, i.e. sugarcane harvesting residues (SCT). This assumption essentially implies that portion of the raw feedstock (SCT) initially fed to the biorefinery, but not consumed towards the main product (i.e. bioethanol), nor to the main co-product (i.e. xylan biopolymers), shall serve as primary fuel source for the co-generation plant of the biorefinery. That would mean, if steam and electricity co-generated from this portion of the raw feedstock fall short of the energy requirement of the biorefinery, then additional raw biomass, just enough to allow the biorefinery energy demand be met, shall be co-fed to the CHP plant. If, on the other hand, the energy (electricity, in particular) generated at the CHP plant is more than the amount required by the biorefinery, then the excess electricity shall be considered as an additional co-product from this energy 'self-sufficient' biorefinery. In either case, the CHP plant is to be designed in such a way that it can convert any biogenic carbon (biomass-derived fuel) fed to it into electricity and steam: basically to meet the energy demand of the biorefinery itself; and, when in surplus, to avail the excess amount to the external grid.

Closing the energy balances around the major processing segments of the biorefinery in a manner where the overall biorefinery would be energy self-sufficient requires: (I) determination of the amount of biogenic carbon recovered from biorefinery

streams and availed to the co-gen plant (determined from mass balance results); (II) determination of the amount of electricity and steam that can be produced from this biomass-derived feed (determined based on the carbon/energy content of the biomass-derived fuel input and the conversion efficiencies at the biomass combustion (combustor), steam generation (boiler) and power generation (turbine) stages of the CHP plant; (III) estimation of the energy demand (electricity and steam) for the biorefinery; and (IV) determination of whether the energy demand of the biorefinery are met based solely on the biogenic carbon derived from the initial raw biomass fed to the biorefinery.

For the present techno-economic and environmental assessment purpose, two steps are followed in closing the energy balances around major production segments of the biorefinery. Firstly, the energy requirement for the production and recovery of bioethanol (which is the main end-product under all three scenarios: MCS, BCS and ICS) shall be estimated based on mass balance results and data from existing literature (Aden et al., 2002; Kazi et al., 2009; and Leibbrandt et al., 2010) which deployed similar process configurations, as in the present biorefinery, for the production of lignocellulosic ethanol and electricity. And secondly, the energy requirement for recovery of xylan biopolymers (the main co-product under the main-case scenario) shall be separately estimated based on available secondary data and mass balance results. In the latter case, the energy demand for major processing steps involved in the purification, concentration and recovery of xylan biopolymers (i.e. cascade of microfiltration and ultrafiltration units, ethanol-based anti-solvent precipitation unit, ethanol recovery plant, and vacuum drying unit to dry the precipitated xylan biopolymers) shall be estimated based on relevant data from literature and other secondary sources (equipment suppliers website and catalogues). The overall energy requirement under all scenarios shall be put in balance to the energy generated at the CHP plant.

3.5. PROCESS ECONOMICS

3.5.1 ESTIMATION OF TOTAL CAPITAL INVESTMENT AND OPERATING EXPENSES

The envisaged biorefinery which would be developed based on the preferred biomass pretreatment method, i.e. alkalinized steam explosion pretreatment, and feedstock type, i.e. sugarcane harvesting residues, was evaluated for its techno-economic viability following established methodologies applicable thereof (Aden et al., 2002; Peters et al., 2003; Perry, 2008; Humbird et al., 2011; Julio et al., 2017; Chaturvedi et al., 2020). As part of the economic assessment, estimation of total capital investment (TCI), annual operating costs (AOC) and project profitability analysis were carried out. The overall approach and steps followed for estimating TCI are shown in Table 3.2. Accordingly, the TCI will be composed of fixed capital investment (FCI) and working capital (WC); the former is again broken down into direct and indirect capital costs. Capital cost estimation was made using 'factorial/factored method' where installed costs for major capital items were first determined and costs for other 'non-major' capital items are estimated based on overall (combined) cost of major capital items, often referred to as Inside battery-limit (ISBL) costs, multiplied by pre-specified factors (Aden et al., 2002; Peters et al., (2003); Perry, 2008; Humbird et al., (2011). All costs estimates were made in terms of USD with 2019 as the currency year. Estimation of annual operating costs (AOC) for the envisaged biorefinery was carried out following well-established methods (Peters et al., 2003; Perry, 2008; Ereev and Patel, 2012; Giuliano et al., 2015; Lindorfer et al., 2019). Steps followed in the estimation of AOC are shown in Table 3.3 with major cost items (fixed, variable and other operating expenses). Fixed operating costs include that for maintenance, labour, capital charges (depreciation), local taxes and insurance. Major variable costs include costs for feedstock, non-feedstock materials, costs for utilities and miscellaneous operating materials. The fixed and variable costs together form direct operating costs

(DOC). Indirect operating costs (IOC) include general overheads, R&D expenditures, sales expenses and reserves. Total AOC shall be the sum of DOC and IOC.

Table 3.2 Approach for the estimation of Total Capital Investment (TCI)

Estimation of Total Capital Investment (TCI) [= FCI and Working Capital (WC)]	
Fixed capital Investment (FCI) is comprised of (I) Direct and (II) Indirect Costs	
(I)	**Direct Capital Costs**
	(a) Major Capital Items, Process plants (Inside battery-limits (ISBL) costs)
1	Biomass pretreatment plant
2	Xylan Biopolymers Recovery Plant
3	Ethanol Production and recovery plant
4	Solids recovery and co-generation plant
[5]	**ISBL direct costs = SUM [(1) + (2) + (3) + (4)]**
	(b) Non-process capital items (Outside battery-limits (OSBL) costs)
6	Storage and handling (Est. = 2 to 4 % of [5])
7	Waste treatment and disposal (Est.= 15% [5])
8	Site preparation and yard improvement (Est.= 5 to 10 % of [5])
9	Buildings and structures (Est.= 20 to 50 % [5])
10	Service facilities (Est.= 5 to 20% of [5])
11	Land (Est.= 1 % of [5])
[12]	**OSBL direct costs = SUM [(6) + (7) + (8) + (9) + (10) + (11)]**
[13]	**Total Direct Costs (TDC) = [5] + [12]**
(II)	**Indirect Costs**
14	Engineering and supervision [= 10 to 20 % TDC]
15	Construction expenses and contractors' fee[= 5 to 10 % of TDC]
16	Plant start-up expenses [Est.= 5 % of TDC]
17	Legal expenses[Est.= 1 to 2 % of TDC]
18	Contingency [Est. = 5 to 15% FCI; take 10 % of TDC [13]]
19	Other indirect costs [Est.= 5 to 10% of TDC]
[20]	**Total Indirect Costs (TIC) = SUM [(14) + (15) + (16) + (17) + (18) + (19)]**
(III)	**Fixed Capital Investment (FCI) = TDC + TIC = [13] + [20]**
(IV)	**Working Capital (WC) = 5 % * FCI**
(V)	**Total Capital Investment (TCI) = FCI + WC = (III) + (IV)**

Table 3.3 Approach for the estimation of Total Operating Costs (TOC/OPEX)

Estimation of Total Operating Costs (OPEX) (Annual basis => 6500 hrs/year, i.e. ~ 75% on time)
(I) Fixed Operating Costs (F-Opex) 1 Maintenance and Repair costs (Est. = 5 - 10% FCI) 2 Operating labour, Labour cost (to be determined based on manning estimates) 3 Laboratory costs (est. =10-20% of operating labour (OpLa)) 4 Supervision (est. = 10-20% OpLa) 5 Plant overheads (Est. = 30 to 50% of OpLa) 6 Depreciation costs (Capital charges) (Est. = 5 to 10 % FCI) 7 Local Taxes (Est. = 2 to 3% FCI) 8 Licence fees and royalities (Est. = 1 to 2 % FCI) **(A) Sub-total (F-Opex) Costs = SUM (1 through 8)**
(II) Variable Operating Costs (V-Opex) 9 Raw Materials (to be determined from flow sheets) 10 Utilities (to be determined from flow sheets) 11 Miscellaneous operating materials [Est. = 5 to 10% of Maintenance costs] 12 Shipping and packaging [can be considered 'negligible'] **(B) Sub-total (V-Opex) Costs = SUM (9 through 12)**
Direct Operating Costs (DOC) = Fixed + Variables = (A) + (B)
(III) Other Operating Expenses 13 General overheads 14 R & D expenditures 15 Sales Expenses (marketting and distribution) 16 Reserves **(C) Sub-total (other Opex) costs= 20 to 30 % DOC = 20 to 30% [(A) + (B)]**
(IV) Annual Total Operating Costs = (A) + (B) + (C)

3.5.2. ECONOMIC FEASIBILITY ANALYSIS

With estimated values of the total capital investment (TCI) and annual operating expenses (AOC), the economic return of the biorefinery project can be quantitatively measured. The discounted cash flow (DCF) method was applied to evaluate the profitability of the biorefinery once it goes operational and starts to generate revenues. Parameters required to this end are discount rate, corporate income tax, plant life, start-up time and method of depreciation (Aden et al., 2002; Perry, 2008; Humbird et al., 2011; Ereev and Patel, 2012). This method takes into account all yearly net (after-tax) cash flows which are then discounted (compounded) to a reference time of interest ('time zero'). The discounted cash flow rate of return (DCFRR), which is the interest rate at which the sum of the present value of all investment items equals the sum of the present values of each year's net cash flows. In other words, it is the discount rate 'i' at which the project breaks even, i.e. it is where the project's net present value (NPV) becomes zero. The DCFRR is determined – either graphically or iterating by trial-and-error – as that value of 'i" which validates the following equation 6.3.

$$\text{NPV} = \sum_{n=0}^{n=t} \frac{CFn}{(1+i)^n} = 0 \quad \text{---------- (6.3)}$$

As part of the economic analysis of the envisaged biorefinery, minimum ethanol selling price (MESP) shall be determined under different process scenarios identified for this purpose. The minimum hemicelluloses selling price (MHSP) shall also be determined for the actual biorefinery scenario where the co-production of xylan biopolymers takes place with bioethanol and electricity. As the minimum selling prices (MSP) are considered good indicator of how worth producing the targeted products, comparison of the MSP results shall be made among identified biorefinery scenarios as well as against prices reported in extant works. Moreover, sensitivity analysis shall also be carried out on of

main biorefinery products (i.e. bioethanol and/or xylan biopolymers) to see how their MSP is influenced when certain input parameters (such as feedstock price, production capacity, FCI, AOC, discount rate) are varied within certain ranges. Unit production cost is obtained by dividing the annual operating costs by the annual production rate.

3.6. GREENHOUSE GAS EMISSIONS REDUCTION POTENTIAL

Modern biorefineries should take due consideration of all possible environmental implication associated with their development; in fact, environmental sustainability is one critical requirement for their advancement (Wellisch et al., 2010; Junqueira et al., 2017; Mandegari et al., 2017; Hassan et al., 2019). Along this line, the present study intends to evaluate the envisaged biorefinery from climate change mitigation points of view in general, and in terms of its potential towards of greenhouse gases (GHG) emissions reduction, in particular. The GHG Emissions Reduction Potential (GHG-ERP), aka GHG emissions savings, resulting from the lignocellulosic biorefinery (producing bioethanol, xylan biopolymers and electricity) shall be estimated based on the apparent (indirect) reduction of GHG emissions that can result from it in comparison to fossil-fuel baseline (Falano et al., 2014; Junqueira et al., 2017). To this end, the RSB GHG Calculation Methodology (v2.13) has been considered for the purpose of estimating the potential GHG emissions savings under the actual biorefinery scenario (MCS) producing bioethanol, xylan biopolymers and electricity; and under the benchmark process scenarios (BCS & ICS) producing bioethanol and electricity based on sugarcane harvesting residues as feedstock of choice. The basic steps and sequence involved under this standardized methodology for life cycle assessment (LCA) of biofuels as well as calculation details involved therein are to be found in the reference document: 'RSB-STD-01-003-01-ver.2.3-RSB GHG Calculation Methodology'.

CHAPTER FOUR: SINGLE-STEP MICROWAVE-ASSISTED HOT WATER EXTRACTION OF HEMICELLULOSES FROM SELECTED LIGNOCELLULOSIC MATERIALS – A BIOREFINERY APPROACH

Chapter published in 'Bioresource Technology' 241 (2017) 669-680, Impact Factor: 7.5

Article Title: Single-Step microwave-assisted hot water extraction of hemicelluloses from selected lignocellulosic materials – a biorefinery approach

Authors: Gezahegn T. Mihiretu, Malin Brodin, Annie F. Chimphango, Karin Øyaas, Bård H. Hoff, and Johann F. Görgens

Objective of Dissertation and Summary of findings of this Chapter

This chapter addresses the first four research objectives through a full-fledged experimental investigation on the effects of microwave-induced pressurized hot water conditions on the extraction of hemicelluloses from two lignocellulosic materials, namely: sugarcane trash (SCT) and aspenwood sawdust (AW). The co-production of hemicellulosic biopolymers with cellulosic ethanol in a multi-product biorefinery setup inherently demands optimal pretreatment conditions with trade-offs between yield and quality of the respective end-products be established. Temperatures from 170-200 °C for AW; and 165-195 °C for SCT; and, a retention time of 8 to 22 minutes for both feedstock types, were selected for statistical optimization purpose. Hemicellulose extraction yields as well as enzymatic digestibility of the resulting solid residues were determined under different set of statistically defined test points.

The study results showed that xylan extraction yield and cellulose digestibility were strongly influenced by temperature. The effect of retention time on xylan yield was significant in the case of AW; but not so for SCT. Under tested experimental conditions, about two-third and half of the original xylan were extracted from AW and SCT respectively. Cellulose digestibilities for AW and SCT were 78 and 74 % respectively. Furthermore, for both AW and SCT little formation of monomeric xylose was observed in the extraction hydrolysates, this suggested that the xylan extracts were predominantly non-monomeric (oligomeric/polymeric). Thus, biomass pretreatment under microwave-induced liquid hot water conditions can be regarded as a viable biorefinery approach for extraction of xylan from lignocellulosic solids with enhanced cellulose digestibility.

Candidate Declaration:

With regard to Chapter 4, page numbers 73-106 of this dissertation, the nature and scope of the candidate's contributions were as follows:

Name of Contribution	Extent of Contribution (%)
Experimental Planning	80
Executing Experiments	100
Interpretation of experimental results	75
Writing of the Chapter	100

The following co-authors have contributed to Chapter 4, page numbers of 73-106 of this dissertation:

Name	Email Address	Name of Contribution	Extent of Contribution (%)
Malin Brodin	malin.brodin@rise-pfi.no	Reviewing of chapter Experimental Planning Interpretation of results Co-ordinating collaboration	10 10 5 40
Annie F. Chimphango	achimpha@sun.ac.za	Reviewing of chapter Interpretation of results Co-ordinating collaboration	40 10 20
Karin Øyaas	Karin.oyass@pfi-rise.no	Reviewing of chapter Co-ordinating collaboration	5 20
Bård H. Hoff	Bard.h.hoff@ntnu.no	Reviewing of chapter Experimental planning	5 10
Johann F. Görgens	jgorgens@sun.ac.za	Reviewing of chapter Interpretation of results Co-ordinating collaboration	40 10 20

Signature of candidate: _____ Date: _____

Declaration by co-authors:

All authors have read and approved the final manuscript and hereby confirm that:

1. The declaration above accurately reflects the nature and extent of contributions by the candidate and co-authors to Chapter 4, page numbers 73-106 of this dissertation,
2. no other authors contributed to chapter 4, page numbers 73-106 of this dissertation, besides those specified above, and
3. Potential conflicts of interest have been revealed to all interested parties and that necessary arrangements have been made to use the material in chapter 4, page numbers 73-106 of this dissertation.

Single-Step Microwave-assisted Hot Water Extraction of Hemicelluloses from selected Lignocellulosic Materials – a Biorefinery Approach

Gezahegn T. Mihiretu[a,b*], Malin Brodin[b], Annie F. Chimphango[a], Karin Øyaas[b], Bård H. Hoff[c], Johann F. Görgens[a]

a: Stellenbosch University, Process Engineering Department, Stellenbosch 7602, South Africa
b: Paper and Fibre Research Institute (PFI), Høgskoleringen 6B, NO-7491 Trondheim, Norway
c: Norwegian University of Science and Technology (NTNU), Department of Chemistry, Høgskoleringen 5, NO-7491 Trondheim, Norway

ABSTRACT

The viability of single-step microwave-induced pressurized hot water conditions for co-production of xylan-based biopolymers and bioethanol from aspenwood sawdust and sugarcane trash was investigated. Extraction of hemicelluloses was conducted using microwave-assisted pressurized hot water system. The effects of temperature and time on extraction yield and enzymatic digestibility of resulting solids were determined. Temperatures between 170-200 °C for aspenwood and 165-195 °C for sugarcane trash; retention times between 8-22 minutes for both feedstocks, were selected for optimization purpose. Maximum xylan extraction yields of 66 and 50 %, and highest cellulose digestibilities of 78 and 74 %, were attained for aspenwood and sugarcane trash respectively. Monomeric xylose yields for both feedstocks were below 7 %, showing that the xylan extracts were predominantly in non-monomeric form. Thus, single-step microwave-assisted hot water method is viable biorefinery approach to extract xylan from lignocelluloses while rendering the solid residues sufficiently digestible for ethanol production.

KEYWORDS: Lignocellulosic Biorefinery, Hemicellulose Extraction, Aspenwood, Sugarcane Trash, Microwave-assisted Pressurized Hot Water Method

*** Corresponding Author:** Process Engineering Department, Stellenbosch University, Stellenbosch 7602, South Africa; Tel: +27-641950543
E-mail: 18935001@sun.ac.za (Mihiretu, G.T.)
(Or, gezahegn_teklu@yahoo.com)

4.1. INTRODUCTION

Hemicelluloses, notably xylan, are the second most abundant carbohydrate polymers in lignocellulosic biomasses such as hardwoods and agricultural residues. Biopolymers in the form of xylan-rich hemicelluloses have potential applications as gels, films, adhesives, coatings, stabilizing and viscosity-enhancing agents in the food, biomedical and pharmaceutical industries (Ebringerova, 2006; Canilha et al., 2013). Due to their ability to self-assemble in spatially cross-linked manner, remarkable hydrophilic property and swelling capacity, hemicellulosic biopolymers have become of special interest in the development of biocompatible hydrogels for applications in wound dressing and advanced drug delivery systems (Silva et al., 2011; Ebringerova, 2006). Recent studies on xylan-based hydrogels have also shown the possibility of modifying and further synthesizing them into newly functionalized biomaterials for innovative applications in nanomedicine (Pahimanolis et. al., 2014; Chimphango et. al., 2012) and tissue engineering (Venugopal et al., 2014; Tan and Marra, 2010).

Despite their potential applications, the path towards large scale production of high-value hemicellulose-based products largely remains underexplored (Spiridon and Popa, 2008). One viable approach in realizing their ultimate economic value is the development of a lignocellulosic biorefinery system, whereby hemicellulosic biopolymers are co-produced with cellulosic ethanol (Chantal et al., 2012; Ragauskas et al., 2006). Such co-production of multiple biorefinery products from single biomass may require: (a) that due consideration of the complex and recalcitrant nature of lignocelluloses be made in view of optimally fractionating the initial biomass to convert its major components into intended end-products, and (b) that selection of suitable pretreatment method and conditions thereof be made in view of attaining acceptable yields and quality for end-products to be co-produced under a biorefinery setup.

There are several pretreatment techniques to enhance the enzymatic digestibility of lignocellulosic biomass for ethanol production, but not all of them are suitable for the extraction of hemicelluloses for application as biopolymers/biomaterials (Trajano and Wyman, 2013; Mosier 2013, Ramirez et al., 2013). Hemicelluloses are thermally so labile that their extraction in oligomeric and polymeric forms typically requires a milder set of pretreatment conditions than those required for enhanced cellulose digestibility (Bond et al., 2013; Tutt et al, 2012). Increasing the severity of pretreatment conditions may favour enhanced cellulose digestibility as well as increased removal of hemicelluloses from the lignocellulosic matrix. However, with increased severity, there is increased decomposition of hemicelluloses, which in turn leads to increased formation of degradation products that have inhibitory effects on the downstream bio-catalytic action of enzymes and fermentation yeasts (Yang et al., 2011; Cardona et al., 2010). Therefore, the development of a biorefinery system meant for co-production of hemicellulosic biopolymers and cellulosic ethanol needs to take into account the potential operational challenges that primarily prevail at the pretreatment stage. Such challenges become even more evident when it comes to defining a single pretreatment step that can both remove hemicelluloses in oligo- and polymeric form and produce enzymatically digestible solids rich in cellulose (Bond et al., 2013; Trajano and Wyman, 2013).

A number of studies have shown that the extraction of hemicelluloses in their oligo- and polymeric form can be realized under pressurized hot water conditions (Aachary and Prapulla, 2011; Teo et al., 2010). The phenomena of auto-ionization of water at elevated temperatures and pressures leads to apparent formation of hydronium (H_3O^+) and hydroxyl (OH^-) ions thereby rendering water to behave like polar and apolar solvent (Mosier 2013; Chemat et al., 2012). These properties of subcritical water are used to deconstruct the lignocellulosic matrix and remove extractible components such as

hemicelluloses (Mosier, 2013; Chemat et al., 2012). From cellulosic ethanol production point of view, however, liquid hot water method with conventional forms of heating usually requires higher temperatures and/or longer retention times which may result in increased decomposition of polymeric extracts of hemicelluloses as well as formation of degradation products thereof (Yan et al., 2016; Yang et al., 2011; Cardona et al., 2010).

Owing to its remarkable dielectric properties and high loss tangent (tan δ), water can be effectively heated up through microwave irradiation (Barba and d'Amore, 2012; Tsubaki et al., 2016). Such unique ability of microwaves to rapidly heat up water to highly elevated temperatures within shorter span of time can make it a potentially attractive source of energy for hydrothermal pretreatment of lignocellulosic biomass. The application of microwaves for the extraction of soluble components from a wide variety of plant biomass was discussed extensively in previous works (Tsubaki et al., 2016). Microwave-assisted hot water dissolution two hardwoods (Formosan sweet gum and mahogany) was mentioned in (Kuo et al., 2002), but the study was mainly on comparing hot water solubility of each wood under microwave and conventional heating modes. The extraction of water-soluble hemicelluloses from flax shive (Jacobs et al., 2003), from spruce and aspen wood (Jacobs et al., 2002; Teleman et al., 2000) using hydrothermal microwave treatment were mentioned, but these analytical studies were mainly focused on the isolation and characterization of the xylan and xylo-oligomers extracts obtained under specific condition. Microwave-assisted extraction of xylan from birch wood under low-temperature alkaline conditions was reported in Panthapulakkal et al., (2013); In Gulbrandsen et al., (2015), the extraction of hemicelluloses from sugarcane bagasse was carried out under microwave irradiation to study the effects of temperature and time on sugar yield and molar mass distribution. The effect of microwave-assisted hot water

pretreatment on digestibility of sugarcane bagasse and rice straw were reported in (Binod et al., 2012) and (Ma et al., 2009) respectively.

Apparently, the technological routes for hemicellulose extraction and cellulosic ethanol production from lignocellulosic biomass have been considered independently. There is as well a clear gap in defining a set of optimal process conditions for single-step extraction of hemicelluloses and digestible solids in a biorefinery setup. Furthermore, for the two lignocellulosic materials selected for this study, no prior study has approached their pretreatment under microwave-assisted hot water conditions with the goal of co-producing hemicellulosic biopolymers and cellulosic ethanol under a biorefinery concept.

The aim of this study was to explore and establish feasible solution space for single-step microwave-assisted pressurized hot water extraction of hemicelluloses from two selected lignocellulosic materials, while simultaneously enhancing the enzymatic digestibility of the solid residue. More specifically, the effects of microwave-induced temperature and retention time on xylan extraction and enzymatic digestibility of the solid residue were investigated for sugarcane trash and aspenwood sawdust. In addition, the extent of delignification, formation of monomeric xylose as well as degradation products at all tested conditions were determined and discussed in light of the study context here.

4.2. MATERIALS AND METHODS

4.2.1. Materials

Sugarcane (*Saccharum officinarum*) trash and aspen (*Populus tremula*) sawdust were used in this study; the former being of South African and the latter of Norwegian origin. Chemicals such as sulphuric acid, potassium hydroxide, sodium hydroxide, citric acid monohydrate, potassium sodium tartrate, 3,5-dinitrosalicyclic acid, phenol, sodium

azide and bovine serum albumin as used in this experimental study were of laboratory grade. Ethanol (95% v/v) was used in the determination of ethanol extractives in raw samples. The enzymes Cellic CTec2 and HTec2, both from Novozymes, were used for enzymatic hydrolysis tests. Glucose standard solutions for cellulase activity evaluation and xylose control solutions as used in acid-hydrolysis tests were prepared from standard-grade glucose and xylose respectively. Unless otherwise mentioned, de-ionized water was used for all test purposes.

4.2.2. Preparation and Characterization of Raw Materials

The sugarcane trash consisted primarily of semi-dried leaves and tops. It was further dried in open air to a moisture level of 8.3 % and shredded to smaller sizes (approx. 5 to 7 cm). To make the sugarcane trash is representative enough as locally-sourced feedstock; the shredded mass was spread on plastic sheet, split into two parts and mixed back manually. This was done twice before they are packed into plastic bags. The shredded sugarcane trash was further reduced in size using Schuttle Buffalo hammer mill fit with 2 mm screen. Likewise, aspenwood sawdust was air-dried to moisture content of 6.3 %, reduced in size using lab-scale knife mill fitted with 2 mm screen.

The resulting milled raw materials were fractioned using lab-scale sieve shaker. Those in the size range of 250 - 1000 μm were uniformly mixed and used for the preparation of the actual test samples. Representative samples from prepared raw materials were characterized for extractives, ash, structural sugars and lignin contents. Determination of extractives was carried out in duplicates based on the NREL two-step method, NREL/TP-510-42619 (Sluiter et al., 2008a). Ash content was determined as per the NREL protocol, NREL/TP-510-42622 (Sluiter et al., 2008b). Lignin contents (acid-soluble and –insoluble) as well as structural sugars were determined in accordance with the NREL two-stage method, NREL/TP-510-42618 (Sluiter et al., 2012).

4.2.3. Hemicellulose Extraction

The raw biomass meant for extraction test purpose was soaked in water overnight for about 18 h at a soaking loading ratio of 50 mL water per g dry biomass. The soaked material was vacuum filtered to remove the liquid and recover the solid residue. Moisture and dry matter contents of the wet solid residue was measured using Sartorius MA-40 automatic moisture analyser. The extraction feed was prepared by mixing about 3 g soaked wet residue (dry weight basis) and calculated amount of water in a PTFE-TFM (polytetrafluoroethylene, modified) liner in such a way that the loading ratio is 15 mL water per g dry biomass. The extraction of hemicelluloses was conducted under microwave-assisted pressurized hot water condition at varying combinations of temperature and holding time (see section 2.9) using Anton Paar Multiwave-3000 microwave system. This system was equipped with a sensor to control an accurate profile of temperature and pressure inside a reference vessel, an infrared (IR) sensor to monitor the temperature at the base of each extraction vessel, and an integrated cooling system. Microwave power of 1000 W, ramp-up time of 10 min and cooling time of 30 min were fixed for all extraction experiments. Following the completion of each extraction test, the slurry was transferred to a 100 mL bottle. The reactor liner was washed with 50 mL of water to recover solid residues and sugar extracts stuck on the inner wall. The wash water was poured into the bottle containing the extraction slurry. The slurry was vacuum filtered using Whatman filter paper to separate the liquid and solid fractions. The solid residue was repeatedly washed with additional 400 (± 25) mL water until the pH of the wash water became neutral. The volume of the liquid fraction and weight of the wet solid residue were recorded. The liquid fraction was stored in schott bottle and kept in refrigerator till required for subsequent hydrolysis tests. About 25 mL samples (2X) were taken from the fresh liquid fraction, syringe-filtered (0.22 μm pore size) into 30 mL plastic

bottles and kept in freezer till required for analysis. The wet solid residues were freeze-dried to about 95 % dry matter content using Heto PowerDry PL6000 freeze dryer and kept in plastic bags till required for subsequent hydrolysis tests (acid and enzymatic).

4.2.4. Enzymatic Hydrolysis

Saccharification experiments were conducted on freeze-dried solid samples as per the NREL Protocol NREL/TP-510-42629 (Selig et al., 2008). The tests were run in 20 mL scintillation vials at 2 % (w/w) substrate loading and 10 mL overall hydrolysis volume, i.e. about 0.21 g of solid sample was used per test. Added to each vialled solid sample were 5 mL of sodium citrate buffer (0.1 M, pH 4.9), 0.1 mL of 2 % sodium azide solution, 10 μL of Bovine Serum Albumin (BSA) and the balance with de-ionized water and finally the enzyme preparations. The enzyme combinations used were Cellic CTec2 and HTec2. The former (i.e. CTec2) was loaded at 15 FPU/g of substrate (dry weight basis) and the later (i.e. HTec2) was taken at 25 % (v/v) of CTec2. The enzymatic activity of CTec2 was determined in accordance with the protocol NREL/TP-510-42628 (Adney et al., 2008) and the estimated activity was around 150 (±10) FPU/mL. Enzymatic hydrolysis tests were carried out in an incubator set at 50 °C shaken at 150 rpm. After 72 h, the hydrolysis was terminated by putting the vials in boiling water for about 5 min and subsequently cooled in cold water. Separation of the slurry into liquid and solid fractions was carried out using vacuum filtration. The vials were subsequently washed with 10 mL of de-ionized water so as to wash out solid residue and liquid remaining therein. Samples were taken from the resulting liquid hydrolysate, syringe-filtered at 0.22 μm, bottled and kept in freezer till required for the intended analytical purposes. The enzymatic hydrolysis tests were run in duplicates.

4.2.5. Sugars Analysis

4.2.5.1. Sugars in Liquid Fraction

Hemicellulosic sugar extracts (xylose in particular) in liquid fractions were analysed based on the NREL two-stage acid hydrolysis method, NREL/TP-510-42623 (Sluiter et al., 2008c). At the second stage of acid-hydrolysis, control samples from 66.67 mM xylose solution were simultaneously acid-hydrolysed under the same autoclaved conditions. The xylose standard solution was prepared as suggested in the NREL protocol so as to account for the xylose loss from degradation. The acid-hydrolysis tests on actual samples as well as on samples from on xylose solution were conducted in duplicates. About 8 mL of the acid hydrolysate was taken for sugar analysis purpose. The pH of the analytical sample was adjusted in the range of pH 4 to pH 6 using 6 M potassium hydroxide and 1 M sulphuric acid solutions. The sample was subsequently filtered using syringe-filter with 0.22 μm pore-size and analysed by High Pressure Liquid Chromatography (HPLC) method using Biorad Aminex HPX-87H column (7.8x300 mm) with 5 mM sulphuric acid as a mobile phase. Column temperature was set at 65 °C. Samples were injected at a volume of 30 μL, eluted at a flowrate of 0.6 mL/min and detected with an RI-detector.

The amount of xylose extract in the liquid fraction was quantified based on the respective xylose concentration from HPLC analysis. The HPLC-read xylose concentration for the actual liquid samples was first adjusted for dilution and further corrected for xylose loses from degradation. The corrected xylose concentration was used to determine the overall amount of xylose extract in the liquid fraction, which in turn was used to determine the overall xylose yield. Furthermore, samples from un-hydrolysed liquid fractions were also directly HPLC-analysed so as to quantify monomeric xylose present therein. The amount of xylose that was in non-monomeric form was determined by

subtracting the amount of monomeric xylose from the overall xylose. The yield for xylose extracts was calculated against the original xylose in the initial raw sample.

4.2.5.2. Sugars in Solid Samples

The content of sugars such as glucose, xylose and arabinose in freeze-dried pretreated samples was determined as per the NREL two-stage acid hydrolysis method NREL/TP-510-42618 (Sluiter et al., 2012). The preparation of analytical samples as well as the HPLC setup for sugar analysis was the same as described under section 4.2.5.1. The concentration of sugars from the HPLC results was used to determine the composition of the raw and pretreated solids for such major structural sugars as glucose and xylose.

4.2.5.3. Sugars in Enzymatic Hydrolysates

The hydrolysate samples from enzymatic hydrolysis tests (section 4.2.4) were analysed for sugars (glucose and xylose) under the same HPLC setup as described in section 4.2.5.1. The HPLC results on the sugar concentrations were used to quantify the amount of enzymatically released sugars. The enzymatic sugar yields for glucose and xylose were calculated as the percentage of the respective sugar in the initial raw sample that was enzymatically released. Enzymatic sugar yield for glucose and xylose were also determined for raw (un-pretreated) samples of sugarcane trash and aspen wood.

4.2.6. Degradation Products in Liquid Fractions

The analytical samples prepared from extraction liquid fractions (section 4.2.3) were analysed for acetic acid, formic acid, furfural and HMF following the NREL method, NREL/TP-510-42623 (Sluiter et al., 2008c). Samples were analysed by similar HPLC setup as in 4.2.5.1 and as per the same NREL protocol.

4.2.7. Lignin Content

The content of lignin in the raw lignocellulosic materials as well as in pretreated solids was determined in accordance with the NREL protocol, NREL/TP-510-42618 (Sluiter et al., 2012). Acid-soluble lignin contents were determined based on absorbance readings taken at 205 nm on liquid samples against a background with de-ionized water. The analysis was conducted using UV-Vis Spectrophotometer (UV-1800, SCHMADZU).

4.2.8. Calculations

4.2.8.1 Structural sugars and lignin

Contents of major structural sugars (cellulose and xylan) and lignin (acid-soluble (ASL) and acid-insoluble (AIL)) in raw as well as pretreated solid samples were determined as per the respective NREL procedure (NREL/TP-510-42618; Sluiter et al., 2012) and were accordingly calculated using the following equations:

$$\text{Cellulose [\%]} = 100 * \frac{(0.90)*(\text{Concentration of Glucose [g/L]in LF})*(\text{Volume of LF})[\text{L}]}{\text{Weight of Initial Sample, ODW [g]}} \quad (1)$$

$$\text{Xylan [\%]} = 100 * \frac{(0.88)*(\text{Concentration of Xylose [g/L] in LF})*(\text{Volume of LF [L]})}{\text{Weight of Initial Sample, ODW [g]}}$$

$$\text{ASL [\%]} = 100 * \frac{(\textbf{UV abs})*(\textbf{Dilution Factor})*(\textbf{Volume of LF [L]})}{\boldsymbol{\varepsilon}\ [\textbf{L/g.cm}]*\textbf{Weight of Initial Sample, ODW [g]}*\textbf{Pathlength[cm]}} \quad (3)$$

$$\text{AIL [\%]} = 100 * \frac{W_{AIR}\,[g] - W_{ASH}\,[g]}{\text{Weight of Initial Sample,ODW [g]}} \quad (4)$$

where, LF=liquid fraction (filtrate); ODW= Oven-dried Weight; UVabs = absorbance reading for the sample from LF; ε= Extinction Coefficient; W_{AIR} =Weight of Acid Insoluble Residue; W_{ASH} =Weight of Acid Insoluble Ash

4.2.8.2 Xylan Extraction Yields (expressed as "Xylose Yields")

The overall extraction yield for xylose (Xo) [%w/w] (i.e. 'xylan' extracts both in monomeric and non-monomeric forms) as quantified in the respective liquid fraction (LF) was determined as follows:

$$\text{Xo [\%]} = 100 * \frac{\text{Amount of Overall Xylose in Liquid Fraction (LF)[g]}}{\text{Amount of Xylose in Initial Raw Sample [g]}} \qquad (5)$$

The Non-monomeric Xylose Yield (NM-XY=X_{nm}) [%w/w], i.e. the extraction yield for xylan that is in non-monomeric form, was determined as follows:

$$\text{Xnm[\%]} = 100 * \frac{\text{(Amount of Overall Xylose in LF)} - \text{(Amount of monomeric Xylose in LF)}}{\text{Amount of Xylose in Initial Raw Sample}} \qquad (6)$$

The monomeric xylose yield (X_m) [% w/w], i.e. the percentage of xylose in the liquid fraction (LF) that is in monomeric form was determined as follows:

$$X_m\ [\%] = 100*(1 - \frac{\text{Xnm}}{\text{Xo}}) \qquad (7)$$

4.2.8.3 Enzymatic sugar yield

Enzymatic hydrolysis yield for glucose and xylose were calculated using the following equations:

$$\text{Glucose Yield** [\%]} = 100* \frac{\text{Amount of enzymatically released glucose [g]}}{\text{Amount of glucose in initial unhydrloyzed sample [g]}} \qquad (8)$$

$$\text{Xylose Yield [\%]} = 100* \frac{\text{Amount of enzymatically released xylose [g]}}{\text{Amount of xylose in initial unhydrloyzed sample [g]}} \qquad (9)$$

N.B. Cellulose digestibility is quantitatively equivalent to the Enzymatic Hydrolysis Glucose Yield. It was determined as percentage of cellulose in the initial unhydrolyzed sample that was enzymatically digested. The amount of digested cellulose was itself determined by multiplying the amount of enzymatically released glucose by the anhydrous correction factor of 0.9.

4.2.8.4. Lignin Removal

The percentage of lignin that was removed as a result of pretreatment was determined as follows:

$$\text{Lignin Removal [\%]} = 100 * \frac{(\text{Lignin in Initial Sample})[\text{g}] - (\text{Lignin in Pretreated Sample})\ [\text{g}])}{\text{Lignin in Initial Sample, ODW [g]}}$$

4.2.9. Experimental Design

The design of experiments on hemicellulose extraction and enzymatic saccharification tests as well as statistical analysis of results thereof was carried out using Design-Expert 8.0.2. Experiments were designed based on central composite design (CCD) as a response surface methodology with temperature and retention time as the two main factors. Parametric values for these two variables were chosen based on preliminary test results (section 4.3.1). The minimum, central and maximum temperature values for aspenwood were respectively set at 175, 185 and 195 °C; similar temperature values for sugarcane trash were set at 170, 180 and 190 °C respectively. For both feedstocks, retention times of 10, 15 and 20 min were set as the minimum, central and maximum values respectively.

The response-factor relationship between major output (mainly, sugar yields) and input parameters was represented by a quadratic model taking the following form:

$$Y = B_0 + B_1*X_1 + B_2*X_2 + B_{12}*X_1*X_2 + B_{11}*X_1^2 + B_{22}*X_2^2 \text{ ------ (I)}$$

Where, Y [% w/w] is the output parameter (representing xylan extraction yield or enzymatic hydrolysis glucose yield); X_1 and X_2 are the independent parameters representing temperature [°C] and retention time [min] respectively; B_0 is the intercept yield value, B_1 and B_2 being the linear effects, B_{11} and B_{22} the quadratic effects from temperature and time respectively; and B_{12} indicating the interaction effect from the two variables. Values of these regression coefficients and their statistical significance as well as the R-Squared values were estimated using analysis of variance (ANOVA) and those model terms with high significance level (i.e. p-value below 0.05 or confidence interval above 95 %) were considered to fit in the regression model above. Besides the ANOVA, Pareto chart analysis was also carried out to ascertain the extent of the observed effect on sugar yields that was separately coming from either temperature or retention time. Contour plots for xylan extraction yields were also generated for each feedstock based on respective statistical models to portray the yield profiles over a wide range and combinations of temperature and time so as to examine how the yield patterns behave with increased severity of pretreatment conditions. Furthermore, for each feedstock, the correlation analysis between cellulose digestibility and degree of removal of hemicelluloses (expressed here as xylose yield), digestibility and lignin removal as well as between xylan extraction yield and degree of lignin removal was carried out.

4.3. RESULTS AND DISCUSSIONS

4.3.1. Selection of experimental set points

Two batches of preliminary tests were carried out on the extraction of hemicelluloses from selected lignocellulosic feedstock under microwave-induced pressurized hot water conditions. The aim was to identify reasonable ranges of values for temperature and retention time, for optimization using a central composite design as response surface methodology. The underlying reason for the design of main experiments (see section 4.2.9) was to establish the microwave-induced conditions where the extraction yield for hemicelluloses, xylan in particular, would be enhanced, while formation of monomeric sugars as well as degradation products thereof is minimized. The first batch was conducted at a fixed time (10 min) and three temperatures (165, 175 and 185 °C for sugarcane trash and 175, 185 and 200 °C for aspenwood) selected based on previous works on liquid hot water methods (Teo et al., 2010; Aachary and Prapulla, 2011; Sukhbaatar et al., 2014). The second batch tests were conducted based on the steepest ascent methodology to follow the direction of increments in the yields. Preliminary test results (data not shown here) showed that extraction yields for both feedstocks were predominantly influenced by temperature and, to a lesser extent, by retention time. For an extraction time of 10 min, the extraction yields for sugarcane trash and aspenwood were observed to increase steeply with an increase in temperature starting from 180 °C and 185 °C respectively. It was also observed that monomeric sugars and degradation products thereof could noticeably form at these same temperatures. These temperatures were thus chosen as centre-point values in designing main extraction tests. For the purpose of this experimental study, an extraction time of 15 min was selected as central value.

4.3.2. Effects of Temperature and Retention Time on the Extraction of Hemicellulose from selected Lignocellulosic Materials under Microwave-induced Liquid Hot Water Conditions

4.3.2.1. Effects on Xylan Extraction from Aspenwood

Results obtained on the extraction of xylan, the major hemicellulosic sugar in aspenwood, under different combinations of microwave-induced liquid hot water temperature and retention time are shown in Table 4.1. The xylan extraction yield (expressed hereinafter as xylose yield) was directly influenced by variations made in both extraction parameters. An increase in retention time from 10 to 20 min increased the xylose yield by less than 10 % for temperatures below 175 °C; by 12 to 40 % for temperatures from 175 to 185 °C; and by up to 66 % for temperatures higher than 185 °C. For extractions at high temperatures (i.e. 185 °C and above) and under the span of retention times (i.e. 8 to 22 min), the overall xylose yield was in the range of 40 to 70 % (w/w). Under the same conditions, the fraction of the xylan extracts that was in monomeric form was in the range of 2.2 to 5.3 %, showing that the extracted xylan was to high extent (more than 90 %) in non-monomeric form. As seen in Table 4.1, the maximal xylan extraction yield (ca. 66.1%) was achieved at 195 °C and 20 minutes with monomeric xylose yield of 5.3 %. Similar, and somehow comparable, results on xylan extraction yield (ca. 67 % xylo-oligomeric, ca. 14 % xylose, temperature of 195 °C) were reported in Romani et al., 2010, where the extraction of hemicelluloses from another hardwood (eucalyptus chips) was quantified at high-temperature conditions under conventional batch-mode hot water pretreatment. In the same study, autocatalytic pretreatment at 200 °C and 36 min could lead to xylan extraction yield of 76 %, of which about 55.7 % was in oligomeric and 20.3 % in monomeric form (Romani et al., 2010; Yan et al., 2016).

Table 4.1: Extraction Results (Sugar Yield, Lignin Removal, Degradation Products), Sugars in Pretreated Solids and Enzymatic Hydrolysis Sugar Yields for Aspenwood

Pretreatment Conditions		Sugar Extract (Xylose), Lignin and Degradation Products in Liquid Fraction								Sugars in Pretreated Solids [%w/w]		Enzymatic Hydrolysis Sugar Yield [%]	
		Xylose Extraction Yield [%w/w]			Lignin Removal [% w/w]	Degradation products [mg] per g raw sample							
Temp [°C]	Time [min]	Overall	Non-Monomeric	Monomeric		Acetic Acid	Formic Acid	Furfural	HMF	Glucose	Xylose	Glucose	Xylose
171	15	6.2	6.2	[n.d]	8.1	[n.d]	[n.d]	[n.d]	[n.d]	59.6	19.9	32.7	25.5
175	10	12.5	12.5	[n.d]	10.5	[n.d]	[n.d]	[n.d]	[n.d]	61.1	19.9	40.8	33.4
175	20	21.9	21.9	[n.d]	13.5	[n.d]	[n.d]	0.09	[n.d]	62.8	18.7	50.9	43.3
185	8	40.4	39.5	2.2	16.2	[n.d]	[n.d]	0.21	[n.d]	68.8	15.8	58.5	52.4
185	15	43.0	41.9	2.4	16.4	3.68	[n.d]	0.30	[n.d]	67.2	15.1	63.1	56.1
185	22	55.9	53.3	4.6	17.7	4.05	[n.d]	0.65	0.04	70.3	13.1	69.2	57.4
195	10	46.8	45.6	2.5	18.9	3.34	[n.d]	0.30	[n.d]	67.3	14.4	65.3	60.2
195	20	66.1	62.6	5.3	19.4	7.16	2.10	2.44	0.06	67.6	11.6	77.8	64.6
199	15	57.8	55.1	4.6	19.5	4.63	[n.d]	0.62	0.04	71.2	12.2	73.8	64.3
Raw Sample Composition [%w/w]			18.7		22.0	[--]	[--]	[--]	[--]	50.3	18.7	18.8	15.6

Table 4.2: Statistical Analysis Results for Xylose Extraction Yield from Aspenwood

Response: Xylose Extraction Yield, XY [% w/w]

ANOVA for Response Surface Reduced Quadratic Model

Analysis of Variance Table [Partial sum of squares - Type III]

Source	Sum of Squares		df	Mean Square		F-Value		p-value	
	O-XY*	NM-XY**		O-XY	NM-XY	O-XY	NM-XY	O-XY	NM-XY
Model	3486	3117	3	1162	1039	110	134	< 0.0001	< 0.0001
A-Temp [oC]	2873	2562	1	2873	2562	272	331	< 0.0001	< 0.0001
B-Time [min]	322	265	1	322	265	30	34	0.0004	0.0002
A^2	292	290	1	292	290	28	38	0.0005	0.0002
Residual	95	70	9	11	8				
Lack of Fit	81	60	5	16	12	4	5	0.0860	0.0756
Pure Error	14	10	4	4	2				
Cor Total	3581	3186	12						

Model Terms and Significance

Level of Significance	Factor	Coefficient	
		O-XY	NM-XY
significant	Intercept	44.0	42.8
	Temp	19.0	17.9
	Time	6.3	5.8
	(Temp)^2	-6.4	-6.4
	R-Squared (R-Sq) Values		
not significant		O-XY	NM-XY
	R-Sq	0.97	0.98
	Adj R-Sq	0.96	0.97

Note: *O-XY= Overall Xylose Yield; ** NM-XY= Non-monomeric Xylose Yield

The quantitative relationship between the response (xylose yield) and input parameters (temperature and time) were statistically analysed using central composite design (CCD) as a response surface methodology. The statistical model results (i.e. ANOVA results for reduced quadratic model with significant model terms, coefficients for the quadratic equation, as well as the R-Square values) both for the overall xylose yield (O-XY) and non-monomeric xylose yield (NM-XY) are shown in Table 4.2. With very low p-value ($p<0.0001$) and high R-Squared value (~0.97), the fitted quadratic models had a high significance (with 95% confidence interval, i.e. CI=95 %) to adequately represent the response-factor relationship. The ANOVA results did also indicate that the xylose yield was significantly influenced by the positive linear effects from both temperature and retention time as well as the negative quadratic effect from temperature. Comparing the magnitudes of the linear effects of the two factors (Table 4.2, coefficients for linear model terms), it can also be observed that the xylan extraction yield was more responsive to variations in temperature than it was to variations made in retention time. To confirm this, Pareto chart analysis was carried out to compare the relative size of standardized effects of temperature and retention time on the xylan extraction yield. The resulting chart (not shown here) could show that both extraction temperature and retention time had significant positive effect on the xylose yield, with temperature (t-value of 20.67) having more significant impact than retention time (t-value of 7.35), when gauged against the Bonferroni and standardized t-value limits, which were 3.96 and 2.78 respectively. Based on the results from both ANOVA and Pareto analysis, for the experimental conditions investigated here, it was evident that the positive linear effect of temperature on the xylan extraction yield was about three-fold more significant than that of retention time.

The contour plot for xylan extraction yield over a wide range of temperature and time was generated based on the reduced quadratic model, derived from CCD experimental results (see Table 4.2) and is shown in Fig 4.1. Considering the region defined by the design points (i.e. Temp: 170 – 199 °C; Time: 8 – 22 min), where the yields are well supported by experimental data, the constant-yield lines for xylan extraction are increasing in the up-right-direction showing that there was net positive effect on the yield with increases from both input parameters. However, from the extended version of the contour lines, it could be observed that there are inflection points around a temperature of 200 °C, beyond which the constant–yield lines continue to increase in the up-left direction, due to the positive effect from retention time, while the net effect of temperature has become negative (as is reflected in the growing size of the negative quadratic effect from increased temperature). These inflection points, in the study context here, can be viewed as good indicators of the maximum temperature and the shortest retention time suitable for xylose yields higher than 45 % (e.g. at 200 °C, a xylose yield of 45 % could be achieved in less than five minutes extraction time). For a given extraction time, the xylose yield can be increased when the temperature is increased up to 200 °C; for higher temperatures though, the yield can be expected to decrease (as discussed below). This observed pattern of contour yield lines is in agreement with reported results in Romani et al., 2010, where the release of xylan and other structural sugars was investigated under high temperature (195-250 °C) conventional batch-mode hot water treatment of eucalyptus chips (a hardwood like aspen). Accordingly, the xylan extraction yield was found to reach its maximal values in the temperature range of 195 to 205 °C, however, the proportion of the xylan extract that was in oligomeric form was observed to decrease for temperatures higher than 195 °C, evidently from increased formation of xylose and its subsequent degradation into furfural.

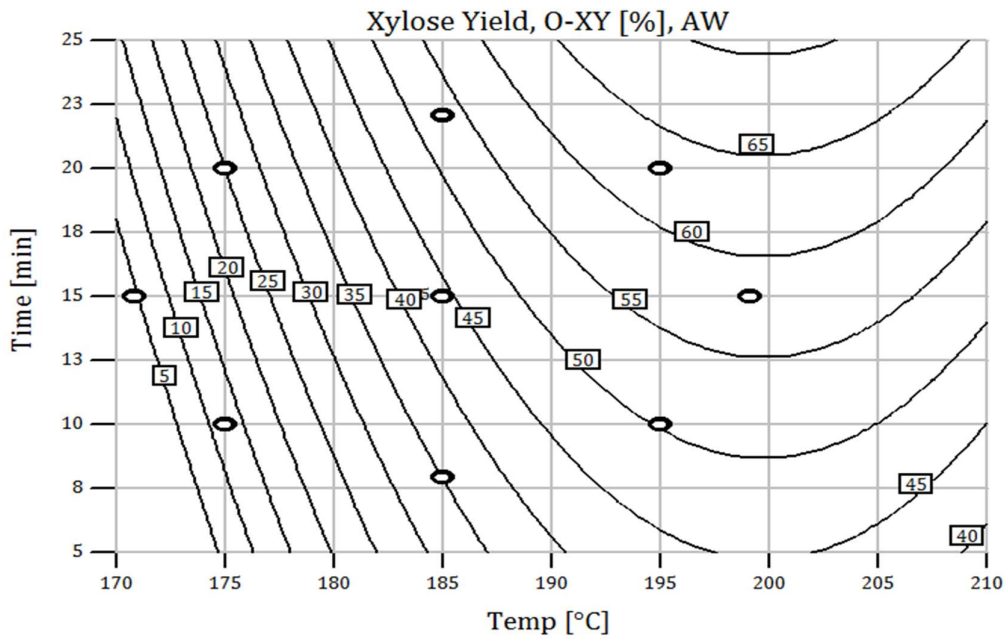

Fig. 4.1: Contour Plot for overall Xylose Yield (O-XY) for Aspenwood (AW) against Temperature and Retention Time

The increase in xylose yield at temperatures of 185 °C and above could primarily be the result of increased acidity level of the extraction medium, mainly from acetic acid. Under these conditions noticeable formation of acetic acid in the extraction hydrolysate was observed (0.36 to 0.72 g/100 g $_{\text{initial dry raw sample, dry weight basis}}$, see Table 4.1). The observed increase of acetate concentration in the extraction medium might have led to increased thermal effect of microwave irradiation through ionic dissipative mechanisms (Barba and d'Amore, 2012; Tsubaki et. al., 2016). Such increased acidity level in the extraction medium might have hastened the progressive depolymerisation of xylan (into xylo-oligomers) and its ultimate conversion into monosaccharides (Trajano and Wyman, 2013; Mosier, 2013). In fact, it is these acetic-acid-derived hydronium ions to which much of the observed auto-catalytic effect under such severity of conditions might be attributed (Carvalheiro et al., 2016; Tsubaki et. al., 2016). To a lesser extent, increased self-ionization and so increased auto-catalytic action of water at such high temperatures can also be part of the reason for enhanced dissolution of hemicelluloses (Trajano & Wyman, 2013;

Mosier, 2013). Furthermore, with increased temperature subcritical water is known to exhibit high rate of diffusion, low viscosity and low surface tension – properties that enhance solubility and extraction of hemicellulosic components (Teo et al., 2010).

A closer look at the results on xylan extraction from aspenwood (see Table 4.1) showed that temperatures of 185 °C and above were not only high enough for enhanced yields, but also severe enough to lead to monomeric xylose formation. It is important to note here that, at such high temperatures, extended extraction time had significant effect on the formation of monomeric xylose as well as degradation products thereof. For instance, at 185 °C, increasing the time from 8 to 22 minutes and, at 195 °C, from 10 to 20 min, led to over 100 % increase in the monomeric xylose yield (see Table 4.1). At the same conditions, the amount of acetic acid in the extraction hydrolysate was observed to increase substantially with increased retention time. Furfural, a degradation product from xylose, was also observed at such severe extraction conditions and results thereof (see Table 1) show that its formation was highly influenced by increases in retention time. For instance, at 185 °C, increasing the retention time from 8 to 22 minutes led to a three-fold increase (from 20.8 mg to 65.0 mg of furfural per 100 g $_{\text{dry initial sample}}$). Whereas at 195 °C, as the retention time was increased from 10 to 20 minutes, an eight-fold increase in furfural formation was observed (from 29.7 mg to 244.4 mg per 100 g $_{\text{initial dry sample}}$). Evidently, the combined effects of elevated temperature and elongated retention time appear to become more pronounced in view of enhanced xylan extraction, enhanced depolymerisation of the xylan extracts and their subsequent degradation into furfural.

As discussed earlier, for aspenwood, the linear positive effect of time on xylose extraction yield would mean that any reduction in this extraction parameter (at such elevated temperatures) would lead to corresponding reduction in xylose yield – both overall and monomeric. The minimization of monomeric xylose formation was thus only

possible by compromising the overall extraction yields, which increased with increased time. Therefore, at such high temperatures (i.e. 185–200 °C), a trade-off needs to be made between high non-monomeric xylose yield and low monomeric xylose yield. In this context, the choice of microwave-assisted pressurized hot water method for the purpose of extracting hemicelluloses from aspenwood is well justified, as high temperatures can be achieved in a relatively short time as used in the present experimental study. In other words, the rapid microwave irradiation effect in reducing the severity of extraction conditions through reduced retention time (Tsubaki et al., 2016; Barba and d'Amore, 2012) can potentially be exploited towards enhanced xylan extraction from aspenwood, while minimizing the formation of monomeric sugars and degradation products thereof.

4.3.2.2. Effects on Xylan Extraction from Sugarcane Trash

For sugarcane trash, results on xylan extraction (presented in Table 4.3) show that the xylose yield was predominantly influenced by temperature. Under the extraction times investigated here (i.e. 10 to 20 min) and for temperatures below 170 °C, the xylan extraction yield increased to values below 10 % (w/w), with no observed formation of monomeric xylose, organic acids and degradation products. For temperatures higher than 170 °C, however, the xylan extraction yield increased significantly (from 20 to 50 % w/w), with noticeable formation of monomeric xylose, degradation products (furfural and HMF) as well as organic acids such as acetic acid and formic acid. The low monomeric xylose yield of 3 to 6 % w/w shows that the xylan extracted from sugarcane trash was to a large extent in non-monomeric form. Comparable monomeric sugar yields of 2 to 5 % (w/w) were reported in Gulbrandsen et al., (2015), after microwave-assisted hot water extraction of hemicelluloses from sugarcane bagasse (temperature =180-190 °C; time = 20 min).

Table 4.3: Extraction Results (Sugar Yield, Lignin Removal, Degradation Products), Sugars in Pretreated Solids and Enzymatic Hydrolysis Sugar Yields for Sugarcane Trash

Pretreatment Conditions		Sugar Extract (Xylose), Lignin and Degradation Products in Liquid Fraction								Sugars in Pretreated Solids (SF) [%w/w]		Enzymatic Hydrolysis Sugar Yield [%]	
		Xylose			Lignin Removal [%w/w]	Degradation Products [mg], per g raw sample							
Temp [°C]	Time [min]	Overall	Non-Monomeric	Monomeric		Acetic Acid	Formic Acid	Furfural	HMF	Glucose	Xylose	Glucose	Xylose
167	15	9.5	9.5	[n.d]	9.1	[n.d]	[n.d]	[n.d]	[n.d]	47.7	26.6	41.4	23.8
170	10	18.6	18.6	[n.d]	10.6	[n.d]	[n.d]	[n.d]	[n.d]	47.7	23.1	49.5	34.5
170	20	23.2	23.2	[n.d]	8.6	[n.d]	[n.d]	[n.d]	[n.d]	48.4	25.2	53.2	32.4
180	8	20.2	19.5	3.5	18.0	5.24	1.87	2.05	0.04	49.9	23.1	52.6	35.9
180	15	21.7	20.9	3.8	16.1	5.69	1.89	2.36	0.05	50.3	22.9	54.4	40.1
180	22	24.2	23.3	3.7	14.3	5.10	1.85	2.68	0.05	49.2	20.7	56.8	42.8
190	10	29.2	28.3	3.2	17.8	9.58	2.56	3.21	0.05	53.2	21.2	62.9	47.6
190	20	29.2	28.2	3.6	15.5	6.76	1.88	4.14	0.06	53.2	20.5	65.4	49.8
194	15	50.9	47.7	6.2	21.4	11.10	2.28	3.29	0.18	61.3	15.3	74.3	53.3
Raw Sample Composition [%w/w]			23.2		18.8	[--]	[--]	[--]	[--]	38.7	23.2	19.2	6.5

Table 4.4: Statistical Analysis Results for Xylose Extraction Yield from Sugarcane Trash

Response: Xylose Extraction Yield, XY [% w/w]

ANOVA for Response Surface Quadratic Model

Analysis of Variance Table [Partial sum of squares - Type III]

Source	Sum of Squares		df	Mean Square		F-Value		p-value	
	O-XY*	NM-XY**		O-XY	NM-XY	O-XY	NM-XY	O-XY	NM-XY
Model	833	707	5	167	141	5	5	0.0333	0.0369
A-Temp	706	590	1	706	590	20	19	0.0029	0.0034
B-Time	18	16	1	18	16	1	1	0.5037	0.5001
AB	5	6	1	5	6	0	0	0.7104	0.6864
A^2	104	95	1	104	95	3	3	0.13	0.1249
B^2	0	0	1	0	0	0	0	0.9429	0.91
Residual	248	219	7	35	31				
Lack of Fit	224	195	3	75	65	13	11	0.0165	0.0209
Pure Error	24	24	4	6	6				
Cor Total	1081	926	12						

Model Terms and Significance

Significance	Factor	Coefficient	
		O-XY	NM-XY
significant	Intercept	21.7	20.9
	A-Temp	9.4	8.6
	B-Time	1.5	1.4
	AB	-1.2	-1.2
	A^2	3.9	3.7
	B^2	0.2	0.3

R-Squared (R-Sq) Values

Significance		O-XY	NM-XY
significant	R-Sq	0.77	0.76
	Adj R-Sq	0.61	0.59

Statistical analysis of the response-factor relationship was carried out using CCD and results obtained both for overall xylose yield (O-XY) and non-monomeric xylose yields (NM-XY) are presented in Table 4.4. As per the generated quadratic model, which itself was of low significance (p-value=0.0333 and R-Squared=0.77), temperature was identified as the sole significant model term (with p-value = 0.0023) with positive linear effect on the xylose yield. The effect from retention time was rather insignificant within 95 % confidence interval. Pareto chart analysis was performed to see the independent effect each extraction factor had on the xylose yield, and results thereof (not shown here) did confirmed what was already deduced from the ANOVA results.

A contour plot based on the statistically generated model (shown in Fig 4.2) also portrays the yield profile over a wide range of temperatures and times. The effect of retention time seems to level out with increased temperature showing that the observed increases in xylan extraction yield were mainly in response to changes in temperature. One plausible explanation hereto could be made on the basis of the high level of ash content in sugarcane trash, which was estimated at 7.89 % (w/w). In the course of the extraction process, those inorganic minerals constituting the ash, once they find their way into the extraction medium, would dissociate into the respective cations and anions. Such inorganic ions may compete for those hydronium (H_3O^+) and hydroxide (OH-) ions from self-ionization of sub-critical water as well as the dissolution of organic acids such as acetic acid and formic acid. As the effectiveness of microwave-assisted hot water extraction process is directly dependent on the apparent concentration of H_3O^+ and OH^-, the reaction they undergo with the inorganic ions and the resulting neutralization effect might have undermined the extent of hemicellulose extraction under such low-acid auto-hydrolytic conditions (Tanjore et al., 2011; Trajano and Wyman, 2013).

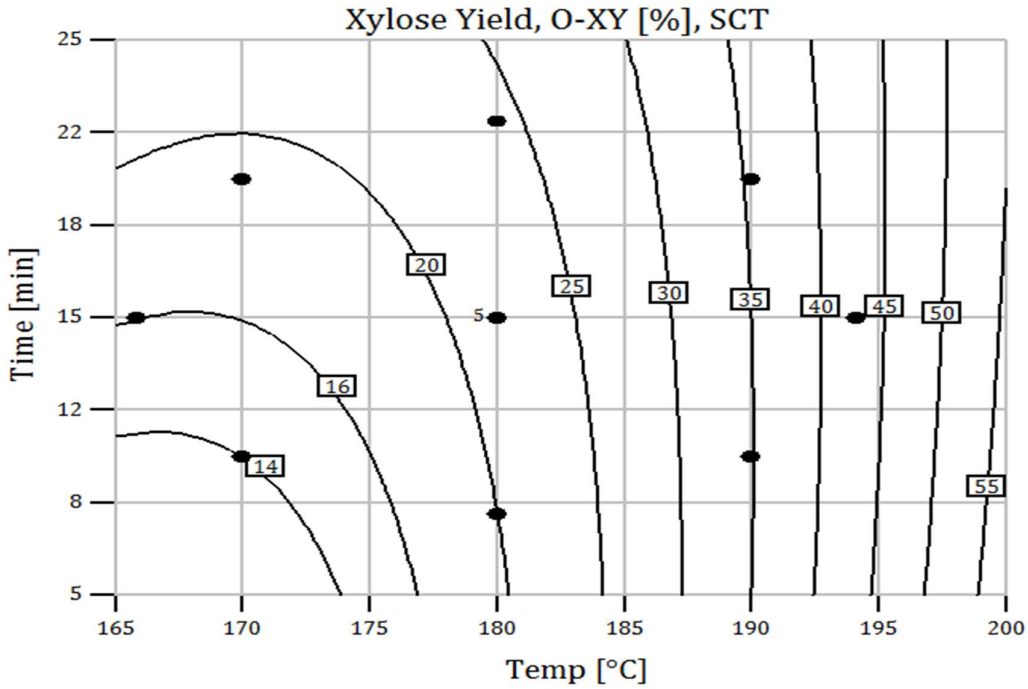

Fig. 4.2: Contour Plot for overall Xylose Yield (O-XY) for Sugarcane Trash (SCT) against Temperature and Retention Time

In the experimental case here, the presence of acids such as acetic acid and formic acid was noticeable for temperatures of 180 °C and above (see Table 4.3) and this can be associated with enhanced extraction yield for xylan, its depolymerisation into xylose as well as formation of degradation products such as furfural and HMF. This means, for sugarcane trash, temperatures starting from 180 °C could be severe enough to cause not only the decomposition of extracted xylan into xylo-oligomers, but also the degradation (dehydration) of xylose into furfural. One point of observation worth emphasizing with respect to hemicellulose extraction is the minimized formation of monomeric xylose even at the most severe conditions tested for both selected lignocellulosic feedstocks. From such low monomeric xylose yield and the high proportion of non-monomeric sugars (i.e. Xylo-oligosaccharides of wide range of degree of polymerization, DP), it can be deduced that the rate of formation of monomeric xylose could be a slow process. This may mean that the formation of monomeric xylose can only be realized after a series of

depolymerisation reactions whereby those initial hemicellulosic extracts (i.e. xylan extracts having high initial DP values) would have a progressively reduced DP, ultimately leading to formation of monomeric xylose. Given the structural and chemical complexity of hemicelluloses, it is likely that their depolymerisation and ultimate conversion into monomeric sugar units would unfold only in a progressive manner where a chain of complex reaction routes with a number of intermediate steps and products are involved. This may mean that, under the extraction conditions investigated in this study; those extracted xylo-oligosaccharides would apparently tend to remain in the extraction broth, while undergoing progressive reduction in DP, long enough before they end up into the monomeric units. This hypothesis is actually well supported by previous kinetic studies on the auto-hydrolytic decomposition of xylan-rich hemicelluloses into monomeric xylose (Carvalheiro et al., 2016; Trajano and Wyman, 2013).

4.3.3. Effect of Microwave-assisted Pressurized Hot Water Temperature and Retention Time on Cellulose digestibility (Enzymatic Hydrolysis Glucose Yield)

4.3.3.1. Effects on Enzymatic Glucose Yield – Aspenwood

Results from enzymatic hydrolysis test (shown in Table 4.1) revealed that the cellulose content as well as the enzymatic digestibility of aspenwood solids were substantially enhanced following their pretreatment under microwave-assisted conditions. For raw aspenwood, the enzymatic hydrolysis glucose yield was 18.85 % (w/w); this yield figure could be enhanced close to 80 % (w/w) after pretreatment, indicating that the cellulose in aspenwood was rendered highly digestible under microwave-induced conditions. The effects of temperature and retention time on the enzymatic hydrolysis sugar yield were statistically analysed (results shown in Table 4.5) and the response-factor relationship was well represented by a quadratic model with high level of significance (p-value<0.0001, R-Squared value=0.99, CI=95%). Accordingly, temperature appears to have positive linear effect and negative quadratic effect on the

enzymatic glucose yield, whereas only a linear positive effect of time was identified as significant. Pareto chart analysis results (data not shown) also showed that temperature (with t-value of 14.27) had more significant effect than retention time (t-value of 6.25).

Table 4.5: Statistical Analysis Results for Enzymatic Hydrolysis Glucose Yield for Aspenwood

Response: Enzymatic Hydrolysis Glucose Yield [%w/w], AW

ANOVA for Response Surface Reduced Quadratic Model

Analysis of variance table [Partial sum of squares - Type III]

Source	Sum of Squares	df	Mean Square	F-Value	p-value Prob > F	Significance
Model	1872	3	624	203	< 0.0001	significant
A-Temp [oC]	1501	1	1501	488	< 0.0001	
B-Time [min]	179	1	179	58	< 0.0001	
A^2	192	1	192	62	< 0.0001	
Residual	28	9	3			
Lack of Fit	14	5	3	1	0.5745	not significant
Pure Error	13	4	3			
Cor Total	1900	12				

Model Terms	
Factor	Coefficient
Intercept	63.8
Temp	13.7
Time	4.73
(Temp)^2	-5.21

R-Squared Values	
R-Squared	0.99
Adj R-Squared	0.98

The observed increase in cellulose digestibility of pretreated solids may primarily be attributed to the removal of hemicelluloses (xylose in particular), both during pretreatment and enzymatic hydrolysis stages. As is shown in Figs. 4.3a and b, the cellulose digestibility of pretreated solids was directly correlated with variations in the values of overall xylose yields. With increased removal of xylose, the pretreated solid was not only getting more cellulose-enriched (see Fig. 4.3c), but the solid ligno-carbohydrate matrix would also become more open-structured – effects which make the solid residue become more accessible to enzymatic attack (Ioelovich & Morag, 2012; Yang B. et al., 2011). Furthermore, the removal of lignin from the solid residue could also be another factor for enhanced digestibility as delignification does likewise lead to a more porous structure. Under the conditions investigated here (see Table 4.1), the degree of lignin removal was observed to increase moderately from 5 to 20 % w/w with increased severity of conditions.

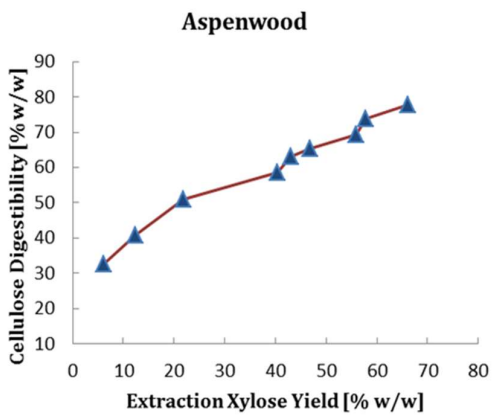

a) Cellulose Digestibility vs Extraction Xylose Yield

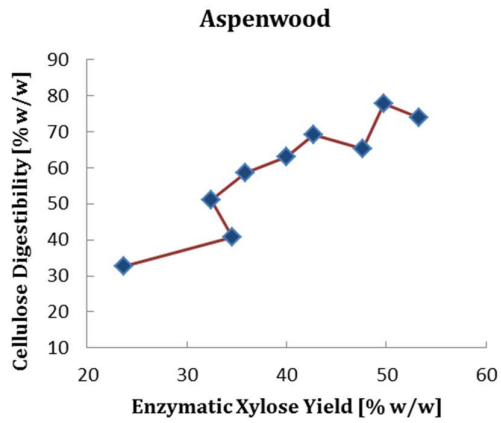

b) Cellulose Digestibility vs Enzymatic Hydrolysis Xylose Yield

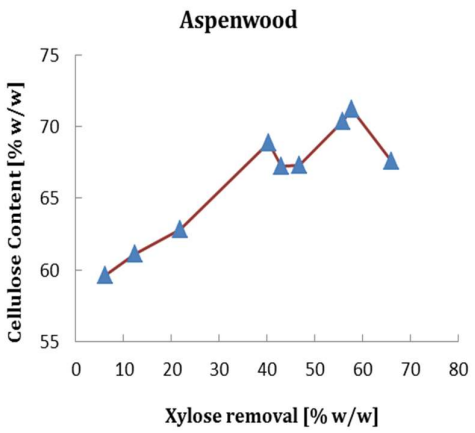

c) Cellulose content in pretreated solids against Xylose (hemicellulose) removal

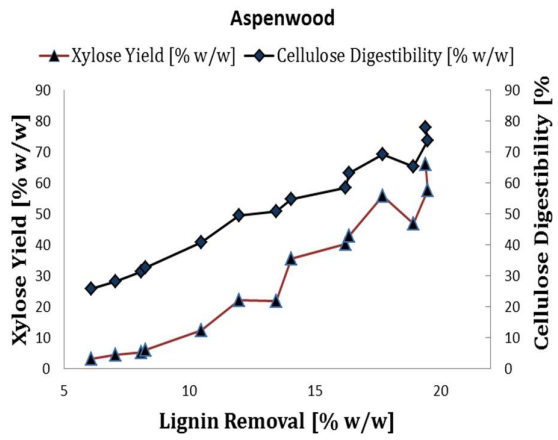

d) Cellulose Digestibility and Extraction Xylose Yield against lignin removal

Fig. 4.3: Cellulose content and digestibility of pretreated solids against degree of removal of Xylose and/or Lignin (Aspenwood)

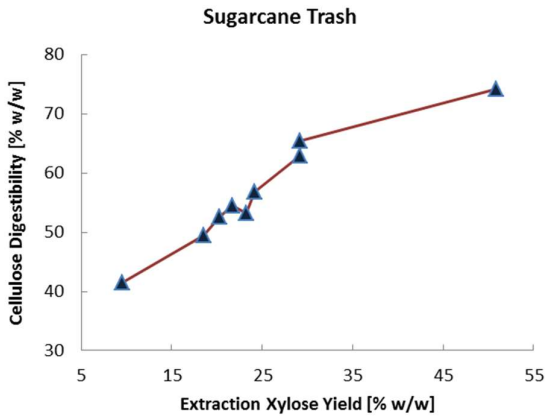

4a) Cellulose Digestibility vs Overall Extraction Xylose Yield (Sugarcane Trash,

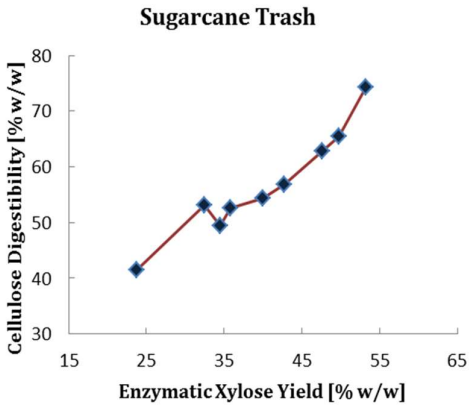

4b) Cellulose Digestibility vs Enzymatic Hydrolysis Xylose Yield (SCT)

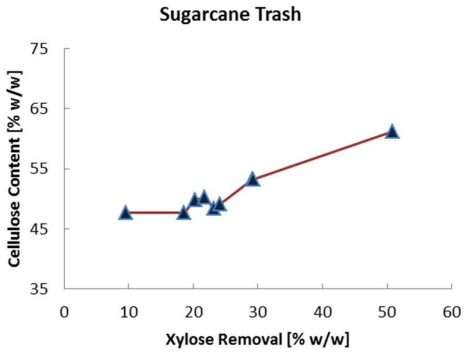

4c) Cellulose content in pretreated solids against xylose (hemicellulose) removal

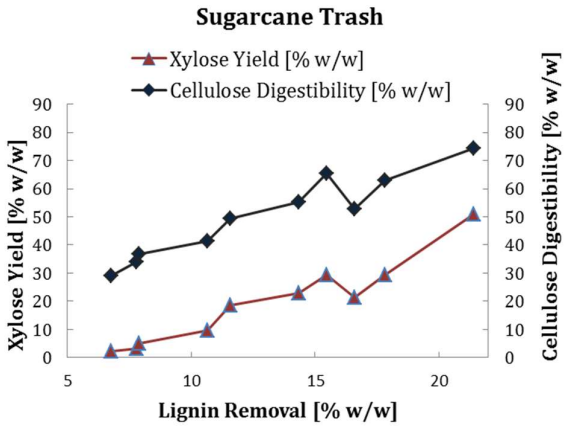

4d) Cellulose Digestibility and Extraction Xylose Yield against lignin removal (SCT)

Fig. 4.4 Cellulose content and digestibility of pretreated solids against removal of xylose (Hemicellulose) and/or lignin (Sugarcane Trash)

4.3.3.2. Effects on Enzymatic Hydrolysis Glucose Yield – Sugarcane Trash

For sugarcane trash, hydrolysis test results (see Table 4.3) showed that the enzymatic glucose yield and cellulose content of the pretreated solids were significantly enhanced following pretreatment under microwave-induced conditions. About 19 % (w/w) of the cellulose present in raw sugarcane trash was enzymatically digested without pretreatment; whereas, under the pretreatment conditions here, up to 75 % (w/w) of the cellulose could be digested, i.e. released in glucose form. An enzymatic glucose yield of 60 % (w/w) was reported in Franco et al. (2013), for sugarcane trash (tops and leaves) hydrothermally pretreated at 190 °C for 10 min under conventional heating mode. In the present study, about 63 % enzymatic glucose yield was achieved at the same pretreatment conditions.

Table 4.6: Statistical Analysis Results for Enzymatic Hydrolysis Glucose Yield for Sugarcane Trash (SCT)

Response: Enzymatic Hydrolysis Glucose Yield, SCT [% w/w]

ANOVA for Response Surface Quadratic Model

Analysis of variance table [Partial sum of squares - Type III]							Model Terms (Equation)	
Source	Sum of Squares	df	Mean Square	F-Value	p-value Prob > F	Significance	Factor	Coefficient
Model	716	5	143	13	0.0021	significant	Intercept	53.7
A-Temp	649	1	649	58	0.0001		A	9.0
B-Time	21	1	21	2	0.2126		B	1.6
AB	0	1	0	0	0.8659		AB	-0.3
A^2	44	1	44	4	0.0879		A^2	2.5
B^2	3	1	3	0	0.6238		B^2	0.7
Residual	78	7	11					
Lack of Fit	60	3	20	4	0.091	not significant	R-Squared Values	
Pure Error	18	4	5				R-Squared	0.90
Cor Total	794	12					Adj R-Squared	0.83

The response-factor relationship were statistically analysed and the resulting quadratic model was statistically significant (with p-value=0.0021; R-Squared value=0.91; CI=95%). Results thereof (shown in Table 4.6) could show that the enzymatic hydrolysis glucose yield for sugarcane trash was predominantly influenced by

temperature. Pareto chart analysis results thereon also showed temperature (with t-value of 3.77) to be the significant factor; whereas retention time to be rather insignificant (t-value=0.75, which is below the reference t-value=2.78). The correlations between xylose removal and enzymatic sugar yields were also analysed and results showed that, the enzymatic digestibility of the cellulose in sugarcane trash was generally observed to increase with increased removal of hemicelluloses – both during pretreatment (Fig. 4.4a) and enzymatic hydrolysis (Fig. 4.4b). The cellulose digestibility was evidently increasing with increased removal of both hemicelluloses and lignin (Fig. 4.4d), showing that hemicelluloses and lignin form physical and structural barrier for enzymatic accessibility of cellulose. With increased removal of hemicelluloses, both the content and structural porosity of the cellulosic component in the lignocellulosic solid apparently increases (Fig. 4.4c) thereby rendering the pretreated biomass more amenable for enzymatic attack (Ioelovich & Morag, 2012; Yang B. et al., 2011).

4.4. CONCLUSION

Single-step microwave-induced pressurized hot water pretreatment was demonstrated as a viable technique for extracting xylan from aspenwood and sugarcane trash, while enhancing their enzymatic digestibility for cellulosic ethanol production. Viable pretreatment conditions for enhanced xylan extraction and cellulose digestibility were established for each feedstock. About two-third of the original xylan in aspenwood and over half of that in sugarcane trash were extracted, with more than 90 % being in non-monomeric form. The cellulose digestibility for both lignocellulosic materials was improved by four-fold. Thus, microwave-induced hot water method can be regarded as viable route for advancing second-generation biorefineries.

ACKNOWLEDGEMENT

This work was supported by the Research Council of Norway (RCN) and the National Research Foundation (NRF), South Africa (BioCoPro, Grant No.: 234288/H30). We kindly acknowledge analytical services rendered by Levine Simmers and Jaco van Rooyen (SU, South Africa); Ingebjorg Leirset and Mirjana Filipovic (RISE-PFI AS, Norway). We also thank Eiric Sundby (HIST, Norway) for availing lab equipment required for the research work.

CHAPTER FIVE: STEAM EXPLOSION PRETREATMENT OF ALKALI-IMPREGNATED LIGNOCELLULOSES FOR HEMICELLULOSE EXTRACTION AND IMPROVED DIGESTIBILITY

Chapter published in 'Bioresource Technology' 294 (2019) 122121, Impact Factor=7.5

Article Title: Single-Step microwave-assisted hot water extraction of hemicelluloses from selected lignocellulosic materials – a biorefinery approach

Authors: Gezahegn T. Mihiretu, Annie F. Chimphango and Johann F. Görgens

Objective of Dissertation and Summary of findings of this Chapter

This chapter, like the preceding one, addresses the first four research objectives whereby the application of steam explosion pretreatment for the extraction of xylan-rich biopolymers from alkali-impregnated lignocellulosic materials was investigated. The extraction of xylan from the same two feedstock types (SCT and AW) was performed under subcritical conditions induced by varying saturated steam temperatures in the range of 176 - 204°C and retention times of 3 - 17 min following the impregnation of biomass samples with sodium hydroxide at 1:20 (w/w) solid loading ratio. Experimental results obtained for xylan extraction yield as well as those for enzymatic cellulose digestibility were statistically analyzed to fix the condition/s for significantly enhanced output parameters.

Accordingly, maximum xylan yields of 51 and 24%, and highest cellulose digestibility of 92 and 81%, were attained for SCT and AW respectively following their pretreatment at 204°C for 10 min. At this thermally most-severe condition, neither xylose nor furfural – a degradation product from xylose – were observed in the hemicellulose extract, which is a strong indication that the xylan extracts have been retained in non-monomeric form. Therefore, applying an alkali impregnation step on lignocellulose biomass prior to their steam explosion pretreatment conditions can be regarded as a viable biorefinery approach for the co-production of xylan biopolymers and bioethanol.

Candidate Declaration

With regard to Chapter 5, page numbers 109-141 of this dissertation, the nature and scope of the candidate's contributions were as follows:

Name of Contribution	Extent of Contribution (%)
Experimental Planning	70
Executing Experiments	100
Interpretation of experimental results	80
Writing of the Chapter	100

The following co-authors have contributed to Chapter 5, page numbers of 109-141 of this dissertation:

Name	Email Address	Name of Contribution	Extent of Contribution (%)
Annie F. Chimphango	achimpha@sun.ac.za	Reviewing of chapter Interpretation of results Experimental Planning	50 10 15
Johann F. Görgens	jgorgens@sun.ac.za	Reviewing of chapter Interpretation of results Experimental planning	50 10 15

Signature of candidate: _____ Date: _____

Declaration by co-authors

All authors have read and approved the final manuscript and hereby confirm that:

1. The declaration above accurately reflects the nature and extent of contributions by the candidate and co-authors to Chapter 5, page numbers 109-141 of this dissertation,
2. no other authors contributed to Chapter 5, page numbers 109-141 of this dissertation, besides those specified above, and
3. potential conflicts of interest have been revealed to all interested parties and that necessary arrangements have been made to use the material in Chapter 5, page numbers 109-141 of this dissertation.

Steam Explosion Pretreatment of alkali-impregnated Lignocelluloses for Hemicellulose Extraction and improved Digestibility

Authors: Gezahegn T. Mihiretu, Annie F. Chimphango, Johann F. Görgens*

Stellenbosch University, Process Engineering Department, Stellenbosch 7602, South Africa

ABSTRACT

The application of steam explosion pre-treatment to extract xylan-rich biopolymers from alkali-impregnated lignocelluloses, while simultaneously increasing the enzymatic digestibility of cellulose, was investigated. Steam-enhanced extraction of xylan from sugarcane trash (SCT) and aspen wood (AW) was performed at varying temperatures (176-204°C) and retention times (3-17 min) after the impregnation of biomass samples with sodium hydroxide at 1:20 (w/w) solid loading ratio. Xylan extraction and cellulose digestibility results were statistically analysed to fix the condition/s for significantly enhanced values. Accordingly, maximum xylan yields of 51 and 24%, and highest cellulose digestibility of 92 and 81%, were attained for SCT and AW respectively following their pre-treatment at 204°C for 10 min. At this most-severe condition, neither xylose nor furfural – a degradation product from xylose – were observed in the hemicellulose extract, indicating steam explosion pre-treatment with alkali impregnation of lignocelluloses as viable biorefinery approach to co-produce xylan biopolymers and bioethanol.

Keywords: xylan extraction; alkaline steam explosion pre-treatment; sugarcane trash; aspen wood; lignocellulosic biorefinery

*** Corresponding Author:** Process Engineering Department, Stellenbosch University,
Private Bag X1, Matieland, Stellenbosch 7602, South Africa
E-mail: jgorgens@sun.ac.za (Görgens, J.F.)

5.1. INTRODUCTION

The development of lignocellulosic biorefinery systems for an integrated production of biofuels and other bio-based co-products is widely regarded for its potential role towards decarbonized economic growth with improved environmental sustainability (Mohan et al., 2016; Medina et al., 2018). Such bioindustrial approaches essentially imply increased use of fibrous plant biomass where those major lignocellulosic components (cellulose, hemicellulose and lignin) patently become of immediate economic interest (Silveira et al., 2015; Cardona et al., 2019). Hemicelluloses are hetero-polysaccharides generally comprising 20-35% of dry lignocellulosic biomass (Isikgor and Becer, 2015; Anwar et al., 2014); however, they have largely remained underutilized despite their abundance and potential applications (Zhang et al., 2014; Liu et al., 2018). Hemicelluloses in hardwoods and herbaceous residues are particularly rich in xylan – a natural biopolymer which, if extracted in its polymeric and/or oligomeric form, can serve as a precursor for developing functional biomaterials having potential applications in the food, agricultural, pharmaceutical, cosmetic and biomedical areas (Hu et al., 2018; Mihiretu et al., 2017; Norström et al., 2015; Zhang et al., 2014; Chimphango et al., 2012).

A number of biomass fractionation techniques have been reported in view of enhancing extraction of xylan and improving digestibility of solid residues for subsequent bioconversion steps (Cantero et al. 2019; Baruah et al., 2018; Mihiretu et al., 2017; Carvalho et al., 2016). Alkaline pretreatment is one widely studied chemical route for the extraction of xylan-rich hemicelluloses from hardwoods and agricultural residues (Carvalho et al., 2016; Kim et al., 2016; Longue Junior et al., 2013). Alkaline extraction of hemicelluloses with minimal depolymerisation and degradation typically takes place under temperatures below 100 °C, hours-long retention times and alkali loadings of 1 to 5% (w/w) per dry biomass (Kim et al., 2016; Singh et al., 2015; Karp et al., 2014). Although

thermally and/or chemically more severe conditions may lead to higher hemicellulose yield, they are very often associated with increased depolymerisation and degradation of extracts (Xu and Sun, 2016; Longue Junior et al., 2013). For instance, in Longue Junior et al. (2013), where the effect of different alkali (NaOH) loadings on the yield of hemicellulose extraction from *Eucalyptus globulus* and degree of polymerization (DP) of the extracts was investigated, it was shown that increasing the alkaline charge from 10 to 50% (w/w, ODW) led to xylan yield increase from 39.3 to 58.6%, whereas a decrease in DP (from 250 to 97) was observed for the respective xylan extracts.

Steam explosion pre-treatment (SEPT) is another widely studied biomass fractionation technique suitably applied for selective removal of hemicelluloses from lignocelluloses – a process primarily catalysed by the hydrolytic action of organic acids (such as acetic acid) that form during pre-treatment under subcritical conditions (Jönsson and Martin, 2016; Singh et al., 2015). In this hydrothermal method, biomass sample is normally subjected to high-pressure saturated steam in the temperature range of 160 °C to 260 °C for few to several (2 to 30) minutes, after which the pre-treated material is discharged with an explosion decompression effect (Duque et al., 2016). Un-catalysed SEPT has been shown technically viable and environmentally benign method for cellulosic ethanol production mainly owing to its ability to remove hemicelluloses, to cause mechanical disruption of the lignocellulosic matrix, to reduce cellulose crystallinity while increasing its surface area and level of porosity – effects which lead to enhanced enzymatic cellulose digestibility (Pielhop et al., 2016; Duque et al., 2016).

However, the acidic conditions of auto-catalysed SEPT typically produce xylan extracts in the form of oligomers, monomers and degradation products thereof. A number of studies have shown that the extent of depolymerisation and formation of degradation products become significant for SEPT temperatures beyond 190 °C. For instance, in

Alvarez et al., (2017), wheat straw pre-treatment at un-catalysed SEPT (200 °C, 4 min) resulted in a liquid fraction (LF) rich in oligosaccharides (ca. 93% overall, and ca. 70% xylo-oligomers) and about 7% monosaccharide sugars with ca. 36% being xylose. From the reported concentrations of furfural (0.3 g/L) and xylose (1 g/L) in the LF, it can be deduced that the actual amount of xylose could be at least 20% higher than the detected amount. In another study by Tomas-Pejo et al., (2011), for wheat straw pre-treated at SEPT (210°C, 5 min), concentrations of xylose and furfural in the LF were reported as 24.7 g/L and 1.4 g/L respectively. In Manfredi et al., (2018), for sugarcane harvesting residue subjected to SEPT (204 °C, 20 min), almost one quarter of the hemicelluloses recovered in the LF were reportedly in monomeric form (24% monomers, 76% oligomers). Similar observations were also made for hardwoods. For instance, pretreatment of *E. globulus* under un-catalysed SEPT conditions, temperatures of 195°C and higher were shown to result in noticeable formation of monomeric xylose and furfural (Romani et al., 2010); with xylose concentration increasing up to a temperature of 210 °C, but from 220 °C onwards, the xylose concentration started to decrease, mainly due to enhanced degradation of the xylose into furfural (Romani et al., 2013; Romani et al., 2010).

From the above SEPT studies on agricultural residues and hardwoods, it can generally be observed that formation of monomeric sugars (mainly xylose) as well as degradation products thereof (furfural) was evidently taking place for SEPT temperatures around 200°C. Even though temperatures close to and beyond 200°C may favour enhanced removal of hemicelluloses, the extent of depolymerisation of extracts thereof as well as further degradation of monomeric units render SEPT rather un-suitable to extract polymeric xylan. Such high-temperature SEPT conditions may, in fact, be desired to produce highly digestible cellulose-rich solids, but they often lead to loss of sugars and enhanced formation of degradation products that have inhibitory effect on enzymatic

action (Jönsson and Martin, 2016; Duque et al., 2016). The addition of acids (such as SO_2, H_2SO_4, CO_2) to the biomass prior to SEPT has also been shown to enhance hemicellulose sugars recovery at lower temperatures; however, this approach substantially increases depolymerisation and degradation of hemicelluloses (Xu et al., 2017; Jönsson and Martin, 2016; Pielhop et al., 2016). In sum, both auto- and acid-catalysed SEPT are not attractive to extract hemicelluloses in their polymeric and/or oligomeric form, for applications as biopolymers for functional biomaterials.

This work intends to improve the extraction of polymeric and/or oligomeric xylan-rich hemicelluloses from two lignocellulosic materials, namely: sugarcane trash (SCT) – an agricultural harvesting residue, and aspen wood (AW) – a hardwood, by impregnating respective biomass samples with an alkaline agent prior to their pre-treatment under SEPT conditions. It was intended to exploit the unique ability of alkaline conditions to preserve hemicellulose extracts in their oligomeric and/or polymeric form, while simultaneously producing cellulose-enriched residue with sufficient digestibility for subsequent cellulosic ethanol production (Kim et al., 2016; Xu and Sun 2016). Adequate performance of such single-step alkali-impregnated SEPT would avoid the need for a two-step lignocellulosic biomass pre-treatment, with the first step mainly aimed at removing hemicelluloses and the second to render cellulose-rich solids sufficiently digestible (Rocha et al., 2012; Oliveira et al., 2013; Ratti et al., 2015). Furthermore, for both selected lignocelluloses, a pretreatment approach with an alkali-impregnation step prior to SEPT has not been applied in a biorefinery context whereby co-production of hemicellulosic (xylan) biopolymers and bioethanol would take place under alkalinized SEPT conditions. However, how and to what extent the xylan extraction yield and enzymatic hydrolysis sugar yields behave under alkalized SEPT conditions was far from clear, thus necessitating this study.

The aim of the present study was to explore and establish steam explosion pretreatment conditions for the extraction of hemicellulosic biopolymers from alkali-impregnated lignocelluloses while simultaneously improving the enzymatic digestibility of the cellulose-enriched solid residue. Put more precisely, the effects of varying SEPT temperature and retention time on xylan extraction yield and enzymatic digestibility of cellulose were examined for NaOH-impregnated sugarcane trash and aspenwood sawdust. In effect, this work attempts to assess the technical viability of alkalized SEPT for co-production of xylan biopolymers and bioethanol from lignocellulosic materials in a biorefinery context. Furthermore, the extent of lignin removal as well as formation of monomeric sugars, degradation products, acetic and formic acids were also considered from a mechanistic point of view.

5.2. MATERIALS AND METHODS

5.2.1. Materials

Sugarcane (*Saccharum officinarum*) trash (SCT) of South African origin and aspen wood (*Populus tremula*) sawdust (AW) of Norwegian origin were used for this study. Laboratory grade chemicals and analytical reagents as used in this experimental study such as sulphuric acid (95-97%), potassium hydroxide (≥85%), sodium hydroxide (≥97%), citric acid monohydrate (≥99%), potassium sodium tartrate (99.0%), 3,5-dinitrosalicyclic acid (98%), phenol, sodium azide (99.5%), sodium chloride (≥99.0%), disodium phosphate (≥99.0%), potassium chloride (≥99%), potassium phosphate monobasic (99%), potassium phosphate dibasic (≥98%), yeast extract, peptone, D-(+)-glucose (≥99.5%), D-(+)-xylose (≥99.0%) and perchloric acid (70%) were from Sigma-Aldrich. The enzymes Cellic CTec2 and HTec2 as used for enzymatic hydrolysis tests were both from Novozymes. Distilled water was used for all test purposes.

5.2.2. Feedstock preparation and characterization

The sugarcane harvesting residues (sugarcane trash), consisted primarily of leaves and tops, were dried in open air to a moisture level of 8.3%. The dried biomass was shredded to smaller sizes (ca. 5 to 7 cm), manually mixed to ensure uniformity of samples before packing in plastic bags. Likewise, aspen wood sawdust was air-dried to a moisture content of 6.3%, manually mixed and kept in plastic bags. Representative samples in the size fraction of 250-1000 μm were prepared in duplicates to determine extractives, structural sugars, lignin, and ash contents. Determination of extractives was based on the NREL two-step method (Sluiter et al., 2008). Ash content was determined as per the NREL protocol in Sluiter et al., (2008). Lignin content and structural sugars were determined as per Sluiter et al., (2012).

5.2.3. Hemicellulose extraction

5.2.3.1. Sample Preparation

About 600 g of prepared raw biomass was taken for each steam explosion pre-treatment test. The dry sample was first soaked in water at a loading ratio of 10:1 [mL/g]. The soaking was left overnight (ca. 18 h). Moisture contents of wet solid residues (WSR) obtained after centrifugal separation of the soaked material were 67 (±3) and 58 (±3) wt % for SCT and AW respectively. This WSR was subsequently impregnated with sodium hydroxide at 5% (w/w), i.e. about 31 g of NaOH was dissolved in 150 mL of water and this caustic solution was thoroughly mixed with the WSR to ensure uniform dispersion of the alkaline therein. The alkali-impregnated wet solid residue was left overnight at room temperature before pre-treatment.

5.2.3.2. Extraction step

The extraction of hemicelluloses from both lignocellulosic materials (SCT and AW) was carried out as per the experimental design under section 5.2.7. Tests were run in steam explosion pre-treatment unit (aka "steamgun", set up by IAP, Graz, Austria). The steamgun reactor (ca. 19 L) is the central component wherein the biomass sample was fed and subjected to high-pressure saturated steam at pre-set temperature and time. The pre-treated material (slurry) was discharged into a receiving tank upon instantaneous depressurization of the reactor to atmospheric pressure. The slurry was collected from the tank and manually mixed to ensure uniform distribution of pre-treated solids therein. Representative samples, ca. 150 g, were taken in triplicates for subsequent analytical purposes. Each steam-exploded sample was subjected to a solid-liquid separation step where the liquid fraction was separated by vacuum filtration and the solid fraction was repeatedly washed until the pH of the wash water became neutral. Weight of the resulting solid fraction, aka water insoluble solids (WIS) as well as volumes of the liquid fraction (LF) and washing water used were recorded for the purpose of determining quantitative distribution of biomass components therein. Moisture and dry matter contents of the WIS were determined by drying ca 5 g samples for about 4 h in a convection oven at 105℃. To do compositional analysis on pre-treated solids, around 30 g representative samples were taken from the respective WIS, oven-dried at 40℃ overnight (~24 h) and prepared in the size range 250-1000 μm. The remaining washed solid was kept at 4℃ till required. Duplicated samples of 50 mL were taken from extraction hydrolysates for the analysis of sugars and degradation products therein.

5.2.4. Enzymatic Hydrolysis Tests

Enzymatic saccharification experiments were carried out in duplicates on water insoluble solids (WIS) as per the NREL protocol (Selig et al., 2008). Each test was

conducted in a 250 mL Erlenmeyer flask at 2% substrate loading and 100 mL overall hydrolysis volume with sodium citrate buffer (0.1M, pH 5). The enzyme combinations used were Cellic CTec2 and HTec2, the former loaded at 15 FPU/g of substrate and the latter at 25% (v/v) of the former. The activity of CTec2 was estimated at 150 (±10) FPU/mL following the NREL protocol (Adney et al., 2008). The hydrolysis test was run in an incubator (50°C, 150 rpm) for 72 h after which the flasks were autoclaved for about 8 min to terminate the enzymatic activity. Separation of the liquid hydrolysate and solid fraction was carried out using vacuum filtration. Liquid analytical samples meant for sugars analysis were syringe-filtered using 0.22 μm filter.

5.2.5. Fermentation Experiments on steam-exploded samples

5.2.5.1. Simultaneous saccharification and fermentation

Simultaneous saccharification and fermentation tests were done on steam-exploded WIS samples selected from three different conditions. Tests were run in duplicates for six days in 250 mL flasks (cotton-plugged and covered with aluminium foil) incubated at 35°C and 150 rpm. With substrate loading of 10% (w/v) and an overall working volume of 100 mL, other inputs, i.e. 10X-YP yeast growing media (10 mL), 1M potassium phosphate buffer solution (5 mL), calculated amounts of water, enzymes and finally inoculum, 10x (1 mL) were sequentially fed into the flask just before the start of the fermentation. The enzyme preparation was from CTec2 and HTec2, the former loaded at 15 FPU/g substrate (dry weight basis) and the latter at 25% (v/v) of the former. *Saccharomyces cerevisiae*, yeast type MH-1000, was used for all fermentation tests. Fermentation tests were run in duplicates following the NREL SSF experimental protocol (Dowe and McMillan, 2008).

5.2.5.2. Inoculum preparation

Yeast inocula were prepared from frozen yeast stock (kept at -80°C) through pre-culturing steps based on the NREL protocol (NREL/TP-510-42630; Dowe and McMillan, 2008). The pre-culturing was accordingly done in an incubator (30°C, 150 rpm) and overnight (24 h). Inocula for actual fermentation tests were prepared from freshly pre-cultured yeast cells. The volume required for each fermentation flask was determined based on optical density (OD) measurements at 600 µm. That volume which, after dilution with YPD medium, led to an OD of 0.8 was taken for each flask.

5.2.5.3. Analytical sample preparation

Representative samples from the final fermentation broth were used to evaluate the yield of ethanol production. Samples, ca. 1.5 mL, were first centrifuged with MIKRO 120 centrifuge (make: Hettich Zentrifugen) at a relative centrifugal force (RCF) of 18,407 xg for five minutes; 0.4 mL of the supernatant was transferred to a 2 mL micro-centrifuge tube and diluted with water by a factor of 4.5. About 110 µL perchloric acid (35% v/v) was added to the diluted sample to precipitate proteinaceous contents therein and the tube was kept in refrigerator (4°C) overnight to allow sufficient time for precipitation. About 85 µL 7 M KOH solution was used to neutralize the acid therein. The 2 mL tubes were again centrifuged at 18,407 x g for two minutes to separate the precipitates from the liquid part. Analytical samples were prepared from de-proteinised supernatant syringe-filtered with 0.22 µm filter.

5.2.6. Analysis

Analysis of extraction hydrolysates for sugars (glucose, xylose, cellubiose and arabinose) as well as for degradation products (acetic acid, formic acid, furfural and hydroxymethylfurfural – HMF) was carried out in duplicates following the NREL two-

stage acid hydrolysis method (Sluiter et al., 2008a-c). Analytical samples were prepared between pH 4 and pH 6, syringe-filtered at 0.22 µm. Samples were analysed by High Pressure Liquid Chromatography (HPLC) method using Biorad Aminex HPX-87H column (7.8x300 mm) with 5 mM sulphuric acid as a mobile phase and column temperature at 65°C. Samples were injected at a volume of 30 µL, eluted at a flowrate of 0.6 mL/min and detected with an RI-detector. As xylan yield is an important output parameter, xylose standard solutions were acid-hydrolysed together with actual extraction hydrolysate samples to account for possible degradation of xylose during acid hydrolysis. The xylose concentration obtained from the HPLC analysis were corrected for xylose losses resulting from degradation. With respect to sugar analysis in enzymatic hydrolysates, analytical samples as prepared under section 5.2.4 were analysed for glucose and xylose under the same HPLC setup. The concentration of ethanol from SSF tests as well as residual sugars therein were determined based on HPLC analysis results on analytical samples prepared for this purpose (Section 5.2.5).

Sugar content in solid samples – both raw and pre-treated – was determined as per the NREL two-stage acid hydrolysis method (Sluiter et al., 2012). Preparation of analytical samples and sugar analysis steps were the same as above. The concentration of sugars in acid-hydrolysates was used to determine the composition of major structural sugars, i.e. cellulose and xylan, in the respective solid samples. The content of acid-insoluble (Klason) lignin was determined in parallel with structural sugars. That was done both before and after pre-treatment following the same NREL protocol (Sluiter et al., 2012).

5.2.7. Calculations

5.2.7.1. Composition of solid biomass samples (major components)

Major structural sugars (cellulose and xylan) and acid-insoluble lignin (AIL) in raw as well as pretreated solid samples were determined using the following equations:

$$\text{Cellulose [\%]} = 100 * \frac{(0.90)*(\text{Concentration of Glucose [g/L]in LF})*(\text{Volume of LF})[\text{L}]}{\text{Weight of Initial Sample, ODW [g]}}$$

$$\text{Xylan [\%]} = 100 * \frac{(0.88)*(\text{Concentration of Xylose [g/L] in LF})*(\text{Volume of LF [L]})}{\text{Weight of Initial Sample, ODW [g]}}$$

$$\text{AIL [\%]} = 100 * \frac{W_{AIR}\,[g] - W_{ASH}\,[g]}{\text{Weight of Initial Sample,ODW [g]}}$$

where, LF = liquid fraction (filtrate); ODW = Oven-dry Weight basis; W_{AIR} =Weight of Acid Insoluble Residue; W_{ASH} =Weight of Acid Insoluble Ash

5.2.7.2. Xylan extraction yield

Xylan yield was calculated as a percentage of original xylan in raw biomass sample that was extracted out and ended up in the liquid fraction (LF). The xylan yield, expressed in terms of xylose (Xo) [%w/w], was determined as follows:

$$\text{Xo [\%]} = 100 * \frac{\text{Amount of Overall Xylose in Liquid Fraction (LF)[g]}}{\text{Amount of Xylose in Initial Raw Sample [g]}} \qquad (4)$$

5.2.7.3. Lignin removal

The degree of removal of Klason lignin was determined as the percentage of original acid-insoluble lignin in initial raw sample that was removed as a result of pretreatment, and it was calculated using the following equation:

$$\text{Lignin Removal [\%]} = 100 * \frac{(\text{Lignin in Initial Sample})[g] - (\text{Lignin in Pretreated Sample})\,[g])}{\text{Lignin in Initial Sample, ODW [g]}}$$

5.2.7.4. Enzymatic hydrolysis sugars yield and ethanol yield

Enzymatic sugar yield (glucose and xylose) were calculated as follows:

$$\text{Glucose Yield [\%]} = 100 * \frac{\text{Amount of enzymatically released glucose [g]}}{\text{Amount of glucose in initial unhydrloyzed sample [g]}} \quad (6)$$

$$\text{Xylose Yield [\%]} = 100 * \frac{\text{Amount of enzymatically released xylose [g]}}{\text{Amount of xylose in initial unhydrloyzed sample [g]}} \quad (7)$$

The ethanol yield was determined from the actual amount of ethanol from fermentation as a percentage of the theoretical maximum yield which itself is determined assuming complete hydrolysis-fermentation of all glucose in the substrate. The yield is calculated based on the following equation (Dowe and McMillan, 2008):

$$\text{\% Yield of Ethanol} = \frac{\text{EtOH Conc at the end of Fermentation}}{(0.51)*(1.111)*\text{F}*\text{CDB}} \text{ X } 100 \quad (8)$$

where,

EtOH Conc = Ethanol concentration

F = Cellulose fraction of dry biomass (g/g)

CDB = Dry biomass concentration at the beginning of the fermentation (g/L)

0.51 = Conversion factor for glucose to ethanol, stoichiometric value

1.111 = Conversion factor for cellulose to equivalent glucose

5.2.8. Experimental Design and Approach

Design of experiments for hemicellulose extraction and statistical analysis of results thereof were done using Design-Expert 8.0.2. Main experiments were performed according to central composite design (CCD), a response surface methodology, with temperature and retention time as main factors. Based on CCD results, the response-

factor relationship between major output and input parameters was represented by a quadratic model. Regression coefficients, their statistical significance as well as the R-Squared values were estimated using analysis of variance (ANOVA) and those model terms with high significance level (i.e. p-value below 0.05 or confidence interval above 95 %) were considered to fit in the regression model.

The choice of parametric values for temperature and time aimed to find a compromise between xylan extraction and degradation thereof at conditions high enough for enhanced cellulose digestibility. Based on un-catalysed SEPT studies on agricultural residues (Alvarez et al., 2017, Tomas-Pejo et al., 2011, Manfredi et al., 2018) and hardwoods (Rocha et al., 2012; Romani et al., 2013; Oliveira et al., 2013; Duque et al., 2016), temperatures from 170 to 200℃ and retention times from 5 to 15 min were considered to design the extraction experiments. The choice of temperature values was made based, in part, on the operational history of the SEPT unit where previous studies have proven stable operational conditions. The alkali loading per unit dry biomass was chosen at a value which would be high enough to avoid formation of monomeric sugars (esp. xylose) thereby ensuring that the xylan extracts are in their non-monomeric form. Preliminary tests were conducted on both feedstocks (section 5.3.2) to fix the alkali loading and validate the range of values considered for the two extraction parameters. Main experiments were accordingly designed with minimum, central, and maximum values of temperature set at 176, 190 and 204℃; and of time at 3, 10 and 17 min respectively.

5.3. RESULTS AND DISCUSSION

5.3.1 Raw material characterization

Compositional analysis of sugarcane trash (SCT) and aspen wood (AW) confirmed that cellulose was the major structural component in both (SCT: ~39%; AW: ~50% w/w) lignocellulosic feedstocks (Table 5.1). Xylan content was lower in AW (19%) than in SCT (23%). Both raw materials had comparable contents of acid-soluble lignin (ca. 3.8%), whereas contents of acid-insoluble lignin in AW and SCT were around 18% and 15% respectively. The acetyl groups in SCT and AW were approximated around 2.3 and 4.6% w/w, showing that hemicelluloses in AW are highly acetylated in comparison to SCT. These compositional figures are comparable to respective values reported for SCT in (Singh et al., 2008; da Silva et al., 2012) and for AW in (Wang et al., 2018). With respect to SCT, significant amounts of extractives (11.4%) and ash (8%) were worth noting (Table 5.1). In Manfredi et al., (2018), 6.3% extractives and 14.6% ash content were reported for SCT.

Table 5.1: Compositional analysis results for selected raw lignocellulosic materials

Component	Composition [%w/w], dry weight basis	
	Sugarcane Trash (SCT)	Aspenwood (AW)
Glucan	38.70 ± 0.96	50.32 ± 1.26
Xylan	23.2 ± 0.70	18.71 ± 0.60
Acid-soluble Lignin	3.69 ± 0.18	3.94 ± 0.19
Acid-insoluble Lignin	15.14 ± 0.76	18.1 ± 1.1
Ash content	7.89 ± 0.42	0.51 ± 0.05
Acetyls	2.25 ± 0.35	4.55 ± 0.65
Water extractives	9.25 ± 0.45	1.75 ± 0.15
Ethanol extractives	2.15 ± 0.14	1.01 ± 0.05

5.3.2 Preliminary Steam Explosion Experiments

Preliminary extraction tests were conducted to verify parametric values for temperature [°C] and retention time [min], and to fix an appropriate value for alkali loading (AL) [%w/w]. A batch of four tests on SCT (each at 180°C for 10 min) carried out at 0%, 1%, 3% and 5% AL resulted in xylan yields of 21.2, 10.9, 25.5 and 35.3% respectively (Table-2). The yield at 0% AL was higher than that at 1% AL, but lower than the yields at 3 and 5% AL. Further analysis of extraction hydrolysates for furfural – degradation product from xylose – showed that about 11.89, 3.64 and 1.13 mg of furfural was present per 100 g raw sample at 0, 1 and 3% AL respectively; and none was detected at 5% AL (Table 5.2). A second batch of three tests carried out on SCT at three temperatures: 180, 190 and 200°C (each for 15 min and at 5% AL) resulted in xylan yields of 36.8, 45.1 and 49.5% respectively (Table 5.2). Despite increased temperature and time, no furfural was detected in all respective extraction hydrolysates, showing that formation of monomeric xylose as well as its degradation to furfural was effectively dampened at 5% AL. Based on these preliminary results, the main extraction experiment for SCT was designed (see section 5.2.7) with 190°C and 10 min as centre-point values for temperature and time, all tests at 5% AL.

For AW, four tests were conducted to see how xylan yield and formation of degradation products vary with alkali loading (AL), temperature and time. Two tests run at (190°C, 10 min) with 0 and 5% AL resulted in about 71% and 16% (w/w) xylan removal. The xylan yield was markedly lowered with the alkali impregnation step; nevertheless no monomeric sugars and degradation products were noticed. Whereas, in case of no alkali addition, there was significant formation of xylose (~ 11% of the xylan removed), degradation products (94.9 mg furfural and 23.3 mg HMF per 100 g raw biomass) (Table 5.2). Two more tests run at 180 and 200°C (each for 15 min and at 5%

AL) resulted in xylan extraction yields of 12.5 and 20.3% respectively. The detection of trace amounts of degradation products (13.4 mg furfural and 1.7 mg HMF per 100 g dry sample) at 200 °C (Table 5.2) showed that, at 5% AL, formation of monomeric sugars and degradation products becomes very likely for temperatures higher than 200°C and retention times longer than 15 min. Such conditions can indeed be sufficiently severe for degradation of polysaccharide sugars to take place, mainly hemicelluloses and, to a lesser extent, cellulose as well (Romani et al., 2010; Rocha et al., 2012; Romani et al., 2013). The extraction conditions for AW were thus delimited with upper temperature and time values of 205°C and 15 min respectively, all tests at 5% AL.

Table 5.2: Preliminary test results on xylan yield and formation of degradation products

Feedstock Type	Pretreatment Conditions			Xylan extraction yield [%w/w]	Concentration of Xylose detected in extraction liquid fraction [g/L]	Formation of degradation products [mg/100g raw sample]	
	Temperature [°C]	Retention Time [min]	Alkaline Loading, AL [%w/w]			Furfural	HMF
SCT	180	10	0	21.4	[n.d]	11.89	4.88
	180	10	1	10.9	[n.d]	3.64	1.36
	180	10	3	25.5	[n.d]	1.13	[n.d]
	180	10	5	35.3	[n.d]	[n.d]	[n.d]
	180	15	5	36.8	[n.d]	[n.d]	[n.d]
	190	15	5	45.1	[n.d]	[n.d]	[n.d]
	200	15	5	49.5	[n.d]	[n.d]	[n.d]
AW	190	10	0	70.6	0.51	94.86	23.31
	190	10	5	16.3	[n.d]	[n.d]	[n.d]
	180	15	5	12.5	[n.d]	[n.d]	[n.d]
	200	15	5	20.3	[n.d]	13.44	1.68

Note: [n.d] = not detected

3.3 Statistical optimization of steam explosion temperature and retention time for xylan extraction from alkali-impregnated lignocelluloses

Results on xylan extraction yields under different alkalinized SEPT conditions are shown in Table 5.3. The effects of temperature [°C] and retention time [min] on xylan yield [%w/w] were also statistically analysed (Table 5.4). The resulting quadratic model (see Table 5.4, model terms and respective coefficients), developed based on central composite design (CCD) method as response surface methodology, adequately represents the response-factor relationship within 95% confidence interval (for SCT: p-value=0.0008, R-Squared=0.93; for AW: p-value<0.0001, R-Squared=0.98). The ANOVA results (Table 5.4) for SCT indicated that xylan extraction yield was significantly influenced by the linear and quadratic effects from both temperature and time, predominantly from the linear effect of the former (p-value=0.0003). For AW, similar statistical observations were made according to which temperature was found to be the main factor to influence the xylan extraction process (Linear effect: p-value <0.0001; Quadratic effect: p-value=0.0081); whereas the effects of retention time on xylan extraction yield appeared insignificant (p-value>0.05) (Table 5.4). No wonder that temperature has so been among the most important factors influencing the xylan extraction process under alkaline as well as steam explosion pre-treatment conditions (Kim et al., 2016; Duque et al., 2016). It was indeed at the highest tested temperature (204°C) where the maximal xylan extraction yields for both feedstocks (SCT=~51%; AW=~24%) were attained (Table 5.3).

Table 5.3: Xylan extraction yield, degree of removal of Klason lignin (KL) and solid's compositional changes resulting from steam explosion pre-treatment of alkali-impregnated SCT and AW Samples

No.	Extraction Conditions		Xylan ExtractionYield [%w/w]		Klason Lignin Removal [%w/w]		Major components in Pretreated Solids (SF), Oven Dry Weight-basis [%]					
							SCT			AW		
	Temp [°C]	Time [min]	SCT	AW	SCT	AW	Gl	Xy	KL	Gl	Xy	KL
1	176	10	34.6 ± 0.87	12.3 ± 0.25	46.8 ± 1.11	5.0 ± 0.10	52.2 ± 1.31	24.8 ± 0.60	12.4 ± 0.29	55.0 ± 1.25	17.7 ± 0.40	19.8 ± 0.37
2	180	5	36.1 ± 1.05	12.0 ± 0.15	53.8 ± 1.10	8.8 ± 0.10	55.4 ± 1.20	23.5 ± 0.70	11.1 ± 0.25	55.4 ± 1.10	17.8 ± 0.30	17.9 ± 0.25
3	180	15	37.0 ± 1.10	12.5 ± 0.30	54.5 ± 1.33	18.6 ± 0.35	51.2 ± 0.90	21.1 ± 0.50	11.6 ± 0.35	56.6 ± 0.75	17.8 ± 0.20	16.8 ± 0.25
4	190	3	35.7 ± 0.80	15.0 ± 0.20	55.5 ± 0.95	6.5 ± 0.10	58.7 ± 1.20	26.6 ± 0.30	10.4 ± 0.20	54.6 ± 0.80	17.0 ± 0.30	18.7 ± 0.35
5	190	10	31.1 ± 1.25	16.3 ± 0.40	61.7 ± 1.45	12.6 ± 0.67	61.4 ± 1.45	24.9 ± 1.10	8.8 ± 0.55	55.7 ± 0.70	17.3 ± 0.48	18.0 ± 0.50
6	190	17	45.2 ± 1.30	16.1 ± 0.25	70.5 ± 1.50	19.6 ± 0.50	62.3 ± 1.07	23.1 ± 1.00	8.3 ± 0.80	56.3 ± 1.05	17.5 ± 0.67	17.4 ± 0.22
7	200	5	42.0 ± 1.10	21.7 ± 0.55	67.8 ± 1.30	14.3 ± 0.22	59.0 ± 1.10	22.8 ± 0.40	10.2 ± 0.25	58.4 ± 1.10	16.9 ± 0.50	19.9 ± 0.27
8	200	15	50.8 ± 1.45	20.3 ± 0.70	65.4 ± 1.67	29.3 ± 1.10	65.4 ± 1.27	20.3 ± 0.84	11.3 ± 0.50	61.0 ± 1.40	17.5 ± 0.50	16.2 ± 0.46
9	204	10	50.7 ± 1.70	23.6 ± 1.20	70.1 ± 2.55	31.3 ± 1.23	64.5 ± 1.50	20.5 ± 1.28	9.5 ± 0.84	59.1 ± 1.67	17.0 ± 0.77	15.5 ± 0.50
	Content in raw sample [%w/w]		23.2 ± 0.70	18.7 ± 0.60	15.14 ± 0.76	18.1 ± 1.1	38.7 ± 0.96	23.2 ± 0.70	15.1 ± 0.76	50.3 ± 1.26	18.7 ± 0.60	18.1 ± 1.1

Table 5.4: Statistical analysis results on xylan extraction yield from alkali-impregnated sugarcane trash (SCT) and aspenwood (AW) under different SEPT conditions

Response: Xylan Extraction Yield [% w/w]
ANOVA for Response Surface, Quadratic Model
Analysis of variance table [Partial sum of squares - Type III]

Source	Sum of Squares		df	Mean Square		F-Value		p-value (Prob > F)	
	SCT	AW		SCT	AW	SCT	AW	SCT	AW
Model	716,4	146,8	5	143,3	29,4	17,3	86,8	0,0008	< 0.0001
A-Temp	350,5	139,5	1	350,5	139,5	42,3	412,4	0,0003	< 0.0001
B-Time	94,8	0,1	1	94,8	0,1	11,4	0,2	0,0117	0,7132
AB	15,1	0,9	1	15,1	0,9	1,8	2,5	0,2194	0,1551
A^2	143,9	4,5	1	143,9	4,5	17,4	13,4	0,0042	0,0081
B^2	145,4	1,2	1	145,4	1,2	17,5	3,4	0,0041	0,106
Residual	58,1	2,4	7	8,3	0,3				
Lack of Fit	45,5	1,0	3	15,2	0,4	4,8	1,0	0,0817	0,4653
Pure Error	12,6	1,3	4	3,2	0,3				
Cor Total	774,4	149,1	12						

Model Terms (Equation)

Factor	Coefficients	
	SCT	AW
Intercept	31,1	16,3
A	6,6	4,2
B	3,4	0,1
AB	1,9	-0,5
A^2	4,6	0,8
B^2	4,6	-0,4

R-Squared Values	SCT	AW
R-Squared	0,93	0,98
Adj R-Squared	0,87	0,97

Besides the quantitative determination of xylan yields, extraction hydrolysates were also analysed for monomeric sugars (xylose, in particular) and degradation products such as furfural and hydroxymethylfurfural (HMF). In the case of SCT, analytical results (data not shown) revealed no formation of monomeric xylose and furfural under all tested conditions, including the most severe ones at which maximal xylan yield of ca. 51% (w/w) was attained, i.e. at (204°C, 10 min) and (200°C, 15 min) (Table 5.3). This was a strong indication that the xylan extracts were retained in their polymeric and/or oligomeric forms, thus proving alkaline impregnation of SCT prior to its pre-treatment with steam explosion as an important step for the extraction of xylan biopolymers. In contrast, up to 93% of hemicellulose removal was reported in Oliveira et al., (2013) for sugarcane straw subjected to un-catalysed SEPT at (200°C, 15 min), with the disadvantage that the majority of the extracted hemicelluloses being in monomeric or oligomeric form (Oliveira et al., 2013; Manfredi et al., 2018). Pre-treatment of sugarcane harvesting residues at SEPT (204°C, 20 min) has reportedly led to 68.5 % hemicelluloses recovery in the liquid fraction, about one-fourth of the hemicellulose extracts being in monomeric form (Manfredi et al., 2018). The same feedstock (=>sugarcane residues) subjected to conventional alkaline pretreatment (condition: 2% NaOH (w/w) loading, 121°C and 60 min) resulted in ca. 40% hemicelluloses extraction yield, with no monomeric sugars noticed in the liquid fraction (Manfredi et al., 2018). In Carvalho et al, (2016), sugarcane straw pre-treated in a conventional-type reactor pressure vessel with 5% (w/w) NaOH loading was shown to result in 55% hemicellulose solubilisation after its pretreatment for 15 min at 175°C. In a recent study by Mihiretu et al., (2017), xylan extraction yield of 51% was reported for the same feedstock (SCT) subjected to microwave-induced pressurized hot water conditions at (194°C, 15 min), also with insignificant formation of monomeric xylose.

Similarly, analysis of extraction hydrolysates for Aspen wood revealed no formation of monomeric xylose and degradation products (data not shown) under most tested conditions, including SEPT (204°C, 10 min) at which the maximal xylan yield was attained (Table 5.3). Trace amounts of furfural (Table 2) were, however, detected in the extraction hydrolysate at (200°C, 15 min), which may suggest that hemicelluloses extracted at such high temperatures (200°C and higher) are likely to degrade with retention time of 15 min and longer, thus making rather elongated times undesirable from xylan extraction point of view. In Mihiretu et al., (2017), the same feedstock (AW) subjected to comparable sub-critical condition (199°C, 15 min) under microwave-induced pressurized hot water method resulted in a higher xylan yield of 58% with noticeable formation of degradation products (e.g. ca. 62 mg furfural per 100 g dry raw sample). In a study by Carvalho et al. (2016), about 47% hemicellulose removal was observed for Eucalyptus sample (a hardwood like aspen wood) subjected to conventional alkaline pretreatment at 175°C for 15 min and 5% NaOH loading per dry sample weight. In Heitz et al., (1991), *Populus tremuloides* – a hardwood species very similar to Aspen wood – was subjected to un-catalysed SEPT at different temperatures and retention times; results showed that about 42, 60 and 65% of the original hemicellulose were respectively removed at 200, 210 and 220°C following their pretreatment for two minutes. The hemicellulose extracts were reported to be in oligomeric and monomeric forms, with the extent of de-polymerization and degradation increasing with increased temperature (Heitz et al., 1991).

Another important observation was the co-solubilisation of lignin that took place along with hemicellulose extraction (Table 5.3). The extent of delignification, expressed here as the percentage of removal of Klason lignin, ranged from 45-71% for SCT and from 5-31% for AW (Table 5.3). Statistical analysis results (not shown here) indicated that the

removal of lignin from both feedstocks was strongly influenced by temperature (SCT: p-value=0.0008, R-squared=0.84; AW: p-value=0.0009, R-squared=0.89); retention time was significant only for AW (p-value=0.003). The extent of lignin removal for SCT was far larger than that for AW (Table 5.3). Such quantitative difference (in delignification) may primarily result from the interplay between two factors, namely: feedstock ash content and acetyl groups originally associated with hemicellulose. While, on the one hand, the apparent alkalinity of the sub-critical pre-treatment condition can be enhanced by the alkaline nature of those mineral constituents of ash (Caillat and Vakkilainen, 2013; Jusko, 2017); on the other hand, acetyl groups – under the prevailing alkaline conditions – are easily cleaved from hemicellulose side chains and become subsequently hydrolysed into acetic acid, the latter chemically neutralizing any alkali present in the extraction medium (Pawar et al., 2017; Castro et al., 2017).

Given the relatively higher ash content in SCT (ca. 8%) compared to that in AW (ca. 0.5%); and, the lower acetyl content in SCT (ca. 2.2%) than that in AW (ca. 4.6%) (Table 5.1), it can be deduced that the extraction conditions were rendered more alkaline in the case of SCT than of AW. For instance, in the present study, SCT subjected to two un-catalysed SEPT conditions of (180°C, 10 min) and (190°C, 10 min), resulted in 10.6 and 22.5% (w/w) lignin removal (data not shown); in contrast, with 5% alkali impregnation prior to same SEPT conditions, the lignin removals were at 51.4 and 62.5% respectively (Table 5.3), thus proving that the SEPT conditions were rendered significantly alkaline with the impregnation step. Similarly, the removal of lignin from AW subjected to SEPT (190°C, 10 min) – with and without alkali addition – were 12.6 and 11.96% respectively (data not shown), indicating that the alkali impregnation step led only to a slight increase in lignin removal. In other words, the alkalinity of extraction conditions for AW were significantly counter-balanced by the neutralization effect of acetic acid. In Mihiretu et al.,

(2017) about 19.5% lignin removal was reported for AW pre-treated at (199℃, 15 min) under un-catalysed pressurized hot water method. Whereas in this study, 50% higher lignin removal was obtained for alkali-impregnated AW pre-treated at comparable SEPT condition (200℃, 15 min) (Table 5.3). In Carvalho et al., (2016), about 60% lignin removal was reported for sugarcane straw subjected to alkaline pretreatment in pressurized reactor vessel at 175 ℃ for 15 min and 5% NaOH loading (dry weight basis). In the same study, *Eucalyptus grandis* subjected to same pretreatment condition led to only 11% lignin removal (Carvalho et al., 2016). In the present study, AW pre-treated with 5% alkali loading at the least sever condition (176℃, 10 min) led to just 5% Klason lignin removal (Table 5.3).

From the discussion on delignification, it can be inferred that the extraction conditions were sufficiently alkaline for SCT and, of course, more alkaline than the conditions for AW. It is well known that removal of lignin and simultaneous extraction of hemicelluloses under alkaline conditions take place as a result of the saponification and disruptive effects of the alkaline agents have on the ester bonds between lignin and structural carbohydrates (Duque et al., 2016; Kim et al., 2016). The observed extent of delignification is thus a direct indicator of how alkaline the pre-treatment condition was – the more alkaline the condition, the higher the degree of removal of both lignin and hemicelluloses. The relatively higher xylan yields for SCT can thus be attributed to the higher degree of alkalinity of SEPT conditions that resulted from both the impregnation step and its ash contents. The rather low xylan yield for aspenwood could mainly be accounted to the neutralization between the carboxylic acids and alkalis, thus significantly reducing the apparent amounts of hydronium and hydroxide ions which are essential for continued cleavage of intermolecular bonds linking lignin with hemicelluloses (Pawar et al., 2017; Kapu et al., 2016). Even though the yield figures for AW seem to be not that high,

as a method, steam explosion pretreatment with an alkali-impregnation step can still be regarded as a viable approach to extract xylan biopolymers from AW. Based on the statistical model generated for AW (Table 5.4), at 5% alkali loading, higher xylan yields are only possible with increased thermal severity of conditions. Accordingly, temperature as high as 235°C may be required to extract about half of the original xylan in AW (pre-treated for 10 min and 5% alkali loading). Even though the alkali loading was fixed for all main experiments, the results thereof could provide sufficient insight as to how varying the alkali loading (used for impregnation purpose) may influence the extent of xylan extraction. For aspenwood, by applying alkali loadings greater than 5%, the pretreatment conditions can be made sufficiently alkaline to make higher xylan extraction yields possible.

5.3.4. Effects of alkaline steam explosion pretreatment temperature and retention time on enzymatic hydrolysis glucose yield (cellulose digestibility)

The effects of alkalinized steam explosion pre-treatment conditions on cellulose digestibility were assessed based on results from standardized enzymatic hydrolysis tests conducted on water-insoluble solid samples obtained after hemicellulose extraction step (Table 5.5). Accordingly, the enzymatic digestibility of both lignocellulosic materials (SCT & AW) was considerably influenced by introducing an alkali impregnation step prior to their pre-treatment under steam explosion conditions, thus proving the selected pre-treatment strategy as an effective approach towards cellulosic ethanol production. Under the experimental conditions investigated here, the enzymatic glucose yield for SCT was in the range of 61% (176°C, 10 min) to 92% (200°C, 5 min), equivalent to 3- to 5-fold increase over the digestibility of raw sample (Table 5.5). For aspenwood, the glucose yields ranged from 54 to 81%, the maximal yield being attained at (204°C, 10 min), which was 2.5 to 4.5-folds over the glucose yield for the raw sample (Table 5.5). The extent of

cellulose digestibility appeared to increase with increased thermal severity of pretreatment conditions. This was statistically validated with results (not shown here) having significant model terms (SCT: $p=0.0006$, R-SQ=0.93; AW: $p=0.0036$, R-SQ=0.88) and the glucose yields for both feedstocks were mainly influenced by the linear effect of temperature (SCT: $p<0.0001$; AW: $p=0.0003$); whereas the effect of retention time (SCT: $p=0.0124$; AW: $p=0.0311$) was significant but not so as temperature.

Table 5.5: Enzymatic hydrolysis sugar yields (glucose and xylose) for steam exploded sugarcane trash (SCT) and aspenwood (AW) under different combinations of temperature and time

No.	Pretreatment Conditions		Removal of Original Xylan after pretreatment (XR-SEPT), after enzymatic hydrolysis (XR-EH) and Combined (overall) xylan removal (XR-COM) [%w/w]						Enzymatic Hydrolysis Sugar Yield [%w/w]			
			SCT			AW			Glucose		Xylose	
	Temperature [°C]	Time [min]	XR-SEPT	XR-EH	XR-COM	XR-SEPT	XR-EH	XR-COM	SCT	AW	SCT	AW
1	176	10	34.6 ± 0.87	39.1 ± 1.10	73.7 ± 1.00	12.3 ± 0.25	69.4 ± 1.50	81.7 ± 1.40	60.9 ± 1.71	54.4 ± 1.20	53.7 ± 1.50	79.2 ± 1.75
2	180	5	36.1 ± 1.05	49.9 ± 1.35	86.0 ± 1.23	12.0 ± 0.15	67.7 ± 1.55	79.7 ± 1.35	68.1 ± 1.85	50.9 ± 1.17	78.1 ± 2.10	76.9 ± 1.77
3	180	15	37.0 ± 1.10	55.0 ± 1.30	92.0 ± 1.25	12.5 ± 0.30	65.7 ± 1.67	78.2 ± 1.55	83.1 ± 1.95	47.6 ± 1.21	87.3 ± 2.14	75.1 ± 1.91
4	190	3	35.7 ± 0.80	45.5 ± 1.05	81.2 ± 0.95	15.0 ± 0.20	71.8 ± 1.60	86.8 ± 1.40	76.9 ± 1.77	55.8 ± 1.25	67.5 ± 1.55	84.5 ± 1.86
5	190	10	31.1 ± 1.25	60.1 ± 1.22	91.2 ± 1.24	16.3 ± 0.40	69.7 ± 1.45	86.0 ± 1.37	82.7 ± 1.68	60.6 ± 1.26	87.2 ± 1.77	83.3 ± 1.70
6	190	17	45.2 ± 1.30	44.6 ± 0.90	89.8 ± 1.15	16.1 ± 0.25	73.8 ± 1.33	89.9 ± 1.15	88.3 ± 1.80	74.2 ± 1.35	81.4 ± 1.65	88.0 ± 1.60
7	200	5	42.0 ± 1.10	53.0 ± 0.85	95.0 ± 0.95	21.7 ± 0.55	70.2 ± 1.15	91.9 ± 1.01	92.2 ± 1.50	65.8 ± 1.10	91.3 ± 1.65	89.7 ± 1.45
8	200	15	50.8 ± 1.45	46.1 ± 1.40	96.9 ± 1.20	20.3 ± 0.70	64.6 ± 1.70	84.9 ± 1.45	90.3 ± 2.70	77.6 ± 2.05	93.7 ± 2.85	81.1 ± 2.15
9	204	10	50.7 ± 1.70	44.6 ± 1.25	95.3 ± 1.35	23.6 ± 1.20	67.1 ± 1.86	90.8 ± 1.68	91.7 ± 2.57	81.4 ± 2.25	90.5 ± 2.50	87.9 ± 2.44
Content in Raw sample, [%w/w]			23.2 ± 0.70	23.2 ± 0.70	23.2 ± 0.70	18.7 ± 0.60	18.7 ± 0.60	18.7 ± 0.60	Yields for un-pretreated Samples			
									19.2 ± 0.65	18.8 ± 0.50	6.6 ± 0.20	15.3 ± 0.40

As discussed earlier (section 5.3.3), removal of lignin from the lignocellulosic matrix and of acetyl groups from hemicelluloses are observed to take place in an enhanced manner with the alkali-impregnation step. Both delignification and de-acetylation processes in effect render the lignocellulosic material structurally open and porous thereby making polysaccharide sugars (holocellulose) more accessible to enzymes (Pawar et al., 2017; Castro et al., 2017; Kim et al., 2016). The cellulose digestibility for SCT was accordingly found significantly enhanced with the alkali-impregnation step when compared to un-catalysed hydrothermal methods. For instance, sugarcane straw subjected to un-catalysed SEPT at (200°C, 15 min) about 80% cellulose conversion to glucose was reported in Oliveira et al., (2013), the enzymatic digestibility being enhanced by the significantly high hemicellulose removal (93%). In this study, alkali-impregnated SCT subjected to the same SEPT conditions led to 90.3% digestibility (Table 5.5). In Mihiretu et al. (2017), cellulose digestibility of ca. 54% was reported for sugarcane trash pre-treated under pressurized hot water conditions at (180°C, 15 min). Whereas in the present study, a higher cellulose digestibility of 83% was for SCT pre-treated at (180°C, 15 min). In a more recent study by Manfredi et al., (2018), sugarcane harvesting residue subjected to un-catalysed SEPT (204°C, 20 min), about 78% enzymatic hydrolysis glucose yield was reported; whereas in the present study, about 91% cellulose digestibility was attained for alkali-impregnated SCT subjected to SEPT (204°C, 10 min) (Table 5.5). In all cases, the comparatively higher glucose yields observed in this study revealed that SCT was, in fact, rendered more digestible with alkali addition than without, thus indicating the important and direct role the alkali impregnation step plays in enhancing cellulose digestibility. The enzymatic glucose yield was indeed strongly correlated with both the degree of removal of lignin and xylan yield (Fig. 5.1A).

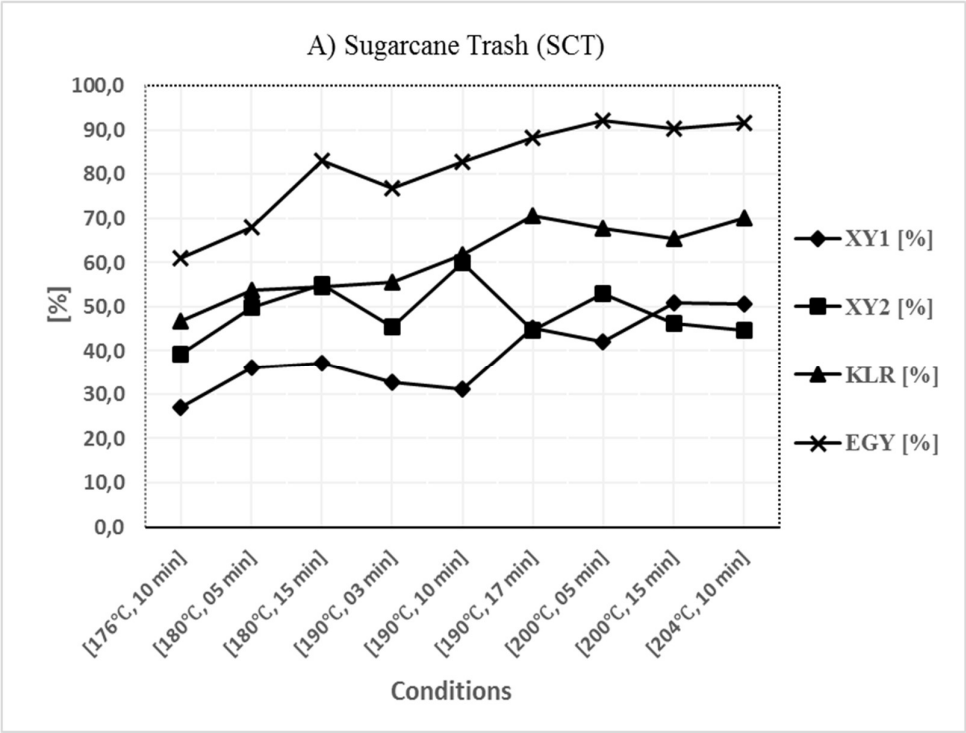

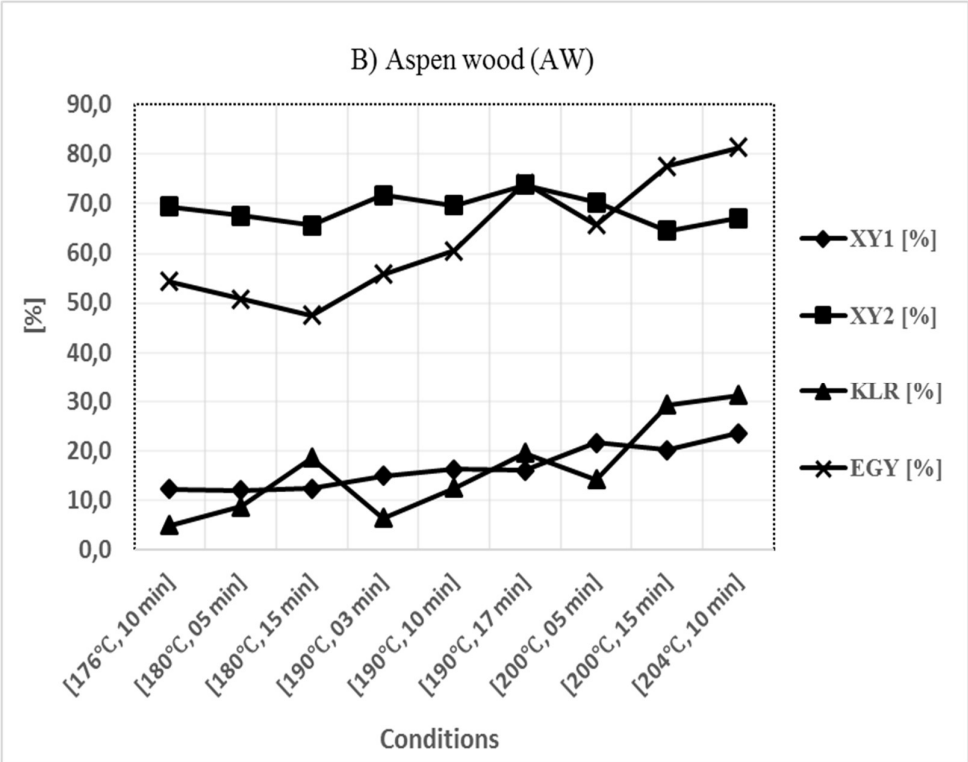

Fig. 5.1: Removal [%w/w] of original xylan during pretreatment (XY1) and enzymatic hydrolysis (XY2); of Klason lignin during pretreatment (KLR) and Enzymatic hydrolysis glucose yield (EGY) for SCT (A) and Aspenwood (B) under different SEPT conditions

For aspenwood, the enzymatic glucose yields on pre-treated solids were varying from 54 to 81% (Table 5.5), the maximal yield being attained at (204°C, 10 min), which is equivalent to 2.5 to 4.5-folds the glucose yield from the un-treated sample. In Mihiretu et al., (2017), AW pre-treated under pressurized hot water condition (199°C, 15 min) resulted in cellulose digestibility of 73.8% which is quite close to that obtained in the present study at (200°C, 15 min) (77.6%). A much lower enzymatic digestibility (ca. 42%) was reported in Dziekonska-Kubezak et al., (2018) for AW subjected to SEPT at (198°C, 15 min); whereas in the same study, AW subjected to alkaline pre-treatment (121°C, 60 min, 2% (w/v) NaOH loading) close to 80% digestibility was reported (Dziekonska-Kubezak et al., 2018). These results strongly suggest that the enzymatic digestibility of AW was significantly enhanced under alkalinized pretreatment conditions where the simultaneous removal of lignin and hemicelluloses can take place. As is seen from Fig. 1B, the enzymatic glucose yield for AW bear direct correlation with the degree of removal of KL and xylan. One point worth noting in this respect is the overall or combined removal of xylan (XR-COM) from pretreatment and enzymatic hydrolysis steps (see Fig. 5.1B; Table 5.5). Such enhanced enzymatic conversion of xylan into xylose can be directly linked to de-acetylation of hemicelluloses which itself takes place efficiently under prevailing alkaline conditions – the higher the degree of removal of acetyl groups, the more enzymatic digestible become xylan (Pawar et al., 2017; Castro et al., 2017). With increased removal of xylan, the cellulosic portion – which is the major component in raw AW – should become more exposed to enzymatic attack. In addition to this, the combined use of cellulase (=>Cellic CTec2) and hemicellulase (=>Cellic HTec2) enzymes might as well have rendered the cellulose more digestible through their enzymatic synergistic effect (Sun et al., 2016).

5.3.5. Fermentation test results

Simultaneous saccharification and fermentation (SSF) experiments were performed on water-insoluble solids from steam explosion pretreatment at three temperatures (two extreme-end: 176°C & 204°C; and one centre-point: 190°C) with a common retention time of 10 min. The resulting ethanol yields (EY), actual amount of ethanol produced expressed as percentage of theoretical amount of ethanol from all cellulose in raw sample, are presented in Fig 5.2. Accordingly, ethanol production yields of 58 to 83% for SCT and 52 to 79% for AW were obtained, with the maximal values (SCT: 83.4%; AW: 79.4%) being attained at the most severe condition (204°C, 10 min). In Manfredi et al., 2018, an ethanol yield of 50.1 ± 5.9% (w/w) was reported for sugarcane residue steam-exploded at (204°C, 20 min) fermented as well under SSF mode. In the same study, a higher ethanol yield (75.2 ± 1.0% (w/w)) was reported for the same feedstock subjected to alkaline pretreatment (121°C, 60 min, 2% (w/v) NaOH loading) and subsequent fermentation under identical SSF condition (Manfredi et al., 2018). Both reported ethanol yields are lower than the highest ethanol yield for SCT (83.4% w/w) in the present study achieved at SEPT (204°C, 10 min). The results from both studies reveal that, for SCT, the ethanol yield can be enhanced remarkably under alkaline conditions, thus strongly suggesting that the alkali-impregnation step prior to SEPT as effective approach to boost ethanol yield. Similarly, in a previous study by Dziekonska-Kubczak et al., (2018), fermentation of steam-exploded aspen wood chips subjected to un-catalysed SEPT (198, 15 min) resulted in 86% ethanol yield against the theoretical maximum value. Comparable ethanol yield (ca. 84%) was also reported by the same study for aspen wood pre-treated under alkaline conditions (121°C, 60 min, 2% (w/v) NaOH loading) (Dziekonska-Kubczak et al., 2018).

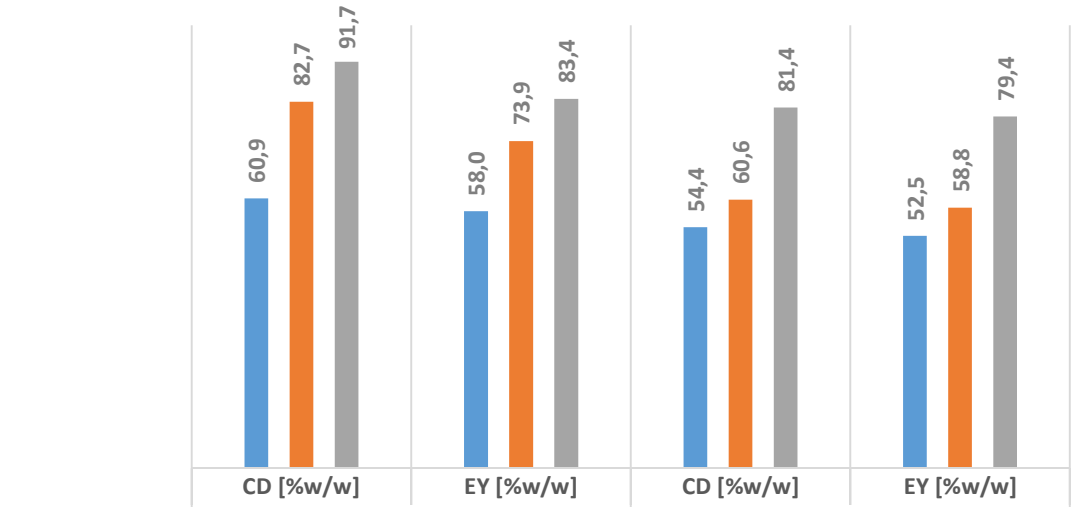

	CD [%w/w]	EY [%w/w]	CD [%w/w]	EY [%w/w]
	Sugarcane Trash		Aspen wood	
[176°C,10 min]	60,9	58,0	54,4	52,5
[190°C,10 min]	82,7	73,9	60,6	58,8
[204°C,10 min]	91,7	83,4	81,4	79,4

Fig. 5.2: Ethanol Yield (EY) [%w/w] and Cellulose Digestibility (CD [%w/w]) for Sugarcane trash and Aspen wood at three SEPT conditions (Temperature: 176, 190 and 204°C; Retention time = 10 min)

The extent of ethanol production from both feedstocks was evidently increasing with increased thermal severity of pretreatment conditions and so was the cellulose digestibility (Fig. 5.2). However, the fermentation efficiency (calculated as the percentage of enzymatically released glucose that was actually fermented into ethanol) as well as the amount of ethanol produced per unit weight of initial raw material were higher for AW than they were for SCT. For instance, at SEPT (204°C, 10 min), the fermentation efficiency for SCT and AW were around 91 and 97% respectively. At the same condition, around 29 g and 38 g of ethanol was produced per 100 g of raw SCT and AW samples respectively. The higher amount of ethanol for AW could be attributed to the larger cellulose content in raw AW (~50%) than that in raw SCT (~39%), as higher initial cellulose content means higher amount of cellulose in the pre-treated solid as well.

5.4. CONCLUSION

An alkali-impregnation step prior to steam explosion pretreatment (SEPT) of lignocelluloses proved viable for co-production of xylan biopolymers and bioethanol. This was demonstrated by impregnating sugarcane trash and aspenwood with NaOH at 5% (w/w) with optimal yields under SEPT temperatures 195-205℃. Xylan was extracted with little or no formation of monomeric sugars and degradation products thereof; this confirms the suitability of alkalised SEPT for xylan biopolymers extraction. The significant increase observed in enzymatic cellulose digestibility indicates the potential of this pretreatment strategy for bioethanol production. Kinetic studies of xylan extraction under alkalized SEPT conditions is worth considering for further research.

ACKNOWLEDGMENTS

This work was supported by the Research Council of Norway (RCN) and the National Research Foundation (NRF), South Africa (BioCoPro, Grant No.: 234288/H30). We kindly acknowledge analytical services rendered by Levine Simmers and Jaco van Rooyen (SU, South Africa). We also like to acknowledge the assistance offered by Lukas J. Swart (SU, South Africa) in the operational aspects of the pilot plant used in this experimental work.

CHAPTER-SIX: TECHNO-ECONOMIC AND ENVIRONMENTAL ASSESSMENT OF A BIOREFINERY FOR CO-PRODUCTION OF XYLAN BIOPOLYMERS AND BIOETHANOL FROM SUGARCANE HARVESTING RESIDUES

Chapter Intended for Publication in 'Bioresource Technology' Journal, IF= 7.539

Article Title: Techno-economic and environmental assessment of a biorefinery for co-production of xylan biopolymers and bioethanol from sugarcane harvesting residues

Authors: Gezahegn T. Mihiretu, Abdul M. Petersen, Annie F. Chimphango and Johann F. Görgens

Declaration: This chapter is a manuscript under preparation due for submission once agreed upon by all authors

Objective of Dissertation and Summary of findings of this Chapter

This chapter addresses objective 5 of the present research primarily aimed at the techno-economic assessment of a lignocellulosic biorefinery for co-production of hemicellulosic biopolymers with bioethanol and electricity. This modelling study was carried out based on the experimental study (Mihiretu et al., 2019) which investigated the effects of alkalinised steam explosion pretreatment (ASEPT) conditions on xylan extraction, cellulose digestibility and ethanol yield for two feedstocks, of which SCT is one. This fractionation method (ASEPT) was found more effective on sugarcane trash (SCT) which was thus considered as a feedstock of choice for this study. This scenario-based modelling study intended to assess how a new line of production for 'xylan biopolymers' will impact the techno-economic viability of a 'biorefinery' that would otherwise produce only bioethanol and electricity from the raw biomass.

The study results suggested that co-production of xylan biopolymers from sugarcane harvesting residues can substantially boost up the economic performance ethanol-centred biorefinery by lowering the selling price of cellulosic ethanol, the main product here but still not competitive enough in the ethanol market. For instance, the study showed that a minimum selling price of 809 USD/ton of xylan biopolymers would be required should the biorefinery avail bioethanol at a price of 0.70 USD/L. The introduction of xylan biopolymers was also observed to render the minimum selling price of ethanol (MESP) much more sensitive to variations made in economic parameters that can have significant impact on it.

Candidate Declaration

With regard to Chapter 6, page numbers 144-196 of this dissertation, the nature and scope of the candidate's contributions were as follows:

Name of Contribution	Extent of Contribution (%)
Study planning	70
Study Execution	60
Interpretation of results	60
Writing of the chapter	100

The following co-authors have contributed to Chapter 6, page numbers of 144-196 of this dissertation:

Name	Email Address	Name of Contribution	Extent of Contribution (%)
Abdul M. Petersen	ampetersen@sun.ac.za	Reviewing of chapter Interpretation of results Study Planning Study execution	25 20 15 40
Annie F. Chimphango	achimpha@sun.ac.za	Reviewing of chapter Interpretation of results	25 10
Johann F. Görgens	jgorgens@sun.ac.za	Reviewing of chapter Interpretation of results Study planning	50 10 15

Signature of candidate: _____ Date: _____

Declaration by co-authors

All authors have read and approved the final manuscript and hereby confirm that:

1. The declaration above accurately reflects the nature and extent of contributions by the candidate and co-authors to Chapter 6, page numbers 144-196 of this dissertation,
2. no other authors contributed to Chapter 6, page numbers 144-196 of this dissertation, besides those specified above, and
3. potential conflicts of interest have been revealed to all interested parties and that necessary arrangements have been made to use the material in Chapter 6, page numbers 144-196 of this dissertation.

TECHNO-ECONOMIC AND ENVIRONMENTAL ASSESSMENT OF A BIOREFINERY FOR CO-PRODUCTION OF XYLAN BIOPOLYMERS AND BIOETHANOL FROM SUGARCANE HARVESTING RESIDUES

Authors: Gezahegn T. Mihiretu, Abdul M. Petersen, Annie F. Chimphango, Johann F. Görgens

Stellenbosch University, Process Engineering Department, Private Bag X1, Matieland
Stellenbosch 7602, South Africa

ABSTRACT

The present modelling study was primarily aimed at evaluating the techno-economic viability of a lignocellulosic biorefinery for co-production of xylan biopolymers, bioethanol and electricity from sugarcane harvesting residues subjected to alkalinized steam explosion pretreatment at (204 ℃, 16.5 bar, 10 min). With a daily capacity of 1000 tons of raw biomass, co-production of xylan biopolymers was shown to have substantially improved the economic performance of the multi-product biorefinery by lowering the selling price of ethanol against higher values under the benchmark processes. A minimum selling price of 809 USD/ton of xylan co-product was determined by fixing ethanol selling price at 0.70 USD/L (market price of ethanol in 2019); higher xylan prices could further lower the ethanol prices. Even though the economic viability of the biorefinery was significantly enhanced with co-production of xylan than without, this multi-product biorefinery complex was rendered rather energy-intensive as a result of such co-production scheme where the recovery of xylan biopolymers necessitated substantial thermal and electrical energy demands. From environmental point of view, the co-production of xylan biopolymers along with bioethanol and electricity was shown to have a positive contribution towards mitigating GHG emissions from fossil sources, but only marginally higher GHG emissions savings than the benchmark processes.

Keywords: Techno-economics; lignocellulosic biorefinery; xylan biopolymers; alkaline steam explosion pre-treatment; sugarcane harvesting residues

6.1. INTRODUCTION

Driven by the growing need to decarbonize conventional fossil-based economic systems by environmentally more sustainable ones, there is undoubtedly a renewed interest to advance the development of second-generation (2G) biorefineries based on lignocellulosic biomass. Advanced biofuels, notably cellulosic ethanol, have probably been at the forefront of technological developments realized therein, albeit with little commercial success – a pitfall limiting industrial-scale development of lignocellulosic biorefineries (Ernsting and Smolker, 2018; Lynd et al., 2017; Littlewood et al., 2013). One strategic approach in enhancing the economics of bioethanol production has been to look at additional sources of fermentable sugars other than cellulose (Humbird et al., 2011; Hahn-Hägerdal et al., 2006). In this context, hemicelluloses – the second most abundant structural sugars in lignocelluloses – have been regarded as a potential source of C-5 sugars which can be co-fermented with C-6 sugars derived from cellulose. Even though technological improvements in more efficient co-fermentation processes can result in enhanced ethanol yield per unit biomass, making lignocellulosic biorefineries economically attractive based on the sole production of such a low-value product as ethanol may remain a challenge (Knudsen and Rønnow, 2020; Pandey et al., 2019).

An alternative biorefinery approach towards enhanced economic utilization of lignocellulosic biomass is to target hemicelluloses as resource base for a high-value biopolymer as functional biomaterial having potential applications in the food, agricultural, biomedical, and biopharmaceutical industries (Ebringerova A., 2006; Elite et al, 2012; Norstroem et al., 2015; Hu et al., 2018). In this context, integrated production of high-value hemicellulose-based products with bioethanol in a multi-product biorefinery may improve the economic viability of cellulosic ethanol production (Rosales-Calderon and Avantes, 2019; Baruah et al., 2018; Mihiretu et al., 2017). Even though such multi-

product biorefinery approach is inevitably expected to lead to increased economic utilization of lignocellulosic biomass, it can also give rise to technical and process optimization challenges owing to the competing nature of each line of production leading to the respective biorefinery product (Serna-loaiza et al., 2019; Rosales-Calderon & Arantes, 2019; Silveira et al., 2015). These technical challenges coupled with the commercial uncertainties often associated with large-scale biorefineries justify the need to assess their techno-economic viability while in their early stage of development.

There are quite a number of techno-economic studies with the aim of utilizing hemicelluloses towards high-value products. For instance, in Geng et al., (2019) the economic potential of biopolymeric hemicellulose extracts (obtained from sugarcane bagasse, switch grass and poplar via alkaline pretreatment) was evaluated for applications as a starting material for the production of xylo-oligomeric prebiotics. A more recent study by Ou et al., (2021) conducted techno-economic assessment of a biorefinery whereby hemicellulose and lignin extracts (obtained via a combination of auto-hydrolysis and mechanical refining pretreatment) would be converted into high-value co-products, i.e. hemicelluloses into xylitol and lignin into polyol. This study revealed that co-production of xylitol and polyol resulted in around 24% reductions in the minimum sugar selling price, i.e. from 446 USD/ton down to 342 USD/ton of sugars produced. The economic gains from such co-production scheme were also shown to outweigh the additional capital investment incurred; however, the envisaged biorefinery was reportedly unable to meet its energy requirement by its own thus necessitating the purchase of external power (Ou et al., 2021). Another recent study by Lan et al., (2021) assessed the economic viability of xylo-oligosaccharides (XOS) produced from miscanthus via autohydrolysis and purification; results showed that the minimum selling price for XOS could vary the purity level and scale of production of XOS as targeted

product. For instance, the minimum selling price for XOS (90% purity) was estimated between 4030 to 8970 USD/ton of XOS depending on the scale of daily production of XOS (i.e. between 50-250 ton/day, the lowest selling price being at the highest capacity).

From ethanol production point of view, several techno-economic assessment (TEA) studies have been carried out based on different feedstock types and different pretreatment approaches. A good summary of such studies comprising of ethanol production capacity, feedstock type and prices, total capital investment (TCI) requirement and minimum ethanol selling price (MESP) has been provided in Dao et al., (2018). Considering the current status of bioethanol production from lignocellulosic residues, it can generally be concluded that industrial-scale production of 2G bioethanol is far from commercial success, be that in terms of price competitiveness and overall project profitability (Saini et al., 2020; Franck et al., 2019; Lynd et al., 2017; Brown et al., 2013). Even though the commercial performance of lignocellulosic bioethanol production is expected to be boosted up by following a multi-product biorefinery approach, how and to what extent that can be achieved through co-production of hemicellulosic biopolymers is also far from clear. That born in mind, a recent study by Mihiretu et al., (2019) has demonstrated experimentally the possibility of co-producing xylan biopolymers and bioethanol by the application of alkali-catalysed steam explosion pretreatment on two feedstock types (namely, sugarcane harvesting residues and aspen wood sawdust) in a biorefinery context. The present study considers whether such a co-production scheme offers improved financial viability through techno-economic assessment. Under the experimental conditions investigated therein, sugarcane residues was shown to have comparatively better results in terms of xylan extraction and ethanol production yields, thus selected for this techno-economic case study (Mihiretu et al., 2019).

Sugarcane harvesting residues represents an attractive bioresource that can be valorised into advanced biofuels and other high-value biopolymeric co-products (Gomez et al., 2014; Pierossi and Bertolani, 2018; Nogueira et al., 2019). Furthermore, the development of lignocellulosic biorefineries based on sugarcane biomass, in general, and sugarcane harvesting residues, in particular, has been identified as one strategic approach for sustainable economic, social and environmental performance of the South African sugar industry (Pierossi and Bertolani, 2018; Pachón et al., 2018; Mandegari et al., 2017; Petersen et al., 2017). In this perspective, such a techno-economic assessment study for the co-production of hemicellulosic biopolymers and bioethanol in a biorefinery setup is intended to shed light on the viability of enhancing the economic utilization of these residues, which may have otherwise remained underutilized.

Along with their techno-economic assessments, large-scale development of biorefineries should also take into account environmental sustainability as one essential dimension requiring due consideration for analysis. In this respect, a number of studies have conducted life cycle assessment (LCA) of lignocellulosic ethanol production (Dao et al., 2018; Chang et al., 2017); and, in terms their GHG reduction potential, 2G bioethanol was generally considered to have better environmental performance compared to 1G bioethanol or against their fossil counterparts (Dao et al., 2018; Soam et al., 2016). Bioethanol produced via biochemical conversion of lignocellulosic biomass was reported to have around 50-95% GHG reduction potential when compared to utilizing non-renewable fossil-fuel baseline (Dao et al., 2018; Soam et al., 2016). For instance, in Soam et al., (2016), production of cellulosic ethanol (intended for use as transportation fuel) from rice straw via steam explosion pretreatment was reported to have around 89% GHG emission reduction against gasoline baseline. However, assessment of the environmental performance of multi-product lignocellulosic biorefinery systems – be it a comprehensive

LCA study or just its relative GHG emissions reduction potential – could be far complicated than it is for sole production of bioethanol.

The primary objective of this study was to assess the techno-economic performance of a lignocellulosic biorefinery system where co-production of xylan biopolymers, bioethanol and electricity from sugarcane harvesting residues would take place through the application of alkalinized steam explosion pretreatment. Material and energy balance results generated through AspenPLUS® process simulations shall constitute the central part of this techno-economic analysis as they serve as the basis for estimating the capital and operational cost items involved therein. As a basis for comparison, the minimum selling price for bioethanol (MESP) was determined under two sets of biorefinery scenarios identified for this purpose: one where co-production of xylan biopolymers takes place with bioethanol and electricity; and the other set where only bioethanol and electricity production takes place. Furthermore, model parameters such as feedstock price, internal rate of return, total capital and operational cost estimates as well as selling price for xylan biopolymers were analysed for their effect on the minimum ethanol selling price as key indicator of the economic performance of the envisaged biorefinery. Additionally, the present study shall touch upon the impact of the envisaged biorefinery towards mitigating climate change effects through apparent reduction of greenhouse gas (GHG) emissions, mainly carbon dioxide. Accordingly, the potential GHG emissions which can be avoided (i.e., GHG savings) under each biorefinery scenario were estimated in g CO_2eq/MJ biofuel using the RSB-Global GHG calculation method.

6.2. METHODOLOGY

6.2.1. Feedstock availability, plant capacity and location

Sugarcane harvesting residues, of South African origin, shall constitute the feedstock type for the standalone biorefinery facility for an integrated production of hemicellulosic (xylan) biopolymers, bioethanol and electricity. The present study primarily intends to assess the techno-economic viability of this multi-product biorefinery against benchmark processes where only bioethanol and electricity are produced based on the same feedstock type and quantitative input. To this end, three process scenarios were identified (described herein under section 6.2.4) each of which shall have a capacity to process 1000 tons of dry biomass on a daily basis. With such processing capacity and around 270 annual operating days, the estimated annual ethanol production under all process scenarios falls fairly well within the capacity range of existing cellulosic ethanol plants based on agricultural residues (Lynd et al., 2017; Franck et al., 2019). The envisaged biorefinery shall be located within reasonable proximity to the biomass source, i.e. in the vicinity of existing sugarcane farms in the regions of KwaZulu-Natal and Mpumalanga (see www.sasa.org.za). Sugarcane residues intended for the biorefinery are assumed to be mechanically collected afield while cane stalks are harvested for subsequent crushing at local sugar mills. Sugarcane residues, consisting mainly of dried leaves and tops, generally make up around 13% (w/w) of the sugarcane biomass which, on average, is grown around 20 million tons annually (Pippo et al., 2011; Pachon et al., 2018; GAIN Report, 2019). On this basis, 10 to 15% of harvestable residues are assumed to be available as feedstock for the biorefinery, which shall have similar duration of annual operational period as that for local sugar mills.

6.2.2. Process Description

6.2.2.1. Process overview

Sugarcane harvesting residues, as characterized in Mihiretu et al., (2019), represents the lignocellulosic feedstock to be processed by the envisaged biorefinery. Alkalinized steam explosion pretreatment is the central processing step in the overall biorefinery complex as it is meant to achieve a dual purpose: extracting xylan-rich hemicellulosic biopolymers from the raw biomass while simultaneously rendering the cellulosic portion more amenable to enzymatic digestion. To ensure efficient recovery of hemicellulose extracts from the lignocellulosic matrix, the pretreated biomass is subsequently separated into solid and liquid fractions through filtration coupled with solids' washing step. The resulting extraction hydrolysate (liquid fraction) containing the xylan extracts as well as other solubilized biomass components is subjected to a series of purification, concentration, separation and dewatering steps leading to xylan biopolymers as a major co-product. Whereas the water insoluble solids (solid fraction) would serve as a substrate for ethanol production via enzymatic hydrolysis and fermentation steps followed by ethanol recovery using conventional distillation and molecular-sieve dehydration units. Along with co-production of xylan biopolymers and bioethanol, recovery of lignin-rich biosolids from side streams (both from xylan and ethanol recovery plants) constitutes an integral part of the biorefinery where the recovered biosolids would serve as fuel for co-generation of steam and electricity. Liquid streams with biogenic contents not recovered in solidified form are directed to wastewater treatment plant where the organic contents therein are anaerobically digested to produce biogas which, together with the biosludge, shall serve as additional fuel to the co-generation plant (Aden et al., 2002; Humbird et al., 2011).

6.2.2.2. Detailed Description of Major Biorefinery Segments

The application of alkalinized steam explosion pretreatment for the extraction of biopolymeric hemicelluloses from sugarcane harvesting residues, while simultaneously enhancing the enzymatic digestibility of the cellulosic portion, is the key aspect of this biorefinery study. The experimental basis hereto was laid by a recent study (Mihiretu et al., 2019) where the optimal conditions for xylan extraction yield and enzymatic cellulose digestibility were established for sugarcane trash alkali-impregnated at 5% NaOH loading on dry biomass prior to its pretreatment. Accordingly, xylan yield of 51% and cellulose digestibility of 91.7% (which corresponded to 83.4% ethanol yield) were attained as optimal values for alkalinized steam explosion pretreatment at (204 °C, 16.7 bar) for 10 min retention time (Mihiretu et al., 2019). These optimized conditions were used as model inputs while simulating the pretreatment process at 50% (w/w) of dry biomass loading in the steam explosion reactor. For the techno-economic study purpose here, the envisaged biorefinery shall comprise of the following major process segments within its battery limit: (1) biomass pretreatment and hemicellulose extraction plant (2) xylan recovery plant; (3) bioethanol production plant; and (4) bio-solids (lignin) recovery plant; (5) wastewater treatment plant; and (6) steam and power co-generation plant. These segments are described in more details as follows.

(I) Biomass pretreatment and hemicellulose extraction steps

The pretreatment and hemicellulose extraction plant (see Fig 6.1) comprises of three major unit processes at forefront: presteaming of raw biomass using low pressure steam (180 °C; 10 bar) to remove non-condensable gases entrapped therein; impregnation of presteamed biomass with an alkaline agent (5% NaOH loading on raw SCT biomass, dry weight basis); and, steam explosion pretreatment of alkali-impregnated biomass using high pressure steam (260 °C; 16.7 bar). Steam required for presteaming

and pretreatment purposes is supplied by the low pressure utility boiler, with the steam intended for pretreatment being further compressed to a pressure of 16.7 bar and heated to a temperature of 260 °C. The steam requirements for presteaming and pretreatment were considered around 10 and 40% (w/w) of the raw biomass respectively (Aden et al., 2002; Petersen et al., 2021). The condition inside the steam explosion reactor was maintained at 204 °C and 16.7 bar (Mihiretu et al., 2019). The presteamer and pretreatment reactor shall each have processing capacity estimated based on the assumption that that the material input (i.e. biomass and water) will occupy 90% (v/v) of the overall holding volume (Aden et al., 2002; Humbird et al., 2011).

Pretreated biomass is discharged into a blowdown tank with instantaneous depressurization effect, a condition which results in substantial release of flash vapour (100 °C) at an amount assumed around 15% (w/w) of the pretreated biomass. The slurry is subsequently separated into solid and liquid fractions using pneumapress filtration system equipped with water spraying unit for simultaneous washing of the solid residues at a loading ratio of 5:1 (w/w) water onto insoluble biomass solids (WIS). This step not only ensures efficient recovery of hemicelluloses extracts which may otherwise remain entrapped in the pretreated solid residue, but also that the resulting solid fraction (WIS) would be clean from pretreatment by-products having potential inhibitory effect on the enzymatic hydrolysis and/or fermentation processes. The liquid hydrolysate with hemicellulose extracts (mainly xylan at 51% recovery therein) and other solubilized biomass components (mainly lignin at 70% recovery therein) is pumped to the xylan recovery plant (see Fig 6.1 and sub-section (II) herein under); whereas the solid fraction (mainly cellulose, 95% recovery) serves as substrate for ethanol production through hydrolysis-fermentation (see sub-section (III) herein under). Biomass solids recovery after filtration and washing steps, i.e. in WIS, was taken at 65% (Mihiretu et al., 2019).

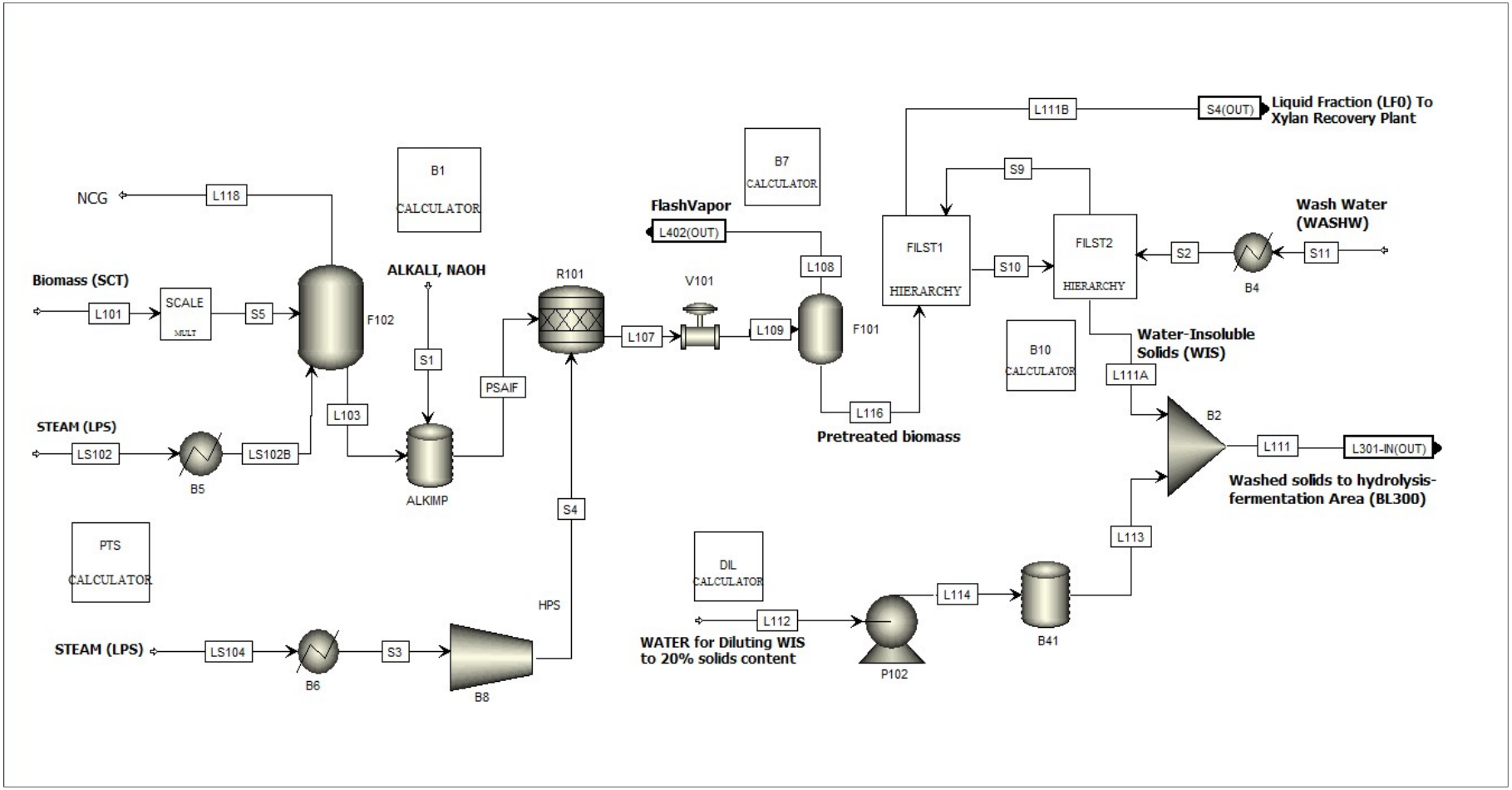

Fig 6.1. ASPEN Process Flowsheet for biomass pretreatment and hemicellulose extraction plant

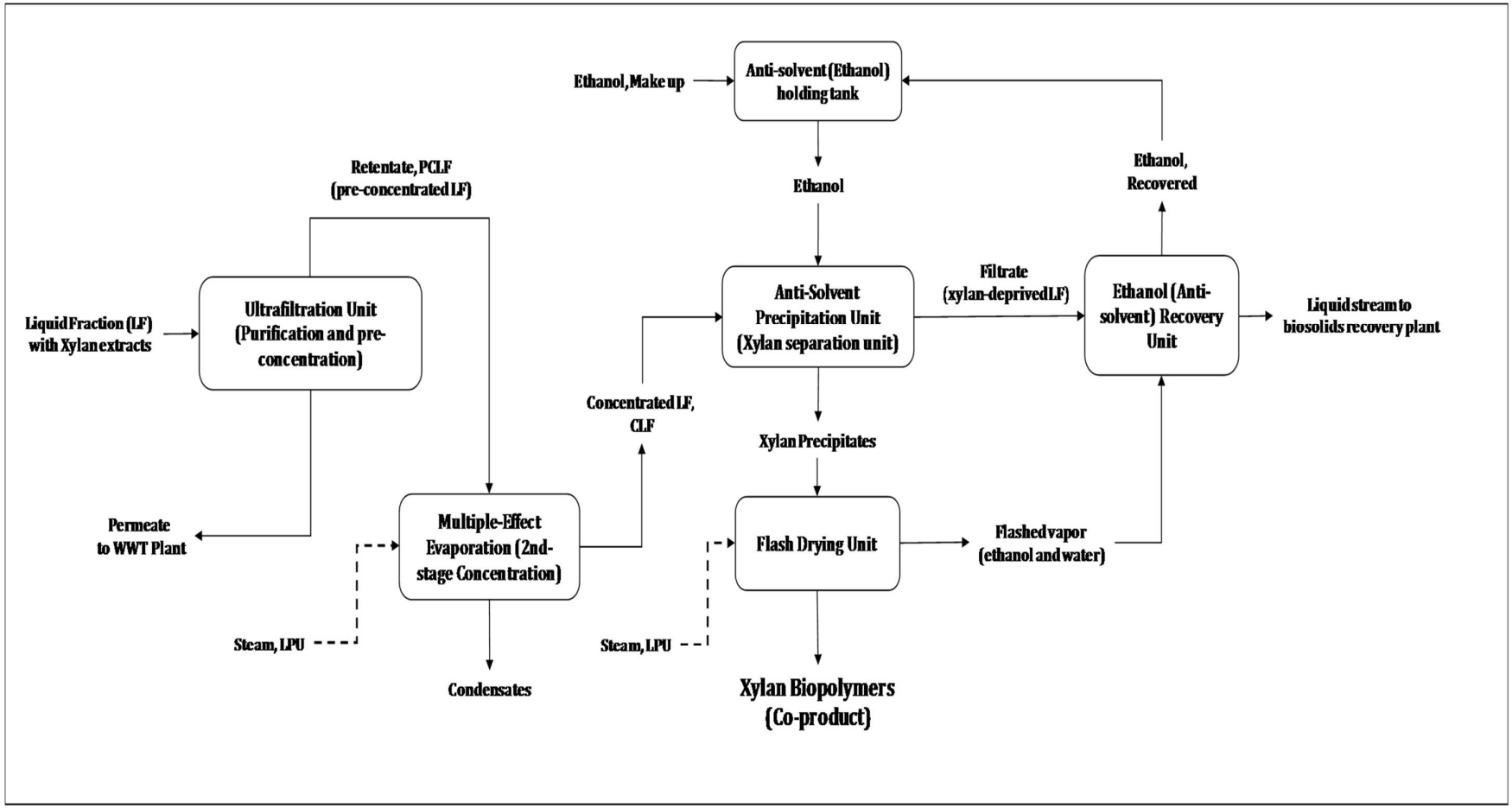

Fig 6.2. Simplified Block Diagram for Xylan Recovery Plant with major processing steps involved therein

(II) Recovery of xylan biopolymers

The recovery of xylan extracts from the extraction hydrolysate shall involve successive separation steps which eventually lead to xylan biopolymers as co-product (see Figure 6.2), namely: (i) pre-concentration of xylan extracts via ultrafiltration (UF) separation system and further concentration using multiple-effect evaporation system; (ii) recovery of xylan extracts using ethanol as an anti-solvent precipitation (ASP) agent; (iii) drying of xylan precipitates using low-temperature flash drying system; and (iv) recovery of ethanol (anti-solvent) from xylan-deprived liquid fraction via distillation.

(i) Concentrating xylan extracts using ultrafiltration and evaporation

The liquid fraction containing the xylan extracts along with other solubilized biomass components is predominantly water (>90% w/w) with low concentration of xylan extracts therein (2.5 to 4.5 g/L), thus necessitating substantial removal of water from it as the first step towards recovering biopolymeric xylan. An ultrafiltration (UF) system was considered for initial removal of close to 50% of the water in the liquid fraction so that the xylan extracts and other solubilized biomass components therein would be pre-concentrated to the range of 15 to 20 g/L. The UF system intended for this purpose shall have spiral-wound ceramic membrane with molecular weight cut-off size of 5 to 15 kDa (~10 kDa), membrane working temperature of 50 - 60 °C and a transmembrane pressure (TMP) in the range of 5 to 7 bar (Buruiana et al., 2014; Bokhary et al., 2017; Al-Rudainy et al., 2019; Persson et al., 2007; Peng et al., 2019). Such configuration is desired to retain significant portion (90±5%) of the xylan extracts and co-solubilized lignin; while monomeric sugars, degradation products and ionic entities being allowed to permeate through the membrane along with water which is pumped to the wastewater treatment plant.

Even though ultrafiltration (UF) systems are widely favoured for their further development and implementation for hemicelluloses recovery, the technology is poised to suffer from inevitable membrane fouling and subsequent impact on its operational efficiency (Al-Rudainy et al., 2019; Bokhary et al., 2017; da Silva et al., 2015). Ultrafiltration (UF) systems are among pressure-driven membrane-based separation technologies which are being widely investigated and considered for biorefinery applications for purification and/or concentration of process streams (Alriols et al., 2014; Abels et al., 2013; Al-Rudainy et al., 2019). Owing to their modular arrangement, commercial availability, applicability for selective removal of targeted entities, ability to be run based on known process configurations and standardized operating procedures, the UF systems may represent key biorefining (separation and purification) step thereby resulting in enhanced economic utilisation of lignocellulosic components towards bio-based products of higher value. However, membrane fouling is one inevitable operational challenge towards successful deployment of the UF systems – a problem which needs to be properly managed and systematically handled to ensure efficient operation of the UF plant. The flux decline that can result from membrane fouling can be overcome by following and implementing industrially established operating procedures in cleaning membrane-based ultrafiltration plants (such as in biopharmaceuticals, food processing, water treatment plants), closely monitoring and controlling the hydrodynamic conditions at the membrane surfaces (Transmembrane pressure, cross-flow velocity, pH) as well as by deploying appropriate cleaning mechanisms which can lead to more stable permeate flux rates (restore the initial permeability of the fouled membranes). Such cleaning can, for instance, be through pulsed backflushing of membranes coupled with chemicals (caustic solution, citric acid, sodium hypochlorite) to further facilitate cleaning of membranes from foulants (Perry, 2008; Abel et al., 2013; Al-Rudainy et al., 2019).

The retentate from the UF unit, i.e. the pre-concentrate, may yet contain significant amount of water which is not removed at the ultrafiltration step, but needs to be removed in view of the energy-intensive nature of the technological process proposed for xylan recovery, i.e. mainly ethanol-based anti-solvent precipitation technique where recovery of ethanol is to take place via distillation. Additionally, the amount of ethanol required for xylan precipitation purpose depends directly on the volumetric quantity of the pre-concentrate, thus necessitating further de-watering to economize on ethanol consumption. A second-stage removal of water employing multiple-effect evaporation (MEE) system was, therefore, considered to remove around two-third of the water in the pre-concentrate. To this end, the amount of low pressure steam (111 °C, 1.46 bar) to be used as heat source for the MEE, the number of effects required and the conditions (pressure and temperature) under each effect were optimized using AspenPlus® simulation software with the aim of minimizing energy requirement and ethanol consumption for xylan recovery. Forward-feed penta-effect evaporation system was considered for further dewatering of the pre-concentrate with decreasing pressures of 0.91>0.71>0.51>0.31>0.1 bar and temperatures of 98.1>91.1>83.1>71.3>49.5 °C set for each consecutive effect along the feed's direction. The MEE was optimized in such a way that the concentrate would leave the final effect at a temperature twice as high as the working temperature (i.e. 25 °C) chosen for the subsequent precipitation process. With the cascade of UF and MEE units, around 85% of the water in the extraction hydrolysate was removed thus resulting in a concentrate having around 47±2% solids of which xylan extracts would make up 44±1% (w/w).

(ii) <u>Recovery of Xylan Biopolymers using Anti-Solvent Precipitation Technique</u>

Owing to the alkaline nature of pretreatment conditions applied, significant removal of lignin could take place during hemicellulose extraction from sugarcane

residues, SCT (Mihiretu et al., 2019). The need to recover this solubilized lignin and use it as fuel source to the CHP plant, on the one hand, and the need to purify the xylan extracts from such, on the other, clearly poses a techno-economic challenge necessitating a viable solution. For the recovery of xylan biopolymers from the concentrate leaving the MEE unit (see Fig 6.2), a process comprising of anti-solvent precipitation (ASP) technique is proposed for selective precipitation of xylan extracts using ethanol as an ASP agent, while leaving lignin therein in solubilized state. The underlying principle here is that solubility of xylan in water can be increasingly lowered with increased addition of ethanol into the aqueous solution thereby causing gradual precipitation of xylan extracts (Peng et al., 2012; Peng et al., 2019). Upon its apparently decreased extent of solubility in water-ethanol mixture, the xylan extracts gradually become supersaturated and subsequently start to precipitate out; whereas the lignin therein remains in dissolved state. The application of ethanol for selective precipitation and recovery of hemicelluloses has been reported in extant literature (Buranov and Mazza., 2010; Weinwurm et al., 2014; Al-Rudainy et al., 2019). These studies also suggest that the solubility of lignin is dependent on the ethanol content and gets maximal with 60 to 70% (v/v) ethanol contents (Buranov et al., 2010; Weinwurm et al., 2014). For the study purpose here, the amount of ethanol (95% v/v) per unit volume of concentrated fraction containing the xylan extracts was taken at 70% (v/v). This approach is desired to result in the recovery of 70-90% (w/w) the xylan extracts in the precipitated form with purity of 90±2.5% (w/w). Even though ethanol-based precipitation of xylan extracts can be appealing in the biorefinery context, the recovery of this ethanol to be re-used as an ASP agent can potentially lead to increased thermal energy demand of the biorefinery complex.

The precipitate from the ASP unit, which is now predominantly xylan (~70% w/w) is subsequently fed to a conical mixer dryer where the xylan product will be recovered to

the level of 88% dry. The drying vessel shall be internally equipped with a rotating screw and externally with a heating jacket or coil into which the heating medium flows in and out. Low pressure steam shall be used as a heating medium to allow indirect heating of the wet product inside the vessel to a temperature of around 85±5 ℃ thus enabling removal of water and residual ethanol therein in vapour form. To ensure that no vapour condensation would take place inside the process vessel, the top cover of the vessel shall also be equipped with a heating compartment (also heated by steam, LPU) where the vapour outlet (mainly water and ethanol) are heated up 95±5 ℃. This vapour mix is directed to the distillation-based recovery unit where ethanol used as anti-solvent is recovered; whereas the dried xylan co-product is collected from the bottom of the dryer. Whereas the filtrate from the precipitation unit (which is a mixture of ethanol, water and soluble biomass components, mainly lignin), is transferred to a separate distillation unit where ethanol used as ASP agent is recovered to the extent of 98%. This means about 2% of the overall ethanol required per batch of precipitation needs to be supplied as make-up ethanol. The distillation bottoms obtained after ethanol recovery is rich in soluble biomass components, especially lignin, which needs to be recovered and be used as fuel source to the steam generation plant (see Fig 6.2).

(III) Bioethanol production and recovery

Ethanol production and recovery essentially consists of two major processing steps: (a) enzymatic hydrolysis and fermentation units where the pretreated and cellulose-rich solid residue obtained after hemicellulose extraction is fed as substrate for ethanol production; and (b) distillation and dehydration units where the produced ethanol is recovered in its anhydrous form, i.e. 99.5% (v/v). For the study purpose here, technological processes for lignocellulosic ethanol production and recovery were assumed to have been well established and standardized. To this end, technical

specifications that pertain with the distillation, rectification and molecular sieve dehydration units were adopted from previous studies on biomass-to-ethanol production (Aden et al., 2002; Kazi et al., 2010; Humbird et al., 2011; Petersen et al., 2021). Some basic input parameters such as cellulose digestibility, ethanol yields and fermentation efficiency were, however, as experimentally determined by Mihiretu et al., (2019).

(IV) Solids recovery, wastewater treatment and co-generation plants

Lignin-rich liquid streams from xylan recovery plant as well as from ethanol production plant (see Fig 6.3) shall be dewatered using multiple effect evaporation and/or pneumatic press filtration systems. In the former case, the liquid stream from ethanol (anti-solvent) recovery unit (see Fig 6.2), a triple-effect evaporation system was deployed to remove water from it so that the resulting concentrate (syrup) leaving the final effect will have around 60% (w/w) solids content. Whereas, in the case of the stream from the actual ethanol production plant, a pneumapress filtration system was used to separate the distillery sludge into solid and liquid fractions. The sludge leaving the distillation column is predominantly water (95±2% w/w), thus necessitating such dewatering step to recover the biogenic solids therein. The pneumapress was intended to remove as much water from the sludge as possible so that the resulting pressate shall minimally have a 50% solids content. Air required for the pneumatic operation of the press filter was compressed to about 8±1.5 atm (Petersen et al., 2021; Humbird et al., 2011). The biosolids so recovered, i.e. the syrup and pressate, fulfil the minimum acceptable moisture content for subsequent combustion at the co-generation plant. The technologies, process configuration and conditions for biosolids recovery were discussed in previous studies and are adopted in this study (Aden et al., 2002; Humbird et al., 2011; Petersen et al., 2021). While the condensate from all triple effects shall serve as process water, the liquid fraction from the pneumatic press filter, which still has significant

organic contents in it, is directed to the wastewater treatment plant where organic contents therein are anaerobically converted into biogas, a by-product which will serve as additional fuel source to the co-generation plant.

In the present modelling study, the recovered biosolids (pressate and syrup) were mainly used for steam generation purpose to meet the process steam demands of the biorefinery complex; whereas the biogas produced at the WWT plant was mainly geared towards biopower generation primarily intended to meet the electricity demands of the biorefinery. The steam generation plant consists of three major units, namely: the combustor, low-pressure utility boiler and back pressure turbine. The lignin-rich biosolids are fed to the combustor where their combustion takes place at very high temperature (1052 °C) using hot air initially preheated to 235 °C. The thermal energy contained in the hot air stream leaving the combustor is primarily used to generate steam at (240 °C; 11 atm) which is directed to the turbine where low pressure steam (175±10 °C; 9±1.5 atm) is extracted to meet the process heat demands of the biorefinery. The hot air, after being used for steam generation, was also used to preheat the ambient air to be used for biomass combustion; the gaseous combustion product is finally filtered through the baghouse and vented off to atmosphere.

With respect to power generation, the biogas produced at the WWT plant is first compressed to about 15 bar which is the pressure to be maintained in the combustion unit where the biogas is combusted at a temperature around 1290 °C. The ambient air required for biogas combustion was also compressed to the same working pressure of 15 bar whereby it is as well preheated to about 432 °C prior to entering the combustor. The combustion product which leaves the combustor at high temperature and pressure (1290 °C; 15 bar) is expanded into a gas turbine where its thermal energy is eventually converted to electrical power. While the process configuration for the co-generation of

steam and electricity was adopted from a recent study by Petersen et al., (2021), technologies for the co-gen and WWT plants are well-established, standardized and fit for purpose here (Aden et al., 2002; Humbird et al., 2011). The co-generation of steam and electricity from recovered biosolids and biogas forms an integral part of the envisaged biorefinery which aims to be energy self-sufficient based solely on biogenic sources (which originally are the sugarcane harvesting residues) for energy production purpose, i.e. no fossil-based energy inputs (e.g. coal, natural gas) for the biorefinery.

6.2.3. Modelling and simulation approach

The envisaged biorefinery, described in the preceding section 6.2.2, was modelled using ASPENPLUS® software (V11) thereby developing the overall biorefinery as well as major process segments within its battery limit into respective ASPEN flowsheets (See Appendix C for detailed flowsheets and summary of simulation results thereof). While developing these ASPEN flowsheets, major processing units were modelled using steady-state unit operation models from ASPEN library as follows. Units such as the steam explosion pretreatment, anti-solvent precipitation, hydrolysis and fermentation were modelled using RSTOIC reactor blocks based on simplified stoichiometric reaction paths (Al-Malah, 2017; Joelsson et al., 2016). The RStoic reactor model, often used to represent equipment when reaction kinetics are unknown, enables calculation of product stream flow rates based on user-specified reaction stoichiometry and extent of conversion of key component. The stoichiometric reaction statements may involve monomeric, oligomeric or polymeric entities. RGIBBS reactor model was used for biosolids and biogas combustion units (Zheng and Furimsky, 2003; Kamari et al., 2021). This model allows reasonable estimation of mass flow rates in the product stream based on the Gibbs free energy minimization algorithm; where equilibrium modelling is performed with the Gibbs free energy of the system set at minimum (Kamari et al., 2021). Distillation,

stripping and rectification units were modelled using the RadFrac block which is a rigorous multistage distillation column applicable for simulating all types of multi-stage vapour-liquid fractionation operations (Al-Malah, 2017; Aden et al., 2002).

With respect to ASPEN thermodynamic property methods, the non-random two-liquid (NRTL) activity model was used for property estimation of liquid and vapour phases (Aden et al., 2002; Al-Malah, 2017). NRTL is among the most commonly used method which can be applied to polar mixtures. The NRTL activity model correlates the activity coefficients of a compound with its mole fraction in the liquid phase concerned. The RKS-BM property method (i.e. Redlich-Kwong-Soave equation-of-state with Boston-Mathias alpha function) was used for biogas combustion and gas turbine units at co-generation plant (Pardo-Planas et al., 2017; Al-Malah 2017; Kamari et al., 2021); whereas the PENG-ROB method was applied for air compression units deployed at the same power generation plant (Doherty et al., 2013; Safarian et al., 2019; Kamari et al., 2021). Non-conventional thermodynamic properties which may pertain to such lignocellulosic components as cellulose, hemicelluloses and lignin were adopted from relevant NREL studies, as they are normally not fully in the ASPEN database (Aden et al., 2002; Kazi et al., 2010; Humbird et al., 2011).

The biorefinery model, once developed in ASPEN flowsheet form, was simulated with the primary objective of establishing material and energy balances which form the basis for sizing major equipment and utilities, and so for estimating capital and operating costs. Mass and energy balances were closed and optimized for the overall biorefinery as well as around major processing units therein (see Appendix C for detailed results summarized by major process flow segments). Primary data from Mihiretu et al., (2019) as well as secondary data from relevant literature were consulted to specify parametric

inputs. Summary of process parameters which have been considered and/or assumed are presented in Table B1-3 of Appendix B.

6.2.4. Biorefinery scenarios

Three process scenarios were identified to examine the impact of co-producing hemicellulosic (xylan) biopolymers on the techno-economic viability of the envisaged bioethanol-centred biorefinery (see Fig 6.3). These scenarios were approached based on how those major biomass components (i.e. cellulose, hemicelluloses and lignin) and, more specifically, how the hemicellulosic portion, of the sugarcane residues end up towards targeted end-products (bioethanol and/or xylan biopolymers and/or electricity). Under all scenarios, bioethanol and electricity shall commonly constitute two of the product mix towards which cellulose and lignin respectively serve as primary inputs. All minor biomass components as well as polysaccharides not consumed towards bioethanol and/or xylan biopolymers shall end up as additional fuel to the co-generation plant. Accordingly, the three process scenarios are briefly defined as follows**:**

(I) **Main-case scenario (MCS): Co-production of bioethanol and hemicellulosic biopolymers scenario.** This scenario represents the actual biorefinery where xylan biopolymers particularly constitute the co-product of interest. Hence, the liquid fraction containing the hemicellulose extracts is subjected to successive separation and purification steps which ultimately recover biopolymeric xylan (see Fig 6.2 & 6.3 and section 2.2 for detailed process description hereon).

(II) **Base-case scenario (BCS): Bioethanol and electricity only scenario.** Under this scenario, ethanol and electricity shall form the product mix with the liquid fraction containing the extracts being pumped to the wastewater treatment plant where hemicellulosic sugars therein are consumed to produce biogas – fuel source for

power generation plant (see Fig 6.3). This scenario shall form the base case against which the main-case biorefinery scenario is compared.

(III) Intermediate-case scenario (ICS): maximum ethanol scenario. Here, bioethanol and electricity shall form the product mix where, in particular, the hemicellulose (xylan) extracts in the liquid fraction are wholly diverted to the ethanol production plant (see Fig 6.3). The ICS is, therefore, about maximizing the ethanol yield by using xylan extracts to produce bioethanol. The use of celluloses and lignin remains similar to that in the BCS and MCS.

It is worth noting that the benchmark processes (i.e. BCS and ICS), share the same process segments for biomass pretreatment, ethanol production, biosolids recovery, wastewater treatment and co-generation plant as in the actual biorefinery scenario (MCS) except that the production line for xylan biopolymers is excluded in either of the cases (see Fig 6.3). In the ICS case, the liquid fraction containing the hemicellulose extracts is to be subjected to ultrafiltration separation with the aim of removing the ionic entities therein (especially the alkaline agents which were used for biomass impregnation purpose needs to be removed to ensure the pH of the hydrolysis-fermentation processes would not be rendered higher than required) in the permeate, whereas much of the hemicelluloses extracts are retained for subsequent diversion to the ethanol production plant. The ultrafiltration unit which was employed under the MCS for pre-concentration of the hemicellulosic extracts in the liquid fraction is identically applied to the ICS.

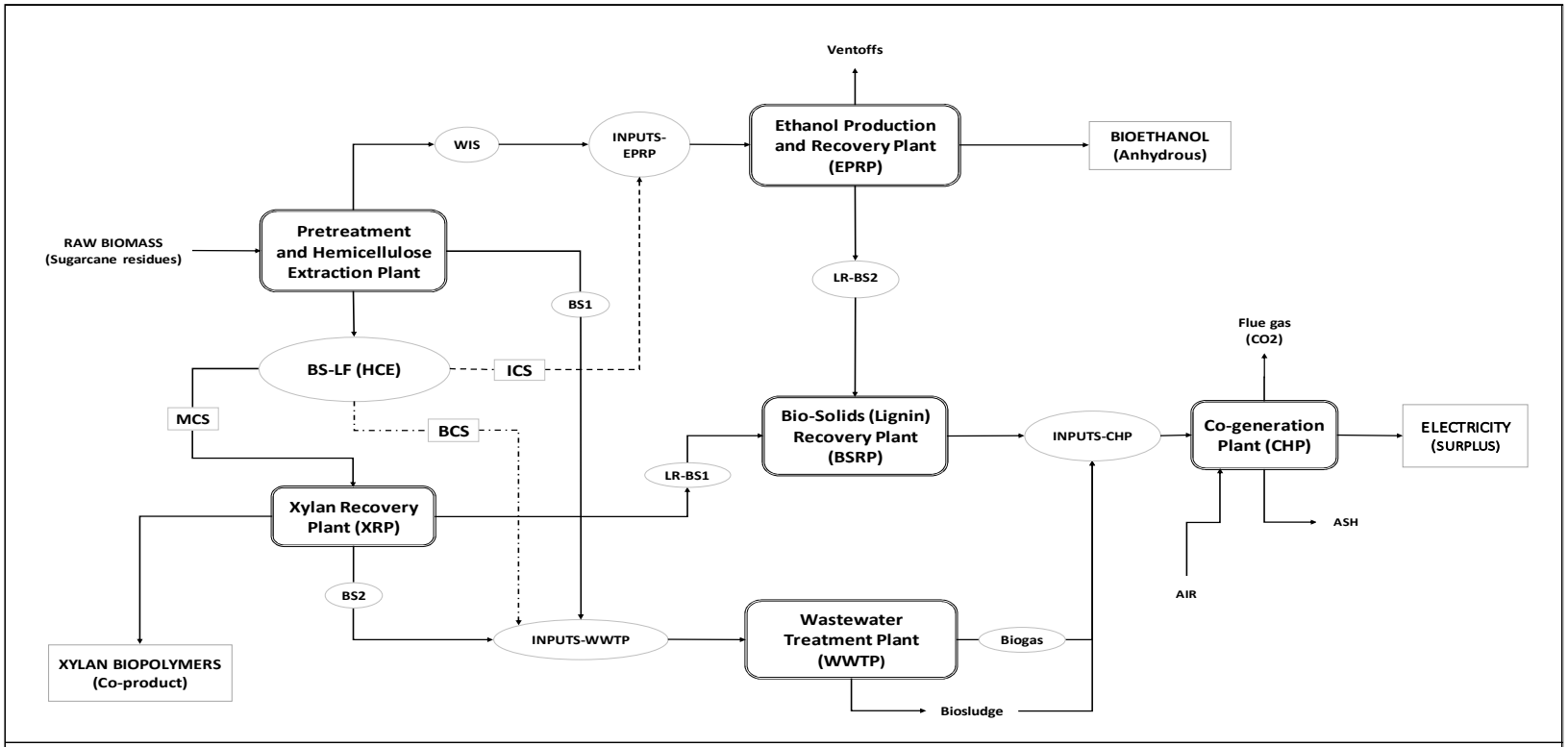

KEYS:
HCE = Hemicellulose (xylan) Extracts
MCS = Main-Case Scenario
BCS = Base-Case Scenario
ICS = Intermediate-Case Scenario
WIS = Water-Insoluble Solids (Solids Fraction)
BS-LF = Biomass solubles (BS) ending up in liquid fraction (LF)
BS1 = Biomass solubles flashed off at the pretreatment plant
BS2 = Biomass solubles permeating through the ultrafiltration unit

NB: BS1 and BS2 are mainly water with relatively little biomass solubles therein, thus headed to the WWTP to recover the water

KEYS, cont.
LR-BS1 = Lignin-rich biomass solubles (from the XRP)
LR-BS2 = Lignin-rich biomass solubles (from the EPRP)
XRP = Hemicellulose (Xylan) recovery plant
EPRP = Ethanol production and Recovery Plant
WWTP = Wastewater treatment plant
BSRP = Biosolids (Lignin) recovery plant
CHP = Steam and Power Generation (Co-generation) Plant
INPUT-'X' = Inputs to Plant 'X'

Fig 6.3. Diagram depicting point of divergence (BS-LF, HCE) among the three biorefinery scenarios (MCS, BCS & ICS)

6.2.5. Process economics

Economic analysis of the lignocellulosic biorefinery intended for co-production of xylan biopolymers, bioethanol and electricity from sugarcane harvesting residues was carried out in a comparative manner based on the three process scenarios described hereinabove (section 6.2.4). Mass and energy balance results generated using ASPENPLUS® simulation software formed the basis for subsequent economic evaluation steps, discussed under the following sub-sections.

6.2.5.1. Equipment sizing and cost estimates

Mass balance results were used as primary inputs for equipment sizing purpose and major process equipment were accordingly sized to appropriate capacity levels. Equipment cost data required for capital items were collected from existing literature (e.g. relevant NREL technical studies such as Aden et al., 2002; Humbird et al., 2011; Kazi et al., 2010) and/or other secondary sources (e.g. equipment suppliers/traders). Equipment cost variations that may arise with different equipment sizes were adjusted using cost-capacity relationships as shown under equation (6.1).

$$C2 = C1 * \left(\frac{S2}{S1}\right) \wedge n \qquad \text{---------- (6.1)}$$

Where, C1 = cost of equipment at capacity S1; C2 = cost of equipment at capacity S2; and n = exponent varying from 0.6 to 0.9 depending on the equipment type

Equipment cost variations that may arise from different years (base year vs. actual year of interest) were adjusted using cost indexes such as "Chemical Engineering Plant Cost Index" (see equation 6.2 below). All costs were adjusted to year 2019.

$$Cost\ in\ Year2 = Cost\ in\ Year\ 1 * \left(\frac{Cost\ Index\ in\ Year\ 2}{Cost\ Index\ in\ year\ 1}\right) \qquad \text{---------- (6.2)}$$

6.2.5.2. Total capital investment and annual operating costs

Capital cost estimates were made mainly based on established methods and procedures (Peters et al., 2003; Perry, 2008) and relevant studies carried out in the biorefinery context as is the present one (Aden et. Al., 2002; Kazi et al., 2010; Humbird et al., 2011; Petersen et al., 2021). Accordingly, major process areas falling within the battery limit of the biorefinery (i.e. the ISBL capital items) were first identified and the capacity of major processing equipment therein were determined based on simulated mass balance results. Preliminary cost estimation for major capital items, referred hereto as Inside battery-limit (ISBL) costs, was carried out using the factorial method. Costs for other 'non-major' capital items were estimated based on the ISBL costs multiplied by pre-specified factors (Aden et al., 2002; Peters et al., 2003; Perry, 2008; Humbird et al., 2011; Ereev and Patel, 2012). Major capital items identified within the ISBL of the biorefinery were biomass pretreatment and hemicellulose extraction plant (including major feedstock preparation units); xylan recovery plant; ethanol production plant; biosolids recovery, wastewater treatment and co-generation plants (see Fig 6.3). Other direct non-process capital items (aka 'outside battery-limit (OSBL)' items) include storage and handling; site preparation; building and structures; waste disposal; service facilities and land (Peters et al., 2003; Perry, 2008; Ereev and Patel, 2012). The ISBL and OSBL costs together make up the total direct costs (TDC). Indirect fixed costs include costs associated with engineering and supervision; construction expenses; start-up expenses; legal expenses, and contingency. The fixed capital investment (FCI) was the sum of total direct costs (TDC) and total indirect costs (TIC). The working capital (WC) was taken 5% of FCI (Aden et al., 2002; Peters et al., 2003; Humbird et al., 2011). Capital cost estimates form an essential part of the economic analysis as other cost estimates (including operating expenses, depreciation and project profitability) depend largely on it.

The envisaged biorefinery was assumed to operate 6500 hours a year over which the annual operating costs are estimated based on fixed, variable and other expenses (Aden et al., 2002; Peters et al., 2003; Perry, 2008; Giuliano et al., 2015; Lindorfer et al., 2019). Fixed operating costs are those for maintenance and repair, labour and supervision, annualized capital depreciation, local taxes and insurance, license fees and royalties. Major variable cost items include those for feedstock, non-feedstock input materials, utilities and miscellaneous materials (estimated 5 to 10% of maintenance costs). Fixed and variable costs together form direct operating costs (DOC). Expenses associated with general overheads, R&D, sales and reserves constitute indirect operating cost (IOC), which is estimated at 20 to 30 % of DOC. The annual operating costs (AOC) will be the sum of DOC and IOC; steps hereto are presented in Table 3.3 under Chapter 3.

Table 6.1. Economic parameters considered for the techno-economic study purpose

Parameter Description	Unit	Parametric value	Remark
Feed processing capacity, dry weight basis	[tons/day]	1000	Feedstock is 90% dry
Annual operating hours	[hr]	6500	75% on-time (9 months operation)
Economic Project lifespan	[Yrs]	20	20 to 30 years, average value considered
Construction period	[months]	30	
Capital expenditures during Constrution Period			TPI = Total Project Investment
Phase-I: First 6 months	[% TPI]	10	Project Completion status [%] by phase: 20, 50 and 30% during the first, second and third phases respectively
Phase-II: Next 12 months	[% TPI]	60	
Phase-III: Last 12 months	[% TPI]	30	
Start-up period	[months]	6	
Capacity utilization (as % full capacity)			
During start-up period	[%]	40	The biorefinery is assumed to operate at full capacity by the third year (after successful startup/commissioning)
Ramp up after start-up period: Year-1	[%]	50	
Year-2	[%]	75	
Year-3	[%]	100	
Depreciation Period			Double declining balance (DDB) and Straight line (SL) methods are applied in conjuction: with DDB values of 200% and 150% for the general plant and steam generation plants respectively
Steam generation plant (SGP)	[years]	20	
General plant (other than the SGP)	[years]	7	
Corporate Income Tax (CIT) rate, SA	[%]	28	Source: SARS
Discount rate	[%]	15	
Year of project analysis	[num]	2019	

Note: SARS= South African Revenue Service

6.2.5.3. Feasibility analysis and minimum selling prices

With estimates of TPI and AOC in place, the economic viability of the biorefinery project can be quantitatively evaluated using the discounted cash flow (DCF). Key parameters required to this end are presented in Table 6.2. Discount rate of 15% and corporate income tax rate of 28% were considered for South African case. The method of depreciation applied was the combination of straight line (SL) and double declining balance (DDB) methods (Aden et al., 2002; Perry, 2008; Kazi et al., 2010; Humbird et al., 2011). The Modified Accelerated Cost Recovery System (MACRS) was followed to determine the annual depreciated values of installed capital items. Accordingly, for steam generation plant (SGP) 20 years of depreciation period was considered; whereas for the rest of the biorefinery segments, referred hereto as 'General Plant' (GP), 7 years of recovery period was taken. Under the double declining balance method, the SGP and GP were respectively made to depreciate at 150% and 200% of that depreciation value found from the SL method (Short et al., 1995; Aden et al., 2002; Humbird et al., 2011).

For the purpose of assessing the profitability of the biorefinery project, minimum selling prices (MSP) for bioethanol and/or xylan biopolymers were determined inter-dependently under the main biorefinery scenario. The MSP was considered as a good indicator of how worth producing the targeted end-products is; market selling prices higher than the MSP apparently indicate enhanced profitability, thus desired. The minimum ethanol selling price (MESP) shall, therefore, serve as a quantitative basis to gauge the economic viability of the three scenarios (MCS, BCS and ICS) against each other as well as against reported prices. MESP was estimated under the following condition:

$$\text{Total annual revenues, TAR} = \text{Total annual Costs, TAC} \quad \text{----------} \quad (6.4)$$

For the main case scenario: TAR = R_{BE} + R_{XB} + R_{EE}; and, for the Base-case and intermediate-case scenarios: TAR = R_{BE} + R_E; where R_{BE}, R_{XB} and R_{EE} are revenues generated from sales of bioethanol (BE), xylan biopolymers (XB) and excess electricity (EE) respectively.

Annual costs for all scenarios: TAC = AOC + ACE + AIT, where AOC is the annual operating costs (fixed and variable costs); ACE is amortized capital expenses (annualized capital costs); and AIT is the annual income tax (tax paid on net revenues). The latter two (i.e. ACE and AIT) were determined using the following equations:

$$\mathrm{ACE} = (\mathrm{TPI}) * \frac{r*(1+r)^n}{(1+r)^n - 1} \qquad \text{----------} \ (6.5)$$

$$\mathrm{AIT} = \frac{R}{(1-R)} * (\mathrm{ACE} - \mathrm{ADC}) \qquad \text{----------} \ (6.6)$$

where, r and R are discount rate and corporate income tax rate respectively; TPI = total project investment; n = economic life of the project; ADC = annual depreciation costs for capital items

Moreover, sensitivity analysis was carried out on the MSP of the main biorefinery product (i.e. bioethanol) under all process scenarios to see how it is influenced by variations made in certain economic parameters including the selling price for xylan biopolymers (under the MCS only) as well as feedstock price, capital investment, discount rate and annual operating costs (under all three scenarios). Similarly, sensitivity analysis of the minimum selling price for the co-product (i.e. xylan biopolymers) was also carried out under the main biorefinery case.

6.2.6. Environmental assessment: GHG reduction potential

One important aspect of the present study was to evaluate the envisaged biorefinery from climate change mitigation point of view where, in particular, its potential towards reduction of GHG emissions shall be determined in comparison to a fossil-based reference. The GHG emissions reduction, aka GHG emissions savings, resulting from the lignocellulosic biorefinery shall be estimated based on the apparent (indirect) reduction of GHG emissions that can be realized against fossil-fuel baseline. To this end, the RSB GHG Calculation Methodology (v2.13) has been considered for the purpose of estimating the potential GHG emissions savings under the actual biorefinery scenario (MCS) producing bioethanol, xylan biopolymers and electricity; and under the benchmark process scenarios (BCS & ICS) producing bioethanol and electricity based on sugarcane harvesting residues as feedstock. The basic steps and sequence involved under this standardized GHG methodology for biofuels and/or bio-based products are depicted by a flow diagram in Fig 6.4. Calculation details involved in this methodology are to be found in the reference document: 'RSB-STD-01-003-01-ver.2.3-RSB GHG Calculation Methodology'.

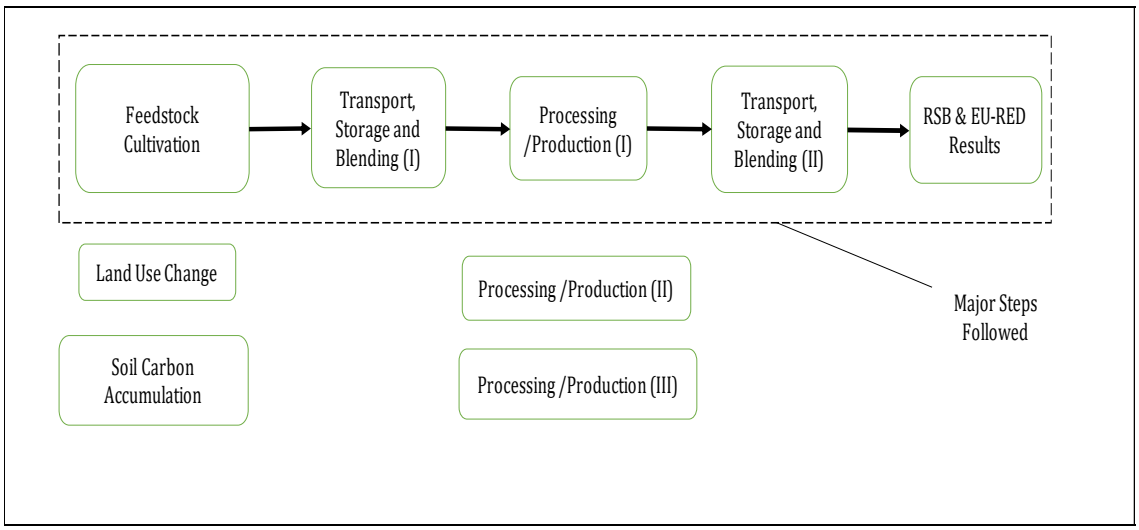

Fig 6.4 Flow Diagram showing basic steps followed in estimating potential GHG Emissions Calculation steps (adopted from RSB GHG Calculator, V2.13)

For the study purpose here, three of the major value chain steps, namely: feedstock cultivation and collection; transport and distribution; and processing (production) steps, (see Fig 6.4) were considered to define the system boundary for estimating the GHG emissions resulting under the three biorefinery scenarios. Whereas 'land use change' as well as 'soil carbon accumulation' have been excluded as sugarcane harvesting residues (the feedstock under consideration) is an agricultural by-product from cane stalks are harvested for the sugar mills. Emissions savings from biofuels is calculated using the following equation (6.7). The functional unit hereto is one MJ of finished biofuel product, in the case here bioethanol. That means, emission saving results (in 'g CO_{2eq}') are to be reported against a lower heating value of ethanol (26.81 MJ/kg), i.e. 'g CO_2eq/MJ biofuel.

$$\text{Emission Saving} = \frac{\text{EF}-\text{E}}{EF} \quad \ldots\ldots\ldots\ldots\ldots\ldots\ldots\ldots\ldots\ldots \quad (6.7)$$

Where, EF = total emissions from fossil fuel comparator; and

EB = total emissions from biofuel or bio-liquids.

It is also worth noting here that under the RSB Global GHG methodology, no emissions are to be allocated to agricultural crop residues such as sugarcane trash which is the feedstock under the present study. Where co-production of additional product takes place along with biofuel (as it is the case in the present study), the RSB GHG calculator divides the GHG emissions between the biofuel (main product) and the co-product in proportion to their energy content determined by the lower heating value (LHV). The allocation factor (AF) for GHG emissions savings for co-product is determined based on the energy yield (EY) of the main product and co-product using the formula:

$$\text{AF} = \frac{\text{EY main product [MJ]}}{(\text{EY main product [MJ]} + \text{EY co-product [MJ]})} \quad \ldots\ldots\ldots\ldots \quad (6.8)$$

6.3. RESULTS AND DISCUSSION

6.3.1. Technical evaluation based on mass and energy balance results

Techno-economic evaluation of the biorefinery complex for an integrated production of xylan biopolymers, bioethanol and electricity was principally carried out based on mass and energy balance results generated using ASPENPLUS® Simulation Software (V11) for the whole biorefinery as well as major processing units within its battery limit as defined and depicted in Fig 6.3. Summary of results on mass and energy balances under all three process scenarios (MCS, BCS & ICS) are presented in Table 6.2 showing how the biomass input, i.e. sugarcane residues fed to the biorefinery on dry weight basis, is processed into targeted material products (i.e. bioethanol and xylan biopolymers) as well as co-generated energy products (i.e. steam and electricity).

From ethanol production point of view, the amount of bioethanol (99.5% EtOH) produced under the main-case scenario (MCS) was around 194 kg (246 L) per ton of sugarcane residues consumed; whereas that under the BCS and ICS was around 221 kg (280 L) and 268 kg (340 L) respectively (see Table 6.2). Under the main- and base-case scenarios, water insoluble solids (WIS) of the pretreated residues was the only substrate for enzymatic hydrolysis where the resulting hexose and pentose sugars are co-fermented into ethanol. However, ethanol production under the MCS was apparently 3% lower than that under the BCS (see Table 6.2). This was due to ethanol consumption for anti-solvent precipitation of xylan extracts from within, i.e. around 3% of ethanol produced under the MCS is consumed internally for xylan recovery purpose.

For the intermediate-case scenario (ICS), where ethanol production per ton of SCT was around 25% and 21% higher than that under MCS and BCS respectively (see Table 6.2), hemicellulosic sugars recovered in the extraction hydrolysate were used as additional substrate for enzymatic hydrolysis along with WIS (see Fig 6.3). Xylan in its

intact form (i.e. in the solid fraction) as well as in its extracted form (i.e. in the liquid fraction) was hydrolyzed into xylose at 90% conversion rate (Mihiretu et al., 2019); and, the resulting xylose was assumed to be fermented into ethanol at 75% conversion rate (Aden et al., 2002; Humbird et al., 2011). Xylose has reportedly been co-fermented with glucose using the yeast strain *Zymomonas mobilis* at 80% ethanol yield from corn stover (Aden et al., 2002) and similar hydrolysis-fermentation conditions were used in the present study as well. Corn stover, the feedstock type in Aden et al., (2002), was also observed to have similar compositional characteristics as sugarcane harvesting residues, the feedstock type used here and characterized in Mihiretu et al., (2019).

Given around 270 operating days a year (ca. 75% on-time), the annual ethanol production for the multi-product biorefinery (MCS) was around 72.6 M L (or, 19.2 M gallons); whereas that for the ethanol-alone benchmark processes was 75.6 M L (or, 19.98 M gallons) and 91.7 M L (24.2 M gallons) under the BCS and ICS respectively. These annual production capacities stand well on par with capacities reported for existing commercial-scale cellulosic ethanol plants which were built based on agricultural residues (Rosales-Calderon and Avantes, 2019; Frank et al., 2019; Lynd et al., 2017; Padella et al., 2019). Along with bioethanol, the multi-product biorefinery would also produce up to 35,679 tons of xylan biopolymers (ca. 90% w/w xylan) on annual basis. This amount of biopolymeric co-product constitutes about 12.1% (w/w) of the sugarcane residues supplied to the biorefinery on dry weight basis; or, about 48.2% (w/w) of the xylan originally therein.

Table 6.2. Mass and energy balance results with biomass input and major output products thereof, by scenario type (MCS, ICS & BCS)

Description of Biomass Input and Output Products		Unit	Quantified Inputs and Outputs, by Scenario type		
			Main-case Scenario (MCS)	Intermediate-case Scenario (ICS)	Base-case Scenario (BCS)
Biomass Input (Sugarcane Trash)	Raw Biomass, dwb*	[kg/hr]	45 360	41 040	41 040
	Cellulose (GL)	[kg/hr]	18 270	16 530	16 530
	Xylan (XY)	[kg/hr]	11 424	10 336	10 336
	Lignin (KL)	[kg/hr]	9 114	8 246	8 246
	Others, minor components (MIC)	[kg/hr]	6 552	5 928	5 928
Major Output and/or Intermediate Products	Bioethanol (99.5% v/v)	[kg/hr]	8 810	10 987	9 081
	Xylan Biopolymers (90% w/w)	[kg/hr]	5 506	[n.a]**	[n.a]**
	Lignin-rich combustible Inputs to Steam Generation Plant (SGP), dwb*	[kg/hr]	16 247	12 930	11 282
	Biogas (29% w/w CH4)	[kg/hr]	4 235	5 505	13 128
Steam and power co-generation, use and supplus Amounts	Electricity (Power generation)				
	Power generation capacity	[kW]	5 535	7 195	15 442
	Consumption for biorefinery processes	[kW]	1 793	2 136	2 796
	Consumption for cooling duties	[kW]	5 635	4 341	3 495
	Surplus power	[kW]	-1 893	718	9 151
	Thermal Energy (steam generation)	[kW]			
	Steam generation capacity	[kW]	67 102	50 327	40 261
	Process Steam Requirement (Total Heat Duty	[kW]	65 313	47 331	37 275
Outputs per ton of raw biomass, dwb*	Bioethanol (main product)	[kg/ton]	194,2	267,7	221,3
	Xylan biopolymers (main co-product)	[kg/ton]	121,4	[n.a]**	[n.a]**
	Biogas (available for power generation)	[kg/ton]	93,4	134,1	319,9
	Electricity (surplus power generated)	[kW/ton]	-41,7	17,5	223,0

Notes: dwb* = dry weight basis; [n.a]** = Not applicable

NB. Under the MCS, negative value for surplus power implies need to supplement the biorefinery's power demand from outside source

Table 6.3. Utilities requirements (thermal and electrical duties) for major process segments of the main-case biorefinery (MCS), base-case (BCS) and intermediate-case (ICS) process scenarios

Major process segments (plants) within the biorefinery complex	Utility Requirement by Scenario Type (MCS, ICS, BCS)														
	Thermal Duty [kW]									Electrical duty [kW] (ELECTUSE)					
	Heating (LPU)			Cooling (COOLW)			Chilling (CHILLW)			Direct consumption			Cooling & Chilling Systems		
	MCS	ICS	BCS	MCS	ICS	BCS	MCS	ICS	BCS	MCS	ICS	BCS	MCS	ICS	BCS
Pretreatment and HC Extraction Plant	11 074	11 074	11 074	0	0	0	0	0	0	551	574	551	0	0	0
Ethanol Production and Recovery Plant	20 580	30 869	20 580	15 569	23 354	15 569	5 920	7 401	5 920	279	419	279	2 143	3 003	2 143
Xylan Recovery Plant	26 840	[n.a]	[n.a]	26 505	[n.a]	[n.a]	0	[n.a]	[n.a]	28	[n.a]	[n.a]	2 209	[n.a]	[n.a]
Wastewater Treatment Plant	4 685	5 387	5 622	13 055	15 815	15 666	0	0	0	335	385	402	1 088	1 318	1 306
Biosolids (lignin) recovery plant	2 134	0	0	2 152	0	0	0	0	0	205	274	339	179	0	0
Co-generation plant	0	0	0	185	240	554	0	0	0	395	483	1 225	15	20	46
Total Duty	65 313	47 331	37 275	57 466	39 408	31 789	5 920	7 401	5 920	1 793	2 136	2 796	5 635	4 341	3 495

One essential aspect of the technical assessment of the envisaged biorefinery had to do with the determination of its thermal and electrical energy requirements and how capably it can meet these energy demands through co-generation of steam and power. Presented under Table 6.3 are the utility requirements for the actual biorefinery (MCS) and benchmark processes (BCS and ICS) determined based on mass and energy balance results closed thereof and expressed herein as thermal and electrical duties. Accordingly, it can be observed that the thermal duties – both for heating and cooling purposes – were highest under the main-case biorefinery scenario (=>MCS) with a total heat duty of 65.3 MW and total cold duty (cooling and chilling combined) of 63.4 MW. Around 90% of the overall process steam demand of the biorefinery complex (=>MCS) was attributed to three major process segments, namely: xylan recovery plant (41.1%), ethanol production plant (31.5%) and biomass pretreatment plant (17.3%). With respect to cooling water requirements, around 96% of the overall cold duty under the MCS was attributed to the xylan recovery plant (46.1%), ethanol production plant (27.1%) and wastewater treatment plant (22.7%) (see Table 6.3). The results clearly show that the xylan recovery plant was the biorefinery segment having the highest thermal duties (heating and cooling demands) followed by the ethanol production plant. For the benchmark processes, which exclude co-production of xylan biopolymers, the overall thermal duty under the BCS and ICS was respectively around 57% and 72% of that under the MCS. Two major process segments, namely: ethanol production and biomass pretreatment plants cover 85 and 88% of the overall heating duty under the BCS and ICS respectively. Whereas around 99% of the overall cooling duties for both benchmark processes were geared towards ethanol production and wastewater treatment plants (see Table 6.3). Obviously, bioethanol production represents the major process area (under BCS and ICS) having the highest thermal duty – both heating and cooling requirements.

Electrical power requirements for the three process scenarios were also analysed based on mass and energy balance results closed thereof (see Tables 6.2. and 6.3). The overall power demand was categorized into two: (1) direct consumption by different electrically-driven units of the biorefinery; and (2) power consumption towards meeting the cooling duties of the biorefinery, i.e. electricity required for water cooling and chilling systems. Accordingly, the overall power consumption for the actual biorefinery was estimated at 7,428 kW three-quarter of which (ca. 76%) being used towards meeting the cooling duties of the biorefinery, while only one-quarter being used directly, i.e. 1793 kW (see Tables 6.2 and 6.3). For the benchmark processes, the overall power consumptions under the BCS and ICS were respectively estimated around 84% and 87% of that under the MCS (see Table 6.2). The overall power consumption used towards meeting the cooling duties of the benchmark processes was also lower than that for the actual biorefinery (Cooling duties: BCS=0.62*MCS; ICS=0.778MCS); however, direct power consumption was higher for the benchmark processes (BCS=1.56*MCS; ICS=1.2*MCS). Under all scenarios, compressors and pumps constitute major power consuming units; larger share (>80%) of the direct power being used for running compressors.

With regard steam and power co-generation capacities, significant variation was observed among the three process scenarios (see Table 6.2; Table 6.3). The steam generation capacity under each process scenario was optimized to a value which is 5±2.5% higher than the respective overall steam requirements (see Tables 6.2 & 6.3). The main-case (MCS) process scenario was accordingly optimized to have steam generation capacity equivalent to 67,102 kW; whereas, the capacities under the base-case (BCS) and intermediate-case (ICS) scenarios were respectively around 75 and 60% of that under the MCS (see Table 6.2). Even though the steam generation capacity under the MCS appears as the highest, that was only apparent, in that, additional raw biomass had to be used

under the MCS (ca. 25% more of the actual amount of biosolids recovered from process streams) to ensure its rather higher process steam demands are fully met using biomass. In terms of electrical power generation (see Table 6.2), the biorefinery complex (=>MCS) was nonetheless found to have the least net power generation capacity (i.e. 122 kW) per ton of sugarcane residues fed to the biorefinery; whereas the highest net power generation was observed under the base-case scenario (BCS) with an estimated capacity of producing 373 kW per ton of raw biomass, which is three-fold that under the MCS (Table 6.2). The net power generation under the ICS was about 44% higher than that under the MCS, but just around 47% of that under the BCS (see Table 6.2).

The variations in the co-generation capacities under the three scenarios was due to varying amounts of combustible biogenic inputs to the steam generation plant (i.e. lignin-rich bio-solids recovered from different process streams; and, in the case of MCS, additional raw biomass directly fed to the combustor); and, to the power generation plant (i.e. biogas produced at the wastewater treatment plant) (see Fig 6.3). Lignin-rich combustible inputs to the steam generation plant (SGP) under the MCS, BCS and ICS were respectively 35.8, 27.5 and 31.5% (w/w) of the raw biomass initially fed to the biorefinery. The amount of combustible solids input under the MCS was apparently about 44 and 26% (w/w) higher than that under the BCS and ICS respectively (see Table 6.2). This was due to additional sugarcane residues fed to the combustor at 4320 kg/hr to enable the biorefinery complex meet its thermal requirements based on biomass.

The main reason for the observed variations in the co-generation capacities of the three scenarios was, however, the extent to which hemicellulosic (xylan) extracts are ending up to the co-generation plant, in general, and to the wastewater treatment (biogas generation) plant, in particular (see Fig 6.3). In this respect, the overall biogas production (ca 29% CH_4; 70% CO_2; 1% H_2O) under the MCS, BCS and ICS were respectively around

93, 320 and 134 kg per ton of raw biomass (see Table 6.2). Biogas production under the main-case scenario (MCS) was the lowest and stands around 32 and 77% of that under the BCS and ICS respectively. This was mainly due to the co-production scheme under the actual biorefinery, where xylan extracts in the liquid fraction are considerably recovered as biopolymeric co-product (see Fig 6.3). Whereas under ethanol-alone base-case scenario (BCS), the scale of biogas production per ton of raw biomass was the highest (see Table 6.2). The reason hereto is that those xylan extracts were wholly ending up to the wastewater treatment plant (see Fig 6.3) where they are ultimately converted into biogas. Under the intermediate case, the same xylan extracts are diverted to the ethanol production plant where they are partly converted into ethanol. The xylose from enzymatic hydrolysis of xylan which is not fermented into ethanol was destined to the WWT plant as it remains soluble in the filtrate after pneumapress filtration of the distillery sludge (see Fig 6.3). Mass balance results indicate that, under the MCS, the xylose ending up to the WWT plant was about 50 and 15% of that under the ICS and BCS respectively. Other non-xylose bio-digestible inputs to the WWT plant, mainly glucose and cellubiose, didn't show significant variation among the three scenarios. For the study purpose here, lignin was assumed to be rather recalcitrant to the anaerobic digestion conditions prevailing at the WWT plant and, whatever amount of it is in was assumed to be out unaffected, at least in quantitative terms (Li et al., 2018; Mulat and Horn, 2018; Khan et al., 2021).

From the technical assessment discussed hereinabove, it can be concluded that the lignocellulosic biorefinery (=>MCS) envisaged for the co-production xylan biopolymers, bioethanol and electricity was certainly more energy-intensive than either of the benchmark processes (=> BCS & ICS) which are intended to produce only bioethanol and electricity from the same biomass input, but under different scenarios. Evidently, the biorefinery complex was rendered to have relatively higher thermal and electrical duties

mainly due to the inclusion of the xylan recovery plant as an integral part of it. Worth noting here is that the extraction of hemicelluloses from the raw biomass and its subsequent recovery as a biopolymeric co-product involve energy-intensive processes which, in particular, have high thermal requirements (see Tables 6.2 & 6.3). One reason hereto was the need to remove as much water from the extraction hydrolysate as possible so that the xylan extracts in the resulting concentrate can be readily separated through ethanol-based anti-solvent precipitation technique. The other reason for the high thermal requirement of the xylan recovery plant is the energy-intensive nature of distillation-based recovery of ethanol which was used (and is reused) as anti-solvent agent (see Table 6.3). Even though ethanol required for selective precipitation of xylan extracts can be conveniently supplied and sourced from within the biorefinery, its recovery after xylan separation can be prohibitively energy intensive, depending on the amount of water in the concentrate containing the xylan extracts. As a result, the overall process steam demand of the biorefinery complex (=>MCS) could only be met with additional raw biomass (i.e. ca 10% more sugarcane residues than required under each of the benchmark processes) to be combusted at the steam generation plant (along with recovered solids) thereby covering around a quarter of its overall steam demand.

Another important observation with respect to the multi-product biorefinery (=>MCS) is that the co-production of xylan biopolymers resulted in not only increased energy demand of the biorefinery, but it does also lead to decreased amount of biogenic material which could end up as combustible input to the co-generation plant. This was especially reflected in the net power generation capacity of the three process scenarios, which depended directly on the extent of biogas generation at the wastewater treatment plant (see Table 6.2 and Fig 6.3). Unlike the benchmark processes (=> BCS & ICS), both of which are self-sufficient in terms of their thermal and electrical energy requirements, the

biorefinery complex (=>MCS) could only meet around 75% of its overall power requirement by the electricity it generates. On the contrary, the benchmark processes enjoy surplus power which can be availed for sale, i.e. around 60% and 10% of the power generated under the BCS and ICS respectively (see Table 6.2). Such variation in the extent of electricity generation among the three process scenarios becomes evident given that power generation was solely from combustion of biogas generated at WWT plant. As discussed earlier, the extent of biogas production was largely dependent on the amount of hemicellulosic (xylan) extracts ending up to the wastewater treatment plant. The amount of biogas available for combustion was thus least for the MCS and highest for the BCS (see Table 6.2). The overall electricity demand of the biorefinery complex can, therefore, be met either through the purchase of electricity from outside to cover the balance; or, by diverting calculated portion of the xylan extracts to the WWT plant thereby allowing more biogas become available for power generation purpose. In sum, the co-production of xylan biopolymers, bioethanol and electricity from sugarcane residues can be regarded as an energy-intensive process exhibiting more thermal and electrical requirements than benchmark processes where bioethanol and electricity are produced.

6.3.2. Economic assessment

6.3.2.1. Total Capital Investment and Annual Operating Costs

Preliminary cost estimates for total capital investments and annual operating expenditures under the three biorefinery scenarios are presented in Tables 6.4 and 6.5 respectively. Accordingly, the total project investment (TPI) for the MCS, BCS and ICS was respectively estimated around 209 M, 191 M and 190 M (USD, 2019). Around two-third (~67%) of the TPI costs under each scenario was allocated to major capital items installed within the battery limit (see Table 6.4). Four major capital-intensive areas, namely:

biomass pretreatment, ethanol production, wastewater treatment and co-generation plants together make up around 67, 86 and 84% of the total installed costs under the MCS, BCS and ICS respectively. Another outstanding capital cost item just for the actual biorefinery case (MCS) is the xylan recovery plant which makes up about 17.2% of the installed capital cost (see Table 6.4). Direct capital costs under each scenario make up around 72% and indirect project costs around 23% of the TPI. The TPI estimates for the benchmark scenarios (BCS & ICS) vary only by small margin, this is due to the fact that they have more processes to share in common than otherwise.

Whereas, the overall capital costs (=> TPI) as well as the total installed costs under the actual biorefinery scenario (=> MCS), which involves co-production of xylan biopolymers, was around 11±0.5% higher than similar costs under the benchmark processes, where ethanol and electricity form the product mix (see Table 6.4). Evidently, the co-production of xylan biopolymers directly led to higher capital requirement; however, the recovery of xylan extracts as a major co-product can also have indirect impacts on the capital costs incurred at wastewater treatment (WWT) and co-generation plants by reducing the amount of hemicellulosic sugars that could have ended towards steam and power generation. As a result, the level of biogas produced at the WWT plant (see Table 6.2) as well as the capital cost associated with it was lowest under the MCS (see Table 6.4). For instance, the capital cost for the WWT plant under the MCS was around 60% lower than that under the BCS where the hemicellulosic extracts are wholly destined to biogas production (see Table 6.4). The relatively lower capital costs for the co-generation plant under the MCS can also be attributed to the co-production of xylan biopolymers as targeted end-product.

Table 6.4: Estimates for Total Capital Investment under the three biorefinery scenarios

Cost Items by Major Process Area	Capital Cost Estimates, by Scenario [10^6 USD, 2019]		
(I) Direct capital costs	Main-case Scenario (MCS)	Base-case Scenario (BCS)	Intermediate-Case Scenario (ICS)
(1) Biomass pretreatment and hemicellulose extraction plant	34,7	34,7	34,7
(2) Ethanol production plant	20,6	20,6	25,6
(3) Xylan recovery plant	24,3	0,0	4,5
(4) Wastewater treatment plant	20,0	32,0	24,6
(5) Biosolids (lignin) recovery plant	13,2	9,2	8,2
(6) Co-generation plant	19,2	23,9	22,0
(7) ISBL Costs [= **(1)+(2)+(3)+(4)+(5)+(6)**]	**131,9**	**120,6**	**119,7**
(8) Storage [= 2% of (7)]	2,6	2,4	2,4
(9) Utilities [=5% of (7)]	6,6	6,0	6,0
(10) Total Installed costs [= **(7)+(8)+(9)**]	**141,1**	**129,0**	**128,0**
(11) Warehouse [=1.5% of (10)]	2,1	1,9	1,9
(12) Site development [=5% of (7)]	6,6	6,0	6,0
(13) Total Direct Costs [= **(10)+(11)+(12)**]	**149,9**	**137,0**	**135,9**
(II) Indirect Costs			
(14) Project supervision and contractor's fees [= 10 % of (13)]	15,0	13,7	13,6
(15) Engineering and construction fees [=20 % of (13)]	30,0	27,4	27,2
(16) Project Contingency [=3% of (13)]	4,5	4,1	4,1
(17) Total indirect costs [= **(14)+(15)+(16)**]	**49,5**	**45,2**	**44,9**
(18) Total Capital Investment [= **(13)+(17)**]	**199,3**	**182,1**	**180,8**
(19) Other unforeseen costs [= 5% of (18)]	10,0	9,1	9,0
(III) Total Project Investment, TPI [= (18)+(19)]	**209,3**	**191,3**	**189,8**

The envisaged biorefinery was assumed to operate 270 days a year, which was based on the assumption of nine months sugarcane harvesting period would ensure the availability of sugarcane trash. Accordingly, the annual operating costs (AOC) under the MCS, BCS and ICS process scenarios were respectively estimated around 37.3, 34.9 and 36.3 M USD (2019) of which, around 32% was fixed, the remaining being variable costs (see Table 6.5). Feedstock was the major cost item accounting for 59-65% of variable expenses and 41-44% of the AOC (see Table 6.5). The feedstock costs under the MCS was 9.4% higher that under the benchmark process, this was due to additional biomass

required to meet the thermal duties of the biorefinery complex. For the study purpose here, sugarcane trash was assumed to cost 55 USD per ton of dry biomass upon delivery to biorefinery site; similar price (54 USD/ton of SCT) was reported in Mandegari et al., (2018). Other cost items were largely considered from literature (Humbird et al., 2011; Aden et al., 2002).

Table 6.5. Estimated Annual Operating Costs for the biorefinery scenarios

Cost Items (Fixed and Variable costs)	Annual operating cost estimates, by scenario type [10^6 USD, 2019]		
(I) Fixed operating costs (FOC)	**MCS**	**BCS**	**ICS**
Maintenance and repair costs (=5% Total Installed costs)	7,1	6,4	6,4
Labour costs (based on manning estimates)	1,8	1,7	1,8
Local taxes and insurance (=1.05% FCI)	2,1	1,9	1,9
Licence fees and royalities (=0.5% FCI)	1,0	1,0	0,9
Subtotal, Fixed Costs	**12,0**	**11,0**	**11,1**
(II) Variable Operating Costs			
Feedstock costs (Raw biomass, SCT)	16,3	14,9	14,9
Costs for non-feedstock input materials			
Enzymes (0.25 USD per gallon of ethanol produced)	5,0	5,0	6,1
Corn steep liquor, CSL (5 cents per gallon of ethanol)	1,1	1,1	1,2
Diammonium phosphate (0,5 cent per gallon of ethanol)	0,2	0,2	0,2
Caustic soda (price assumed at 125 USD/ton)	1,7	1,7	1,7
Other (miscellaneous) inputs (5 cents per gallon of ethanol)	1,0	1,0	1,2
Waste disposal (1.5% of total installed costs)	2,1	1,9	1,9
SubTotal, Variable Costs	**25,3**	**23,8**	**25,2**
Total Operating Costs	**37,3**	**34,9**	**36,3**

6.3.2.2. Determination and analysis of minimum hemicellulose selling price (MHSP)

One key aspect of the present study was the extraction of xylan-rich hemicelluloses and recovery of xylan biopolymers as a major co-product of the biorefinery. Consequently, the economic value of this biopolymeric co-product was assessed to examine its financial impact on the bioethanol-centred biorefinery. For this purpose, the 'Minimum Hemicellulose Selling Price' (MHSP) was determined by fixing the selling price for ethanol at 0.70 USD/L, which is the 'current' (=>2019) price for cellulosic ethanol (Cheng et al., 2019). Accordingly, the MHSP value was estimated around 809 USD/ton of xylan biopolymers (see Table 6.6 for details as to how this minimum selling price was arrived at and parametric inputs used to that end). A minimum selling price of 1576 USD/ton was reported in Geng et al., (2019) for hemicelluloses extracted from sugarcane bagasse via alkaline route in a Greenfield facility intended for co-production of hemicelluloses and cellulosic sugars.

Even though the minimum selling price for hemicellulosic co-product (MHSP) was determined at fixed selling price of cellulosic ethanol (i.e. 0.70 USD/L), even more important is to see how the MHSP value varies over a wider range of ethanol selling prices. This combinatorial approach will provide a broader mix of selling prices for xylan biopolymers and bioethanol at which the envisaged biorefinery may have to become profitable. In this sense, values of MHSP [USD/kg] resulting from different ethanol selling prices ranging from 0 to 1.20 [USD/L] are graphically represented in Fig 6.5 (A). Evidently, the MHSP value was decreasing with increased ethanol prices; such an inverse relationship between the MESP and MHSP values is a clear indication that co-production of hemicellulosic biopolymers in a biorefinery setup can improve the financial viability of bioethanol production by allowing lower ethanol selling prices (see succeeding section 6.3.2.3 on the analysis of MESP under the three scenarios).

One very important observation that can be drawn from the MHSP vs. MESP in Fig 6.5 (A) is that the linear plot represents a combination of those minimum selling prices for bioethanol and xylan biopolymers required for the project to break even, i.e. combination of prices along this line shall represent and essentially define the minimum sales required for profitability of the envisaged biorefinery (=MCS). Price combinations within the triangle defined by this line and the two axes (MESP as horizontal and MHSP as vertical) would not turn out profitable; whereas price combinations beyond this line will make the project profitable. The practical implication of this combinatorial approach is that the co-production of xylan biopolymers along with bioethanol opens up the possibility of exercising higher degree of flexibility in the selling prices of either or both of these products of the biorefinery. From this, it can be deduced that the would-be biorefinery shall have better chance of being more profitable, flexible and competitive by co-producing xylan biopolymers along with bioethanol, rather than producing ethanol only. This is probably where the strongest impact of hemicellulose extraction and co-production of xylan biopolymers can be observed so far the economic viability of bioethanol-centred biorefinery is concerned.

Table 6.6. Determination of minimum selling prices for hemicelluloses (MHSP) and bioethanol (MESP) by scenario type

Description of required input parameters	Denotation	Unit	Parametric Values, by Scenario		
			MCS	BCS	ICS
Total project Investment (TPI)	TPI	[USD]	209 278 197	191 256 070	189 844 498
Total Annual Operating Costs	AOC	[USD]	37 310 036	34 856 209	36 277 384
Discount rate	r	[%]	15	15	15
Corporate income tax rate, SA	TR	[%]	28	28	28
Biorefinery operational life span	n	[num]	25	25	25
Annual capital depreciaction costs	ADC	[USD]	8 371 128	7 650 243	7 593 780
Electricity selling price, SA	ESP	[USD/kwh]	0,069	0,069	0,069
Revenue from sales of electricity per unit volume of ethanol produced	ER/AEP	[USD/L]	-0,01	0,03	0,01
Revenue from sales of xylan biopolymers per unit volume of ethanol produced	XBR/UVE	[USD/L]	0,49	0,00	0,00
Selling price xylan biopolymers (NB. only for MESP determination)	XBSP	[USD/kg]	1,00	0,00	0,00
Selling price for ethanol (NB. Only for MHSP determination)	ETSP,2G	[USD/L]	0,70	0,70	0,70
Annual ethanol production (AEP)	AEP	[L]	72 357 536	74 581 597	90 238 763
Annual production of xylan biopolymers (XYB)	AXBP	[kg]	35 678 880	0,00	0,00
Estimated Annual power generation (APG)	APG	[kwh]	35 864 208	46 623 578	100 061 372
Percentage of APG consumed within and by the biorefinery	APGC	[%]	134	41	90
Annual revenue from sales of excess electricity (ER)	ER	[USD]	-846 324	1 907 697	690 423
Annual revenue from sales of xylan biopolymers (XBR)	XBR	[USD]	35 678 880	0,00	0,00
Annual revenue from sales of bioethanol (ETR)	ETR	[USD]	50 996 668		
Amortized Capital Expenses (Annualized capital costs)	ACE	[USD]	32 375 212	29 587 200	29 368 830
Annual income tax	AIT	[USD]	9 334 922	8 531 039	8 468 075
Annual revenue from bioethanol to be sold at the minimum selling price	BER	[USD]	44 187 613	71 066 751	73 423 866
Annual revenue from hemicelluloses to be sold at the minimum selling price			28 869 825		
Minimum ethanol selling price, MESP	**MESP**	**[USD/L]**	**0,6107**	**0,9529**	**0,8137**
Minimum hemicelluloses selling price, MHSP	**MHSP**	**[USD/kg]**	**0,8092**		

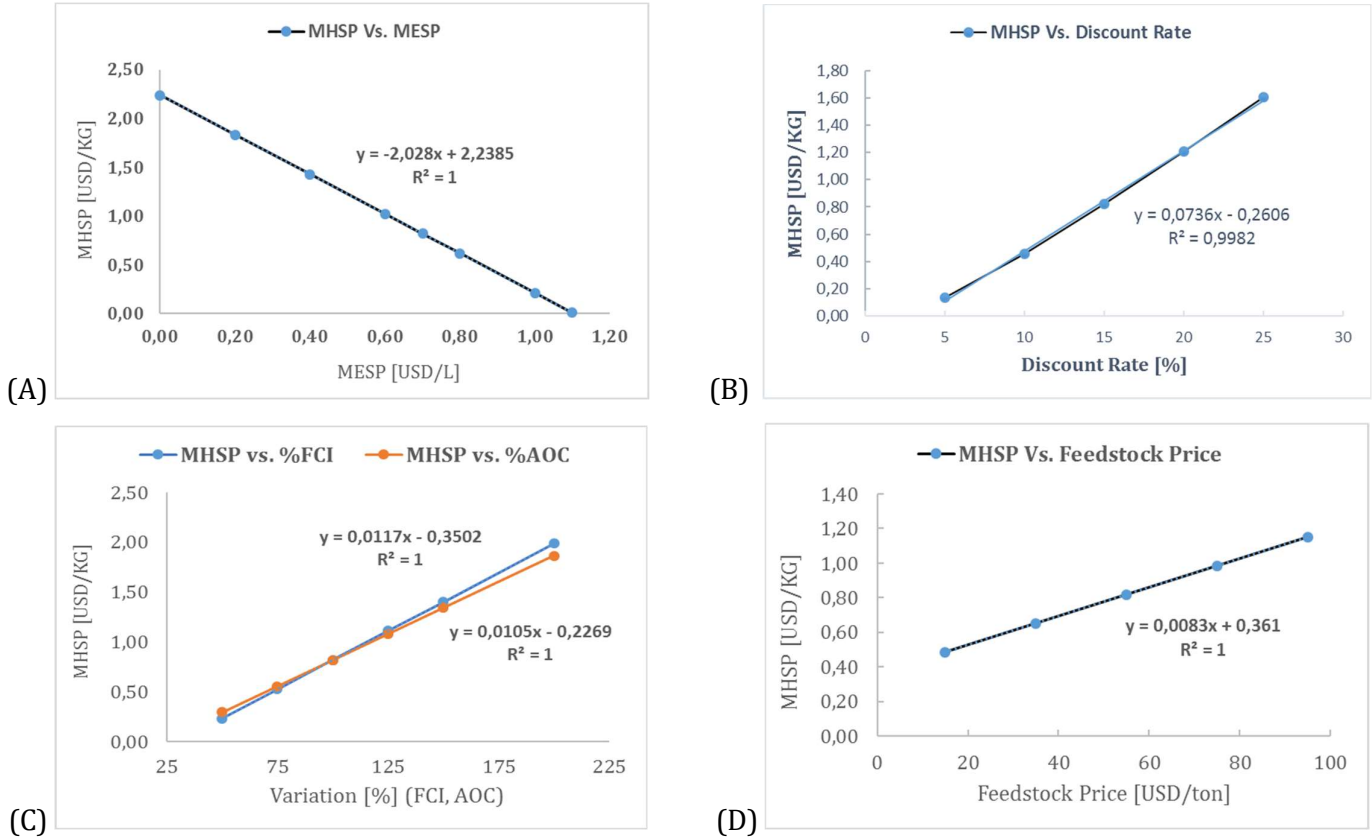

Fig 6.5 Minimum hemicellulose selling prices (MHSP) against varying values of (A) minimum ethanol selling prices (MESP); (B) Discount rate (r); (C) percentile changes in Total capital investment (FCI) and Annual operating costs (AOC); and (D) Feedstock price

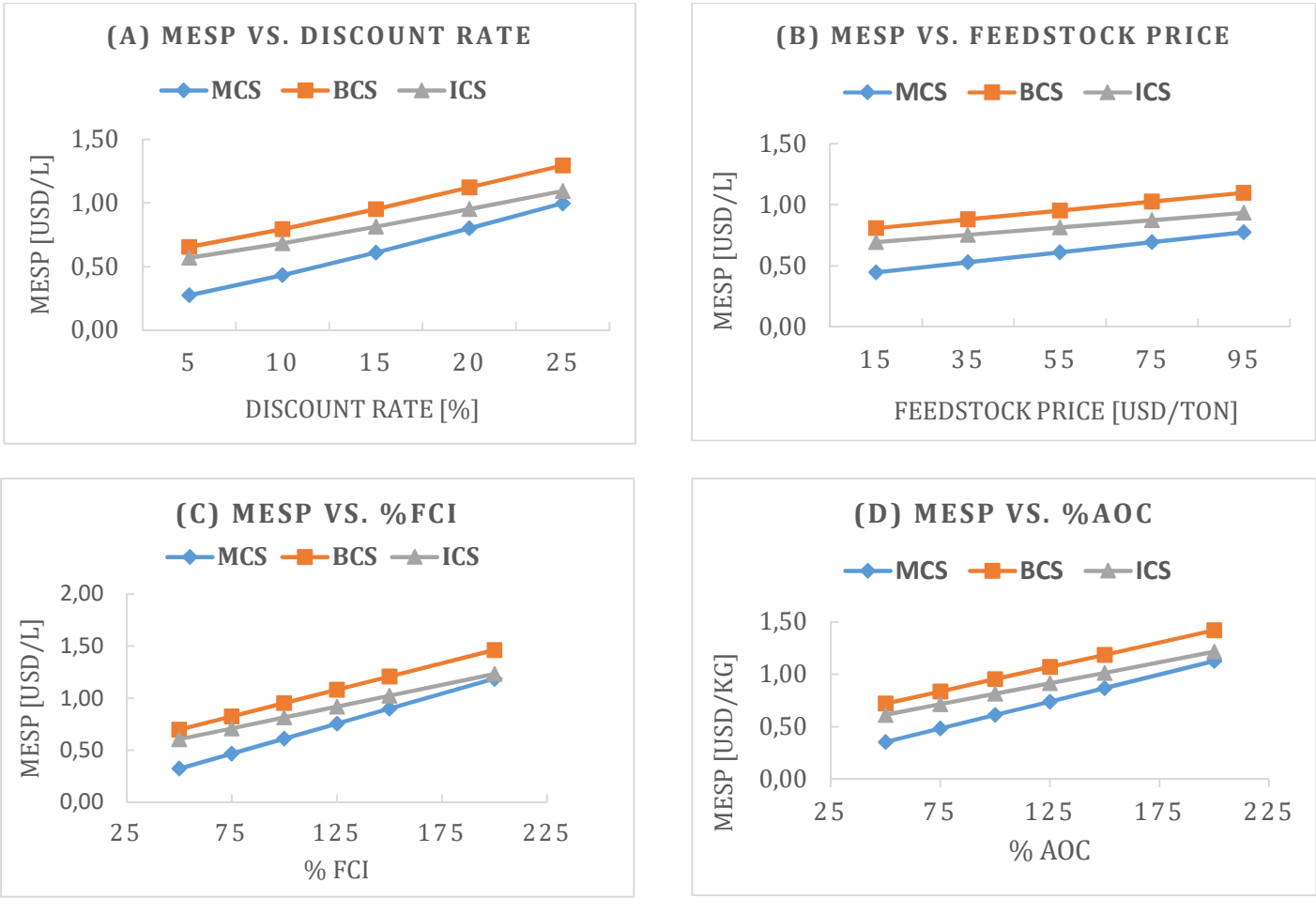

Fig 6.6 Minimum ethanol selling prices (MESP) against (A) discount rate; (B) feedstock price; (C) percentile changes in Fixed capital investment, FCI; and, (D) percentile change in annual operating costs, AOC

Even though the minimum hemicellulose selling price (MHSP) is inversely correlated to ethanol selling price (and vice versa), that was only by keeping other economic parameters at fixed value (see Table 6.6). Presented in Fig 6.5 are also plots showing how the MHSP value changes with variations made in other key economic parameters such as feedstock price, discount rate, total capital investment (TCI), and annual operating costs (AOC). Unlike minimum ethanol selling price (MESP), the other factors appear to be directly correlated with MHSP with positive slopes which indicate their extent of impact on MHSP (see Fig 6.5 b, c and d). From the slopes displayed on the respective plots in Fig 6.5, it can be observed that the minimum hemicellulose selling price is most influenced by (i.e. it is most sensitive to) changes in the discount rate (slope = 0.0736) and least sensitive to changes in feedstock price (slope = 0.0083) (see Fig 6.5). For instance, against feedstock prices (see Fig 6.5 (D)), the MHSP was observed to change from 0.49 to 0.99 USD/kg of xylan biopolymers (two-fold increase in MHSP) when the feedstock price was varied from 15 to 75 USD/ton of sugarcane trash (five-fold increase in feedstock price). Variations made in the discount rate were, however, observed to have more pronounced impact on the MHSP (see Fig 6.5 (B)). Varying the discount rate from 5 to 25 (five-fold increase) led to more than eleven-fold increase in MHSP, i.e. from 0.14 to 1.60 USD/kg of xylan biopolymers. With regard to the impact of varying percentages of FCI and AOC on the MHSP (see Fig 6.5 (C)), it can be observed that the MHSP was equally sensitive to variations in FCI and AOC. For instance, when the FCI was varied between 75 to 150% of the value stated in Table 6.6, the MHSP value increased by about 252%; whereas, for the same percentile increase in AOC, the MHSP was increased by about 216%, thus having comparable impact on MHSP as does FCI.

6.3.2.3. Analysis of Minimum Ethanol Selling Price (MESP) by process scenarios

The economic viability of the present bioethanol-centred biorefinery project was assessed at preliminary level based on minimum ethanol selling price (MESP) determined for each process scenario (MCS, BCS and ICS). For the purpose of this comparative assessment, the selling price for 'xylan biopolymers' was assumed to be 1000 USD/ton which is ca. 25% higher than the minimum hemicellulose selling price determined in the preceding section, i.e. 0.809 USD/kg of xylan co-product (see Table 6.6). In a recent study by Geng et al., (2019), minimum hemicellulose selling price (MHSP) of 641 and 1685 USD/ton of hemicellulose was reported for hemicelluloses produced from sugarcane bagasse under two different greenfield scenarios, GHA and GH scenarios respectively (GH: 'greenfield and total hemicellulose'; GHA: 'greenfield and hemicellulose A'). In the same study, MHSP of 841 and 1934 USD/ton of hemicelluloses were reported for hemicelluloses produced from switchgrass, under the GHA and GH scenarios respectively (Geng et al., 2019). Both sugarcane bagasse and switchgrass are xylan-rich lignocellulosic feedstock like sugarcane residues, the minimum hemicellulose selling prices as reported in Geng et al., (2019) may serve as a reference against which the minimum selling price of 809 USD/ton for xylan biopolymers can be roughly compared. It is important to note here that, in the study context here, the minimum selling prices for xylan biopolymers and bioethanol are inversely related and are interdependent on each other. That may mean a wider range of selling prices can be considered for xylan co-product in order to fix the corresponding minimum selling price for the main biorefinery product, i.e. bioethanol. A selling price of 1000 USD/ton for xylan biopolymers was only considered for the purpose of fixing a certain value for MESP under the MCS scenario, against which the MESP values under the benchmark scenarios (BCS & ICS) will be compared. Other economic parameters required for the determination of MESP are similarly presented in Table 6.6.

Accordingly, the MESP value under the MCS, BCS and ICS were respectively estimated at 0.61, 0.95 and 0.81 USD/L of ethanol (see Table 6.6). Evidently, the MESP value in the base-case and intermediate-case scenarios is higher than the MESP value in the main biorefinery case by 56% and 33% respectively. Minimum ethanol selling price of ca. 2.4 USD/gal (or, 0.64 USD/L) of cellulosic ethanol produced via combined dilute alkaline de-acetylation and disk refining was reported in Chen et al., (2015). A more recent techno-economic study by Cheng et al., (2019) reported a higher MESP of 4.52 to 4.91 USD/gal (or, 1.26±0.25 USD/L) for cellulosic ethanol produced from sugarcane bagasse fractionated through sequential de-acetylation, hot water and disk-refining pretreatment. Minimum ethanol selling prices falling in the range of 1 to 2.5 USD/gal were also reported in previous NREL studies (Aden et al., 2002; Kazi et al., 2010; and Humbird et al., 2011). A minimum ethanol selling price of 0.57 USD/L has been reported for the Raizen cellulosic ethanol plant based on sugarcane biomass (located in Brazil, still operational); this MESP value has so far been considered as lowest cellulosic ethanol price (Susmozas et al., 2020). This reportedly lowest MESP value represents around 93%, 60% and 70% of the respective MESP values determined for the MCS, BCS and ICS scenarios of the present study. That implies, the economic viability of the biorefinery cannot be achieved with sole production of ethanol. However, the very introduction of hemicellulose extraction step and recovery of xylan extracts as biopolymeric co-product can significantly improve the price competitiveness of ethanol by lowering the MESP value (as discussed in the preceding section 6.3.2.2). In fact, it can be shown that a minimum selling price of ca. 1070 USD per ton of xylan biopolymers would suffice to establish the price competitiveness of bioethanol produced under the main biorefinery case in comparison to the lowest selling price currently reported for cellulosic ethanol produced at commercial level (Susmozas et al., 2020).

Factors such as feedstock price, total capital investment (TCI), annual operating costs (AOC) and discount rate were quantitatively varied to see how sensitively the MESP value responds to variations made thereof (see Fig 6.6). With respect to feedstock, varying the price of sugarcane trash from 15 to 95 USD/ton could lead to a corresponding increase in MESP from 0.45 to 0.77, 0.81 to 1.10, and 0.69 to 0.93 USD/L for the MCS, BCS and ICS respectively (see Fig 6.6. B). The increase in MESP was highest for the MCS (61%), whereas for both BCS and ICS, the increase in MESP was only around 31%. This indicates that MESP was more sensitive to feedstock price when xylan biopolymers are co-produced with bioethanol than not. Similarly, varying the discount rate between 5 and 25% resulted in more than three-fold increase in MESP for the MCS; whereas the increase in MESP for both BCS and ICS was only two-fold (see Fig 6.6 (A)). The MESP value under the MCS scenario was again more sensitive towards discount rate than it is under the BCS and ICS scenarios. Total capital investment (TCI) and annual operating costs (AOC) were also observed to have similar impacts on MESP: varying them between 75% and 150% (see Fig 6.6 C&D), the corresponding increase in MESP for the MCS, BCS and ICS was respectively 92, 46 and 44% in the case of FCI, and 80, 42 and 42% in the case of AOC. From such simplified analysis, it can be inferred that the minimum selling price for ethanol (MESP) can be lowered (becomes more competitive) with reductions in feedstock cost, capital investment, operating expenses, and discount rate whether co-production of xylan biopolymers takes place than not. On the contrary, the MESP value can only be improved with increased selling prices for xylan biopolymers.

6.3.3. Environmental assessment: GHG Emissions Reduction Potential

GHG Emission savings under the three biorefinery scenarios (MCS, BCS & ICS) were estimated in accordance with the RSB GHG Calculator (V2.3) and results thereof are presented in Table 6.7 (B). Basic input parameters required for the calculation of GHG emissions savings are presented under Table 6.7 (A). The inputs considered under the 'feedstock cultivation' and 'transport' stages were similarly considered under all three scenarios; whereas, those inputs under the 'processing' stages, which themselves are mainly extracted from mass and energy balance results, vary by scenario type. Bioethanol has been considered as the main biorefinery product and was used as a functional unit while expressing the emission saving results in g CO2eq/MJ biofuel. Accordingly, the GHG emissions savings estimated using the RSB-Global (and EU-RED) method were 28.4 (39.5), 32.6 (47.2) and 31.7 (44.2) g CO2eq/MJ biofuel for the MCS, BCS and ICS process scenarios respectively. The corresponding emissions reduction potential results relative to fossil baseline values of 90 g CO2eq/MJ (RSB-Global) and 94 g CO2eq/MJ (EU-RED-II) were 68.5 (57.9), 63.8 (49.8) and 64.8 (53.0)% for the three scenarios (see Table 6.8 (B). GHG emissions reduction that can be associated with cellulosic ethanol production have been reported by a number of LCA studies and the reduction potential generally falls in the range of 60 to 110% against gasoline as fossil fuel comparator (Wang et al., 2012; Padella 2019; Pereira et al., 2019).

The results indicate that the GHG emission savings under the actual biorefinery scenario (MCS) were somewhat greater than the savings from the benchmark scenarios (BCS, ICS) by a factor of 6.5±1.3%. This is apparently due to the allocation of the GHG emissions under MCS between the main product (bioethanol) and the co-product (xylan biopolymers) in proportion to their energy content (see Table 6.8 (A)). Under the RSB Global method, no emissions were allocated to sugarcane trash as agricultural crop

residues are assumed to have zero emissions until collected. Though not that large, there are positive emissions savings from excess electricity under the benchmark processes (1.71 and 0.11 gCO2eq/MJ biofuel for the BCS and ICS respectively). The negative emission saving under the MCS (-0.203 gCO2eq/MJ) may rather imply an indirect contribution towards GHG emissions (see Table 6.7 (B)). The conclusion that can be drawn from this brief assessment of the three process scenarios is that, from environmental point of view, the co-production of hemicellulosic biopolymers along with bioethanol and electricity may not result in significantly higher GHG emissions reductions in comparison to the benchmark processes.

Table 6.7 (A): Major Input parameters considered and used in estimating GHG emission savings for the biorefinery using the RSB GHG Methodology V2.13

Major Supply Chain Steps for Emission Calculations Purpose	Description of Input parameter	Unit	Value considered and/or assumed	Remark
(I) Feedstock Cultivation Stages	Feedstock (SCT) moisture content, dry basis	[%w/w]	10	Sugarcane trash/residues (SCT) is the feedstock of interest being harvested; wet-basis moisture content is right after harvesting and before further drying
	Feedstock moisture content, wet basis	[%w/w]	25	
	Feedstock (SCT) Lower Heating Value (LHV)	[MJ/kg]	17,5	
	Feedstock (SCT) harvesting residue yield	[ton/ha]	12	
(II) Transport Stages (feedstock and finished products)	Transport distance assumed for dried feedstock (SCT), from farm to biorefinery site	[km]	50	The envisaged biorefinery is assumed to be located within 50 km radius from the cane farm; products are assumed to be availed to end-users within few km from biorefinery site
	Transport distance assumed for xylan biopolymers (main co-product)	[km]	1,5	
	Transport distance assumed for bioethanol (main product)	[km]	5	
(III) Processing/production Stage	**Main Product: Bioethanol**			
	Amount produced per ton of dry biomass	[kg/ton]	MCS=221=BCS; ICS=268	Values vary by scenario type (MCS, BCS and ICS)
	Feedstock efficiency	[kg/kg]	MCS=4,52= BCS; ICS=3,74	
	Moisture content	[%w/w]	0,5	
	Lower heating value (LHV)	[MJ/kg]	26,81	
	Main Co-product: Xylan biopolymers			
	Amount produced per kg of main product	[kg/kg]	0,6104	
	Feedstock efficiency	[kg/kg]	7,46	
	Moisture content	[%w/w]	10	
	Lower heating value (LHV)	[MJ/kg]	15,5	
	Co-product: Electricity			
	Usage per kg of main product	[kWh/kg]	MCS=0.82; BCS=0,69; ICS=0,59	Values vary by scenario type
	Excess amount per kg of main product	[kWh/kg]	MCS= (0,21); BCS=1,21; ICS=0,08	

Table 6.7 (B) GHG Emission Savings by scenario type, estimated based on the RSB GHG Methodology (RSB-Global & EU-RED II)

Biorefinery Scenario	GHG Emissions Savings [g CO2eq/MJ Biofuel] by scenario type						Emission allocated by supply chain step [g CO2eq/MJ biofuel]						Emission Savings from excess electricity [gCO2eq/MJ Biofuel]
	Calculated value, by method type		Baseline Value, by method type		Emissions Savings [%] against Base value		Feedstock Cultivation		Transport and distribution		Processing		
	RSB-Global	EU-RED	RSB-Global	EU-RED (II)	RSB-Global	EU-RED (II)	RSB-Global	EU-RED (II)	RSB-Global	EU-RED (II)	RSB-Global	EU-RED (II)	
MCS	28,40	39,53	90	94	68,45	57,94	0,00	12,96	13,62	13,62	17,59	15,46	-0,23
BCS	32,57	47,22	90	94	63,81	49,77	0,00	17,10	12,52	12,52	20,05	19,35	1,74
ICS	31,68	44,21	90	94	64,79	52,96	0,00	13,92	12,12	12,12	19,57	18,29	0,11

6.4. CONCLUSIONS

The techno-economic viability of a lignocellulosic biorefinery for co-production of xylan biopolymers, bioethanol and electricity from sugarcane harvesting residues was carried out against benchmark processes which produce only bioethanol and electricity. The study results revealed that co-production of xylan biopolymers can substantially improve the economic performance ethanol-centred biorefinery by lowering the selling price of ethanol. A minimum hemicellulose selling price (MHSP) of 809 USD/ton of xylan biopolymers would be required should the biorefinery avail bioethanol at a price of 0.70 USD/L, a value which can further be lowered to a more competitive price by increasing MHSP to higher values. However, the multi-product biorefinery complex was found to be rather energy-intensive as a result of such co-production scheme where the recovery of xylan biopolymers necessitated substantial thermal and electrical energy demands. From environmental point of view, the co-production of hemicellulosic biopolymers along with bioethanol and electricity was shown to have a positive contribution towards mitigating GHG emissions from fossil sources, but there was only marginal difference between the GHG emissions savings attained under the main biorefinery case and that under the benchmark processes.

CHAPTER SEVEN: CONCLUSIONS AND FUTURE DIRECTIONS

7.1. CONCLUSIONS

The development of next-generation biorefinery systems in the perspective of advancing low-carbon bioeconomy has been highly regarded towards unlocking the economic potential of abundantly available lignocellulosic biomass. In this context, the present research was conceived with the aim of developing a multi-product biorefinery intended for the co-production of hemicellulosic (xylan) biopolymers, bioethanol and electricity from selected agro-industrial materials: namely, sugarcane harvesting residues (SCT) and aspen wood sawdust (AW). Accordingly, the research was designed to have both experimental and modelling parts, the former to investigate the suitability of selected biomass pretreatment technologies for the purpose of extracting biopolymeric hemicelluloses as well as for enhanced cellulose digestibility; whereas the latter was primarily meant to evaluate the techno-economic viability of the most promising pretreatment approach having reasonable chance of being scaled up. Two pretreatment approaches were formulated for the study purpose here, namely: microwave-assisted pressurized hot water method and alkalinized steam explosion pretreatment methods.

Two full-fledged experiments were, therefore, conducted in a statistically designed manner and results thereof could provide significant insights as to how the selected pretreatment techniques influence xylan extraction yield and cellulose digestibility (Mihiretu et al., 2017; Mihiretu et al., 2019). Accordingly, single-step microwave-induced pressurized hot water pretreatment was demonstrated to be a viable technique for the extraction of xylan-rich hemicelluloses from aspenwood and sugarcane trash, while enhancing the enzymatic digestibility of cellulose for improved ethanol production. Optimal pretreatment conditions for enhanced xylan yield and cellulose digestibility were

also established for each feedstock type. About two-third of the original xylan in aspenwood and over half of that in sugarcane trash were extracted, with more than 90% of the xylan extracts being in non-monomeric form. Cellulose digestibility for both lignocellulosic materials was improved by four-fold against that for un-pretreated biomass samples. With respect to the second set of experimental work, alkali-catalysed steam explosion pretreatment of lignocelluloses was also proven as viable approach for co-production of xylan biopolymers and bioethanol in a biorefinery set up. This was demonstrated by impregnating sugarcane trash and aspenwood samples with sodium hydroxide at 5% (w/w) loading ratio. Optimal extraction yields were attained under SEPT temperatures of 195-205℃ where xylans were extracted with little or no formation of monomeric sugars and degradation products thereof; thus confirming the suitability of alkalised SEPT for xylan biopolymers extraction. The significant increase observed in enzymatic digestibility of cellulose further reinforces the potential of this pretreatment strategy for bioethanol production.

With respect to the modelling part, a techno-economic case study for the co-production of xylan biopolymers, bioethanol and electricity from sugarcane harvesting residues of South African origin was carried out based on alkalinized steam explosion pretreatment method. This modelling study was approached in a scenario-based manner where the envisaged biorefinery was assessed against two benchmark processes which produce only bioethanol and electricity. The study results revealed that co-production of xylan biopolymers substantially improved the economic performance of the biorefinery complex by lowering the selling price of ethanol. A minimum hemicellulose selling price (MHSP) of 809 USD/ton of xylan biopolymers would be required should the biorefinery avail bioethanol at a price of 0.70 USD/L, a value which can further be lowered to a more competitive price by increasing MHSP to higher values.

However, the multi-product biorefinery complex was found to be rather energy-intensive as a result of such co-production scheme where the recovery of xylan biopolymers necessitated substantial thermal and electrical energy demands. From this, it can be deduced that going beyond bioethanol and introducing new production lines that lead to high-value co-products can prove viable approach in making bioethanol-centred lignocellulosic biorefineries economically more competitive. From environmental point of view, the co-production of hemicellulosic biopolymers, along with bioethanol and electricity, was shown to have a positive contribution towards of mitigating GHG emissions from fossil sources, but there was only marginal difference between the GHG emissions savings attained in the main biorefinery case (MCS) and that under the benchmark processes (BCS & ICS).

7.2. RECOMMENDATIONS FOR FURTHER RESEARCH

The present research may not be about coming up with the next big idea towards realizing technologically mature and commercially viable lignocellulosic biorefinery system, but rather about exploring credibly anticipated techno-economic challenges which are likely encountered in the course of developing multi-product biorefinery complexes. While the overall findings within the scope of the experimental and techno-economic studies are as stated hereinabove, the present work does have its own limitations in covering quite a number of important areas which deserve due consideration. The following recommendations are intended to point out what further studies along this line of research should focus on:

I. Despite the fact that co-production of high-value biopolymeric products with bioethanol leads to enhanced economic viability of the envisaged biorefinery, it is yet worth emphasizing that there are as well significant technological challenges and bottlenecks which have to be overcome to make that happen. One salient area

where such technical challenge stands out is the presence of non-xylan biomass components (notably, lignin) which are substantially co-solubilized along with xylan and so pose separation challenges in subsequent biorefining steps leading to a major biopolymeric co-product. In this respect, the technology considered as potentially applicable for xylan-lignin separation was the Anti-solvent Precipitation (ASP) technique where ethanol is used as an agent to selectively precipitate xylan extracts while leaving lignin in its solubilized state. Although ethanol precipitation of natural polysaccharides has been widely reported in literature, the ASP technology needs to be developed for large-scale applications tailored for xylan biopolymers production. The same applies for membrane-based separation and purification technologies (such as ultrafiltration systems) which were duly considered for the co-production of xylan biopolymers.

II. One advantage of using ethanol as an ASP agent is that it can be conveniently sourced from within the biorefinery. However, ethanol-based recovery of xylan biopolymers may render the envisaged biorefinery rather energy-intensive, as the recovery of ethanol itself necessitates high thermal (heating and cooling) demands in the form of steam and electricity. In connection to this, it is equally important to take due note of the amount of washing water that is to be used during solid-liquid separation of pretreated solids. Even though this washing step is meant to ensure efficient recovery of hemicellulose extracts from pretreated residues (sludge), it can also be the main reason for the energy optimization challenge that can arise during ethanol-based xylan recovery process. More thorough optimization studies is worth considered, as the techno-economic viability of the overall biorefinery can be strongly impacted by outcomes thereof.

III. Another important area whereon further research might be required is the kinetics underlying alkalinized steam explosion pretreatment (ASEPT) applied for hemicellulose extraction. Although this pretreatment approach was shown to be viable for the extraction of biopolymeric hemicelluloses (Mihiretu et al., 2019); the underlying kinetics for the hemicellulose extraction process is worth researched in more depth. The chemical interplay that might be taking place between the introduced alkaline agents and those weak organic acids of biomass origin under subcritical extraction conditions, should be a subject of continued research. Furthermore, significant biomass ash content (as is the case for sugarcane residues) may imply more complex chemical reactions could be taking place, which can potentially influence the extraction yield and efficiency of the pretreatment approach. This could as well constitute one important aspect of this kinetics study.

IV. Owing to their limited level of penetration, microwaves can indeed be suitable enough for small-scale extraction processes taking place within limited spatial distance that can be covered by microwaves both effectively and directly. As a result, they may not be directly applicable for large-scale biomass pretreatment purpose as they do for lab-scale applications. Furthermore, the extraction experiments under microwave-assisted pressurized hot water conditions were conducted at so small a scale that translating those lab-scale extraction setups to an industrial scale is nothing straightforward, but full of foreseeable technical challenges that can limit this technique from becoming a viable biomass pretreatment method for large-scale biorefinery complexes. As a result, microwave-based biomass pretreatment technique was considered to fall beyond

the scope of this research work and was thud left for further research and technological development.

V. Another important aspect of the present research whereon a more comprehensive study is required is the environmental sustainability of the multi-product biorefinery complex. The environmental dimension has only been briefly addressed in terms of GHG emissions reduction potential under each biorefinery scenario. However, full-fledged life-cycle assessment of the biorefinery complex is worth considered for further study.

VI. As a final note, markets for bio-based products (e.g. xylan biopolymers intended for functionalized biomaterial applications) are undoubtedly one critical in dictating the economics of their large-scale production in a biorefinery setup. It is, therefore, important to keep closer eye on commercial trends and developments across potential application areas which can ensure markets for xylan biopolymers, be that at the niche level or well-established one.

REFERENCES

- Adney B., and Baker, J., (2008), Measurement of Cellulase Activities; Laboratory Analytical Procedure (LAP); Technical Report NREL/TP-510-42628
- Adney, B., and Baker, J., 2008. Measurement of Cellulase Activities; Laboratory Analytical Procedure (LAP); Technical Report NREL/TP-510-42628
- Agbor V.B., Cicek N., Sparling R., Berlin A., and Levin D.B., Biomass pretreatment: Fundamentals toward application, Biotechnology Advances 29 (2011), 675-685
- Aguilar-Reynosa A., Romani A., Ma R., Jasso R., Aguilar C.N., Garrote G., and Ruiz H.A., (2017), Microwave heating processing as alternative of pretreatment in second-generation biorefinery: an overview, Energy Conversion and Management 136, 50-65; https://doi.org/10.1016/j.enconman.2017.01.004
- Ajao O., Marinova M., Savadogo O., and Paris J. (2018), Hemicellulose based integrated forest biorefineries: Implementation strategies, Industrial Crops and Products 126 (2018) 250-260
- Albersheim P., An J., Freshour G., Fuller M.S., Guillen R., Ham K-S., Hahn M.G., Huang J., O'Neill M., Whitcombe A., Williams M.V., York W.S., and Darvill A., (1994), Structure and function studies of plant cell wall polysaccharides, Biochem Soc Trans (1994) 22 (2): 374–378, https://doi.org/10.1042/bst0220374
- Al-Dajani, W. W., Tschirner, U. W., & Jensen, T. (2009). Pre-extraction of hemicelluloses and subsequent kraft pulping part II: Acid- And autohydrolysis. Tappi journal, 8(9), 30-37
- Alina Kowalczyk-Jusko (2017) The influence of the ash from biomass on the power boiler pollution, Journal of Ecological Engineering, 2017, 200-204
- Al-Malah K.I.M., (2017), Aspen Plus®: Chemical Engineering Applications, 1st Ed, 2017
- Al-Rudainy B., Galbe M., Hernandez MA., Jannasch P., and Wallberg O., (2019), Impact of lignin content on the properties of hemicellulose hydrogels, Polymers 2019, 11, 35
- Alvarez C., Gonzalez A., Negro M.J., Ballesteros I., Oliva J.M. and Saez F. (2017), Optimized use of hemicellulose within a biorefinery for processing high value-added xylo-oligosaccharides, Industrial Crops and Products, 99 (2017) 41-48
- Anwar Z., Gulfraz M., and Irshad M. (2014) Agro-industrial lignocellulosic biomass a key to unlock the future bio-energy: a brief review, Journal of Radiation Research and Applied Sciences 7 (2014), 163-173

- Bahcegul E., Toraman H.E., Oskan N., and Bakir U. (2012), Evaluation of alkaline pretreatment temperature on a multi-product basis for the co-production of glucose and hemicellulose based films from lignocellulosic biomass, Bioresource Technology, 103 (2012), 440-445
- Balat M., Balat H., Oz Cahide., (2008), Progress in bioethanol processing; Progress in Energy and Combustion Science 34 (2008) 551–573
- Banerjee R., Avanthi A., Kumar S., and Sherpa KC., (2017), Bioconversion of hemicelluloses of lignocellulosic biomass to ethanol: an attempt to utilize pentose sugars, Journal of Biofuels, 2017, pp 431-444
- Barba, A.A., d'Amore, M., 2012. "Microwave Materials Characterization", InTech, Relevance of dielectric properties in microwave assisted processes, edited by Sandra Costanzo, ISBN 978-953-51-0848-1
- Baruah J., Nath BK, Sharma R., Kumar S., Deka RC., Baruah DC., and Kalita E. (2018) Recent trends in the pretreatment of lignocellulosic biomass for value-added products, Frontiers in Energy Research/Bioenergy and Biofuels
- Bauer, F., Coenen, L., Hansen, T., Mccormick, K., & Voytenko Palgan, Y. (2017). Technological Innovation Systems for Biorefineries – A Review of the Literature. Biofuels, Bioproducts and Biorefining, 11(3), 534-548. https://doi.org/10.1002/bbb.1767
- Bennich T., Belyazid S., Kopainsky B., and Diemer A., (2018), The bio-based economy: Dynamics governing transition pathways in the Swedish forestry sector, Sustainability 2018, 10, 976
- Bezerra M.A., Santelli R.E., Oliveira E.P., Villar L.S., and Escaleira L.A., (2008), Response surface methodology (RSM) as a tool for optimization in analytical chemistry, Talanta 76 (5), 965-977, 2008
- Bian J, Peng F, Peng P, Xu F, Sun RC. (2010), Isolation and fractionation of hemicelluloses by graded ethanol precipitation from Caragana korshinskii. Carbohydrate Research 2010; 345:802–9.
- Binod P., Janu K.U., Sindhu R., Pandey A., (2011) Hydrolysis of Lignocellulosic Biomass for Bioethanol Production, in Biofuels: Alternative Feedstocks and Conversion Processes, Elsevier Inc.

- Binod, P., Satyanagalakshmi, K., Sindhu, R., Janu, K.U., Sukumaran, R.K., and Pandey, A., 2012. Short Duration Microwave assisted Pretreatment enhances the enzymatic Saccharification and Fermentable Sugar Yield from Sugarcane Bagasse; Renewable Energy, 37, 109-116
- Bokhary A., Cui L., Lin H.J., and Liao B.Q., (2017), A review of membrane technologies for integrated forest biorefinery. J. Membr. Sci. Res. 3:120-141
- Bond, J.Q., Alonso, D. M., and Dumesic, J.A., 2013. "Catalytic Strategies for Converting Lignocellulosic Carbohydrates to Fuels and Chemicals", in Aqueous Pretreatment of Plant Biomass for Biological and Chemical Conversion to Fuels and Chemicals, Edited by Charles E. Wyman, pp. 61-102
- Brienzo M., Siqueira A.F., Milagres A.M.F., (2009) Search for optimum conditions of sugarcane bagasse hemicellulose extraction, Biochemical Engineering Journal 46, 199–204
- Brown T.R., and Brown R.C., (2013), Techno-economics of advanced biofuels pathways, RSC Adv., 2013,3, 5758-5764, https://doi.org/10.1039/C2RA23369J
- Buranov A., and Mazza G., (2010), Extraction and characterization of hemicelluloses from flax shives by different methods, Carbohydrate Polymers, 79 (1): 17-25. DOE: 10.1016/j.carbpol.2009.06.014
- Buruiana C-T., and Vizireanu C., (2014), Prebiotic xylo-oligosaccharides from lignocellulosic materials: production, purification and applications - An Overview, The Annals of the University Dunarea de Jos of Galati, Fascicle VI - Food Technology 38 (2):18-31
- Busse-Wicher M., Gomes T.C.F., Tryfona T., Nikolovski N., Stott K., Grantham N.J., Bolam D.N., Skaf M.S., and Dupree P., (2014), The pattern of xylan acetylation suggests xylan may interact with cellulose microfibrils as a twofold helical screw in the secondary plant cell wall of Arabidopsis thaliana, The Plant Journal 79 (3), https://doi.org/10.1111/tpj.12575
- Caillat S., Vakkilainen E., (2013), Large-scale biomass combustion plants: an Overview, in Biomass Combustion Science, Technology and Engineering, 2013
- Canilha L., Rodrigues R.C.L.B., Antunes F.A.F., Chandel A.K., Milessi T.S.S., Felipe M.G.A., and da Silva S.S., (2013), Bioconversion of Hemicellulose from Sugarcane Biomass Into Sustainable Products, InTech

- Cano M.E., Garcia-Martin A., Morales P.C., Wojtusik M., Santos V.E., Kovensky J., and Ladero M., (2020), Production of oligosaccharides from agro-food wastes, Germination 2020, 6. 31; doi:10.3390/fermentation6010031
- Cantero D., Jara R., Navarrete A., Pelaz L., Queiroz J., Rodríguez-Rojo S., and Cocero MJ., (2019) Pretreatment Processes of Biomass for Biorefineries: Current Status and Prospects, Annual Review of Chemical and Biomolecular Engineering, 289-310
- Cardona C, Quintero J, Paz I (2010) Production of bioethanol from sugarcane bagasse: status and perspectives. Bioresource Technol 101:4754–4766
- Carrasco C., Baudel H.M., Sendelius J., Modig T., Roslander C., Galbe M., Hahn-Hagerdal B., Zacchi G., and Liden G., (2010), SO2-catalyzed steam pretreatment and fermentation of enzymatically hydrolyzed sugarcane bagasse, Enzyme and Microbial Technology, 2010, 64-73
- Carvalheiro et al., (2008), Hemicellulose biorefineries: a review of biomass pretreatments, Journal of Scientific & Industrial Research, Vol 67, 849-864
- Carvalheiro, F., Duarte, L. C., Girio, F., and Moniz, P., (2016), "Biomass Fractionation Technologies for a Lignocellulosic Feedstock Based Biorefinery", Ed. Mussatto S.L., Hydrothermal/Liquid Hot Water Pretreatment (Autohydrolysis): A Multipurpose Process for Biomass Upgrading, pp. 315-347
- Carvalho D.M., Queiroz J.H., and Colodette J.L. (2016), Assessment of alkaline pretreatment for the production of bioethanol from eucalyptus, sugarcane bagasse and sugarcane straw, Industrial Crops and Products, 2016, 932-941
- Castro RCA., Fonseca BG., Lima dos Santos HT., Ferreira IS., Mussatto SI., and Roberto IC., (2017) Alkaline deacetylation as a strategy to improve sugars recovery and ethanol production from rice straw hemicellulose and cellulose, Industrial crops and products, 2017, 65-73
- Chandel A.K., Garlapati V.K., Singh A.K., Antunes F.A.F., and da Silva S.S., (2018), The path forward for lignocellulose biorefineries: bottlenecks, solutions, and perspective on commercialization, Bioresource Technology 264, 370-381
- Chang F.C., Lin L-D., Ko C.H., Hsieh H.C., Yang B.Y., Chen W.H., and Hwang W.S., (2017), Life cycle assessment of bioethanol production from three feedstocks and two fermentation waste re-utilization schemes. Journal of Cleaner Production, 143:973-979
- Chantal B., Danielle J.C. & Shri R., 2011, Biorefinery Co-Products: Phytochemicals, Primary Metabolites and Value-added Biomass Processing, 1st Ed. Wiley

- Chaturvedi T., Torres A.I., Stephanopoulos G., Thomsen M.H., and Schmidt J.E., (2020), Developing process designs for biorefineries - Definitions, Categories and Unit Operations, Energies 2020, 13(6), 1493; https://doi.org/10.3390/en13061493
- Chemat F., Vian M.A., and Cravotto G., (2012), Green Extraction of Natural Products: Concept and Principles; Int. J. Mol. Sci. 2012, 13, 8615-8627
- Chen et al., (2013), Understanding of alkaline pretreatment parameters for corn stover enzymatic saccharification, Biotechnology for Biofuels 2013 6:8.
- Chen H. (2014), Chemical Composition and Structure of Natural Lignocellulose. In: Biotechnology of Lignocellulose. Springer, Dordrecht. https://doi.org/10.1007/978-94-007-6898-7_2
- Chen Y., Xie Y., Ajuwon K.M., Zhong R., Li T., Chen L., Zhang H., Beckers Y., and Everaert N., (2021), Xylo-oligosaccharides, preparation and application to human and animal health: A review, Front. Nutr. 8:731930. Doi:10.3389/fnut2021.731930
- Cherubini F., and Ulgiati S., (2010), Crop residues as raw materials for biorefinery systems - A LCA case study, Applied Energy 87(1), 47-57, 2010
- Cherubini F., Jungmeier G., Bird D.N., (2012), Greenhouse Gas (GHG) and energy analysis of bioethanol oriented biorefinery based on wood, IEA Bioenergy Task 38
- Chimphango A.F.A., van Zyl W.H., and Görgens J.F. (2012) In situ enzymatic aided formation of xylan hydrogels and encapsulation of horse radish peroxidase for slow release, Carbohydrate Polymers 88, 1109-1117
- Chrysikou LP., Bezergianni S., and Kiparissides C., (2018), Environmental analysis of a lignocellulosic-based biorefinery producing bioethanol and high-added value chemicals, Sustainable Energy Technologies and Assessments, 28 (2018), 103-109
- Clark J.H., Luque R., and Matharu A.S., (2012) Green Chemistry, Biofuels and Biorefinery, Annual Review of Chemical and Biomolecular Engineering, 2. 3:183-207
- Dalton L. J. et al. Extraction of Wood Hemicelluloses through NaOH Leaching, (2010), Cerne, Lavras, v. 16, n. 4, p. 423-429
- Dao C.N., Mupondwa E., Li L.T.X., and Lopez E.C.C., (2018), A review of techno-economic analysis and life-cycle assessment of second-generation bioethanol production via biochemical processes, CSBE18-215
- Davis K.M., Rover M., Brown R.C., Bai X., Wen Z., and Jarboe L.R., (2016), Recovery and utilization of lignin monomers as part of the biorefinery approach, Energies 2016, 9(10), 808; https://doi.org/10.3390/en9100808

- Davis R., Tao L., Tan ECD., Biddy MJ., Beckham GT., Scarlata C., Jacobson J., Cafferty K., Ross J., Lukas K., Knorr D and Schoen P., (2013), Process design and economics for the conversion of lignocellulosic biomass to hydrocarbons: Dilute-acid and enzymatic deconstruction of biomass to sugars and biological conversion of sugars into hydrocarbons, Technical Report, NREL/TP-5100-60223
- Doherty W., Reynolds A., and Kennedy D., (2013), Aspen Plus simulation of biomass gasification in a steam blown dual fluidized bed, Book Chapter: Materials and processes for energy: communicating current research and technological developments, A. Mendez-Vilas (Ed.), Formatex Research Centre, 2013
- Dowe N., and McMillan J., (2008), SSF Experimental Protocols — Lignocellulosic Biomass Hydrolysis and Fermentation; Laboratory Analytical Procedure (LAP); Technical Report NREL/TP-510-42630
- Dragone G., Kerssemakers A.A.J., Driessen J.L.S.P., Yamakawa C.K., Brumano L.P., and Mussatto S.I. (2020), Innovation and strategic orientations for the development of advanced biorefineries, Bioresource Technology 302 (2020) 122847
- Duque A., Manzanares P., Ballesteros I., and Ballesteros M., (2016), Steam explosion as lignocellulosic biomass pretreatment, in 'Biomass fractionation technologies for a lignocellulosic feedstock based biorefinery', 2016, 349-368
- Dziekonska-Kubczak U., Berlowska J., Dziugan P., Patelski P., Balcerek M., Pielech-Przybylska K., Czyzowska A., and Domanski J., (2018), Comparison of steam explosion, dilute acid and alkali pretreatments on enzymatic saccharification and fermentation of hardwood sawdust, BioResources 13(3), 6970-6984
- Ebringerova A. and Heinze T., (2000), Xylan and xylan derivatives - biopolymers with valuable properties, 1 - Naturally occurring xylans structures, procedures and properties; Macromolecular Rapid Communications 21(9):542-556
- Ebringerova A., (2006) Structural diversity and application potential of hemicelluloses. Macromol Symp 232:1–12
- Egito, E.S.T., da Silva, A. E., Marcelino, H.R., Gomes, M.C.S., Oliveira, E.E., and Nagashima, T., 2012. Xylan, a Promising Hemicellulose for Pharmaceutical Use, in Products and Applications of Biopolymers, Edited by Verbeek C.J.R., InTech
- Ereev S.Y. and Patel M.K. (2012), Standardized cost estimation for new technologies (SCENT) - methodology and tool, Journal of Business Chemistry
- Ernsting A. and Smolker R. (2018) Dead End Road: The false promises of cellulosic biofuels, Report by Biofuel watch, September 2018

- Ewanick S., and Bura R. (2010), Hydrothermal pretreatment of lignocellulosic biomass, Bioalcohol production, 2010, 3-23
- Falano T., Jeswani H.K., and Azapagic A., (2014), Assessing the environmental sustainability of ethanol from integrated biorefineries, Biotechnology Journal, 9(6), 753-765, 2014
- Farzad S., Mandegari M.A., Guo M., Haigh K.F., Shah N., and Görgens J.F., (2017), Multi-product biorefineries from lignocelluloses: a pathway to revitalization of the sugar industry? Biotechnology for Biofuels, 10 (87), 2017
- Fengel D, Wegener G. (1989) Wood chemistry, ultrastructure, reactions. New York: Walter de Gruyter.
- Field J.L., Richard T.L., Smithwick E.A.H., Cai H., Laser M.S., LeBauer D.S., Long S.P., Paustian K., Qin Z., Sheehan J.J., Smith P., Wang M.Q., and Lynd L.R., (2020), Robust paths to net greenhouse gas mitigation and negative emissions via advanced biofuels, PNAS, 2020; http://doi.org/10.1073/pnas.1920877117
- Fitzpatrick M., Champagne P., Cunningham M.F. and Whitney R.A. (2010); A biorefinery processing perspective: Treatment of lignocellulosic materials for the production of value-added products, bioresource technology 101 (2010) 8915-8922
- Franck Per-Ake, Bokinge P., Nystrom I. (2019), Production of liquid advanced biofuel - global status, Report by CIT Industriell Energi AB
- Franco H.C.J., Pimenta M.T.B., Carvalho J.L.N., Magalhaes P.S.G., Rossell C.E.V., Braunbeck O.A., Vitti A.C., Kolln O.T., and Neto J.R., (2013), Assessment of sugarcane trash for agronomic and energy purposes in Brazil, Scientia Agricola, 305-312
- Gabrielii I., Gatenholm P., Glasser WG, Jain RK, Kenne L. (2000), Separation, characterization and hydrogel formation of hemicellulose from aspen wood, Carbohydrate Polymers 2000; 43:367–74
- GAIN Report: South African sugar production forecast to grow despite revenue pressures, USDA Foreign Agricultural Services, Report No.: SA1912, 2019
- Galbe M. and Wallberg O., (2019), Pretreatment for biorefineries: a review of common methods for efficient utilization of lignocellulosic materials, Biotechnology for Biofuels, 12:294 (2019); https://doi.org/10.1186/s13068-019-1634-1
- Gao C., Ren J., Zhao C., Kong W., Dai Q., Chen Q., Liu C., and Sun R., (2016), Xylan-based temperature/pH sensitive hydrogels for drug controlled release, Carbohydrate Polymers, 151, 189-197, 2016

- Geng W., Venditti R.A., Pawlak J.J., Assis T.D., Gonzalez R.W.., Philips R.B., and Chang H., (2019), Techno-economic analysis of hemicellulose extraction from different types of lignocellulosic feedstocks and strategies for cost optimization. Biofuels, Bioproducts and Biorefinery, 14(2), 225-241. http://doi.org/10.1002/bbb.2054
- Girio FM., Fonseca C., Carvalheiro F., Duarte LC., Marques S., and Bogel-Likasik R., (2010), Hemicelluloses for fuel ethanol: a review, Bioresource Technology, 2010, pp 4775-4800
- Giuliano A., Poletto M., and Barletta D., (2015), Process design of a multi-product lignocellulosic biorefinery, Computer-aided Chemical Engineering, Vol 37, 2015, 1313-1318; https://doi.org/10.1016/B978-0-444-63577-8.50064-4
- Gomez E.O., de Souza R.T.G., de Moraes Rocha, de Almeida E., and Cortez L.A.B., (2014), Sugarcane trash as feedstock for second generation processes, p. 637-660, In Luis Augusto Barbosa Cortez, Sugarcane Bioethanol - R&D for productivity and Sustainability,http://dx.doi.org/10.5151/blucherOA-sugarcane-SUGARCANEBIOETHANOL_56
- Guilherme M.R., Aouada F.A., Fajardo A.R., Martins A.F., Paulino A.T., Davi M.F.T., Rubira A.F., and Muniz E.C., (2015), Superabsorbent hydrogels based on polysaccharides for application in agriculture as soil conditioner and nutrient carrier: A review, European Polymer Journal 72, 365-385, 2015
- Gulbrandsen, T. A., Johmsen, I. A., Opedal, M.T., Toven, K., Øyaas, K., Pranovich, A., Mokkola, J., and Hoff, B.H., (2015), Extracting Hemicelluloses from Softwood and Bagasse as Oligosaccharides using pure Water and Microwave Heating, Cellulose Chemistry and Technology, 49(2), 117-126
- Guo F., Shi W., Sun W., Li X., Wang F., Zhao J., and Qu Y., (2014) Differences in the adsorption of enzymes onto lignins from diverse types of lignocellulosic biomass and the underlying mechanism, Biotechnology for Biofuels, 2014, 7:38
- Hagman L., Blumenthal A., Eklund M., Svensson N., (2018), The role of biogas solutions in sustainable biorefineries, Journal of Cleaner Production, 172, 3982-3989
- Hahn-Hägerdal B., Galbe M., Gorwa-Grauslund M.F., Lidén G., and Zacchi G., (2006), Bioethanol - the fuel of tomorrow from residues of today: review, Trends Biotechnol., 2006, 24(12):549-56; doi: 10.1016/j.tibtech.2006.10.004
- Hames B., Ruiz R., Scarlata C., Sluiter A., Sluiter J., and Templeton D., (2008), Preparation of Samples for Compositional Analysis; Laboratory Analytical Procedure (LAP); Technical Report NREL/TP-510-42620

- Harmsen P.F.H., Huijgen W.J.J., Bermudez Lopez L.M., Bakker R.R.C., (2010), Literature Review of Physical and Chemical Pretreatment Processes for Lignocellulosic Biomass, ECN-E--10-013
- Hassan S.S., Williams G.A., and Jaiswal A.K., (2019), Moving towards the second generation of lignocellulosic biorefineries in the EU: Drivers, challenges and opportunities, Renewable and Sustainable Energy Reviews, 101, 590-599, 2019
- Hatakeyama H., Hatakeyama T. (2009), Lignin Structure, Properties, and Applications. In: Abe A., Dusek K., Kobayashi S. (eds) Biopolymers. Advances in Polymer Science, vol 232. Springer, Berlin, Heidelberg. https://doi.org/10.1007/12_2009_12
- Heitz M., Capek-Menard E., Koeberle P.G., Gagne J., and Chronet E., (1991) Fractionation of *Populus tremuloides* at the pilot plant scale: optimization of steam pretreatment conditions using the STAKE II Technology, Bioresource Technology 35, 23-32
- Hendriks A.T.W.M., Zeeman G., (2009), Pretreatments to enhance the Digestibility of Lignocellulosic Biomass; Bioresource Technology 100, 10–18
- Hinderer S., Brauchle E. and Schenke-Layland K., (2015), Generation and assessment of functional biomaterial scaffolds for applications in cardiovascular tissue engineering and regenerative medicine, Adv. Healthcare Mater. 4, 2326-2341
- Holm-Nielsen J.B., and Ehimen E.A., (2014), Biorefinery plant design, engineering and process optimization, Ch-4, Advances in Biorefineries, Biomass and Waste Supply Chain Exploitation, pp. 89-111, http://doi.org/10.1533/9780857097385.1.89
- Holopainen-Mantila U., Marjamaa K., Merali Z., Kasper A., de Bot P., Jaaskelainen A-S., Waldron K., Kruus K., and Tamminen T., (2013), Impact of hydrothermal pretreatment to chemical composition, enzymatic digestibility and spatial distribution of cell wall polymers, Bioresource Technology 138, 156-162
- Hu L., Du M., and Zhang J., (2018), Hemicellulose-based hydrogels present status and application prospects: a brief review. Open Journal of Forestry, 8, 15-28, https://doi.org/10.4236/ojf.2018.81002
- Hu L., Fang X., Du M., Luo F., and Guo S., (2020), Hemicellulose-based polymers processing and application, American Journal of Plant Sciences, 11, 2066-2079. Doi:10.4236/ajps.2020.1112146
- Huang H.-J., Ramaswamy S., Tschirner U.W., Ramarao B.V., (2008), A review of separation technologies in current and future biorefineries. Sep. Purif. Technol. 2008; 62:1–21. doi: 10.1016/j.seppur.2007.12.011

- Huang L.Z., Ma M.G., Ji X.X., Choi S.E., and Si C., (2021), Recent developments and applications of hemicellulose from wheat straw: A review, Front. Bioeng. Biotechnol., https://doi.org/10.3389/fbioe.2021.690773
- Humbird D., Davis R., Tao L., Kinchin C., Hsu D., Aden A., Schoen P., Lukas J., Olthof B., Worley M., Sexton D., and Dudgeon D. (2011), Process Design and economics for biochemical conversion of lignocellulosic biomass to ethanol, Dilute acid pretreatment and enzymatic hydrolysis of corn stover, NREL Technical Report NREL/TP-5100-47764
- Humpert D., Ebrahimi M., and Czermak P., (2016), Membrane technology for the recovery of lignin: A review, Membranes 2016, 6, 42; doi:10.3390/membranes6030042
- Hung M.T. and Liu J.C., (2006), Microfiltration for separation of green algae from water, Colloids Surf B Biointerfaces, 2006, 51 (2): 157-164; DOE: 10.1016/j.colsurfb.2006.07.003
- IEA Bioenergy (2017), The role of industrial biorefineries in a low-carbon economy: Summary and conclusions from IEA Bioenergy/IEA IETS Workshop, exCo:2017:07
- Iolovich M. & Morag E. (2012), Study of enzymatic hydrolysis of mild pretreated lignocellulosic biomasses; Bioresources, 7(1), 1040-1052
- IRENA (2019), Advanced biofuels: What holds them back?, International Renewable Energy Agency (IRENA), [ISBN 978-92-9260-158-4, www.irena.org/publications]
- Iroba K.L., Dumonceaux T., Baik O-D., and Tabil L.G., (2013), Effect of alkaline pretreatment on chemical composition of lignocellulosic biomass using radio frequency heating, Biosystems Engineering 116 (2013), 385-398
- Isikgor F.H. and Becer C.R. (2015), Lignocellulosic biomass: a sustainable platform for the production of bio-based chemicals and polymers, Polymer Chemistry (Abr: Polym.Chem.) 2015, 6, 4497
- Jaafar Z., Mazeau K., Boissiere A., Gall S.L., Villares A., Vigouroux J., Beury N., Moreau C., Lahaye M., and Cathala B., (2019), Meaning of xylan acetylation on xylan-xylose interactions: a quartz crystal microbalance with dissipation (QCM-D) and molecular dynamic study, Carbohydrate Polymers 226, 115315, https://doi.org/10.1016/j.carbpol.2019.115315
- Jacobs A., Lundqvist J., Stalbrand H., Tjerneld F., and Dahlman O., (2002), Characterization of water-soluble hemicelluloses from spruce and aspen employing SEC/MALDI mass spectroscopy, Carbohydr. Res. 337, 711-717

- Jacobs A., Plam M., Zacchi G., and Dahlman O., (2003), Isolation and characterization of water-soluble hemicelluloses from flax shive, Carbohydr. Res. 338, 1869-1876
- Joelsson E., Erdei B., Galbe M., and Wallberg O., (2016), Techno-economic evaluation of integrated first- and second-generation ethanol production from grain and straw, Biotechnol Biofuels (2016), 9:1, doi10.1186/s13068-015-0423-8
- Jönsson A-S., (2013), Microfiltration, Ultrafiltration and Diafiltration, Ch8: Separation and Purification Technologies in Biorefineries, https://doi.org/10.1002/9781118493441.Ch8, 2013
- Jönsson L.J., Alriksson B., and Nilvebrant N-O., (2013), Bioconversion of lignocellulose: inhibitors and detoxification, Biotechnol Biofuels. 28; 6 (1):16. doi: 10.1186/1754-6834-6-16
- Jönsson L.J., and Martin C. (2016), Pretreatment of lignocellulose: formation of inhibitory by-products and strategies for minimizing their effects, Bioresource technology, 2016, 199/103-112
- Julio R., Albet J., Vialle C., Vaca-Garcia C., and Sablayrolles C., (2017), Sustainable design of biorefinery processes: existing practices and new methodology (2017) Biofuels, Bioproducts and Biorefining, 11(2). 373-395. ISSN 1932-104X; https://doi.org/10.1002/bbb.1749
- Junqueira T.L., Chagas M.F., Gouveia V.L.R., Rezende M.CAF., Watanabe M.DB., Jesus C.DF., Cavalett O., Milanez A.Y., and Bonomi A., (2017), Techno-economic analysis and climate change impacts of sugarcane biorefineries considering different time horizons, Biotechnology for Biofuels, 10(1), 50, 2017
- Kamari M.L., Maleki A., Nazari M.A., Sadeghi M., Rosen M.A., and Pourfayaz F., (2021), Assessment of biomass-based polygeneration plant for combined power, heat, bioethanol and biogas, Applied Thermal Engineering 198 (2021) 117425
- Kamm et al., (2006) Lignocellulose-based Chemical Products and Product Family Trees, in the book: Biorefineries - Industrial Processes and Products, Status Quo and Future Directions, Vol.2, by Kamm B., Gruber P.R., & Kamm KM. (2006)
- Kapoore R.V., Butler T.O., Pandhal J., and Vaidyanathan S., (2018), Microwave-assisted extraction for microalgae: from biofuels to biorefinery, Biology, MDPI, doi: 10.3390/biology7010018
- Kapu N.S., Yuan Z., Chang X.F., Beatson R., Martinez D.M., and Trajano H.L. (2016) Insight into the evolution of the proton concentration during autohydrolysis and dilute-acid hydrolysis of hemicellulose, Biotechnology for Biofuels (2016) 9:224

- Karaaslan M.A., Tshabalala M.A., Yelle D.J., and Buschle-Diller G., (2011), Nanoreinforced biocompatible hydrogels from wood hemicelluloses and cellulose whiskers, Carbohydrate Polymers, 86, 192-201; https://doi.org/10.1016/j.carbpol.2011.04.030
- Karp E.M., Donohoe B.S., O'Brien M.H., Ciesielski P.N., Mittal A., Biddy M.J., and Beckham G.T., (2014), Alkaline pretreatment of corn stover: bench-scale fractionation and stream characterization, ACS Sustainable Chemistry & Engineering, 2, 1481-1491
- Karp S.G., Woiciechowski A.L., Soccol V.T. and Soccol C.R., (2013) Pretreatment Strategies for Delignification of Sugarcane Bagasse: A Review, Brazilian Archives of Biology and Technology, Vol.56, n.4: pp. 679-689
- Kazi F.K., Fortman J., Anex R., Kothandaraman G., Hsu D., Aden A., and Dutta A., (2010), Techno-economic analysis of biochemical scenarios for production of cellulosic ethanol, Technical Report NREL/TP-6A2-46588, 2010
- Kekana P., Sithole B., and Ramjugernath D., (2016), Stirred cell ultrafiltration of lignin from black liquor generated from South African kraft mills, South African Journal of Science, 112 (11/12); DOI: 10.17159/sajs.2016/20150280
- Khan M.U., Ahring B.K.,Anaerobic biodegradation of wheat straw lignin: the influence of wet explosion pretreatment, Energies 2021, 14,5940, https://doi.org/10.3390/en14185940
- Kilpelaeinen P., Kitunen V., Pranovich A., Ilvesnieme H., and Willfoer S., (2013), Pressurized Hot Water Flow-through Extraction of Birch Sawdust with Acetate pH Buffer, 8(4), 5202-5218
- Kim D., (2018), Physico-Chemical Conversion of Lignocellulose: Inhibitor Effects and Detoxification Strategies: A Mini Review, Molecules. 2018, 23 (2):309, doi: 10.3390/molecules23020309
- Kim J.S., Lee Y.Y., and Kim T.H. (2016) A review of alkaline pretreatment technology for bioconversion of lignocellulosic biomass, Bioresource technology 199, 42-48
- Kim S. and Holtzapple M.T., (2005), Lime pretreatment and enzymatic hydrolysis of corn stover; Bioresource Technology, 96(18), 1994–2006
- Klein M., and Poverenov E., (2020), Natural biopolymer-based hydrogels for use in food and agriculture, A review; Journal of the Science of Food and Agriculture, Vol 100 (6), pp. 2337-2347, https://doi.org/10.1002/jsfa.10274

- Knudsen J.D., and Rønnow B., (2020), Extended fed-batch fermentation of a C5/C6 optimized yeast strain on wheat straw hydrolysate using an online refractive index sensor to measure the relative fermentation rate, Scientific Reports, 10(6705), 2020
- Krishna S.H., Reddy J.T., and Chowdary G.V., (2001), Simultaneous saccharification and fermentation of lignocellulosic wastes to ethanol using a thermotolerant yeast; Bioresource Technology 77 (2001) 193-196
- Krishnan C. et al., (2010), Alkali-Based AFEX Pretreatment for the Conversion of Sugarcane Bagasse and Cane Leaf residues to Ethanol, Biotechnol. Bioeng.107: 441–450
- Kumar, R., G. Mago, V. Balan, and C. E. Wyman. (2009), Physical and chemical characterizations of corn stover and poplar solids resulting from leading pretreatment technologies. Bioresource Tech. 100(17): 3948-3962.
- Kuo L., Jen J., Lee M., Hwang Y., and Cheng Y., (2002), A microwave-assisted extraction method for determining hot water solubility of wood, Wood Fiber Sci. 34 (1), 72-76
- Lahtinen M.H., Valoppi F., Juntti V., Heikkinen S., Kilpelainen P.O., Maina N.H., and Mikkonen K.S., (2019), Lignin-rich PHWE hemicellulose extracts responsible for extended emulsion stabilization, Front. Chem. 17:871. Doi:10.3389/fchem.2019.00871
- Lan K., Xu Y., Kim H., Ham C. and Kelley S.S., (2021). Techno-economic analysis of producing xylo-oligosaccharides and cellulose microfibers from lignocellulosic biomass. Bioresource Technology, v 340, 2021, 125726. http://doi.org/10.1016/j.biotech.2021.125726
- Lawther JM, Sun RC, Banks WB. Effects of extraction conditions and alkali type on yield and composition of wheat straw hemicellulose. J Appl Polym Sci 1996;60:1827–37
- Li J., Henriksson G., and Gellerstedt G. (2007), Lignin depolymerization/repolymerization and its critical role for delignification of aspenwood by steam explosion, Bioresource Technology, 2007, 3061-3068
- Li M., Pu Y., and Ragauskas A.J., (2016), Current understanding of the correlation of lignin structure with biomass recalcitrance, Front. Chem. 4:45. doi: 10.3389/fchem.2016.00045
- Li T., and Takkellapati S., (2018), The current and emerging sources of technical lignins and their applications, Biofuel Bioprod Biorefin. 2018, 0:1-32; doi:10.1002/bbb.1913

- Li W., Khalid H., Zhu Z., Zhang R., Liu G., Chen C. and Thorin E., (2018), Methane production through anaerobic digestion: participation and digestion of cellulose, hemicellulose and lignin (2018), Applied Energy, 226(C), 1219-1228; DOI:10.1016/j.apenergy.2018.05.055
- Li Z., Qin M., Xu C., and Chen X., (2013), Hot water extraction of hemicelluloses from aspen wood chips of different sizes, Bioresources, 8(4), 5690-5700
- Li Zhu, O'Dwyer J.P., Chang V.S., Granda C.B., & Holtzapple M.T., (2008), Structural features affecting biomass enzymatic digestibility; Bioresource Technology 99 (2008) 3817–3828
- Liguori R. and Faraco V. (2016) Biological processes for advancing lignocellulosic waste biorefinery by advocating circular economy, Bioresource Technology, 215, 13-206
- Lindblad M.S., Albertsson A-C., Ranucci E., Laus M., and Giani E., (2005), Biodegradable polymers from renewable sources: rheological characterization of hemicellulose-based hydrogels, Biomacromolecules 2005, 6,2, 684-690; https://doi.org/10.1021/bm049515z
- Lindorfer J., Lettner M., Fazeni K., Rosenfeld D., Annevelink B., and Mandi M., (2019), Technical, economic and environmental assessment of biorefinery concepts: Developing a practical approach for characterization, IEA Bioenergy: Task 42:2019:01
- Littlewood J., Wang L., Turnbull C., and Murphy R.J. (2013) Techno-economic potential of bioethanol from bamboo in China, Biotechnology for Biofuels, 2013, 6:173
- Liu C., and Wyman C.E., (2004), Impact of fluid velocity on hot water only pretreatment of corn stover in a flow-through reactor, Applied Biochemistry and Biotechnology, 113-116 (1-3):977-87, DOI: 10.1385/ABAB:115:1-3:0977
- Liu H., Chen T., Dong C., and Pan X., (2020), Biomedical applications of hemicellulose-based hydrogels, Curr Med Chem. 2020; 27(28): 4647-4659, doi:10.2174/0929867327666200408115817
- Liu W., Yuan Z., Mao C., Hou Q., and Li K. (2012), Extracting hemicelluloses prior to aspen chemi-thermomechanical pulping: effects of pre-extraction on pulp properties, Carbohydrate Polymers, 87 (2012), 322-327
- Liu X., and Lee D-J., (2015), Some recent research and development in drying technologies: product perspective, Drying Technology, 33 (11), 1339-1349, 2015

- Liu Z., Xu D., Xia N., Zhao X., Kong F., Wang S., and Fatehi P., (2018), Preparation and application of phosphorylated xylan as a flocculant for cationic ethyl violet dye, Polymers 2018, 10, 317
- Longue Junior D., Ayoub A., Venditti RA., Jameel H., Colodette JL., and Chang H. (2013), Ethanol precipitation of hetero-polysaccharide material from hardwood by alkaline extraction prior to the kraft cooking process, BioResources 8(4), 5319-5332
- Longue Junior, D., Colodette J.L., Brumano G.C.B., da Silva E.D., and Alves M.M.A., (2013), Effect of process variables on quality improvement of TGW pulps of Eucalyptus, Cerne, Lavras, (4) 567-574, 2013
- Lu Y., He Q., Fan G., Cheng Q., and Song G., (2021), Extraction and modification of hemicellulose from lignocellulosic biomass: A review. Green Processing and Synthesis, vol. 10, no. 1, 2021, pp. 779-804. doi:10.1515/gps-2021-0065
- Lynd L.R., Liang X., Biddy M.J., Allee A., Cai H., Foust T., Himmel M.E., Laser M.S., Wang M., and Wyman C.E., (2017) Cellulosic ethanol: status and innovation, Current Opinion in Biotechnology, 2017, 45:202-211
- Ma, H., Liu, W-W., Chen, X., Wu, Y-J., and Yu, Z-L., 2009. Enhanced Saccharification of Rice Straw by Microwave Pretreatment, Bioresource Technology, 100, 1279–1284
- Macrelli S., Mogensen J., and Zacchi G., (2012), Techno-economic evaluation of 2nd generation bioethanol production from sugarcane bagasse and leaves integrated with the sugar-based ethanol process, Biotechnol Biofuels, Doi:10.1186/1754-6834-5-22
- Mandegari M.A., Farzad S., and Görgens J.F., (2017), Recent trends on techno-economic assessment (TEA) of sugarcane biorefineries, Biofuel Research Journal, 493), 704-712
- Manfredi A.P., Ballesteros I., Saez F., Perotti N.I., Martinez M.A., and Negro M.J. (2018), Integral process assessment of sugarcane agricultural crop residues conversion to ethanol, Bioresource Technology 260 (2018) 241-247

- Manfredi A.P., Ballesteros I., Saez F., Perotti N.I., Martinez M.A., and Negro M.J. (2018), Integral process assessment of sugarcane agricultural crop residues conversion to ethanol, Bioresource Technology 260 (2018) 241-247

- Michael C. Flickinger & Stephen W. Drew, (1999) Encyclopedia of Bioprocess Technology: Fermentation, Biocatalysis and Bioseparation; Volumes 1-5, 1999 by John Wiley & Sons, Inc.

- Mihiretu G.T., Brodin M., Chimphango A.F., Oyass K., Hoff B.H., and Görgens J.F., (2017), Single-step microwave-assisted hot water extraction of hemicelluloses from selected lignocellulosic materials – a biorefinery approach, Bioresource Technology, 241, 669-680
- Mihiretu GT., Chimphango AF., and Görgens JF., (2019) Steam explosion pretreatment of alkali-impregnated lignocelluloses for hemicellulose extraction and improved digestibility, Bioresource Technology, 294, 122121
- Mohan S.V., Nikhil G.N, Chiranjeevi P., Reddy C.N., Rohit M.V., Kumar A.N., and Sarkar O., (2016), Waste biorefinery models towards sustainable circular bioeconomy: critical review and future perspectives, Bioresource Technology 215, 2-12, 2016
- Mosier, N.S., (2013). Fundamentals of Aqueous Pretreatment of Biomass, in "Aqueous Pretreatment of Plant Biomass for Biological and Chemical Conversion to Fuels and Chemicals", Ed. Wyman C.E., pp. 129-143
- Mulat D.G., and Horn S.J., (2018), Biogas production from lignin via anaerobic digestion; Lignin valorisation: Emerging approaches, Energy and Environment, series; pp. 391-412
- Myers R.H., Montgomery D.C., Vining G.G., Borror C.M., and Kowalski S.M., (2004), Response surface methodology: a retrospective and literature survey, Journal of Quality Technology, 36 (1), 53-77, 2004
- Narjary B., Aggarwal P., Kumar S., and Meena M.D. (2013), Significance of hydrogel and its application in agriculture, Indian farming 62 (10): 15-17, 2013
- Nechita P., Mirela R., and Ciolacu F., (2021), Xylan Hemicellulose: A renewable material with potential properties for food packaging applications. Sustainability 2021, 13, 13504. https://doi.org/10.3390/su132413504
- Negro M.J., Manzanares P., Ballesteros I., Oliva J.M., Cabanas A., and Ballesteros M., (2003), Hydrothermal pretreatment conditions to enhance ethanol production from poplar biomass, Biotechnology for Fuels and Chemicals, 87-100, 2003
- Nogueira L.A.H., Kang S., and Skeer J., IRENA (2019), Sugarcane bioenergy in southern Africa: Economic potential for sustainable scale-up, IRENA, Abu Dhabi
- Norstrom E., Fogelstrom L., Nordqvist P., Khabbaz F. and Malmstrom E. (2015), Xylan - A green binder for wood adhesives, European Polymer Journal, 67(2015), 483-493

- Oliveira F.M.V., Pinheiro I.O., Souto-Maior A.M., Martin C., Goncalves A.R., and Rocha G.J.M. (2013), Industrial-scale steam explosion pretreatment of sugarcane straw for enzymatic hydrolysis of cellulose for production of second generation ethanol and value-added products; Bioresource Technology, 130, 168-173
- Oriez V., Peydecastaing J., and Pontalier P-Y., (2019), Lignocellulosic Biomass Fractionation by Mineral Acids and Resulting Extract Purification Processes: Conditions, Yields, and Purities, Molecules. 2019 Dec; 24(23): 4273, doi:10.3390/molecules24234273
- Ou L., Dou C., Yu J.H., Kim H., Park Y.C., Park S., Kelley S., and Lee E.Y., (2021) Techno-economic analysis of sugar production from lignocellulosic biomass with utilization of hemicellulose and lignin for high value co-products. Biofuels, Bioproducts and Biorefinery, 15(2), 404-415. http://doi.org/10.1002/bbb.2170
- Pachón E.R., Vaskan P., Raman J.K., and Gnansounou E., (2018), Transition of a South African sugar mill towards a biorefinery: A feasibility Study, Applied Energy, 229(1), 2018, 1-17; https://doi.org/10.1016/j.apenergy.2018.07.104
- Padella M., O'Connell A., and Prussi M., (2019), What is still limiting the development of cellulosic ethanol? Analysis of the current status of the sector; Appl. Sci. 2019,9,4523; doi:10.3390/app9214523
- Pahimanolis, N., Sorvari, A., Luong, N.D., Seppala, J., 2014. Thermoresponsive Xylan Hydrogels via copper-catalysed azide-alkyne cycloaddition, Carbohydrate Polymers 102, 637-644
- Pandey A.K., Kumar M., Kumari S., Kumari P., Yusuf F., Jakeer S., Naz S., Chandna P., Bhatnagar I., and Gaur N.A., (2019), Evaluation of divergent yeast genera for fermentation-associated stresses and identification of a robust sugarcane distillery waste isolate *Saccharomyces cerevisiae* NGY10 for lignocellulosic ethanol production in SHF and SSF; Biotechnology for Biofuels, 12(40), (2019)
- Panthapulakkal S., Pakharenko V. & Sain M. (2013), Microwave Assisted Short-Time Alkaline Extraction of Birch Xylan; J Polym Environ (2013) 21:917–929
- Parawira W., and Tekere M., (2009), Biotechnological strategies to overcome inhibitors in lignocellulose hydrolysates for ethanol production: review; Critical Reviews in Biotechnology, vol. 31, 20-31, https://doi.org/10.3109/07388551003757816

- Pardo-Planas O., Atiyeh H.K., Philips J.R., Aichele C.P., and Mohammad S., (2017), Process simulation of ethanol production from biomass gasification and syngas fermentation, Bioresource Technology, 245, 925-932
- Parikh D.M., (2015), Vacuum drying: basics and application, Part 1. Chemical Engineering, Vol 122, no. 4, Apr. 2015
- Pauly M., Gille S., Liu L., Mansoori N., de Souza A., Schultink A., and Xiong G., (2013), Hemicellulose biosynthesis, Planta 238 (4), 627-642, 2013
- Pawar PM-A, Maceluch MD, Chong S-L,Gandla ML, Bashar SS, Sparrman T, Ahvenainen P., Hedenstrom M, Özparpucu M, Rüggeberg M, Serimaa R, Lawoko M., Tenkanen M., Jonsson LJ and Mellerwicz EJ (2017), In muro deacetylation of xylan affects lignin properties and improves saccharification of aspen wood, Biotechnol biofuels (2017); 10:98: DOI 10.1186/s13068-017-0782-4
- Peng F, Ren JL, Xu F, Bian J, Peng P, Sun RC. (2012), Fractionation and characterization of alkali extracted hemicelluloses from pea shrub. Biomass Bioenergy 2012; 39:20–30
- Peng F, Ren JL, Xu F, Bian J, Peng P, Sun RC. Fractional study of alkali-soluble hemicelluloses obtained by graded ethanol precipitation from sugar cane bagasse. J Agric Food Chem 2010b; 58:1768–76
- Peng F, Ren JL, Xu F, Bian J, Peng P, Sun RC., (2010a), Comparative studies on the physico-chemical properties of hemicelluloses obtained by DEAE-cellulose-52 chromatography from sugarcane bagasse. Food Res Int 2010a; 43:683–93
- Peng F, Ren JL, Xu F, Bian J, Peng P, Sun RC., (2010b), Fractional study of alkali-soluble hemicelluloses obtained by graded ethanol precipitation from sugar cane bagasse. J Agric Food Chem 2010b; 58:1768–76
- Peng Feng, Peng Pai, Xu Feng and Sun Run-Cang (2012), Fractional purification and bioconversion of hemicelluloses, Biotechnology Advances 30 (2012) 879–903
- Peng X., Nie S., Li X., Huang X. and Li Q. (2019) Characteristics of the water-and alkali-soluble hemicelluloses fractionated by sequential acidification and graded-ethanol from sweet maize stems, Molecules 2019, 24, 212
- Pengilly C., Garcia-Aparicio M.P., Diedericks D., Brienzo M., and Görgens J.F., (2015), Enzymatic hydrolysis of steam-pretreated sweet sorghum bagasse by combinations of cellulase and endo-xylanase, Fuel 154, 352-360, 2015
- Perry R.H., (2008), Perry's Chemical Engineers Handbook, 8th Edition, McGraw-Hill

- Persson T., Nordin A-K., Zacchi G., and Joensson A-S. (2007) Economic evaluation of isolation of hemicelluloses from process streams from thermomechanical pulping of spruce, Applied Biochemistry and Biotechnology, Vol. 136-140, pp. 741-752, 2007
- Peters M.S., Timmerhaus K.D., and West R.E., (2003), Plant design and economics for chemical engineers, Fifth Edition, McGraw-Hill, 2003
- Petersen A.M., Okoro O.V., Chireshe F., Moonsamy T., and Gorgens J.F., (2021), Systematic cost evaluations of biological and thermochemical processes for ethanol production from biomass residues and industrial off-gases, Energy Conversion and Management 243 (2021) 114398
- Petersen A.M., Van der Westhuizen W.A., Mandegari M.A., and Görgens J.F., (2017), Economic analysis of bioethanol and electricity production from sugarcane in South Africa, Biofuels, Bioprod. Bioref. 12:224–238 (2018), DOI: 10.1002/bbb.1833
- Pielhop T., Amgarten J., Rudolf von Rohr P., and Studer M.H., (2016), Steam explosion pretreatment of softwood: the effect of the explosion decompression on enzymatic digestibility, Biotechnology for Biofuels, 2016, 9:152
- Pierossi M.A., and Bertonali F.C., (2018), Sugarcane trash as feedstock for biorefineries: Agricultural and logistics issues, in Book: Advances in Sugarcane Biorefinery: Technologies, Commercialization, Policy Issues and Paradigm shift for Bioethanol and By-products, Edited by: Chandel A.K., and Silveira M.H.L.; pp. 17-39;
- Pippo W.A., Luengo C.A., Alberteris L.A.M., Garzone P., and Cornacchia G., (2011), Energy recovery from sugarcane trash in the light of 2nd generation biofuels. Part1: Current situation and environmental aspects, Waste Biomass Valor (2011), 2:1-16
- Popa V.I., and Spiridon I., (1998), Hemicelluloses: structure and properties, Chap-9 of the book 'Polysaccharides: structural diversity and functional versatility (Edited by Dumitriu S.), pp. 297-311
- Popa V.I., and Spiridon I., (2008), Hemicelluloses: major sources, properties and applications, Monomers, Polymers and Composites from Renewable Resources, 2008, pp. 289-304; https://doi.org/10.1016/B978-0-08-045316-3.00013-2
- Q. Yu., Zhuang X., Wang W., Qi W., Wang Q., Tan X., Kong X., and Yuan Z., (2016), Hemicellulose and lignin removal to improve the enzymatic digestibility and ethanol production, Biomass and Bioenergy 94, 105-109, 2016
- Qing Q. Yang B., Wyman C.E., (2010), Xylooligomers are strong Inhibitors of Cellulose Hydrolysis by Enzymes, Bioresource Technology, 2010, 101:9624-40

- Ragauskas A.J., Williams C.K., Davison B.H., Britovsek G., Cairney J., Eckert C.A., Frederick W.J., Jr., Hallett J.P., Leak D.J., Liotta C.L., et al. The Path Forward for Biofuels and Biomaterials. Science. 2006; 311: 484–489. doi: 10.1126/science.1114736
- Rahikainen JL., Martin-Sampedro R., Heikkinen H., Rovio S., Marjamaa K., Tamminen T., Rojas OJ., and Kruus K. (2013), Inhibitory effect of lignin during cellulose bioconversion: the effect of lignin chemistry on non-productive enzyme adsorption, Bioresource Technology 2013, 270-278
- Ralph J., Lapierre C., and Boerjan W., (2019), Lignin structure and its engineering, Current Opinion in Biotechnology, Vol.56, pp. 240-249; https://doi.org/10.1016/j.copbio.2019.02.019
- Ramaswamy S., Huang H.J., and Ramaroa B.V., (2013). Separation and purification technologies in biorefineries, John Wiley and Sons. http://doi.org/10.1002/9781118493441
- Ramirez, R.S., Holtzapple, M., and Piomonte, N., 2013. "Fundamentals of Biomass Pretreatment at High pH", in Aqueous Pretreatment of Plant Biomass for Biological and Chemical Conversion to Fuels and Chemicals, Edited by Charles E. Wyman, pp. 145-167
- Rao M., Muralikrishna G. (2006), Hemicelluloses of ragi (finger millet, Eleusine coracana, indaf-15): isolation and purification of an alkali-extractable arabinoxylan from native and malted hemicellulose B. J Agric Food Chem 2006;54:2342–9
- Ratti R.P., Delforno T.P., Sakamoto I.K., and Varesche M.B.A. (2015), Thermophilic hydrogen production from sugarcane bagasse pretreated by steam explosion and alkaline delignification, Int'nal J. of Hydrogen energy, 2015, 6296-6306
- Rezende C.A., Aparecida de Lima M., Maziero P., Ribeiro de Azevedo E., Garcia W., and Polikarpov I., (2011), Chemical and morphological characterization of sugarcane bagasse submitted to a delignification process for enhanced enzymatic digestibility, Biotechnology for biofuels 4(1), 54, 2011
- Riya S., Meng L., Wang Y., Lee C.G., Zhou S., Toyota K., and Hosomi M., (2020), Dry anaerobic digestion for agricultural waste recycling, IntechOpen, DOI:10.5772/intechopen.91229
- Robak K., and Balcerek M., (2018), Review of second generation bioethanol production from residual biomass, Food Technol Biotechnol. 2018; 56 (2): 174-187; doi: 10.17113/ftb.56.02.18.5428

- Robak K., and Balcerek M., (2018), Review of second generation bioethanol production from residual biomass, Food Technol Biotechnol. 2018; 56 (2): 174-187; doi: 10.17113/ftb.56.02.18.5428
- Rocha GJM., Goncalves AR., Oliveira BR., Olivares EG., and Rossel CEV (2012), Steam explosion pretreatment reproduction and alkaline delignification reactions performed on a pilot scale with sugarcane bagasse for bioethanol production, Industrial crops and products, 2012, 274-279
- Roehr M., (2001) The Biotechnology of Ethanol, Classical and Future Applications, WILEY-VCH Verlag GmbH, Weinheim
- Rohde V., Boeringer S., Tuebke B., Adam C., Dahmen N., and Schmiedl D., (2019), Fractionation of three different lignins by thermal separation techniques - A comparative study, Special Issue "Biobased value chains for a growing bioeconomy" of GCB-Bioenergy, Global Change Biology Bioenergy, 11(1), 206-217; http://doi.org/10.1111/gcbb.12546
- Romani A., Garrote G., Alonso J.L., and Parajo J.C., (2010) Bioethanol production from hydrothermally pretreated *Eucalyptus globulus* wood, Bioresource Technology, 8706-8712
- Romani A., Garrote G., Ballesteros I., and Ballesteros M. (2013), Second generation bioethanol from steam exploded *Eucalyptus globulus* wood, Fuel 111 (2013) 66-74
- Rosales-Calderon, O., Arantes, V. A review on commercial-scale high-value products that can be produced alongside cellulosic ethanol. *Biotechnol Biofuels* **12,** 240 (2019). https://doi.org/10.1186/s13068-019-1529-1
- Sabiha-Hanim S. & Siti-Norsafurah A.M., (2012), Physical Properties of hemicellulose films from sugarcane bagasse, Procedia Engineering 42 (2012) 1390-1395
- Safarian S., Richter C., and Unnthorsson R., (2019), Waste biomass gasification simulation using Aspen Plus: Performance evaluation of wood chips, sawdust and mixed paper wastes, Journal of Power and Energy Engineering, 7:12-30
- Saini R., Hegde K., Brar SK., and Vezina P., (2020), Advanced biofuel production and road to commercialization: An insight into bioconversion potential of Rhodosporidium sp., Biomass and Bioenergy 132 (2020) 105439
- Santos N.M., Puls J., Sakke B., and Navaard P., (2013), Effects of Nitren Extraction on a dissolving pulp and Influence on Cellulose dissolution in NaOH-Water; Cellulose 20: 2013-2026

- Schaidle J.A., Moline C.J., and Savage P.E., (2011), Biorefinery sustainability assessment, Environmental Progress & Sustainability Energy, 30(4), 743-753, 2011
- Schroeder T., Lauven L.-P., Sowlati T., and Geldermann J. (2019), Strategic planning of a multi-product wood-biorefinery production system, Journal of Cleaner Production, 211 (2019), 1502-1516
- Schulze P., Leschinsky M., Seidel-Morgenstern A., and Lorenz H., (2019), Continuous separation of lignin from organosolv pulping liquors - combined lignin particle formation and solvent recovery, Industrial & Engineering Chemistry Research, 58(9); DOI: 10.1021/acs.iecr.8b04736
- Selig M., Weiss N., and Ji Y., (2008), Enzymatic Saccharification of Lignocellulosic Material; Laboratory Analytical Procedure (LAP); Technical Report NREL/TP-510-42629
- Serna-Loaiza S., Miltner A., Miltner M., and Friedl A., (2019), A Review on the feedstocks for the sustainable production of bioactive compounds in biorefineries, Sustainability 2019, 11(23), 6765; https://doi.org/10.3390/su11236765
- Short W., Packey D.J., and Holt T., (1995), "A manual for the economic evaluation and energy efficiency and renewable energy technologies" NREL Report TP-462-5173
- Shuangliang LV., Quiang Yu., Zhuang X., Yuan Z., Wang W., Wang Q., Qi W. and Tan X., (2013), The influence of hemicellulose and lignin removal on the enzymatic digestibility from sugarcane bagasse; bioenergy resources (2013) 6:1128-1134
- Shuntaro Tsubaki and Jun-Ichi Azuma (2011), Application of Microwave Technology for Utilization of Recalcitrant Biomass, Advances in Induction and Microwave Heating of Mineral and Organic Materials, Stanisław Grundas, IntechOpen, DOI: 10.5772/14040; Available from: https://www.intechopen.com/books/advances-in-induction-and-microwave-heating-of-mineral-and-organic-materials/application-of-microwave-technology-for-utilization-of-recalcitrant-biomass
- Silva E.M., Hogez H., and Larondelle Y., (2007), Optimization of extraction of phenolics from Inga edulis leaves using surface response methodology, Separation and Purification Technology, 55 (3), 381-387, 2007
- Silva T.C.F., Habibi Y., Colodette J.L. and Lucia L.A., (2010), The influence of the chemical and structural features of xylan on the physical properties of its derived hydrogels, The Royal Society of Chemistry 2010

- Silveira M.H.L., Morais A.R.C., da Costa Lopes A.M., Olekszyszen D.N., Bogel-Lukasik R., Andreaus J., and Ramos L.P. (2015), Current Pretreatment Technologies for the Development of Cellulosic Ethanol and Biorefineries, ChemSusChem,8,3366–3390
- Singh J., Suhag M., and Dhaka A. (2015) Augmented digestion of lignocellulose by steam explosion, acid and alkaline pretreatment methods: A review, Carbohydrate Polymers 117 (2015) 624-631
- Singh P., Suman A., Tiwari P., Arya N., Gaur A., and Shrivastava AK., (2008) Biological pretreatment of sugarcane trash for its conversion to fermentable sugars, World Journal of Microbiology and Biotechnology, 24 (5), 667-673, 2008
- Singh R., Shukla A., Tiwari S., and Srivastava M., (2014), A review of delignification of lignocellulosic biomass for enhancement of ethanol production potential, Renewable and Sustainable Energy Reviews 32, 713-728, 2014
- Sluiter A., Hames B., Ruiz R., Scarlata C., Sluiter J., and Templeton D., (2008), Determination of Sugars, Byproducts, and Degradation Products in Liquid Fraction Process Samples; Laboratory Analytical Procedure (LAP); Technical Report NREL/TP-510-42623 [=> Sluiter et al., (2008b)]
- Sluiter A., Hames B., Ruiz R., Scarlata C., Sluiter J., and TempletonD., (2008), Determination of Ash in Biomass; Laboratory Analytical Procedure (LAP); Technical Report NREL/TP-510-42622 [=> Sluiter et al., (2008d)]
- Sluiter A., Hames B., Ruiz R., Scarlata C., Sluiter J., Templeton D., and Crocker D., (2012), Determination of Structural Carbohydrates and Lignin in Biomass; Laboratory Analytical Procedure (LAP); Technical Report NREL/TP-510-42618
- Sluiter A., Hames, B., Ruiz, R., Scarlata, C., Sluiter J., and Templeton D. 2008. Determination of Sugars, Byproducts, and Degradation Products in Liquid Fraction Process Samples; Laboratory Analytical Procedure (LAP); Technical Report NREL/TP-510-42623 [=>Sluiter et al., (2008c)]
- Sluiter A., Hyman D., Payne C., and Wolfe J., (2008), Determination of Insoluble Solids in Pretreated Biomass Material; Laboratory Analytical Procedure (LAP); Technical Report NREL/TP-510-42627 [=> Sluiter et al., (2008a)]
- Sluiter A., Ruiz R., Scarlata C., Sluiter J., and Templeton D., (2008), Determination of Extractives in Biomass; Laboratory Analytical Procedure (LAP); Technical Report NREL/TP-510-42619 [=> Sluiter et al., (2008a)]

- Soam S., Kappor M., Kumar R., Borjesson P., Gupta R.P., and Tuli D.K., (2016), Global warming potential and energy analysis of second generation ethanol production from rice straw in India. Applied Energy, 184.353-364
- Song T., Pranovich A., and Holmborn B., (2012), Hot water extraction of spruce wood of different particle size, Bioresources 7(3), 4214-4225
- Spiridon I and Popa V.I., (2008), Hemicelluloses: major sources, properties and applications, Monomers, Polymers and Composites from Renewable Resources, 2008, pp. 289-304; https://doi.org/10.1016/B978-0-08-045316-3.00013-2
- Sukhbaatar, B., Hassan, E.B., Kim, M., Steele, P., and Ingram, L., 2014. Optimization of Hot-compressed Water Pretreatment of Bagasse and Characterization of extracted Hemicelluloses, Carbohydrate Polymers, 101, 196-202
- Sun JX, Sun XF, Sun RC, Su YQ. Fractional extraction and structural characterization of sugarcane bagasse hemicelluloses. Carbohydrate Polymers 56 (2004b)195–204
- Sun S., Sun S., Cao X., and Sun R., (2016), The role of pretreatment in improving the enzymatic hydrolysis of lignocellulosic materials, A review; Bioresource Technology,199, 2016, 49-58; https://doi.org/10.1016/j.biortech.2015.08.061
- Sun S.L., Wen J.L., Ma M.G. & Sun R.C., (2013), Successive alkali extraction and structural characterization of hemicelluloses from sweet sorghum stem, Carbohydrate Polymers 92 (2013) 2224-2231
- Sun S.S., Wen J.L., Ma M.G., Song X.L., Sun R.C., (2014), Integrated biorefinery based on hydrothermal and alkaline treatments: Investigation of sorghum Hemicelluloses; Carbohydrate Polymers 111 (2014) 663–669
- Susmozas A., Martin-Sampedo R., Ibarra D., Eugenio M.E., Iglesias R., Manzanares P., and Moreno A., (2020), Process strategies for the transition of 1G to advanced bioethanol production, Processes (MDPI), 2020,8,1310; http://doi.org/10.3390/pr8101310
- Tagami A., Gioia C., Lauberts M., Budnyak T., Moriana R., Lindstroem M.E., and Sevastyanova O., (2018), Solvent fractionation of softwood and hardwood kraft lignins for more efficient uses: compositional, structural, thermal, antioxidant and sorption properties, Industrial Crops and Products, 129:123-134; DOI: 10.1016/j.indcrop.2018.11.067
- Tan, H., and Marra, K.G., 2010. Injectable, Biodegradable Hydrogels for Tissue Engineering Applications, Review, Materials, 3, 1746-1767

- Tan, H., and Marra, K.G., 2010. Injectable, Biodegradable Hydrogels for Tissue Engineering Applications, Review, Materials, 3, 1746-1767
- Teleman A., Lundqvist J., Stalbrand H., Tjerneld F., and Dahlman O., (2000), Characterization of acetylated 4-O-methylglucuronoxylan isolated from aspen employing 1H and 13C NMR Spectroscopy, Carbohyd. Res. 329, 807-815
- Teo C.C., Tan S.N., Yong J.W.H., Hew C.S., and Ong E.S., (2010), Pressurized hot water extraction (PHWE); Journal of Chromatography A, 1217 (2010) 2484–2494
- Thuvander J., and Jönsson A-S., (2016), Extraction of galactoglucomannan from thermomechanical pulp mill process water by microfiltration and ultrafiltration - Influence of microfiltration membrane pore size on ultrafiltration performance, Chemical Engineering Research and Design 2016, 105, 171-176. DOE: 10.1016/j.cherd.2015.12.003
- Thuvander J., Lipnizki F., and Jönsson A-S., (2019), On-site recovery of hemicelluloses from thermomechanical pulp mill process water by microfiltration and ultrafiltration, Journal of Wood Chemistry and Technology, 39: 215-224, DOE: 10.1080/02773813.2019.1565865
- Toma´s-Pejo E., Alvira P., Ballesteros M., Negro M.J., (2011), Pretreatment Technologies for Lignocellulose-to-Bioethanol Conversion, Ch.7, Biofuels: Alternative Feedstocks and Conversion Processes, Elsevier Inc.
- Tomani P. (2010), The LignoBoost Process, Cellulose Chemistry and Technology, 44 (1-3), 53-58, 2010
- Torres, A.F., Slegers, P.M., Noordam-Boot, C.M., Dolstra, O., Vlaswinkel, L., Boxtel, A.J., and Trindade, L.M. (2016). Maize feedstocks with improved digestibility reduce the costs and environmental impacts of biomass pretreatment and saccharification; Biotechnology for Biofuels, 9, 63. https://doi.org/10.1186/s13068-016-0479-0
- Trajano, H.L., and Wyman, C.E., (2013), Fundamentals of Biomass Pretreatment at low pH, in "Aqueous Pretreatment of Plant Biomass for Biological and Chemical Conversion to Fuels and Chemicals", Ed. Wyman C.E., pp. 103-128
- Tsubaki, S., Azuma, J. -I., Yoshimura, T., Maitani, M.M., Suzuki, E., Fujii, S., and Wada, Y., 2016. "Microwave-Induced Biomass Fractionation." Biomass Fractionation Technologies for a Lignocellulosic Feedstock Based Biorefinery, edited by Mussatto S.L., pp. 103-126

- Tutt M., Kikas T. and Olt J., (2012), Influence of different pretreatment methods on bioethanol production from wheat straw; Agronomy Research Biosystems Engineering Special Issue 1, 269-276
- Ubando A.T., Felix C.B., and Chen W-H., (2020), Biorefineries in circular bioeconomy: A comprehensive review, Bioresource Technology, Volume 299, March 2020, 122585
- Valinhas RV, Pantoja LA., Maia ACF., Miguel MGCP, Vanzela APFC, Nelson DL, and Santos AS., (2018), Xylose fermentation to ethanol by new *Galactomyces geotrichum* and *Candida akabanesis* strains. Peer J 6:e4673
- Valoppi F., Lahtinen M.H., Bhattarai M., Kirjoranta S.J., Juntti V.K., Peltonen L.J., Kilpelaeinen P.O., and Mikkonen K.S., (2019), Centrifugal fractionation of softwood extracts improves the biorefinery workflow and yields functional emulsifiers, Green Chem., 2019, 21, 4691-4705, https://doi.org/10.1039/C9GC02007A
- Vena P.F., Garcia-Aparicio M.P., Brienzo M., Görgens J.F., and Rypstra T., (2013), Effect of Alkaline Hemicellulose Extraction on Kraft Pulp Fibers from Eucalyptus Grandis, Journal of Wood Chemistry and Technology, 33:157-173, 2013
- Venugopal J.R., Sridhar S., and Ramkrishna S., (2014), Electrospun plant-derived natural biomaterials for tissue engineering, Plant Science Today (2014) 1(3): 151-154; http://dx.doi.org/10.14719/pst.2014.1.3.65
- Walker J. C.F., (2006) Primary Wood Processing – Principles and Practice, 2nd Ed.
- Wan Azelee, N.I., J.M. Jahim, A. Rabu, A.M. Abdul Murad and F.D. Abu Bakar et al., 2014. Efficient removal of lignin with the maintenance of hemicellulose from kenaf by two-stage pretreatment process. Carbohydr. Polym., 99: 447-453. DOI: 10.1016/j.carbpol.2013.08.043
- Wang M., Han J., Dunn B., Cai H., and Elgowainy A., (2012), Well-to-wheels energy use and greenhouse gas emissions of ethanol from corn, sugarcane and cellulosic biomass for US use, Environmental Research Letters, 7 045905
- Wang T., Li C., Song M., and Fan R., (2019), Xylo-oligosaccharides preparation through acid hydrolysis of hemicelluloses isolated from press-lye, Grain & Oil Science and Technology, 2019
- Wang Y. and Zhang J. (2006), A novel hybrid process enhanced by ultrasonication, for xylan extraction from corncobs and hydrolysis of xylan to xylose by xylanase, Journal of Food Engineering 77 (2006), 140-145

- Wang Z., Winestrand S., Gillgren T., and Jonsson LJ., (2018), Chemical and structural factors influencing enzymatic saccharification of wood from aspen, birch and spruce, Biomass and Bioenergy, 109 (2018), 125-134
- Weinwurm F., Drljo A., Silva T.L.S., and Friedl A., (2014), Principles of ethanol organosolv lignin precipitation: process simulation and energy demand, Italian Association of Chemical Engineering, 2014
- Wellisch M., Jungmeier G., Karbowski A., Patel M.K., and Rogulska M., (2010), Biorefinery systems - potential contributors to sustainable innovation, Biofuels, Bioproducts and Biorefining: Innovation for a sustainable economy, 4(3), 275-286
- Winters P., (2011), The current status of cellulosic biofuel commercialization, Biotechnology Industry Organization (BIO), 'www.bio.org'
- Xu J., Zhou G., Li J., and Mo L., (2017), Effects of steam explosion pretreatment on the chemical composition and fiber characteristics of cornstalks, J. of Bioresources and bioproducts, 2017, 153-157
- Xu J.-K., and Sun R.-C., (2016), Recent advances in alkaline pretreatment of lignocellulosic biomass, in "Biomass Fractionation Technologies for a Lignocellulosic feedstock based biorefinery" Ed. S.I. Mussatto, pp. 431-459
- Xu L. and Tschirner U. (2012), Peracetic acid pretreatment of Alfalfa stem and Aspen biomass, BioResources 7(1), 203-216
- Yan, L., Ma, R., Li, L., and Fu, J., 2016. Hot Water Pretreatment of Lignocellulosic Biomass: An Effective and Environmentally Friendly Approach to Enhance Biofuel Production; Chem. Eng. Technol. 39, No. 10, 1759–1770
- Yang B., and Wyman C.E., (2008), Pretreatment: the key to unlocking low-cost cellulosic ethanol, 2008, Biofuels, Bioprod. Bioref. 2:26–40
- Yang B., Dai Z., Ding S. & Wyman C.E., (2011), Enzymatic hydrolysis of cellulosic biomass; Biofuels (2011) 2(4), 421–450
- Yang J., Summanen P.H., Henning S.M., Hsu M., Lam H., Huang J., Tseng C-H., Dowd S.E., Finegold S.M., Heber D., and Li Z., (2015), Xylo-oligosaccharide supplementation alters gut bacteria in both healthy and prediabetic adults: a pilot study, Frontiers in Physiology, 2015; 6:216; doi: 10.3389/fphys.2015.00216
- Yang R., Xu S., Wang Z., and Yang W. (2005), Aqueous extraction of corncob xylan and production of xylo-oligosaccharides, LWT Food Science & Technology 38., 677-682

- Yang, B., Dai, Z., Ding, S.Y., and Wyman, C.E., 2011. Enzymatic hydrolysis of cellulosic biomass; Biofuels, 2(4), 421–450
- Ye C-L. and Jiang C-J., (2011), Optimization of extraction process of crude polysaccharides from *Plantago asiatica* L. by response surface methodology, Carbohydrate Polymers, 84 (1), 495-502, 2011
- Yu Z., Jameel H., Chang H., and Park S., (2011), The effect of delignification of forest biomass on enzymatic hydrolysis, Bioresource Technology 102 (19), 9083-9089, 2011
- Zeitoun R, Pontalier PY, Marechal P, Rigal L. Twin-screw extrusion for hemicellulose recovery: influence on extract purity and purification performance. Bioresource Technology 2010;101:9348–54
- Zhang B., Ning D., Yang Y., Nostrand J.D.V., Zhou J., and Wen X., (2020), Biodegradability of wastewater determines microbial assembly mechanisms in full-scale wastewater treatment plants, Water Research 169 (2020), 115276
- Zhang H., Zhang Y., Shao H., and Hu X., (2004), Prediction of molecular weight distribution of cellulose by using the rheological method, Appl Polym Sci 94: 598–603, 2004; https://doi.org/10.1002/app.20732
- Zhang M., Jiang H., and Lim R-X., (2010), Recent developments in microwave-assisted drying of vegetables, fruits and aquatic products - drying kinetics and quality considerations, Drying Technology 28 (11), 1307-1316, 2010
- Zhang S., Guan Y., Fu G-Q, Chen B-Y, Peng F., Yao C-L and Sun R-C (2014), Organic/Inorganic superabsorbent hydrogels based on xylan and montmorillonite, Journal of Nanomaterials, 2014
- Zhang W. and Geng A., (2012), Improved ethanol production by a xylose-fermenting recombinant yeast strain constructed through a modified genome shuffling method, Biotechnology for Biofuels, 2012, 5:46
- Zhang W., Zhang X., Lei F., and Jiang J., (2020). Co-production of bioethanol and xylo-oligosaccharides from sugarcane bagasse via autohydrolysis pretreatment. Renewable Energy, Elsevier, 2297-2305. DOI:10.1016/j.renene.2020.10.034
- Zhang Y., Pan Z., Zhang R., (2009) Overview of biomass pretreatment for cellulosic ethanol production, Int J Agric & Biol Eng, 2009; 2(3): 51-68
- Zhang Y-H.P., (2008) Reviving the carbohydrate economy via multi-product lignocellulose biorefineries, Journal of industrial microbiology & biotechnology 35 (5), 367-375, 2008

- Zhang YH.P., Ding SY., Mielenz J.R., Cui JB., Elander R.T., Laser M., Himmel M.E., McMillan J.R., and Lynd L.R., (2007), Fractionating recalcitrant lignocellulose at modest reaction conditions, Biotechnology and Bioengineering, Vol. 97, No. 2, June 1, 2007; https://doi.org/10.1002/bit.21386
- Zhang, S., Guan, Y., Fu, G-Q., Chen, B-Y., Peng, F., Yao, C-L., and Sun, R.C., 2014. "Organic/Inorganic Superabsorbent Hydrogels Based on Xylan and Montmorillonite", Journal of Nanomaterials (Hindawe), Research Article, Vol 2014, ID 675035
- Zhao X., Zhang L., and Liu D., (2012), Biomass recalcitrance, Part I: the chemical compositions and physical structures affecting the enzymatic hydrolysis of lignocellulose, 2012, 465-482, https://doi.org/10.1002/bbb.1331
- Zhao Y., Shakeel U., Rehman MSU, Li H., Xu X. and Xu J., (2020), Lignin-carbohydrate complexes (LCCs) and its role in biorefinery, Journal of Cleaner Production, 253 (2020), 120076
- Zhao Y.L., Sun H., Yang B., and Weng Y.X., (2020), Hemicellulose-based film: potential green films for food packaging. Polymers 12:1775. Doi:10.3390/polym12081775
- Zheng L., and Furimsky E., (2003), ASPEN simulation of cogeneration plants, Energy Conversion and Management, 44:1845-1851
- Zhong K., and Wang Q., (2010), Optimization of ultrasonic extraction of polysaccharides from dried longan pulp using response surface methodology, Carbohydrate polymers, 80 (1), 19-25, 2010
- Zhu Li, O'Dwyer J.P., Chang V.S., Cesar B. Granda C.B., and Holtzapple M.T., (2008), Structural features affecting biomass enzymatic digestibility; Bioresource Technology 99 (2008) 3817–3828

- Zhu Li, O'Dwyer J.P., Chang V.S., Cesar B. Granda C.B., and Holtzapple M.T., (2008), Structural features affecting biomass enzymatic digestibility; Bioresource Technology 99 (2008) 3817–3828

- Zhuang X., Wang W., Yu Q., Qi W., Wang Q., Tan X., Zhou G., and Yuan Z., (2016), Liquid hot water pretreatment of lignocellulosic biomass for bioethanol production accompanying with high valuable products, Bioresource Technology 199, 68-75, 2016
- Zhuang X., Yu Q., Yuan Z., Kong X., and Qi W., (2015), Effect of hydrothermal pretreatment of sugarcane bagasse on enzymatic digestibility, Journal of Chemical Technology & Biotechnology 90 (8), 1515-1520, 2015

APPENDIX-A.1: CHAPTER-2, Summary of Literature Review

Table A-1.1: Biomass Pretreatment Methods Assessed in terms of their suitability for hemicellulose extraction and cellulose digestibility

No.	Pretreatment Method	Advantages	Disadvantages/Drawbacks/	Salient Features and typical pretreatment conditions	References
1	**Chemical Routes**				
1.1.	**Acid-based**				
1.1.1	**Dilute Acid Treatment (DAT)**	*Can achieve reasonably high sugar yields from hemicelluloses (HC), higher solubilization of such; lower corrosion and degradation products, cost and ease of use than concentrated acid method (CAT); improved enzymatic hydrolysis*	*High temperature conditions can lead to increased degradation of hemicelluloses (HC), resulting acidic compounds cause equipment corrosion and corrosion products which have undesired effects on downstream processes; formation of inhibitors necessitates second stage treatment to neutralize their effects*	*Low acid concentration and high temperature (140-190 °C; if second stage treatment is required 190 to 230°C); Low Conc = [0.5 to 1 % H2SO4) & Temp=121-160°C; Another range: 0.22 to 0.98%, temp: 140 to 200°C; time: 1 min to 1 or 2 hrs; 80 to 90% hemicellulose recovery is possible*	Sharara et al., (2012); Tomas-Pejo et al., (2013); Yang and Wyman, (2008); Galbe and Wallberg, (2019)
1.1.2	**Concentareted Acid Treatment (CAT)**	*Substantial conversion of structural sugars (cellulose and hemicelluloses) into fermentable sugars*	*High acid and energy consumption; equipment corrosion; significant operational problems; very expensive and associated costs on acid recovery after the treatment largely limit its application; high degradation rate, esp. at higher temp; longer reaction time*	*can remove mostly cellulose and hemicellulose, resulting in lignin-enriched solid phase; less attractive for ethanol production, due to higher inhibitors formation; acid recovery is key for economic viability of this method; H2SO4 is the most commonly used acid; polysaccharide solubilization is reached at different acid concentration levels: H2SO4 @72%; HCL@41%; TFA (Trifluoracetic acid) @100%*	
1.2	**Alkaline Methods (NaOH, KOH, Ca(OH)2)**	*Hemicelluloses degradation lowered substantially when compared to acid-based routes; process results in very few degradation products; improved digestibility of cellulose; can take place at lower temp and pressure; cheap and efficient method (R6)*	*High cost of alkali, esp. sodium hydroxide, and cost of recovery; limitation due to possible conversion of alkali into irrecoverable salts; possibly longer processing time*	*Effective for lignin solubilization while exihibiting only minor effects on cellulose and hemicelluloses; NaOH most commonly used and well-established alkaline agent; Lower PT temperatures and pressures compared to other methods; PT time is inversely related to temperature (e.g. lime PT at 25°C => time in weeks; if at 150°C in 2 hrs); short pretreatment times (1 to 3 hrs) and high temps (85-135°C) or longer PT times (24 hrs) and lower temperatures (50-65°C); temp: 30-130°C, reaction time: 10 min - 18 hrs have been reported*	Carvalheiro et al., (2008); Sharara et al., (2012); Yang and Wyman, (2008); Kim et al., (2016); Xu et al., (2016)

Table A-1.1 (Cont.) Biomass Pretreatment Methods Assessed in terms of their suitability for hemicellulose extraction and cellulose digestibility

1.3.	**Oxidizing Agents (e.g H2O2, Ozone, etc.)**				
1.3.1	**Alkaline/Oxidative (Peroxides with alkalines)**	*more enhanced hemicelluloses solubilization than alkali alone; more enhanced enzymatic conversion of cellulose; can yet take place at milder temperatures*	*safety issues can arise with use of peroxides; substantial lignin co-solubilization*	*Similar reaction mechanism as alkaline PT, but have faster kinetics at lower temperature; can thus be more effective than the alkaline alone; lignin solubilization is substantial; highly PH-dependent; PT are applied in batch mode; 1-3% H2O2; rxn time; 45 min to 5 hrs; temp: 30-80℃; optimal PH=11.5*	Carvalheiro et al., (2008); Kim et al., (2016)
1.3.2	**Wet Oxidation**	*reduced temperature, shorter reaction times, high enzymatic hydrolysis*	*expensive route mainly due to capital costs; significant lignin removal*	*Autohydrolysis in the presence of air or oxygen or Na2CO3 as a catalyst; Na2CO3 is the most employed chemical agent; considerable delignification is correalted with increased carboxylic acid content; Time: 5-15 min at temperatures from 170 to 200℃ and pressures from 10 to 12 bar*	Carvalheiro et al., (2008); Tomas-Pejo et al., (2013)
1.3.3	**Ozonolysis**	*Minimized formation of inhibitors; takes place at atmospheric pressure and temperature*	*Large amount of ozone is required; process is very expensive;*	*Its effect is mainly limited to lignins, not to hemicelluloses and cellulose; ozone incorporates conjugated double bonds and functional groups with high electron densities*	Canilha et al. (2013); Tomas-Pejo et al., (2013)
1.4	**Organosolv**	*Produces a highly digestible cellulose substrate*	*Significant amount of furfural, HMF, and soluble phenolic compounds from lignin in the prehydrolysate obtained after pretreatment; cost associated with solvent recovery is high*	*uses organic or aqueous solvents to extract lignin and provide more accessible cellulose; For economic reasons, low-molecular weight alcohols with lower boiling points such as ethanol and methanol are favored; typical pretreatment temperatures range: 100 to 250℃*	Tomas-Pejo et al., (2013); Galbe and Wallberg, (2019)
1.5	**Nitren Extraction**	*Leads to improved solubility of hemicelluloses (xylan, in particular) in NaOH*	*Not that attractive for industrial application as removal of nickel is both costy and laborious*	*Nickel-based Organometallic Complex is used as an agent; selective in dissolving and extracting xylan from paper-grade pulps; usually applied in the pulp & paper mills to dissolve out xylan; Typical PT condition: 2 to 7% aqueous solution of nitren; 10:1 liquid to solid ratio; reaction time=30min at 30℃*	Santos et al., (2013)

Table A-1.1 (Cont.) Biomass Pretreatment Methods Assessed in terms of their suitability for hemicellulose extraction and cellulose digestibility

2	**Physicochemical Routes**				
2.1	**Pressurized/Liquid Hot Water (HLW)**	*Effective in recovering hemicellulosic sugars at high yields, produces highly digestible cellulose; can be cost attractive; low environmental negative effect*	*excessive water and energy requirements; HLW configuration can be challenging to implement commercially*	*Batch or Flow-through modes; HW passing through biomass at high flow rates and pressures; Temp: 220-240℃; time: seconds to hours; liquid-to-solid ratio: 2 to 100 (w/w), typically at 10; temp: 130-240℃; pH 4 to 7; hemicellulosic sugars are retained primarily in oligomeric form and monomers formation is minimized; lower concentration of solubilized lignins*	Carvalheiro et al., (2008); Tomas-Pejo et al., (2013); Yang and Wyman (2008); Teo et al., (2010); Harmsen et al., (2010)
2,2	**Steam Explosion Pretreatment (SEPT)**	*Substantial removal of hemicelluloses; potential for lower environmental impact; feasibility at industrial scale development, it's one of the most widely employed technologies for 2G bioethanol production; yields high hemicellulose solubility*	*generation of some toxic/inhibitory compounds from sugar degradation (esp. pentoses and hexoses);*	*Steam explosion fractionates the biomass into: (i) a liquid fraction rich in monomeric and oligomeric sugars mainly from hemicelluloses solubilization, and; (ii) a solid fraction of digestible cellulose and lignin; it's a thermonechanochemical process where steam condenses at high pressure thereby wetting the material, which is driven out of reactor through a nozzle by induced force; due to decreased pressure condensed moisture evaporates and disintegration of lignocellulosic matrix takes place; material is heated at high-pressure steam (20-50 bar; 210-290℃); for short period (seconds to few minutes)*	Carvalheiro et al., (2008); Tomas-Pejo et al., (2013); Duque et al., (2016)
2,3	**Ammonia-based Pretreatments**				
2.3.1	**Ammonia Fiber Explosion (APEX)**	*high total sugar yields; negligible presence of inhibitors; improved cellulose digestibility; successfully applied for herbaceous and agricultural residues; moderate on hardwoods (not attractive for softwoods)*	*high costs associated with ammonia awa its recovery; use of pressurized vessels makes them quite costly; considerable safety issues*	*Can result in more than 90% conversion of cellulose and hemicellulose into fermentable sugars; most of AFEX-treated hemicellulose is oligomeric; biomass is normally treated in batch mode with anhydrous ammonia: 1-2kg ammonia/kg biomass; temp: 40-140℃; pressure: 250-300 psi; time: few minutes;*	Yang et al., (2008); Carvalheiro et al., (2008); Sharara et al., (2012);
2.3.2	**Ammonia Recycling Percolation (ARP)**	*enhanced cellulosic hydrolysis; high enzymatic digestibility of pretreated biomass which is attributed to simultaneous removal of lignin and hemicelluloses*	*Process is not that economical; a major challenge for ARP is to reduce liquid loadings to keep energy costs low*	*aqueous ammonia is used in flow-through mode using a column reactor containing the biomass; ammonia to biomass ratio= 1:1, 2:1 or 3:1 depending on how high the pressure is; pressures can be: 1.4 to 4.8MPa; temp: from 60 to 200℃; rxn time: 5 to 45 minutes (R3)*	Carvalheiro et al., (2008); Sharara et al., (2012); Yang and Wyman, (2008)

Table A-1.2. Summary of reported results on hemicellulose (xylan) extraction from different lignocellulosic materials under selected pretreatment methods: alkaline, Pressurized Liquid Hot Water (PLHW) & Steam Explosion Pretreatment (SEPT)

(1) Summary of results on alkaline extraction of hemicelluloses (xylan) from different lignocellulosic biomass

Feedstock description	Pretreatment/Extraction Method and Conditions	Reported Results	Remark	References
Sugarcane bagasse (dried at 60℃; Particle size distribution, PSD: 1 mm)	Alkaline: 0.5M NaOH solution; biomass-to-solvent loading ratio (BSLR) = 1:25 g/mL; 55℃; 120 min	Ca. 25 % Hemicellulose (HC) yield, mainly xylan extracts	Ethanol was used to recover hemicellulose (xylan) extracts	Sabiha-Hanim et al., (2012)
Sugarcane bagasse (air-dried; PSD: 0.27 - 0.91 mm)	Ultrasound-assisted alkaline pretreatment: NaOH solution 0.25, 1.00, 1.75, 2.50 and 3.25% (w/v); Solvent-to-biomass loading ratio (SBLR): 10–20 mL/g; 30-50℃; 5-50 min	Xylan yield: 69.64–93.10%; Arabinan yield: 61.19–86.22%	maximum xylan yield at 0.75 mm size, SBLR of 10 mL/g, 1% NaOH, 30℃ and 20 min	Velmurugan & Muthukumar., (2012)
Sugarcane bagasse (air-dried and dewaxed, PSD: milled to pass through 25 meshes)	Alkaline with solution of hydrogen peroxide (H2O2); 2 to 6% (w/v) of H2O2; time= 4-16 hrs; temp= 20-60℃	38.3–94.5% HC extraction yield, mainly xylan	optimal extraction condition: 6% (w/v) H2O2, 4 hrs, 20℃	Brienzo et al., (2009)
Rice straw (oven-dried at 50℃ for 16 hrs; milled to pass through 0.7mm size screen	Alkaline peroxide pretreatment with 2% (w/v) of H2O2: Temperature = 20-70℃; pH 11.5; retention time = 12 hrs;	44.2–71.9% HC recovery	Optimal Temp was 40℃; (high yield and minimal degradation)	Fang et al., (2000)
Wheat Straw (prepared in accordance with TAPPI Protocol: T-257 cm-85)	Cold alkaline extraction with 80 to 120 g/L NaOH solution; Retention time: 30-60 min; Temperature: 20-40℃	39.4% HC recovery	Optimal condition: 40℃; 90 min; alkali conc. of 100 g/L	Garcia et al., (2013)
Sweet Sorghum Stem (dewaxed sample oven-dried at 60℃ for 3 hrs, ground and screened to 20-40 mesh size)	Sequential hemicellulose extraction: Distilled water at 90℃; alkaline extraction, KOH conc= 0.3, 0.6, 1.0, 1.5 & 2.0% at 75℃; KOH-EtOH solution (60% ethanol) at 75℃	76.3% HC recovery	Highest extraction yield observed at 1.5% KOH concentration (conc.)	Sun et al., (2013)
Sugarcane harvesting residues, air-dried at 40DC to moistire content of 10%; cut to 10-12 cm size	Alkaline pretreatment with 2% NaOH (w/w) loading per dry biomass, 121℃ and 60 min	40% hemicellulose extraction yield	No monomeric sugar formation was noticed	Manfredi et al., 2018
Sugarcane straw, dried to 85% dry matter content; size below 10 mm	Alkaline Pretreatment with 5-15% NaOH (w/w) loading per dry biomass, 175℃ and 15 min; liquor-to-biomass loading=7:1 Lts/kg	55, 61 and 66% HC extraction yield	yield increased with alkali charge; glucose removal of 19, 27 and 36% were also observed	Carvalho et al, (2016)

(1) Summary of results on alkaline extraction of hemicelluloses (xylan) from different lignocellulosic biomass, Cont.

Peashrub (*C. Korshinskii*) (sun-dried and chipped to 1 to 2 cm; ground to pass through 0.8 mm screen size	Sequential extraction of HC with 0.5, 1.0 and 2.0 M KOH solution; solid-liquid ratio, SLR of 1:25 (g/mL); 600 min; 25℃	92.4% HC overall recovery (64.1, 15.6, and 12.5% respective KOH conc.)	Samples were dewaxed in Soxhlet apparatus refluxing for 6 hrs with 2:1 (v/v) tolune-ethanol mixture	Peng et al., (2012)
Hybrid Poplar, bark-free wood (air-dried, PSD=1.8 to 0.7 mm)	Alkaline extraction with 8% NaOH solution at 20:1 mL/g liquid-to-solid ratio; 10 hrs; 90℃	91.7% hemicelluloses extraction yield	Samples were partially delignified prior to their pretreatment	Zhang et al., (2014)
Birch wood (dried, chipped and screened between 2-4 mm & 4-6 mm)	Alkaline Hemicellulose pre-extraction with 1.0, 1.5, 2.0 & 2.5M NaOH solutions; 60 min; Temp= 80, 95, 110 & 125℃	6.6% of wood mass was extracted as polymeric xylan with molar mass of 20 kDa	Optimal condition: 95℃ and 2.5M NaOH solution	Testova et al., (2014)
Birch wood (oven-dried at 40℃, ground to 2 mm size)	Microwave-assisted Alkaline Extraction; with 1-4 % (w/w) NaOH Loading; 10:1 (v/w) solvent-to-biomass ratio; 10-600 seconds; room temp; 110-1100 W microwave power	60% Xylan extraction yield	Optimal condition: 110W power and 10 min	Panthapulakkal et al., (2013)
Eucalyptus globulus	Alkaline extraction of hemicelluloses with different alkali (NaOH) loadings (10-50% w/w ODW basis); 100℃; 60 min	39.3 to 58.6%, xylan extraction yield	Degree of polymerization of xylan extracts was decreasing with increased alkali charge	Longue Junior et al., (2013)
Eucalyptus globulus (chipped to pass through 0.3x3x3 cm for actual samples preparation)	Alkaline Pretreatment with 5, 10 and 15% NaOH (w/w) loading per dry biomass, 175℃ and 15 min; liquor-to-biomass ratio: 2:1 Lts/kg	47, 55, 61% HC extraction yield	HC removal was increasing with increased alkali charge; corr. glucose removal of 0,6, 4,5 and 9,5% were observed	Carvalho et al, (2016)
Sweetgum (hardwood type)	Alkaline pretreatment with 50% NaOH-to-wood loading ratio; 10:1 water-to-wood loading ratio; 100℃; 60 min	66.4% HC recovery (yield)	Mainly in oligomeric form	Longue Junior et al., (2013)

(2) Summary of results on Pressurized Liquid Hot Water (PLHW) and Steam Explosion (SEPT) Pretreatments for hemicellulose (xylan) extraction from lignocellulosic materials (agricultural residues and hardwood types)

Feedstock description	Pretreatment/Extraction Method and Conditions	Reported Results	Remark	References
Cornstover, PSD=250-420 µm	Tubular Pressurized Liquid Hot Water (PLHW) extraction method, flow-through mode: water flowrate of 2.8, 5.6 and 10.7 mL/min; 200°C	60 to 82% xylan removal in 8 min as flowrate increased from 2.8 to 10.7 cm/min	Extracts were mainly in oligomeric form	Liu and Wyman (2004)
Cornstover, PSD=250-420 µm	PLHW extraction method, batch mode: Temperatures =: 180, 200 and 220°C; 16 min	47.3% xylan yield attained at 200°C after 16 min	Extracts were mainly in oligomeric form	Liu and Wyman (2003)
Sugarcane bagasse, milled to 40-80 mesh size	PLHW batch extraction mode; Temp := 170-190°C; time := 10-50 min; water-to-biomass ratio = 10:1	85% xylan removal	optimal condition: 180°C; 30 min	Sukhbaatar et al., (2014)
Sugarcane bagasse, 0.9-3 mm size fraction	Microwave-assisted PLHW extraction: Temp=175-190°C; time= 2-20 min; water-to-biomass loading ratio=10:1	62% HC extraction yield	Optimal condition: 183°C, 11 min; extracts mainly oligomeric	Gulbrandsen et al., (2014)
Sugarcane Trash; samples prepared 90% dry and within PSD = 250-1000 µm	Microwave-assisted PLHW extraction; Temp=167-194°C; time= 8-22 min; water-to-biomass loading ratio=15:1mL/g	9.5 to 50.9% xylan yield	Xylan extracts were mainly in oligomeric form	Mihiretu et al., (2017)
Aspenwood sawdust, 93.5% dry matter content, PSD=250-1000 µm	Microwave-assisted PLHW extraction: Temp=171-199°C; time= 8-22 min; water-to-biomass loading ratio=15:1mL/g	6.2-66.1% xylan yield	Xylan extracts were mainly in oligomeric form	Mihiretu et al., (2017)
Eucalyptus globulus	PLHW, batch-mode extraction: Temp=210°C; water-to-biomass ratio= 8:1 mL/g	44% original xylan recovery (7.43g xylan/100 g sample)	Mainly xylo-oligomeric extracts	Romani et al., (2014)
Eucalyptus globulus, milled to pass through 8 mm screen	PLHW, batch-mode extraction: Temp=160°C; 30-66 min; water-to-biomass ratio= 8:1 mL/g	6,78-13,7 g xylan removal per 100 g initial dry biomass	Mainly oligomeric extracts	Garotte et al., (2007)
Eucalyptus globulus , milled to pass through 8 mm screen	PLHW, batch-mode extraction: Temp=145-190°C; up to 450 min; water-to-biomass loading: 6 - 10 mL/g	71.5 to 80.1% xylan removal, mainly in oligomeric form	Mainly oligomeric extracts	Garotte et al., (1999)

(2) Summary of results on Pressurized Liquid Hot Water (PLHW) and Steam Explosion (SEPT) Pretreatments for hemicellulose (xylan) extraction from lignocellulosic materials (agricultural residues and hardwood types), CONT.

Birch wood sawdust	PLHW, flow-through mode: water flowrate of 4 mL/min; water-to-biomass loading ratio= 12:1 mL/g; Temp: 160, 170 & 180℃	41% HC extraction yield	Mainly oligomeric extracts	Klipelainen et al., (2013)
Eucalyptus globulus , milled to pass through 8 mm screen	Autohydrolysis, pressurized hot water pretreatment in a Parr reactor, Temp=195-250℃; liquid-to-solid ratio=8kg/kg	Upto 76% xylan removal; maximal at 210℃ (mainly oligomeric and monomeric xylose yield was 27%)	temperatures higher than 210℃ led to increased degradation of xylose	Romani et al., (2010)
Wheat straw	Steam explosion pretreatment (SEPT): 200℃, 4 min	93% overall hemicellulose removal (70% oligomers and 23% monomeric form)	mainly xylo-oligomeric extraxts	Alvarez et al., (2017)
Sugarcane straw (green leaves without grinding, not washed and minced)	Un-catalysed SEPT at Temp= 180, 190 & 200℃ for 15 min	hemicellulose removal from 67.1 (180℃, 15 min) to 92.7% at (200℃, 15 min)	mainly in oligomeric and monomeric forms (increased with increased temperature)	Oliveira et al., (2013)
Sugarcane trash, 91.5% dry matter content; shredded to size range of 5-7cm	SEPT on alkali-impregnated samples (5% (w/w) NaOH per biomass, ODW-basis): Temp=171-204℃; Time=3-17min	xylan extration yield of 31 to 51 % (w/w)	No monomeric extracts (polymeric and oligomeric form)	Mihiretu et al., (2019)
Populus tremuloides (hardwood type); chipped to size of 20x20x2 mm	Sequential PT: SEPT (180-230℃; 0.7-4.0 min) => Washing 2X with water at 70℃ for 30 min; alkali delignification of washed solids with 5% (w/v) NaOH loading, 10% (w/v) solids loading at 100℃ for 30 min	Hemicelluloses extraction yield ranged from 5% at (180℃, 0.7min) to 65% (w/w) at (220℃, 2 min)	extracts mainly in oligomeric and monomeric; 75% alkaline delignification at maximal HC removal (220℃, 2 min)	Chornet et al., (1991)
Eucalyptus globulus, milled to pass through 8 mm screen	SEPT; Temp=173-216℃; time=5,87-34 min	Hemicellulose solubilization from 60.6 at (173℃, 20 min) to 95.5% at (216℃, 20 min)	mainly in xylo-oligomeric and monomeric forms; xylose yield increasing with severity	Romani et al., (2013)
Eucalyptus globulus chips, air-dried	SEPT; Temp=183℃; time=5 or 10 min (first cycle), 3 min (second cycle)	32-67% (w/w) extraction of pentosans (hemicelluloses)	increased yield with longer time; mainly oligomeric	Martin-Sampedro et al., (2014)
Aspen wood sawdust, dried to 93.7% dry matter content	SEPT on alkali-impregnated samples (5% (w/w) NaOH per biomass, ODW-basis); Temp=171-204℃; Time=3-17min;	xylan extration yield of 12.3 to 23.6 % (w/w)	monomeric xylose was absent in extracts (polymeric and/or oligomeric form)	Mihiretu et al., (2019)

Table A-1.3. Summary of reported results on enzymatic cellulose digestibility for different lignocellulosic materials under selected pretreatment methods: alkaline, Pressurized Liquid Hot Water (PLHW) & Steam Explosion Pretreatment (SEPT)

(1) Summary of results on alkaline pretreatment for enzymatic cellulose digestibility

Feedstock description	Pretreatment Method and Conditions	Reported Results	Remark	References
Sugarcane bagasse	Dilute Alkaline PreTreatment (APT) with liquid-to-solid ratio (w/w) of 10:1; 60℃; 2 hrs	78.3% glucan hydrolysis yield (cellulose digestibility)	pretreated samples hydrolyzed with cellulase at 20 FPU/g substrate together with 300 nkat β-glycosidase/g substrate at 50 °C in pH 5.0.	Moe et al., (2014)
Rice straw (leaves & stems) crushed by a blender and screened to less than 3 mm	APT with 1.0 - 4.0% NaOH conc-n; Temp= 60-100℃; time= 30-90 min	highest cellulose digestibility of 85.49% attained for rice straw pretreated at 100℃ for 60 min using 4.0% NaOH concentration	Enzymatic hydrolysis performed as per NREL protocol; cellulase from *Trichoderma reesei* 60 FPU/g cellulose and b-glucosidase from *Aspergillus niger* 30 CBU/g cellulose;	Kim and Han, (2012)
Sugarcane straw (agricultural crop residue = ACR)	APT with 2.0% (w/v) NaOH loading; 121°C; 60 min; water-to-biomass ratio=10:1 mL/g	80.0% Celluloce digestibility;	standardized enzymatic hydrolysis tests followed	Manfredi et al., (2018)
Sugarcane trash, sun-dried, milled to pass through 2 mm screen	APT with NaOH loading of 1.2% (w/v), sample loading=12.5, 15.0 and 17.5%(w/v); 121℃; 15 min	Reducing sugars concentration after enzymatic hydrolysis=104.04g/L; ethanol concentration after SSF=25.91 g/L	hydrolysis condition: (pH of 5.0, 50℃, 160rpm, 48hrs; Cellic CTec2 at 50 FPU/g dry biomass), SSF (30℃, 160rpm, inoculum of *S. cerevisiae* TISTR 5596 (10^7 cells/mL)	Srinorakutara et al., (2014)
Sugarcane "leave waste" (SLW), dried at 60℃ for 72hrs, milled to < 1mm size	Sequential Steam Salt-alkaline Pretreatment (1) with salt (ZnCl2) conc-n (0.1, 1.05 & 2.0M) at 121℃, 30min; and then (2) with alkali (NaOH) conc-n (0.1, 1.05 & 2M) at 121℃, 30 min; solids loading (5, 10 and 15% (w/v))	Reducing sugar yield after enzymatic hydrolysis: 0.42-1.22g/g (minimum at 1.05M ZnCl2, 0.10M NaOH & 15%(w/v) solids loading; and, maximum at 2.0M ZnCl2, 2.0M NaOH & 10%(w/v) loading	Saccharification condition: 10% substrate loading; pH=4,8 (0.05N sodium citrate buffer); 50℃, 150 rpm, for 72 hrs; enzyme loading at 10 FPU/g; upto 80% lignin removal was reported at the condition that led to maximal reducing sugar yield	Moodley and Kana, (2017)
Poppy Stalks (=> *Papaver sommiferum*)	APT with NaOH loading of 1 to 3.5% (w/v); temp= 50-100℃; time=10-110 min	61 to 94 % glucan recovery; maximum glucose yield was 80℃; 70min and 2.40% conc. (499.35mg/gm of glucan)	pH adjusted to 4.8; Cellulase at 30PFU/gm of dry biomass; 50℃; 72 hrs in incubator shaker at 150rpm	Uzunlu et al., (2014)
Aspen wood chips, dried to 92.8% dry matter content (7% moisture content)	APT with NaOH loading of 0.5 and 2.0% (w/v); 5% (w/v) substrate loading; 121°C; 60 min	enzymatic sugar yields of 64 & 80% attained at 0.5 & 2.0% (w/v) NaOH loadings	standardized enzymatic hydrolysis tests (=> NREL protocol) followed	Dziekonska-Kubczak et al., (2018)
Vineyard pruning (*Vitis vinifera*), air-dried, milled to 2mm size, ground to 0.5 mm for actual samples (<10% moisture content)	Alkaline pretreatment with NaOH loading of 0.5 to 2.5% (w/v); 80-120℃; 30-60min	47.3-96.9% enzymatic glucose yield	hydrolysis conditions: 5% solids loading, pH of 5.0 (0.1M sodium citrate buffur), 50℃, 100 rpm, 48 hrs; enzyme loading: 0.23 g Cellic CTec2 per g of dry substrate	Franco Catana et al., (2015)
Commercial bamboo chips re-chipped to 3-5mm width and 15-25mm length; washed and dried to moisture content of 22%;	Two-stage alkaline pretreatment: NaOH pre-extraction at 4-10% (w/v) alkali loading, 100℃, 30-180 min; followed by alkaline peroxide pretreatment (AHPT): 0-6% (w/w) of peroxide loading, 75℃ and 180 min; Liquid-to-solids loading ratio=10 L/kg	Optimal enzymatic hydrolysis yields: 92.4% cellulose-to-glucose conversion and 74.1% xylan-to-xylose conversion;	Hydrolysis conditions: (5% solids loading; pH of 5.0, 50℃, 150rpm, 96hrs; enzyme loading (Cellic CTec2 and beta-glucosidase) at 5.5 - 18 FPU/g cellulose; Optimal pretreatment and/or hydrolysis condition: 8% NaOH loading, 4% (or 6%) peroxide loading; 9 FPU/g enzyme loading	Yuan et al., (2018)

(2) Steam explosion (SEPT) and pressurized liquid hot water (PLHW) pretreatments for enzymatic cellulose digestibility

Feedstock description	Pretreatment/Extraction Method and Conditions	Reported Results	Remark	References
Rapeseed straw; air-dried and hammer-milled to <1cm size	Pressurized Liquid hot water (PLHW) method: 217℃, 42 min, solid-to-liquid loading ratio 6% (w/v)	69% of theoritical ethanol yield, 23g/L; maximum yield of 0.12gm EtOH per g of dry straw	SSF Conditions: 10% substrate loading, 40℃, pH 4.8, 150rpm, 71 hrs; Enzyme Loading (40FPU/g-substrate, 15% IU/g-substrate); yeast loading: 0.25 g/L (= 4% (v/v) S. cereviceae inoculum)	Sasikumar and Viruthagiri (2010)
Sugarcane Trash samples, 91.7% dry, PSD= 250-1000 µm	Microwave-assisted PLHW method: 167-194℃; 8-22 min; water-to-biomass loading ratio 15:1 mL/g dry weight basis, dwb	Enzymatic glucose yields from 41.4% at (167℃, 15 min) to 74.3% at (194℃, 15 min)	Hydrolysis experiments were carried out as per the NREL Protocol (NREL/TP-510-42629; Selig et al., 2008)	Mihiretu et al., (2017)
Aspen wood sawdust, 93.5% dry matter content, PSD=250-1000 µm	Microwave-assisted PLHW method: 171-199℃; 8-22 min; water-to-biomass loading ratio of 15:1mL/g, dwb	Enzymatic glucose yields from 32.7 % at (171℃, 15 min) to 77.8% at (195℃, 20 min)	Hydrolysis experiments were carried out as per the NREL Protocol (NREL/TP-510-42629; Selig et al., 2008)	Mihiretu et al., (2017)
Eucalyptus globulus , milled to pass through 8 mm screen	Autohydrolysis, PLHW pretreatment in a Parr reactor, 195-250℃; liquid-to-solid ratio=8kg/kg	Cellulose-to-glucose conversion (w/w)= 40% at 195℃, 65-97% for 200-220℃ and almost complete (100%)** conversion at 230, 240 and 250℃	Hydrloysis conditions: 20g/g solid loadings; pH 4.85 (0.05N sodium citrate buffer); 0.005% sodium azide; 48.5℃, 150 rpm, 96hrs; enzyme preparation: Cellulase (Celluclast) at 10.3FPU/g-substrate and 10 IU beta-glucosidase/FPU (novozym 188);	Romani et al., (2010)
Sugarcane straw (green leaves without grinding, not washed and minced)	Un-catalysed SEPT: 180, 190 & 200℃ for 15 min; followed by alkaline delignification at 100℃, for 1 hr, with 15% (w/w) NaOH loading per unit OD weight of pretreated solid	cellulose-to-glucose conversion (digestibility): 58.8 to 80.0 % (without delignification); 85.1 to 71.5% (with the alkaline delignification step)	Saccharification condition: 10% solids loadings; pH 4.8; 0.05N sodium citrate buffer; 45℃, 100 rpm, 72 hrs; enzyme loadings: Celluclast 1.5L at 15 FPU/g and novozym 188 at 10IU/g	Oliveira et al., (2013)
Sugarcane harvesting residues	Un-catalysed SEPT at 204℃ for 20 min;	78% enzymatic hydrolysis glucose yield	Saccharification condition: 20% solids loadings; pH 4.8; 0.05M sodium citrate; 50℃, 72 hrs; enzyme preparation: Cellic CTec2 and HTec2 at different combinations	Manfredi et al., (2018)
Sugarcane trash, 91.5% dry matter content; shredded to size range of 5-7 cm	Alkaline SEPT on alkali-impregnated samples (5% (w/w) NaOH per biomass, ODW-basis);171-204℃; 3-17 min	Enzymatic hydrolysis glucose yield: 60.9 to 92.2% (w/w)	Hydrolysis condition: 2% solids loading; pH 4.8; 0.05N sodium citrate buffer; 50℃, 150 rpm, 72 hrs; enzyme preparation: Cellic CTec2 at 15 FPU/g and Cellic HTec2 at 25% (v/v) of CTec2	Mihiretu et al., (2019)
Aspen wood chips, dried to 92.8% dry matter content	Uncatalyzed SEPT: 198℃, 5 min	42% enzymatic sugar (glucose) yield	standardized enxymatic hydrolysis tests (=> NREL protocol) followed	Dziekonska-Kubczak et al., (2018)
Populus tremuloides (hardwood); chipped to size of 20x20x2 mm	Sequential PT: SEPT (180-230℃; 0.7-4.0 min); Washing 2X with water at 70℃ for 30 min; delignification of washed solids with 5% (w/v) NaOH loading, 10% (w/v) solids loading at 100℃ for 30 min	maximal glucose recovery of 90% of theoritical value at the most severe SEPT conditions	Saccharification (hydrolysis) conditions: 2% solids loadings; pH 4.8; 0.05N sodium citrate buffer; 0.005% sodium azide; incubated at 50℃ for 48hrs; enzyme preparation: Cellulase (Celluclast) at 1.0 FPU/mL and 1mL/mL cellubiase (novozym 188)	Chornet et al., (1991)
Eucalyptus globulus , milled to pass through 8 mm screen	SEPT; Temp=173-216℃; time=5,87-34 min	Cellulose-to-glucose conversion (w/w)= 50-96%, increasing with increased severity of SEPT condition	Saccharification condition: 5% solids loadings; pH=4.85; 0.05N sodium citrate buffer; 50℃, 150 rpm, for 96 hrs; enzyme preparation: Cellulase (Celluclast 1.5L) at 15 FPU/g and 10IU/FPU beta-glucosidase (novozym 188)	Romani et al., (2013)
Aspen wood sawdust dried to 93.7% dry matter content	Alkaline SEPT on alkali-impregnated samples (5% (w/w) NaOH per biomass, dwb); 171-204℃; 3-17min;	Enzymatic hydrolysis glucose yield: 47.6 to 81.4% (w/w)	Saccharification condition: 2% solids loadings; pH 4.8; 0.05N sodium citrate buffer; 50℃, 150 rpm, for 72 hrs; enzyme preparation: Cellic CTec2 at 15 FPU/g and Cellic HTec2 at 25% (v/v) of CTec2	Mihiretu et al., (2019)

APPENDIX-B: CHAPTER-6 CONCEPTUAL FLOW DIAGRAMS AND TABLES

A) Conceptual Process Flow Diagrams for the envisaged biorefinery with identified streams to and from major processing units/plants

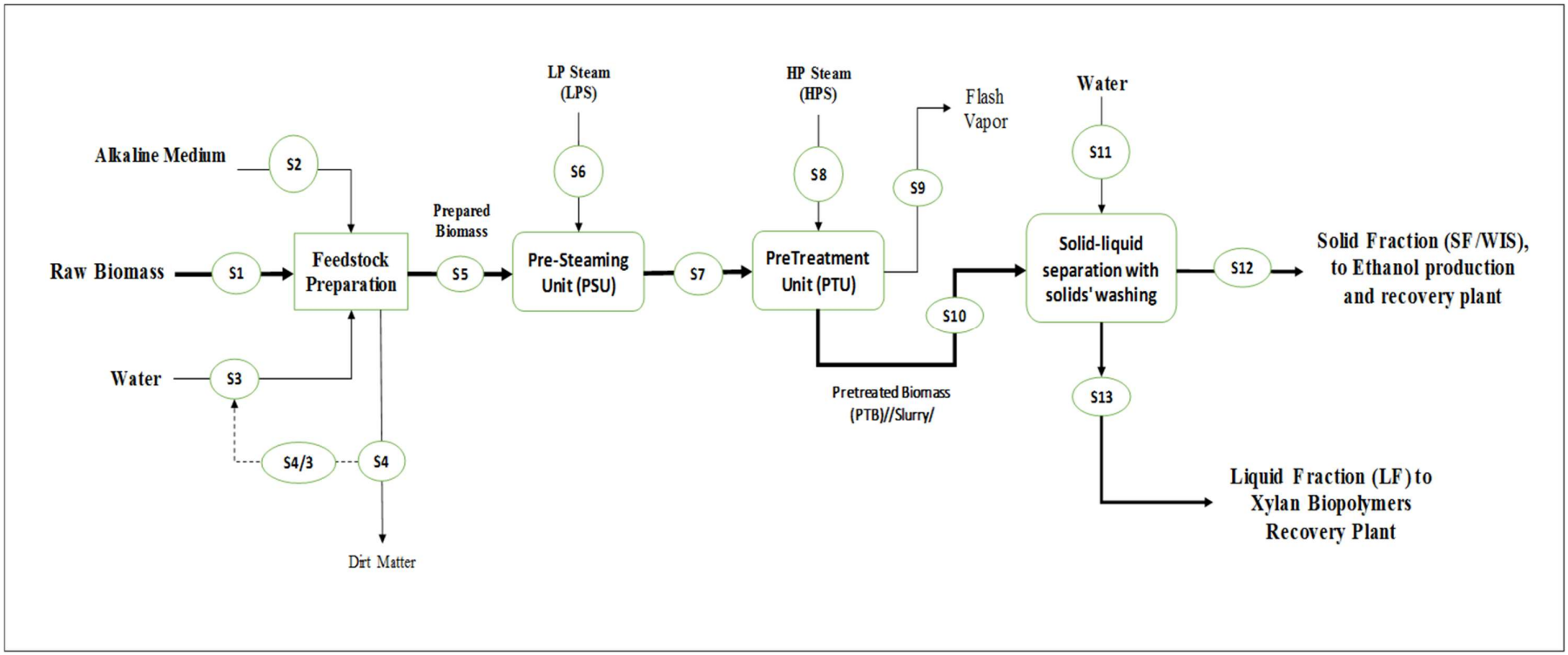

Fig B-1.1: Simplified flow diagram for Feedstock Preparation, biomass pretreatment and Solid-Liquid Separation steps

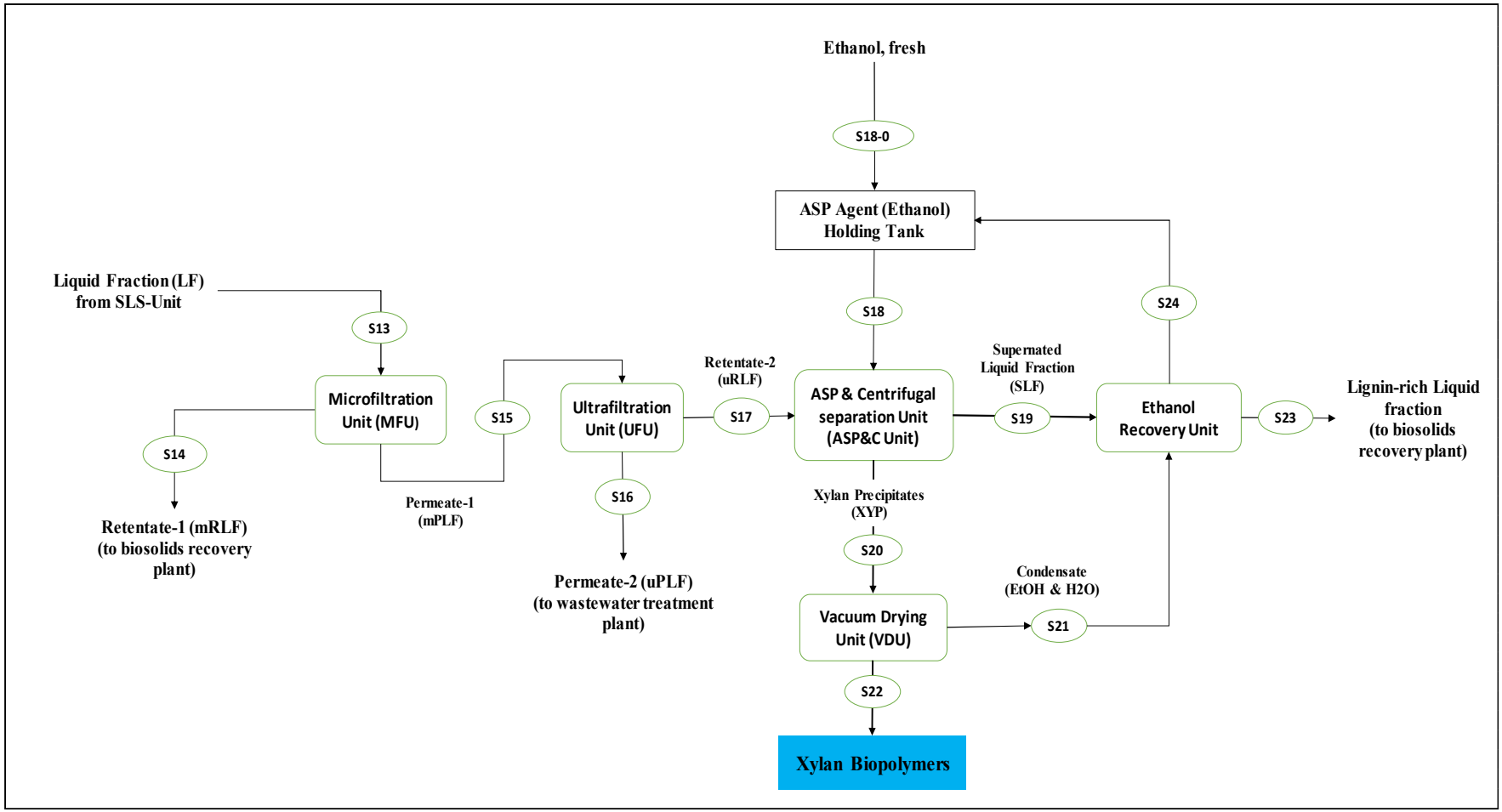

Fig B.1-2: Simplified process flow diagram for the recovery (separation and purification) of xylan biopolymers from the Liquid fraction

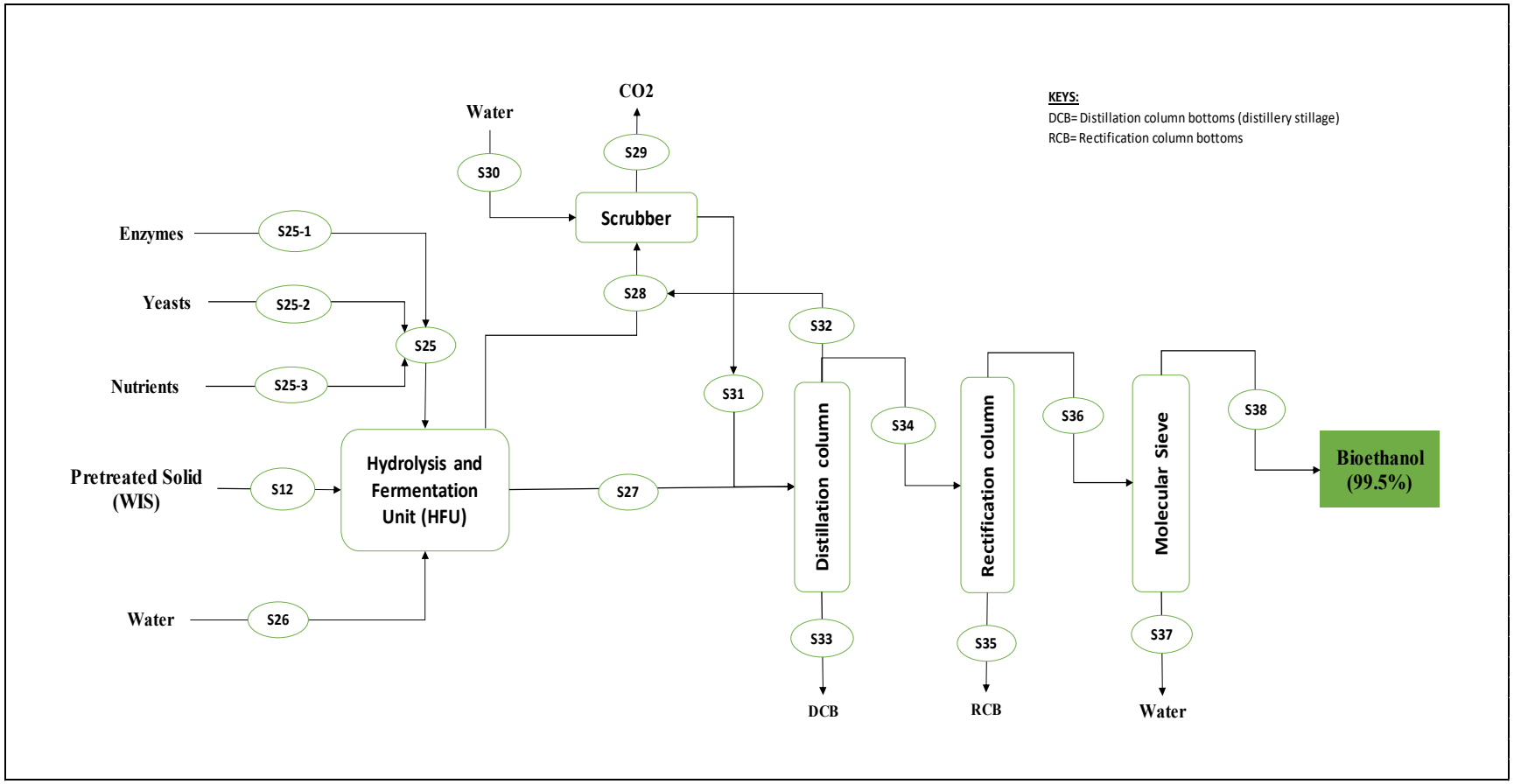

Fig B.1-3: Simplified process flow diagram for ethanol production (enzymatic hydrolysis and fermentation) and ethanol recovery plant

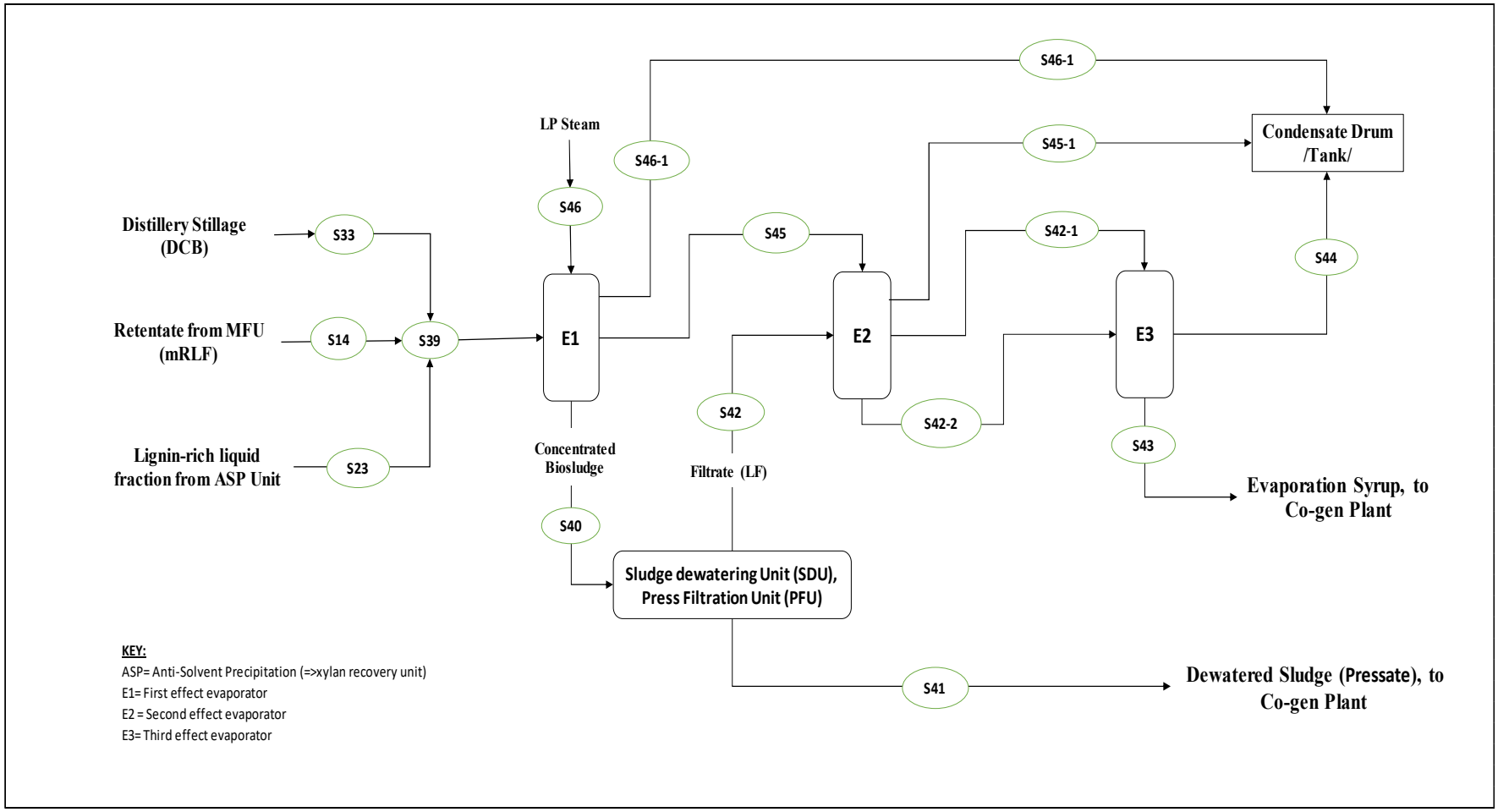

Fig 6.B-1.4 Simplified process flow diagram for biosolids (lignin) recovery plant

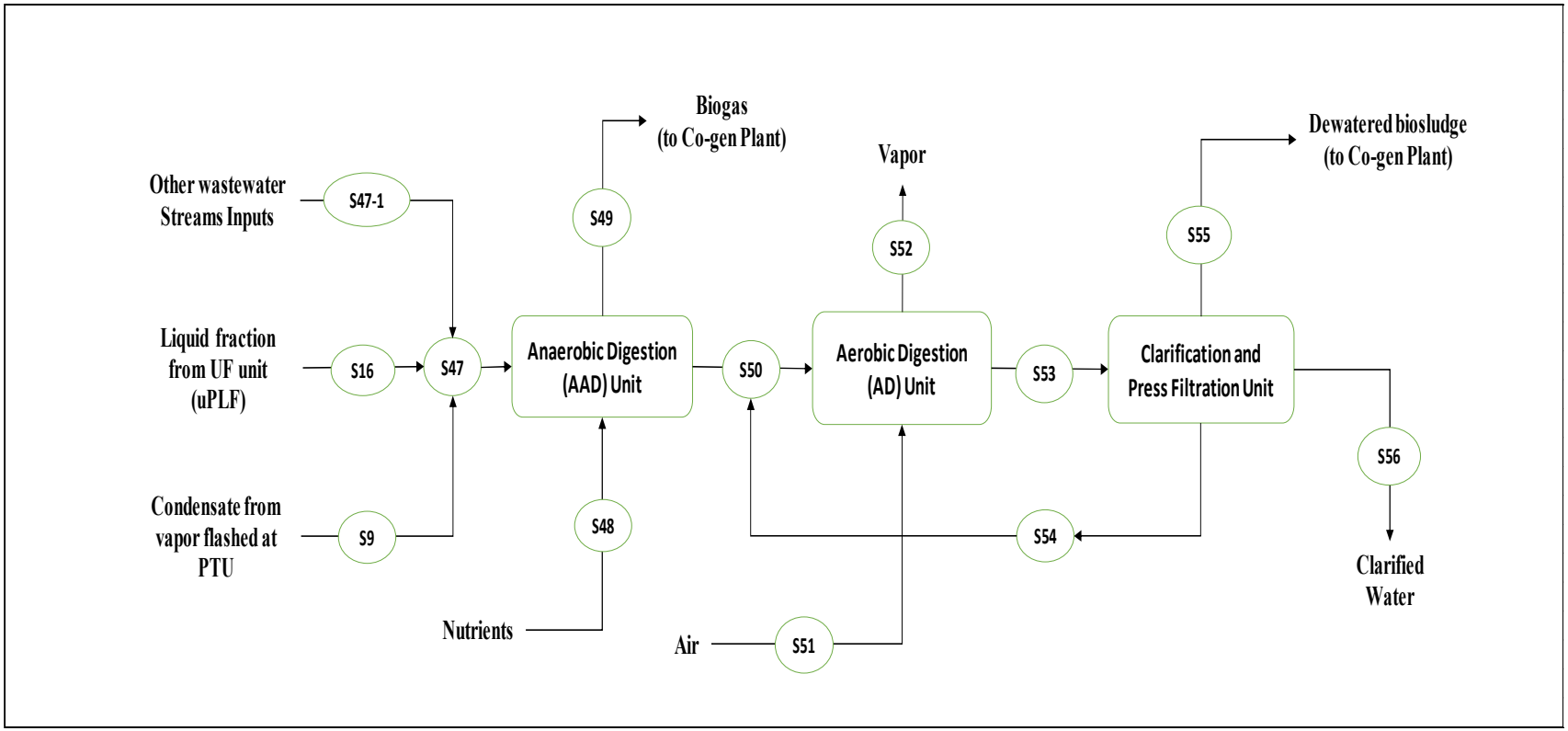

Fig B.1-5: Simplified process flow diagram for wastewater treatment plant

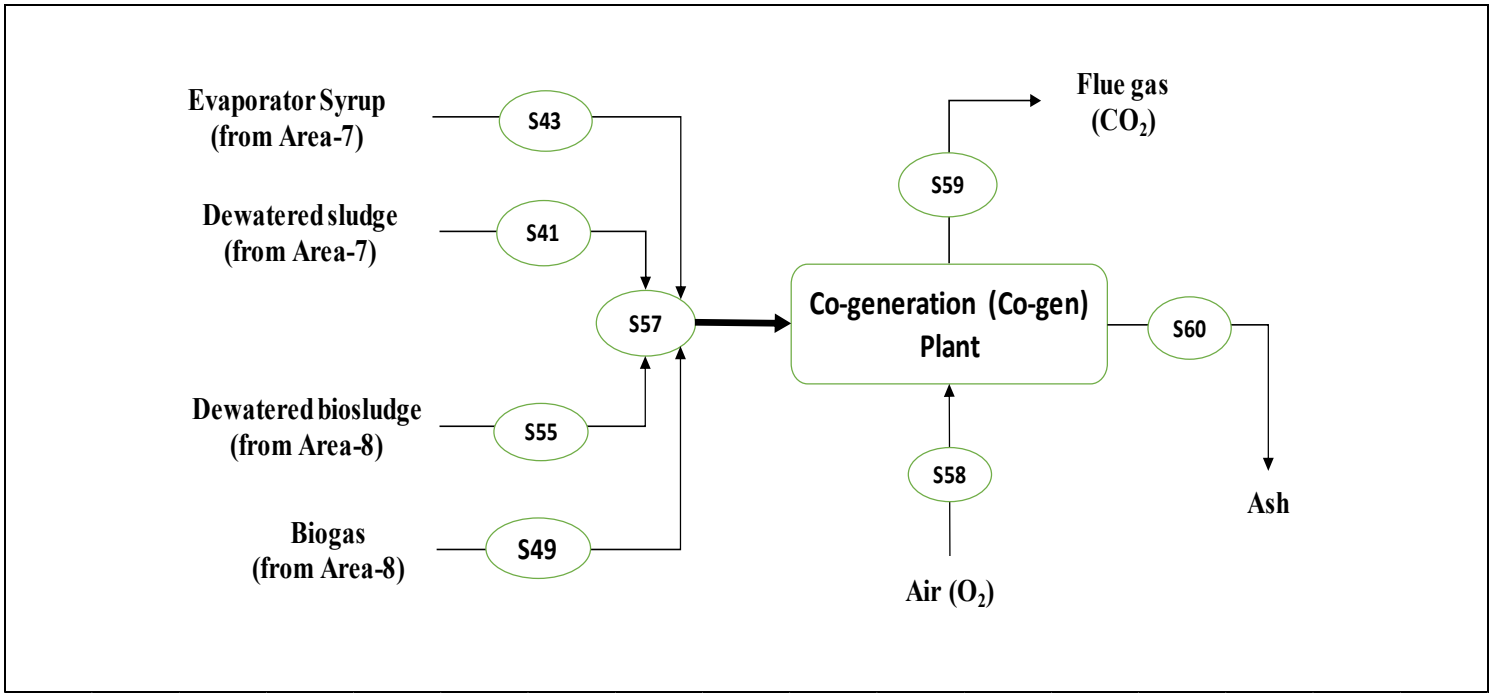

Fig B.1-6: Simplified flow diagram for the co-generation plant

Table B-1.3: Basic process parameters considered and/or assumed for techno-economic assessment purpose (CHAPTER SIX)

Parameter Description, by Process Area	Unit	Parametric value	References
Feedstock Handling and Preparation (AREA-1)			
Daily feedstock processing capacity, dry weight basis (dwb)	[ton/day]	1000	Mihiretu et al., (2019)
Dry matter content (DMC) of raw biomass	[%w/w]	90,0	""
Washing water to biomass loading ratio	[m^3/ton]	10,0	""
DMC of washed and de-watered biomass	[%w/w]	32,0	""
Percentage of non-biomass material in raw biomass	[%w/w]	1,00	""
Alkali-to-biomass loading ratio (biomass impregnation)	[%w/w]	5,0	""
Water per unit weight of alkali (alkaline medium preparation)	[m^3/ton]	30,0	""
DMC of alkali-impregnated biomass (prepared feed)	[%w/w]	33,0	""
Water loss during WW clarification and recycling	[%v/v]	2,0	""
Biomass Pretreatment/Hemicellulose Extraction/ conditions (AREA-2)			
Presteaming conditions			
Inlet Temperature	[°C]	25	Aden et al., (2002); Humbird et al., (2011)
Outlet Temperature	[°C]	100	
Retention Time	[min]	20	
Steam explosion pretreatment conditions			
Temperature	[°C]	204	Mihiretu et al., (2019)
Pressure	[bar]	16,5	""
Retention Time	[min]	10	""
Pretreated material per unit initial biomass, dwb	[w/w]	5,4	""
Flash vapor per unit pretreated biomass	[w/w]	0,6	Aden et al., (2002); Mihiretu et al., (2019)
Solids recovery in pretreated biomass (slurry)	[%w/w]	98	
Solid-liquid separation of slurry with washing (AREA-3)			
Washing water per unit raw biomass, dwb	[m^3/ton]	5,72	Mihiretu et al., (2019)
Solids recovery in WIS (SF)	[%w/w]	57	""
Biomass ending up in liquid fraction (LF)	[%w/w]	43	""
Xylan extraction yield	[%w/w]	51	""
Removal of klason lignin (KL), recovery in the LF	[%w/w]	70	""
Cellulose loss into LF	[%w/w]	5	""
Minor biomass components (other than xylan, cellulose and KL) ending in LF	[%w/w]	97	""

Table B-1.3: Cont.

Recovery of biopolymeric hemicellulose extracts (AREA-4)			
(1) Purification and pre-concentration of liquid fraction (LF) via membrane separation (cascade of MF & UF units)			
(I) Initial purification of LF using Microfiltation (MF) Units			
Membrane nominal molecular cutoff size	[kDa]	50	Hung et al., 2006; Persson et al., 2007; Arkhangelsky et al., 2015; Bokhary et al., 2018
Membrane operating temperature (room conditions)	[°C]	25	
Transmembrane pressure (TMP) of 1.5 to 3 bar	[bar]	2,5	
Biopolymeric extracts (xylan and KL) in retentate	[%]	3	
Biopolymeric extracts (xylan and KL) in permeate (filterate)	[%]	97	
(II) Pre-concentration of permeate from MF unit via Ultrafiltration(UF)			
Membrane molecular weight cutoff size	kDa	10	Buruiana et al., 2014; Bokhary et al., 2017; Al-Rudainy et al., 2019; Persson et al., 2007; Peng et al., 2019
Membrane working temperature	[°C]	55	
Transmembrane pressure (TMP)	[bar]	6	
Biopolymeric extracts (xylan and lignin) retained by UF membrane	[%]	85-90	
Pre-concentration level attained/desired	[%, w/v]	15-20	
(2) Anti-solvent precipitation of hemicelluloses (xylan biopolymers) from pre-concentrated LF (retentate from UF unit)			
Ethanol (95%) per unit volume of pre-concentrated LF	[%v/v]	70	Buranov et al., 2010; Weinwurm et al., 2014; Al-Rudainy et al., 2019
Working temperature of ethanol precipitation unit	[°C]	25	
Recovery of xylan biopolymers in precipitate (precipitation yield)	[%w/w]	80	
Purity level for precipiated xylan biopolymers	[%]	85-90	
Moisture content of precipitate containing the xylan biopolymers	[%w/w]	30	
(3) Drying precipitated xylan biopolymers under vacuum conditions			Parikh, 2015; Zhang et al., 2010; Liu and Lee, 2015
Drying temperature	[°C]	30	
Vacuum pressure	[bar]	0,2	

Table B-1.3: Cont.

Ethanol Production (Hydrolysis/Fementation) (AREA-5)			
Enzymatic hydrolysis conditions			
Total solids (solids in WIS) loading	[%w/v]	10	Mihiretu et al., (2019)
Cellulase loading (Cellic CTec2)	[%w/v]	1,2	""
Hemicellulase loading (Cellic HTec2)	[%w/v]	0,3	""
Enzyme loading (combined)	[%v/v]	1,5	""
Enzymatic sugar yield (Glugan-to-glucose)	[%w/w]	92	""
Enzymatic sugar yield (Xylan-to-xylose)	[%w/w]	91	""
Fermentation conditions (Yeast strain: *Zymomonas mobilis* **)**			
Seed propagation (inoculum preparation)			
Inoculum level	[%v/v]	10	
Corn Steep Liquor (CSL) loading	[%w/w]	0,5	Aden et al., (2002); Kazi et al., (2009); Humbird et al., (2011)
Diammonium phosphate (DAP) loading	[%w/w]	0,67	
Batch time	[hrs]	24	
Fermenter turnaround time	[hrs]	12	
Co-fermentation conditions			
Inoculum level	[%v/v]	10	
Corn Steep Liquor (CSL) loading	[%w/w]	0,25	Aden et al., (2002); Kazi et al., (2009); Humbird et al., (2011)
Diammonium phosphate (DAP) loading	[%w/w]	0,33	
residence time	[hrs]	72	
Temperature	[°C]	40	
Sugars Conversions to ethanol			
Glucose to ethanol	[%]	90-95	
Xylose to ethanol	[%]	75-85	
Amount of CO2 released per unit wt of ethanol produced	[w/w]	0,96	
Parameters for ethanol recovery from fermentation beer (distillation and dehydration units) (AREA-6) are adopted from relevant NREL previous studies			Aden et al., (2002); Kazi et al., (2009); Humbird et al., (2011)
Process parameters for biosolids (lignin) recovery, waste water treatment as well as co-generation plant are mainly adopted from relevant NREL studies (AREAS-7,-8 & -9)			

APPENDIX-C: ASPEN Simulation Results by Flowsheet and Model Type: Overall biorefinery and Major Processing Blocks

(I) Simulation results by Flowsheet: material and energy balances

Table C.1: List of ASPEN Flowsheets (Denotation and Description)

Denotation and Description of ASPEN Flowsheets developed for the overall biorefinery complex (Main Flowsheet) and major processing blocks (BL-XYZ) within its battery limit around which mass and energy balances are closed

No.	Denotation	Flowsheet Description
1	Main Flowsheet	Overall biorefinery (integrated production of bioethanol, xylan biopolymers and biopower/electricity)
2	BL100	Biomass pretreatment and hemicellulose extraction Plant
3	BL200	Seed propagation plant
4	BL300	Enzymatic hydrolysis and fermentation plant
5	BL400	Bioethanol recovery plant (Bioethanol as main biorefinery product)
6	BLNEW11	Xylan recovery plant (xylan biopolymers as main co-product)
7	BLNEW22	Biosolids recovery plant (Triple-effect evaporation system to remove water from lignin-rich liquid waste stream from BLNEW11)
8	BL700	Biosolids recovery plant (Pneumapress filtration system to remove water from lignin-rich distillery sludge from BL400)
9	BL800	Steam generation plant (combustor, low pressure boiler and back pressure steam turbine)
10	BL900	Wastewater treatment plant (Biogas generation plant)
11	BL1000	Condensing extraction steam turbine (CEST)
12	BL1100	Biopower generation plant (based on biogas as combustible fuel input)

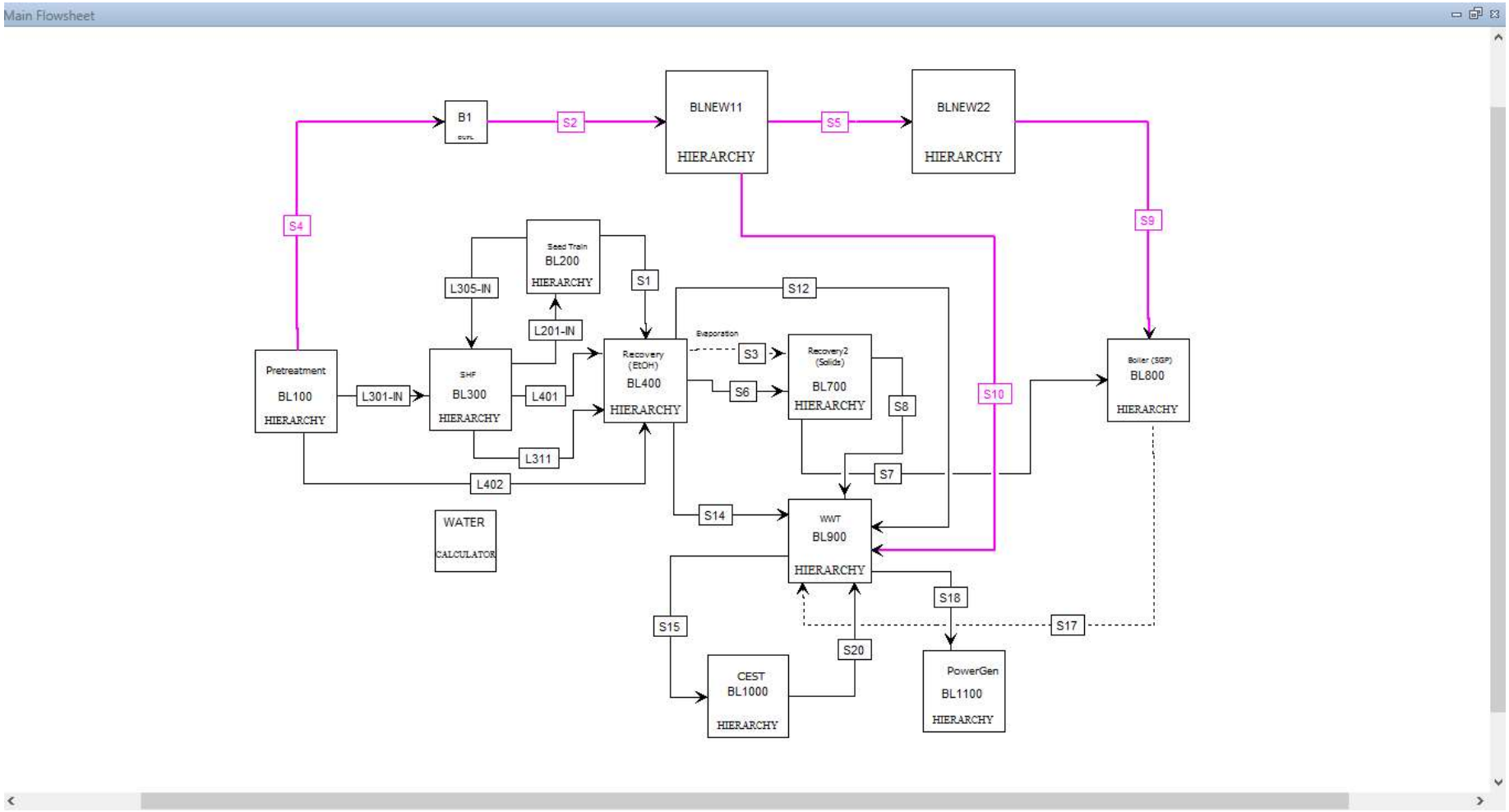

Fig C.1: Main Flowsheet for the overall biorefinery system

TABLE C.2.: Summary of mass and energy balance results for the overall biorefinery (Main Flowsheet)

		Material																			
Stream Name	Units	L201-IN	L301-IN	L305-IN	L311	L401	L402	S1	S2	S4	S5	S6	S7	S8	S9	S10	S12	S14	S15	S18	S20
Description																					
From		BL300	BL100	BL200	BL300	BL300	BL100	BL200	B1	BL100	BLNEW11	BL400	BL700	BL700	BLNEW22	BLNEW11	BL400	BL400	BL900	BL900	BL1000
To		BL200	BL300	BL300	BL400	BL400	BL400	BL400	BLNEW11	B1	BLNEW22	BL700	BL800	BL900	BL800	BL900	BL900	BL900	BL1000	BL1100	BL900
Stream Class		MIXCISLD	MIXCISLD	MIXCISLD	MIXCISLD	MIXCISLD	MIXCISLD	MIXCISLD	MIXCISLD	MIXCISLD	MIXCISLD	MIXCISLD	MIXCISLD	MIXCISLD	MIXCISLD	MIXCISLD	MIXCISLD	MIXCISLD	MIXCISLD	MIXCISLD	MIXCISLD
Total Stream																					
Temperature	C	28,6	40,0	30,1	37,0	37,0	129,7	30,0	76,5	76,5	90,5	125,0	83,3	98,7	85,1	55,0	50,0	113,3	239,5	35,0	170,4
Pressure	atm	1,0	1,0	3,0	1,0	1,0	2,5	1,0	1,0	1,0	1,0	2,3	1,0	3,0	0,5	3,0	2,5	1,6	11,0	2,0	7,9
Molar Vapor Fraction		0,0	0,0	0,0	1,0	0,0	1,0	1,0	0,0	0,0	0,0	0,0	0,0	0,0	0,0	0,0	0,0	0,0	1,0	1,0	0,0
Molar Liquid Fraction		1,0	1,0	1,0	0,0	1,0	0,0	0,0	1,0	1,0	0,9	1,0	0,8	1,0	0,9	1,0	1,0	1,0	0,0	0,0	1,0
Molar Solid Fraction		0,0	0,0	0,0	0,0	0,0	0,0	0,0	0,0	0,0	0,1	0,0	0,2	0,0	0,1	0,0	0,0	0,0	0,0	0,0	0,0
Mass Vapor Fraction		0,0	0,0	0,0	1,0	0,0	1,0	1,0	0,0	0,0	0,0	0,0	0,0	0,0	0,0	0,0	0,0	0,0	1,0	1,0	0,0
Mass Liquid Fraction		1,0	0,8	0,9	0,0	1,0	0,0	0,0	1,0	1,0	0,8	1,0	0,5	1,0	0,6	1,0	1,0	1,0	0,0	0,0	1,0
Mass Solid Fraction		0,0	0,2	0,1	0,0	0,0	0,0	0,0	0,0	0,0	0,2	0,0	0,5	0,0	0,4	0,0	0,0	0,0	0,0	0,0	0,0
Molar Enthalpy	cal/mol	-72571,1	-73943,7	-68750,8	-91029,2	-69822,3	-56988,7	-64972,4	-76094,3	-76094,3	-102157,6	-68024,3	-91254,4	-67657,4	-161731,2	-73407,4	-67868,3	-66709,1	-56220,6	-54055,1	-65661,0
Mass Enthalpy	kcal/kg	-3529,7	-3367,5	-3526,8	-2145,0	-3592,4	-3162,0	-1650,0	-3774,6	-3774,6	-3975,4	-3597,4	-2950,7	-3696,9	-4198,2	-3928,2	-3765,7	-3691,6	-3120,7	-1864,7	-3644,7
Molar Entropy	cal/mol-K	-47,0	-45,4	-45,0	0,0	-43,2	-10,0	1,7	-62,3	-62,3	-142,6	1,02E+27	-89,5	-36,7	-327,1	-52,1	-37,5	-34,3	-11,2	-9,3	-31,7
Mass Entropy	kcal/kg-K	-2,3	-2,1	-2,3	0,0	-2,2	-0,6	0,0	-3,1	-3,1	-5,5	5,41E+25	-2,9	-2,0	-8,5	-2,8	-2,1	-1,9	-0,6	-0,3	-1,8
Molar Density	mol/cc	0,1	0,0	0,1	0,0	0,1	0,0	0,0	0,1	0,1	0,0	0,0	0,0	0,1	0,0	0,1	0,1	0,1	0,0	0,0	0,0
Mass Density	gm/cc	1,1	1,0	1,0	0,0	1,0	0,0	0,0	1,0	1,0	1,0	0,9	1,2	1,0	1,1	1,0	1,0	0,9	0,0	0,0	0,9
Enthalpy Flow	kW	-42308,3	-509045,1	-43819,5	-22471,8	-825223,3	-49990,0	-3268,5	-571674,6	-571674,6	-99905,6	-784858,5	-50905,6	-736884,4	-58761,5	-280018,3	-59533,5	-66845,2	-365752,3	-9184,2	-427168,3
Average MW		20,6	22,0	19,5	42,4	19,4	18,0	39,4	20,2	20,2	25,7	18,9	30,9	18,3	38,5	18,7	18,0	18,1	18,0	29,0	18,0
Mole Flows	kmol/hr	501,3	5919,4	548,0	212,3	10162,4	754,2	43,3	6459,8	6459,8	840,9	9920,8	479,7	9364,9	312,4	3279,9	754,2	861,6	5593,9	146,1	5593,9
Mass Flows	kg/hr	10306,4	129979,1	10683,2	9008,2	197520,3	13593,7	1703,3	130225,6	130225,6	21608,6	187596,0	14834,3	171386,8	12035,1	61293,5	13593,7	15569,4	100775,0	4235,0	100775,0
GLUCOSE	kg/hr	786,4	32,4	292,9	0,0	1324,2	0,0	0,0	426,7	426,7	198,3	1324,2	59,8	1264,4	198,3	218,2	0,0	0,0	0,0	0,0	0,0
CELLULOS	kg/hr	78,3	15662,2	78,3	0,0	1566,2	0,0	0,0	0,0	0,0	0,0	1566,2	1566,2	0,0	0,0	0,0	0,0	0,0	0,0	0,0	0,0
XYLOSE	kg/hr	273,9	423,3	54,8	0,0	1007,0	0,0	0,0	5566,9	5566,9	0,0	1007,0	45,5	961,5	0,0	0,0	0,0	0,0	0,0	0,0	0,0
XYLAN	kg/hr	30,3	5054,3	30,3	0,0	606,5	0,0	0,0	0,0	0,0	0,0	606,5	606,5	0,0	0,0	0,0	0,0	0,0	0,0	0,0	0,0
BIOMASS	kg/hr	0,0	0,0	521,5	0,0	521,5	0,0	0,0	0,0	0,0	0,0	521,5	521,5	0,0	0,0	0,0	0,0	0,0	0,0	0,0	0,0
MICROORG	kg/hr	0,0	0,0	0,0	0,0	131,0	0,0	0,0	0,0	0,0	0,0	131,0	131,0	0,0	0,0	0,0	0,0	0,0	0,0	0,0	0,0
CELLOB	kg/hr	0,0	30,8	0,0	0,0	0,0	0,0	0,0	405,4	405,4	188,4	0,0	0,0	0,0	188,4	207,3	0,0	0,0	0,0	0,0	0,0
EXTRACT	kg/hr	10,7	214,8	10,7	0,0	214,8	0,0	0,0	2825,2	2825,2	1313,0	214,8	9,7	205,1	1313,0	1444,4	0,0	0,0	0,0	0,0	0,0
ASH	kg/hr	144,4	2888,0	144,4	0,0	2888,0	0,0	0,0	0,0	0,0	0,0	2888,0	2888,0	0,0	0,0	0,0	0,0	0,0	0,0	0,0	0,0
ETHANOL	kg/hr	0,0	0,0	0,0	174,0	9028,3	0,0	0,0	0,0	0,0	82,1	83,9	1,1	80,1	0,6	0,0	0,0	77,8	0,0	0,0	0,0
WATER	kg/hr	8835,2	102730,8	9323,4	236,2	176999,8	13585,6	33,3	113752,6	113752,6	13822,5	176252,9	6586,1	168294,6	4334,8	58499,3	13585,6	15491,5	100775,0	75,2	100775,0
CO2	kg/hr	0,0	0,0	8,1	8597,6	213,1	0,0	1265,7	0,0	0,0	0,0	0,0	0,0	0,0	0,0	0,0	0,0	0,0	0,0	2963,2	0,0
O2	kg/hr	0,0	0,0	0,1	0,1	0,0	0,0	403,7	0,0	0,0	0,0	0,0	0,0	0,0	0,0	0,0	0,0	0,0	0,0	0,0	0,0
NH3	kg/hr	0,0	0,0	14,0	0,3	19,8	0,0	0,5	0,0	0,0	0,0	0,0	0,0	0,0	0,0	0,0	0,0	0,0	0,0	0,0	0,0
AACID	kg/hr	0,1	2,7	0,1	0,0	2,7	7,7	0,0	35,5	35,5	7,3	2,6	0,1	2,5	3,6	18,2	7,7	0,1	0,0	0,0	0,0
H3O+	kg/hr	0,0	0,0	0,0	0,0	0,0	0,0	0,0	0,0	0,0	0,0	0,0	0,0	0,0	0,0	0,0	0,0	0,0	0,0	0,0	0,0
OH-	kg/hr	0,0	0,0	0,0	0,0	0,0	0,0	0,0	0,0	0,0	0,0	0,0	0,0	0,0	0,0	0,0	0,0	0,0	0,0	0,0	0,0
FURF	kg/hr	0,0	0,5	0,0	0,0	0,5	0,4	0,0	6,6	6,6	2,6	0,5	0,0	0,5	2,1	3,4	0,4	0,0	0,0	0,0	0,0
SODIU-01	kg/hr	6,7	134,3	6,7	0,0	134,3	0,0	0,0	1765,7	1765,7	820,6	134,3	6,1	128,2	820,6	902,8	0,0	0,0	0,0	0,0	0,0
KH2PO4	kg/hr	0,0	0,0	9,7	0,0	9,7	0,0	0,0	0,0	0,0	0,0	9,7	0,4	9,2	0,0	0,0	0,0	0,0	0,0	0,0	0,0
MGSO4-01	kg/hr	0,0	0,0	8,1	0,0	8,1	0,0	0,0	0,0	0,0	0,0	8,1	0,4	7,7	0,0	0,0	0,0	0,0	0,0	0,0	0,0
DIAMM-01	kg/hr	0,0	0,0	39,8	0,0	39,8	0,0	0,0	0,0	0,0	0,0	39,8	1,8	38,0	0,0	0,0	0,0	0,0	0,0	0,0	0,0
LIG	kg/hr	140,3	2805,0	140,3	0,0	2805,0	0,0	0,0	5441,0	5441,0	5173,8	2805,0	2410,0	395,0	5173,8	0,0	0,0	0,0	0,0	0,0	0,0

	Heat	
Stream Name	S3	S17
QCALC kW	-8188,936	67102,1453
TBEGIN C	76,21249	1052,31588
TEND C	110	278,3

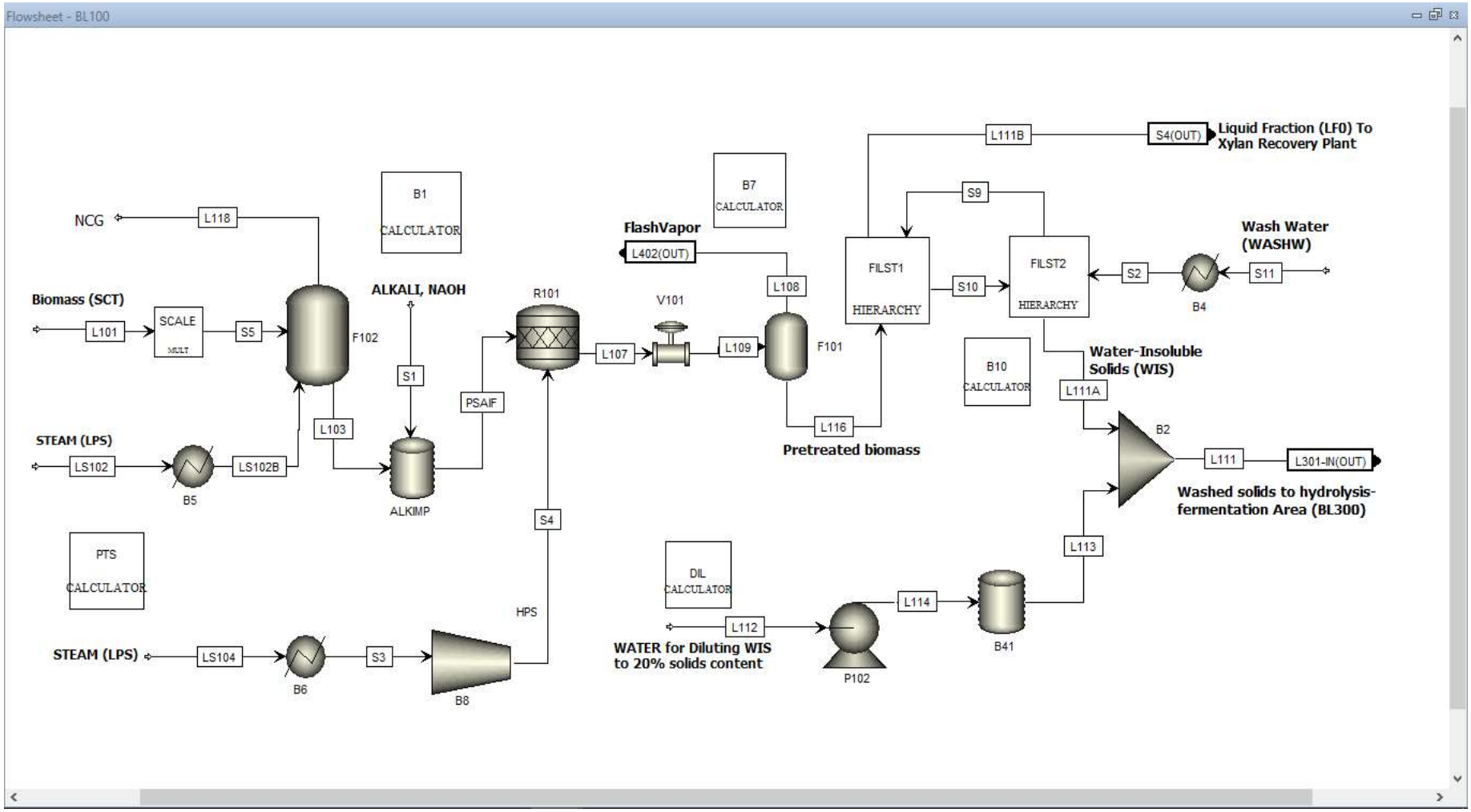

Fig C.2: ASPEN Flowsheet for biomass pretreatment and hemicellulose extraction plant (BL100)

TABLE C.3.: Summary of mass and energy balance results around biomass pretreatment and hemicellulose extraction plant (BL100)

		Material																								
Stream Name	Units	L101	L103	L107	L108	L109	L111	L111A	L111B	L112	L113	L114	L116	L118	LS102	LS102B	LS104	PSAIF	S1	S3	S4	S5	S6	S9	S10	S11
Description		Biomass (SCT)																								
From			F102	R101	F101	V101	B44	FILST2	FILST1		B41	P102	F101	F102		B5		ALKIMP		B6	B8	SCALE	B2	FILST2	FILST1	
To		SCALE	ALKIMP	V101		F101		B2		P102	B2	B41	FILST1		B5	F102	B6	R101	ALKIMP	B8	R101	F102	B44	FILST1	FILST2	FILST2
Stream Class		MIXCISLD	MIXCISLD	MIXCISLD	MIXCISLD	MIXCISLD	MIXCISLD	MIXCISLD	MIXCISLD	MIXCISLD	MIXCISLD	MIXCISLD	MIXCISLD	MIXCISLD	MIXCISLD	MIXCISLD	MIXCISLD	MIXCISLD	MIXCISLD	MIXCISLD	MIXCISLD	MIXCISLD	MIXCISLD	MIXCISLD	MIXCISLD	MIXCISLD
Total Stream																										
Temperature	C	25,0	61,5	204,0	129,7	-231,5	40,0	41,0	76,5	25,0	25,0	25,0	129,7		90,0	180,1	90,0	51,7	25,0	180,1	259,2	25,0	31,9	41,0	76,5	25,0
Pressure	atm	1,0	4,7	16,3	2,5	2,5	1,0	1,0	1,0	1,0	3,0	3,0	2,5	4,7	9,9	9,9	10,9	1,0	1,0	9,9	16,3	1,0	1,0	1,0	1,0	1,0
Molar Vapor Fraction		0,0	0,0	0,0	1,0	0,0	0,0	0,0	0,0	0,0	0,0	0,0	0,0		0,0	1,0	0,0	0,0	0,0	1,0	1,0	0,0	0,0	0,0	0,0	0,0
Molar Liquid Fraction		0,9	0,9	0,9	0,0	0,9	1,0	0,9	1,0	1,0	1,0	1,0	0,9		1,0	0,0	1,0	0,9	1,0	0,0	0,0	0,9	1,0	1,0	0,9	1,0
Molar Solid Fraction		0,1	0,1	0,1	0,0	0,1	0,0	0,1	0,0	0,0	0,0	0,0	0,1		0,0	0,0	0,0	0,1	0,0	0,0	0,0	0,1	0,0	0,0	0,1	0,0
Mass Vapor Fraction		0,0	0,0	0,0	1,0	0,0	0,0	0,0	0,0	0,0	0,0	0,0	0,0		0,0	1,0	0,0	0,0	0,0	1,0	1,0	0,0	0,0	0,0	0,0	0,0
Mass Liquid Fraction		0,5	0,5	0,7	0,0	0,7	0,8	0,6	1,0	1,0	1,0	1,0	0,6		1,0	0,0	1,0	0,5	1,0	0,0	0,0	0,5	0,8	1,0	0,6	1,0
Mass Solid Fraction		0,5	0,5	0,3	0,0	0,3	0,2	0,4	0,0	0,0	0,0	0,0	0,4		0,0	0,0	0,0	0,5	0,0	0,0	0,0	0,5	0,2	0,0	0,4	0,0
Molar Enthalpy	cal/mol	-92407,8	-89919,0	-92315,6	-56988,7	-92315,6	-73943,7	-83131,2	-76094,3	-68311,3	-68310,0	-68310,0	-103358,6		-67137,7	-56638,9	-67137,4	-103747,0	-809710,5	-56638,9	-56004,1	-92407,8	-74098,6	-70085,7	-89451,4	-68311,3
Mass Enthalpy	kcal/kg	-2743,6	-2759,0	-3101,7	-3162,0	-3101,7	-3367,5	-2957,3	-3774,6	-3791,9	-3791,8	-3791,8	-3091,4		-3726,7	-3143,9	-3726,7	-3169,4	-20244,2	-3143,9	-3108,7	-2743,6	-3374,5	-3785,3	-2945,6	-3791,9
Molar Entropy	cal/mol-K	-77,9	-72,6	-84,8	-10,0	1,16E+28	-45,4	-56,8	-62,3	-39,0	-39,0	-39,0	-113,3		-35,4	-11,9	-35,4	-114,7	-2494,3	-11,9	-11,5	-77,9	-46,0	-44,6	-73,2	-39,0
Mass Entropy	kcal/kg-K	-2,3	-2,2	-2,8	-0,6	3,89E+26	-2,1	-2,0	-3,1	-2,2	-2,2	-2,2	-3,4		-2,0	-0,7	-2,0	-3,5	-62,4	-0,7	-0,6	-2,3	-2,1	-2,4	-2,4	-2,2
Molar Density	mol/cc	0,0	0,0	0,0	0,0	0,0	0,0	0,0	0,1	0,1	0,1	0,1	0,0		0,1	0,0	0,1	0,0	0,0	0,0	0,0	0,0	0,0	0,1	0,0	0,1
Mass Density	gm/cc	1,2	1,1	1,0	0,0	1,2	1,0	1,1	1,0	1,0	1,0	1,0	1,1		1,0	0,0	1,0	1,1	0,5	0,0	0,0	1,2	1,0	1,0	1,1	1,0
Enthalpy Flow	kW	-6381,6	-253616,7	-339951,5	-49990,0	-339951,5	-509045,1	-223517,8	-571674,6	-286599,1	-286593,5	-286593,5	-289952,1		-13175,9	-11115,4	-57644,1	-298350,3	-44733,7	-48630,1	-48085,1	-242501,2	-510111,3	-504363,9	-222636,5	-505245,2
Average MW		33,7	32,6	29,8	18,0	29,8	22,0	28,1	20,2	18,0	18,0	18,0	33,4		18,0	18,0	18,0	32,7	40,0	18,0	18,0	33,7	22,0	18,5	30,4	18,0
Mole Flows	kmol/hr	59,4	2425,2	3166,4	754,2	3166,4	5919,4	2311,9	6459,8	3607,5	3607,5	3607,5	2412,1	0,0	168,7	168,7	738,3	2472,7	47,5	738,3	738,3	2256,4	5919,4	6187,8	2140,1	6359,6
Mass Flows	kg/hr	2000,0	79040,0	94240,0	13593,7	94240,0	129979,1	64989,5	130225,6	64989,5	64989,5	64989,5	80646,3	0,0	3040,0	3040,0	13300,0	80940,0	1900,0	13300,0	13300,0	76000,0	129979,1	114568,9	64988,4	114570,0
GLUCOSE	kg/hr	0,0		459,2	0,0	459,2	32,4	32,4	426,7	0,0	0,0	0,0	459,2	0,0	0,0	0,0	0,0	0,0	0,0	0,0	0,0	0,0	32,4	95,3	127,8	0,0
CELLULOS	kg/hr	435,0	16530,0	15662,2	0,0	15662,2	15662,2	15662,2	0,0	0,0	0,0	0,0	15662,2	0,0	0,0	0,0	0,0	16530,0	0,0	0,0	0,0	16530,0	15662,2	0,0	15662,2	0,0
XYLOSE	kg/hr	0,0	0,0	5990,2	0,0	5990,2	423,3	423,3	5566,9	0,0	0,0	0,0	5990,2	0,0	0,0	0,0	0,0	0,0	0,0	0,0	0,0	0,0	423,3	1243,6	1666,9	0,0
XYLAN	kg/hr	272,0	10336,0	5054,3	0,0	5054,3	5054,3	5054,3	0,0	0,0	0,0	0,0	5054,3	0,0	0,0	0,0	0,0	10336,0	0,0	0,0	0,0	10336,0	5054,3	0,0	5054,3	0,0
LIG	kg/hr	217,0	8246,0	8246,0	0,0	8246,0	2805,0	2805,0	5441,0	0,0	0,0	0,0	8246,0	0,0	0,0	0,0	0,0	8246,0	0,0	0,0	0,0	8246,0	2805,0	1215,5	4020,5	0,0
CELLOB	kg/hr	0,0	0,0	436,2	0,0	436,2	30,8	30,8	405,4	0,0	0,0	0,0	436,2	0,0	0,0	0,0	0,0	0,0	0,0	0,0	0,0	0,0	30,8	90,6	121,4	0,0
EXTRACT	kg/hr	80,0	3040,0	3040,0	0,0	3040,0	214,8	214,8	2825,2	0,0	0,0	0,0	3040,0	0,0	0,0	0,0	0,0	3040,0	0,0	0,0	0,0	3040,0	214,8	631,1	845,9	0,0
ASH	kg/hr	76,0	2888,0	2888,0	0,0	2888,0	2888,0	2888,0	0,0	0,0	0,0	0,0	2888,0	0,0	0,0	0,0	0,0	2888,0	0,0	0,0	0,0	2888,0	2888,0	0,0	2888,0	0,0
WATER	kg/hr	920,0	38000,0	50510,6	13585,6	50510,6	102730,8	37741,2	113752,6	64989,5	64989,5	64989,5	36924,9	0,0	3040,0	3040,0	13300,0	38000,0	0,0	13300,0	13300,0	34960,0	102730,8	110888,9	34060,1	114570,0
AACID	kg/hr	0,0	0,0	45,9	7,7	45,9	2,7	2,7	35,5	0,0	0,0	0,0	38,2	0,0	0,0	0,0	0,0	0,0	0,0	0,0	0,0	0,0	2,7	7,9	10,6	0,0
H3O+	kg/hr	0,0	0,0	0,0	0,0	0,0	0,0	0,0	0,0	0,0	0,0	0,0	0,0	0,0	0,0	0,0	0,0	0,0	0,0	0,0	0,0	0,0	0,0	0,0	0,0	0,0
OH-	kg/hr	0,0	0,0	0,0	0,0	0,0	0,0	0,0	0,0	0,0	0,0	0,0	0,0	0,0	0,0	0,0	0,0	0,0	0,0	0,0	0,0	0,0	0,0	0,0	0,0	0,0
FURF	kg/hr	0,0	0,0	7,5	0,4	7,5	0,5	0,5	6,6	0,0	0,0	0,0	7,1	0,0	0,0	0,0	0,0	0,0	0,0	0,0	0,0	0,0	0,5	1,5	2,0	0,0
SODIU-01	kg/hr	0,0	0,0	1900,0	0,0	1900,0	134,3	134,3	1765,7	0,0	0,0	0,0	1900,0	0,0	0,0	0,0	0,0	1900,0	1900,0	0,0	0,0	0,0	134,3	394,5	528,7	0,0

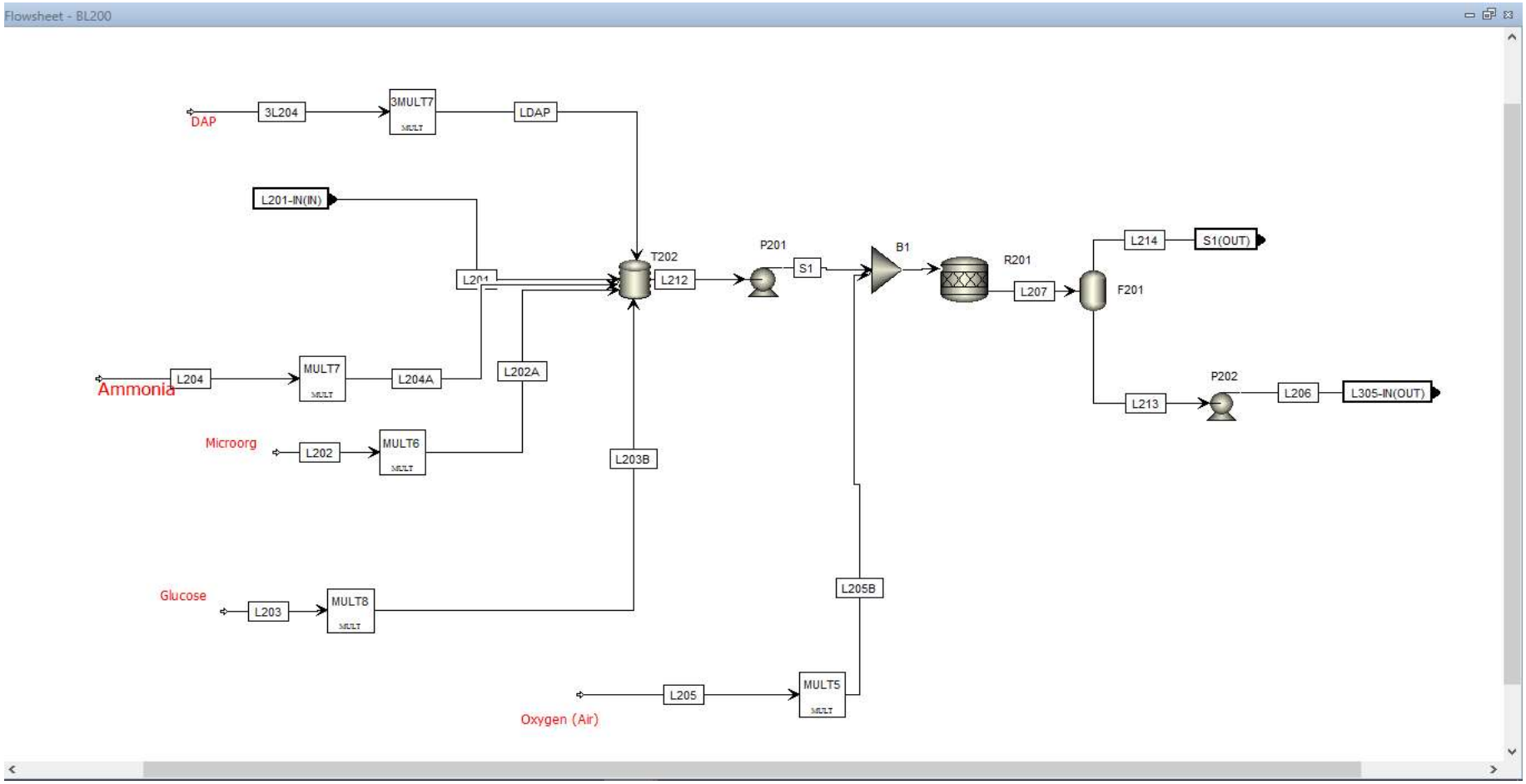

Fig C-3: Flowsheet for seed propagation plant (BL200)

TABLE C.4.: Summary of mass and energy balance results around seed propagation plant (BL200)

		Material																	
Stream Name	Units	3L204	L201	L202	L202A	L203	L203B	L204	L204A	L205	L205B	L206	L207	L209	L212	L213	L214	LDAP	S1
Description																			
From					MULT6		MULT8		MULT7		MULT5	P202	R201	B1	T202	F201	F201	3MULT7	P201
To		3MULT7	T202	MULT6	T202	MULT8	T202	MULT7	T202	MULT5	B1		F201	R201	P201	P202		T202	B1
Stream Class		MIXCISLD	MIXCISLD	MIXCISLD	MIXCISLD	MIXCISLD	MIXCISLD	MIXCISLD	MIXCISLD	MIXCISLD	MIXCISLD	MIXCISLD	MIXCISLD	MIXCISLD	MIXCISLD	MIXCISLD	MIXCISLD	MIXCISLD	MIXCISLD
Total Stream																			
Temperature	C	25,0	28,6	30,0	30,0	30,0	30,0	30,0	30,0	30,0	30,0	30,1	30,0	28,0	29,6	30,0	30,0	25,0	29,7
Pressure	atm	1,0	1,0	1,0	1,0	1,0	1,0	1,0	1,0	1,0	1,0	3,0	1,0	1,0	1,0	1,0	1,0	1,0	3,0
Molar Vapor Fraction		0,0	0,0	0,0	0,0	0,0	0,0	0,9	0,9	1,0	1,0	0,0	0,1	0,1	0,0	0,0	1,0	0,0	0,0
Molar Liquid Fraction		1,0	1,0	0,0	0,0	1,0	1,0	0,1	0,1	0,0	0,0	1,0	0,9	0,9	1,0	1,0	0,0	1,0	1,0
Molar Solid Fraction		0,0	0,0	1,0	1,0	0,0	0,0	0,0	0,0	0,0	0,0	0,0	0,0	0,0	0,0	0,0	0,0	0,0	0,0
Mass Vapor Fraction		0,0	0,0	0,0	0,0	0,0	0,0	0,4	0,4	1,0	1,0	0,0	0,1	0,1	0,0	0,0	1,0	0,0	0,0
Mass Liquid Fraction		1,0	1,0	0,0	0,0	1,0	1,0	0,6	0,6	0,0	0,0	0,9	0,8	0,9	1,0	0,9	0,0	1,0	1,0
Mass Solid Fraction		0,0	0,0	1,0	1,0	0,0	0,0	0,0	0,0	0,0	0,0	0,1	0,1	0,0	0,0	0,1	0,0	0,0	0,0
Molar Enthalpy	cal/mol	-283995,8	-72571,1	-31114,8	-31114,8	-299993,9	-299993,9	-29540,1	-29540,1	33,2	33,2	-68750,8	-68476,3	-68664,3	-74306,1	-68752,9	-64972,4	-283995,8	-74303,9
Mass Enthalpy	kcal/kg	-2150,6	-3529,7	-1263,5	-1263,5	-1665,2	-1665,2	-875,6	-875,6	1,0	1,0	-3526,8	-3268,9	-3037,1	-3402,7	-3527,0	-1650,0	-2150,6	-3402,6
Molar Entropy	cal/mol-K	-731,1	-47,0	-104,4	-104,4	-260,6	-260,6	-8,7	-8,7	0,1	0,1	-45,0	-41,6	-45,1	-48,8	-45,0	1,7	-731,1	-48,8
Mass Entropy	kcal/kg-K	-5,5	-2,3	-4,2	-4,2	-1,4	-1,4	-0,3	-0,3	0,0	0,0	-2,3	-2,0	-2,0	-2,2	-2,3	0,0	-5,5	-2,2
Molar Density	mol/cc	0,0	0,1	0,0	0,0	0,1	0,1	0,0	0,0	0,0	0,0	0,1	0,0	0,0	0,1	0,1	0,0	0,0	0,1
Mass Density	gm/cc	1,0	1,1	0,9	0,9	18,9	18,9	0,0	0,0	0,0	0,0	1,0	0,0	0,0	1,2	1,0	0,0	1,0	1,2
Enthalpy Flow	kW	-2,6	-42308,3	0,0	0,0	-34,5	-1312,9	-0,9	-32,8	0,0	1,6	-43819,5	-47089,3	-43750,7	-43753,6	-43820,8	-3268,5	-99,6	-43752,3
Average MW		132,1	20,6	24,6	24,6	180,2	180,2	33,7	33,7	32,0	32,0	19,5	20,9	22,6	21,8	19,5	39,4	132,1	21,8
Mole Flows	kmol/hr	0,0	501,3	0,0	0,0	0,1	3,8	0,0	1,0	1,1	41,6	548,0	591,3	547,9	506,3	548,0	43,3	0,3	506,3
Mass Flows	kg/hr	1,0	10306,4	0,0	0,0	17,8	677,9	0,8	32,2	35,0	1330,0	10683,2	12386,4	12386,3	11056,3	10683,2	1703,3	39,8	11056,3
GLUCOSE	kg/hr	0,0	786,4	0,0	0,0	17,8	677,9	0,0	0,0	0,0	0,0	292,9	292,9	1464,3	1464,3	292,9	0,0	0,0	1464,3
CELLULOS	kg/hr	0,0	78,3	0,0	0,0	0,0	0,0	0,0	0,0	0,0	0,0	78,3	78,3	78,3	78,3	78,3	0,0	0,0	78,3
XYLOSE	kg/hr	0,0	273,9	0,0	0,0	0,0	0,0	0,0	0,0	0,0	0,0	54,8	54,8	273,9	273,9	54,8	0,0	0,0	273,9
XYLAN	kg/hr	0,0	30,3	0,0	0,0	0,0	0,0	0,0	0,0	0,0	0,0	30,3	30,3	30,3	30,3	30,3	0,0	0,0	30,3
LIG	kg/hr	0,0	140,3	0,0	0,0	0,0	0,0	0,0	0,0	0,0	0,0	140,3	140,3	140,3	140,3	140,3	0,0	0,0	140,3
BIOMASS	kg/hr	0,0	0,0	0,0	0,0	0,0	0,0	0,0	0,0	0,0	0,0	521,5	521,5	0,0	0,0	521,5	0,0	0,0	0,0
MICROORG	kg/hr	0,0	0,0	0,0	0,0	0,0	0,0	0,0	0,0	0,0	0,0	0,0	0,0	0,0	0,0	0,0	0,0	0,0	0,0
EXTRACT	kg/hr	0,0	10,7	0,0	0,0	0,0	0,0	0,0	0,0	0,0	0,0	10,7	10,7	10,7	10,7	10,7	0,0	0,0	10,7
ASH	kg/hr	0,0	144,4	0,0	0,0	0,0	0,0	0,0	0,0	0,0	0,0	144,4	144,4	144,4	144,4	144,4	0,0	0,0	144,4
WATER	kg/hr	0,0	8835,2	0,0	0,0	0,0	0,0	0,0	0,0	0,0	0,0	9323,4	9356,7	8835,2	8835,2	9323,4	33,3	0,0	8835,2
CO2	kg/hr	0,0	0,0	0,0	0,0	0,0	0,0	0,0	0,0	0,0	0,0	8,1	1273,8	0,0	0,0	8,1	1265,7	0,0	0,0
O2	kg/hr	0,0	0,0	0,0	0,0	0,0	0,0	0,0	0,0	35,0	1330,0	0,1	403,8	1330,0	0,0	0,1	403,7	0,0	0,0
NH3	kg/hr	0,0	0,0	0,0	0,0	0,0	0,0	0,4	14,5	0,0	0,0	14,0	14,5	14,5	14,5	14,0	0,5	0,0	14,5
AACID	kg/hr	0,0	0,1	0,0	0,0	0,0	0,0	0,0	0,0	0,0	0,0	0,1	0,1	0,1	0,1	0,1	0,0	0,0	0,1
H3O+	kg/hr	0,0	0,0	0,0	0,0	0,0	0,0	0,0	0,0	0,0	0,0	0,0	0,0	0,0	0,0	0,0	0,0	0,0	0,0
OH-	kg/hr	0,0	0,0	0,0	0,0	0,0	0,0	0,0	0,0	0,0	0,0	0,0	0,0	0,0	0,0	0,0	0,0	0,0	0,0
FURF	kg/hr	0,0	0,0	0,0	0,0	0,0	0,0	0,0	0,0	0,0	0,0	0,0	0,0	0,0	0,0	0,0	0,0	0,0	0,0
SODIU-01	kg/hr	0,0	6,7	0,0	0,0	0,0	0,0	0,0	0,0	0,0	0,0	6,7	6,7	6,7	6,7	6,7	0,0	0,0	6,7
KH2PO4	kg/hr	0,0	0,0	0,0	0,0	0,0	0,0	0,3	9,7	0,0	0,0	9,7	9,7	9,7	9,7	9,7	0,0	0,0	9,7
MGSO4-01	kg/hr	0,0	0,0	0,0	0,0	0,0	0,0	0,2	8,1	0,0	0,0	8,1	8,1	8,1	8,1	8,1	0,0	0,0	8,1
DIAMM-01	kg/hr	1,0	0,0	0,0	0,0	0,0	0,0	0,0	0,0	0,0	0,0	39,8	39,8	39,8	39,8	39,8	0,0	39,8	39,8

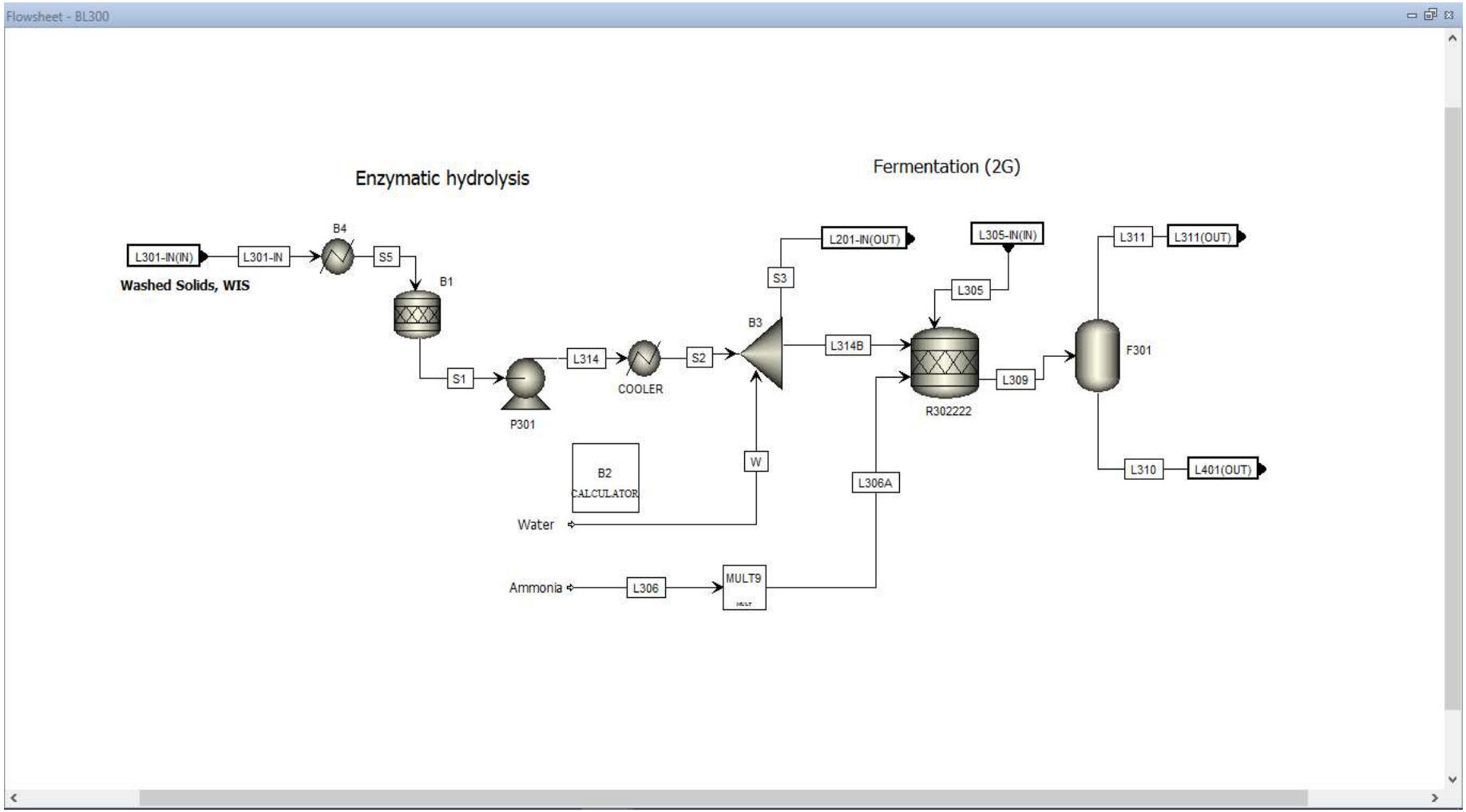

Fig C-4: Flowsheet for the enzymatic hydrolysis and fermentation plant (BL300)

TABLE C.5.: Summary of mass and energy balance results around hydrolysis-fermentation plant (BL300)

		Material													
Stream Name	Units	L301-IN	L305	L306	L306A	L309	L310	L311	L314	L314B	S1	S2	S3	S5	W
Description															
From					MULT9	R302222	F301	F301	P301	B3	B1	COOLER	B3	B4	
To		B4	R302222	MULT9	R302222	F301			COOLER	R302222	P301	B3		B1	B3
Stream Class		MIXCISLD	MIXCISLD	MIXCISLD	MIXCISLD	MIXCISLD	MIXCISLD	MIXCISLD	MIXCISLD	MIXCISLD	MIXCISLD	MIXCISLD	MIXCISLD	MIXCISLD	MIXCISLD
Total Stream															
Temperature	C	40,0	30,1	25,0	25,0	37,8	37,0	37,0	50,0	28,6	50,0	31,0	28,6	50,0	25,0
Pressure	atm	1,0	3,0	1,0	1,0	1,0	1,0	1,0	2,0	1,0	1,0	1,0	1,0	1,0	1,0
Molar Vapor Fraction		0,0	0,0	1,0	1,0	0,0	0,0	1,0	0,0	0,0	0,0	0,0	0,0	0,0	0,0
Molar Liquid Fraction		1,0	1,0	0,0	0,0	1,0	1,0	0,0	1,0	1,0	1,0	1,0	1,0	1,0	1,0
Molar Solid Fraction		0,0	0,0	0,0	0,0	0,0	0,0	0,0	0,0	0,0	0,0	0,0	0,0	0,0	0,0
Mass Vapor Fraction		0,0	0,0	1,0	1,0	0,0	0,0	1,0	0,0	0,0	0,0	0,0	0,0	0,0	0,0
Mass Liquid Fraction		0,8	0,9	0,0	0,0	1,0	1,0	0,0	0,9	1,0	0,9	0,9	1,0	0,8	1,0
Mass Solid Fraction		0,2	0,1	0,0	0,0	0,0	0,0	0,0	0,1	0,0	0,1	0,1	0,0	0,2	0,0
Molar Enthalpy	cal/mol	-73943,74	-68750,83	-10931,72	-10931,72	-70256,15	-69822,26	-91029,17	-75293,34	-72571,13	-75293,96	-75676,23	-72571,13	-73751,51	-68311,31
Mass Enthalpy	kcal/kg	-3367,5	-3526,8	-641,9	-641,9	-3529,2	-3592,4	-2145,0	-3359,1	-3529,7	-3359,1	-3376,1	-3529,7	-3358,7	-3791,9
Molar Entropy	cal/mol-K	-45,4	-45,0	-23,7	-23,7	-42,3	-43,2	0,0	-51,5	-47,0	-51,5	-52,8	-47,0	-44,8	-39,0
Mass Entropy	kcal/kg-K	-2,1	-2,3	-1,4	-1,4	-2,1	-2,2	0,0	-2,3	-2,3	-2,3	-2,4	-2,3	-2,0	-2,2
Molar Density	mol/cc	0,0	0,1	0,0	0,0	0,1	0,1	0,0	0,1	0,1	0,1	0,1	0,1	0,0	0,1
Mass Density	gm/cc	1,0	1,0	0,0	0,0	1,0	1,0	0,0	1,2	1,1	1,2	1,2	1,1	1,0	1,0
Enthalpy Flow	kW	-5,09E+05	-4,38E+04	-4,77E-01	-1,81E+01	-8,48E+05	-8,25E+05	-2,25E+04	-5,08E+05	-8,04E+05	-5,08E+05	-5,10E+05	-4,23E+04	-5,08E+05	-3,36E+05
Average MW		22,0	19,5	17,0	17,0	19,9	19,4	42,4	22,4	20,6	22,4	22,4	20,6	22,0	18,0
Mole Flows	kmol/hr	5919,4	548,0	0,0	1,4	10374,7	10162,4	212,3	5798,8	9524,4	5798,8	5798,8	501,3	5919,4	4226,9
Mass Flows	kg/hr	129979,1	10683,2	0,6	24,3	206528,5	197520,3	9008,2	129979,1	195821,0	129979,1	129979,1	10306,4	129979,1	76148,3
GLUCOSE	kg/hr	32,4	292,9	0,0	0,0	1324,2	1324,2	0,0	15727,0	14940,7	15727,0	15727,0	786,4	32,4	0,0
CELLULOS	kg/hr	15662,2	78,3	0,0	0,0	1566,2	1566,2	0,0	1566,2	1487,9	1566,2	1566,2	78,3	15662,2	0,0
XYLOSE	kg/hr	423,3	54,8	0,0	0,0	1007,0	1007,0	0,0	5477,6	5203,7	5477,6	5477,6	273,9	423,3	0,0
XYLAN	kg/hr	5054,3	30,3	0,0	0,0	606,5	606,5	0,0	606,5	576,2	606,5	606,5	30,3	5054,3	0,0
BIOMASS	kg/hr	0,0	521,5	0,0	0,0	521,5	521,5	0,0	0,0	0,0	0,0	0,0	0,0	0,0	0,0
MICROORG	kg/hr	0,0	0,0	0,0	0,0	131,0	131,0	0,0	0,0	0,0	0,0	0,0	0,0	0,0	0,0
CELLOB	kg/hr	30,8	0,0	0,0	0,0	0,0	0,0	0,0	0,0	0,0	0,0	0,0	0,0	30,8	0,0
EXTRACT	kg/hr	214,8	10,7	0,0	0,0	214,8	214,8	0,0	214,8	204,1	214,8	214,8	10,7	214,8	0,0
ASH	kg/hr	2888,0	144,4	0,0	0,0	2888,0	2888,0	0,0	2888,0	2743,6	2888,0	2888,0	144,4	2888,0	0,0
ETHANOL	kg/hr	0,0	0,0	0,0	0,0	9202,2	9028,3	174,0	0,0	0,0	0,0	0,0	0,0	0,0	0,0
WATER	kg/hr	102730,8	9323,4	0,0	0,0	177236,0	176999,8	236,2	100556,5	167869,5	100556,5	100556,5	8835,2	102730,8	76148,3
CO2	kg/hr	0,0	8,1	0,0	0,0	8810,7	213,1	8597,6	0,0	0,0	0,0	0,0	0,0	0,0	0,0
O2	kg/hr	0,0	0,1	0,0	0,0	0,1	0,0	0,1	0,0	0,0	0,0	0,0	0,0	0,0	0,0
NH3	kg/hr	0,0	14,0	0,6	24,3	20,1	19,8	0,3	0,0	0,0	0,0	0,0	0,0	0,0	0,0
AACID	kg/hr	2,7	0,1	0,0	0,0	2,7	2,7	0,0	2,7	2,6	2,7	2,7	0,1	2,7	0,0
H3O+	kg/hr	0,0	0,0	0,0	0,0	0,0	0,0	0,0	0,0	0,0	0,0	0,0	0,0	0,0	0,0
OH-	kg/hr	0,0	0,0	0,0	0,0	0,0	0,0	0,0	0,0	0,0	0,0	0,0	0,0	0,0	0,0
FURF	kg/hr	0,5	0,0	0,0	0,0	0,5	0,5	0,0	0,5	0,5	0,5	0,5	0,0	0,5	0,0
SODIU-01	kg/hr	134,3	6,7	0,0	0,0	134,3	134,3	0,0	134,3	127,5	134,3	134,3	6,7	134,3	0,0
KH2PO4	kg/hr	0,0	9,7	0,0	0,0	9,7	9,7	0,0	0,0	0,0	0,0	0,0	0,0	0,0	0,0
MGSO4-01	kg/hr	0,0	8,1	0,0	0,0	8,1	8,1	0,0	0,0	0,0	0,0	0,0	0,0	0,0	0,0
DIAMM-01	kg/hr	0,0	39,8	0,0	0,0	39,8	39,8	0,0	0,0	0,0	0,0	0,0	0,0	0,0	0,0
LIG	kg/hr	2805,0	140,3	0,0	0,0	2805,0	2805,0	0,0	2805,0	2664,8	2805,0	2805,0	140,3	2805,0	0,0

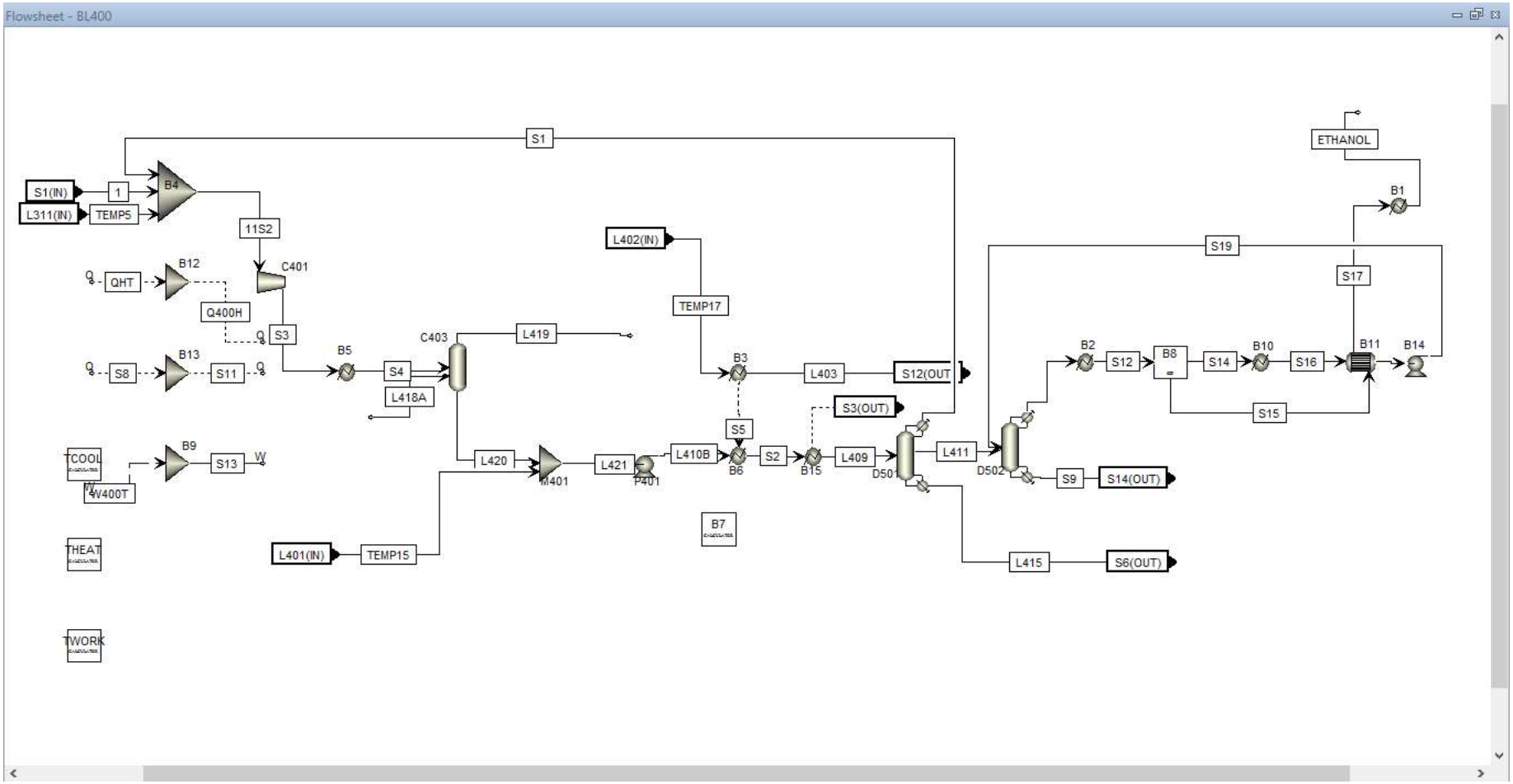

Fig C-5: Flowsheet for bioethanol production and recovery plant (BL400)

TABLE C.6.: Summary of mass and energy balance results around ethanol recovery plant (BL400)

Material

Stream Name	Units	1	11S2	ETHANOL	L403	L409	L410B	L411	L415	L418A	L419	L420	L421	S1	S2	S3	S4	S9	S10	S12	S14	S15	S16	S17	S18	S19	TEMP5	TEMP15	TEMP17
Description																													
From			B4	B1	B3	B15	P401	D501	D501		C403	C403	M401	D501	B6	C401	B5	D502	D502	B2	B8	B8	B10	B11	B11	B14			
To		B4	C401			D501	B6	D502		C403		M401	P401	B4	B15	B5	C403		B2	B8	B10	B11	B11	B1	B14	D502	B4	M401	B3
Stream Class		MIXCISLD	MIXCISLD	MIXCISLD	MIXCISLD	MIXCISLD	MIXCISLD	MIXCISLD	MIXCISLD	MIXCISLD	MIXCISLD	MIXCISLD	MIXCISLD	MIXCISLD	MIXCISLD	MIXCISLD	MIXCISLD	MIXCISLD	MIXCISLD	MIXCISLD	MIXCISLD	MIXCISLD	MIXCISLD	MIXCISLD	MIXCISLD	MIXCISLD	MIXCISLD	MIXCISLD	MIXCISLD
Total Stream																													
Temperature	C	30,0	36,6	35,0	50,0	110,0	36,4	116,3	125,0	25,0	25,5	27,2	36,3	62,4	76,2	125,2	35,0	113,3	90,6	120,0	120,0	120,0	35,0	93,6	71,0	71,1	37,0	37,0	129,7
Pressure	atm	1,0	1,0	1,0	2,5	4,0	4,0	2,1	2,3	2,1	1,0	1,0	1,1	2,0	4,0	2,5	2,5	1,6	1,6	1,4	1,4	1,4	1,5	1,4	1,5	3,0	1,0	1,0	2,5
Molar Vapor Fraction		1,0	1,0	0,0	0,0	0,0	0,0	1,0	0,0	0,0	1,0	0,0	0,0	1,0	0,0	1,0	1,0	0,0	1,0	1,0	1,0	1,0	0,0	1,0	0,0	0,0	1,0	0,0	1,0
Molar Liquid Fraction		0,0	0,0	1,0	1,0	1,0	1,0	0,0	1,0	1,0	0,0	1,0	1,0	0,0	1,0	0,0	0,0	1,0	0,0	0,0	0,0	0,0	1,0	0,0	1,0	1,0	0,0	1,0	0,0
Molar Solid Fraction		0,0	0,0	0,0	0,0	0,0	0,0	0,0	0,0	0,0	0,0	0,0	0,0	0,0	0,0	0,0	0,0	0,0	0,0	0,0	0,0	0,0	0,0	0,0	0,0	0,0	0,0	0,0	0,0
Mass Vapor Fraction		1,0	1,0	0,0	0,0	0,0	0,0	1,0	0,0	0,0	1,0	0,0	0,0	1,0	0,0	1,0	1,0	0,0	1,0	1,0	1,0	1,0	0,0	1,0	0,0	0,0	1,0	0,0	1,0
Mass Liquid Fraction		0,0	0,0	1,0	1,0	1,0	1,0	0,0	1,0	1,0	0,0	1,0	1,0	0,0	1,0	0,0	0,0	1,0	0,0	0,0	0,0	0,0	1,0	0,0	1,0	1,0	0,0	1,0	0,0
Mass Solid Fraction		0,0	0,0	0,0	0,0	0,0	0,0	0,0	0,0	0,0	0,0	0,0	0,0	0,0	0,0	0,0	0,0	0,0	0,0	0,0	0,0	0,0	0,0	0,0	0,0	0,0	0,0	0,0	0,0
Molar Enthalpy	cal/mol	-64972,4	-86603,2	-65850,1	-67868,3	-68314,6	-69702,4	-56546,3	-68024,3	-68288,4	-88115,7	-68248,1	-69704,2	-85991,4	-68955,5	-85776,5	-87050,4	-66709,1	-55288,9	-54781,9	-55766,3	-54296,6	-67012,4	-54792,4	-66007,1	-66005,1	-91029,2	-69822,3	-56988,7
Mass Enthalpy	kcal/kg	-1650,0	-2066,2	-1436,1	-3765,7	-3531,9	-3603,7	-2430,8	-3597,4	-3790,6	-2070,6	-3753,9	-3603,8	-2064,6	-3565,1	-2046,5	-2076,9	-3691,6	-1338,3	-1326,1	-1737,0	-1184,1	-2087,3	-1195,0	-2056,0	-2056,0	-2145,0	-3592,4	-3162,0
Molar Entropy	cal/mol-K	1,7	0,4	-81,2	-37,5	-38,7	-42,9	-16,4	1,02E+27	-38,9	0,9	-39,0	-42,9	-5,1	-40,5	0,9	-2,8	-34,3	-43,1	-41,4	-27,8	-48,8	-59,1	-50,1	-56,0	-56,0	0,0	-43,2	-10,0
Mass Entropy	kcal/kg-K	0,0	0,0	-1,8	-2,1	-2,0	-2,2	-0,7	5,41E+25	-2,2	0,0	-2,1	-2,2	-0,1	-2,1	0,0	-0,1	-1,9	-1,0	-1,0	-0,9	-1,1	-1,8	-1,1	-1,7	-1,7	0,0	-2,2	-0,6
Molar Density	mol/cc	0,0	0,0	0,0	0,1	0,0	0,1	0,0	0,0	0,1	0,0	0,1	0,1	0,0	0,1	0,0	0,0	0,1	0,0	0,0	0,0	0,0	0,0	0,0	0,0	0,0	0,0	0,1	0,0
Mass Density	gm/cc	0,0	0,0	0,8	1,0	0,9	1,0	0,0	0,9	1,0	0,0	1,0	1,0	0,0	1,0	0,0	0,0	0,9	0,0	0,0	0,0	0,0	0,8	0,0	0,8	0,8	0,0	1,0	0,0
Enthalpy Flow	kW	-3,27E+03	-2,64E+04	-1,52E+04	-5,95E+04	-8,73E+05	-8,91E+05	-6,97E+04	-7,85E+05	-6,45E+04	-2,56E+04	-6,54E+04	-8,91E+05	-6,23E+02	-8,81E+05	-2,61E+04	-2,65E+04	-6,68E+04	-1,90E+04	-1,88E+04	-6,34E+03	-1,25E+04	-7,61E+03	-1,26E+04	-7,50E+03	-7,50E+03	-2,25E+04	-8,25E+05	-5,00E+04
Average MW		39,4	41,9	45,9	18,0	19,3	19,3	23,3	18,9	18,0	42,6	18,2	19,3	41,7	19,3	41,9	41,9	18,1	41,3	41,3	32,1	45,9	32,1	45,9	32,1	32,1	42,4	19,4	18,0
Mole Flows	kmol/hr	43,3	261,7	198,0	754,2	10986,7	10986,7	1059,6	9920,8	811,9	249,4	824,2	10986,7	6,2	10986,7	261,7	261,7	861,6	295,7	295,7	97,7	198,0	97,7	198,0	97,7	97,7	212,3	10162,4	754,2
Mass Flows	kg/hr	1703,3	10970,9	9080,5	13593,7	212505,4	212505,4	24649,9	187596,0	14625,9	10611,7	14985,1	212505,4	259,4	212505,4	10970,9	10970,9	15569,4	12216,6	12216,6	3136,1	9080,5	3136,1	9080,5	3136,1	3136,1	9008,2	197520,3	13593,7
GLUCOSE	kg/hr	0,0	0,0	0,0	0,0	1324,2	1324,2	0,0	1324,2	0,0	0,0	0,0	1324,2	0,0	1324,2	0,0	0,0	0,0	0,0	0,0	0,0	0,0	0,0	0,0	0,0	0,0	0,0	1324,2	0,0
CELLULOS	kg/hr	0,0	0,0	0,0	0,0	1566,2	1566,2	0,0	1566,2	0,0	0,0	0,0	1566,2	0,0	1566,2	0,0	0,0	0,0	0,0	0,0	0,0	0,0	0,0	0,0	0,0	0,0	0,0	1566,2	0,0
XYLOSE	kg/hr	0,0	0,0	0,0	0,0	1007,0	1007,0	0,0	1007,0	0,0	0,0	0,0	1007,0	0,0	1007,0	0,0	0,0	0,0	0,0	0,0	0,0	0,0	0,0	0,0	0,0	0,0	0,0	1007,0	0,0
XYLAN	kg/hr	0,0	0,0	0,0	0,0	606,5	606,5	0,0	606,5	0,0	0,0	0,0	606,5	0,0	606,5	0,0	0,0	0,0	0,0	0,0	0,0	0,0	0,0	0,0	0,0	0,0	0,0	606,5	0,0
BIOMASS	kg/hr	0,0	0,0	0,0	0,0	521,5	521,5	0,0	521,5	0,0	0,0	0,0	521,5	0,0	521,5	0,0	0,0	0,0	0,0	0,0	0,0	0,0	0,0	0,0	0,0	0,0	0,0	521,5	0,0
MICROORG	kg/hr	0,0	0,0	0,0	0,0	131,0	131,0	0,0	131,0	0,0	0,0	0,0	131,0	0,0	131,0	0,0	0,0	0,0	0,0	0,0	0,0	0,0	0,0	0,0	0,0	0,0	0,0	131,0	0,0
CELLOB	kg/hr	0,0	0,0	0,0	0,0	0,0	0,0	0,0	0,0	0,0	0,0	0,0	0,0	0,0	0,0	0,0	0,0	0,0	0,0	0,0	0,0	0,0	0,0	0,0	0,0	0,0	0,0	0,0	0,0
EXTRACT	kg/hr	0,0	0,0	0,0	0,0	214,8	214,8	0,0	214,8	0,0	0,0	0,0	214,8	0,0	214,8	0,0	0,0	0,0	0,0	0,0	0,0	0,0	0,0	0,0	0,0	0,0	0,0	214,8	0,0
ASH	kg/hr	0,0	0,0	0,0	0,0	2888,0	2888,0	0,0	2888,0	0,0	0,0	0,0	2888,0	0,0	2888,0	0,0	0,0	0,0	0,0	0,0	0,0	0,0	0,0	0,0	0,0	0,0	0,0	2888,0	0,0
ETHANOL	kg/hr	0,0	204,1	9040,3	0,0	9232,2	9232,2	9118,1	83,9	0,0	0,2	203,9	9232,2	30,2	9232,2	204,1	204,1	77,8	11300,3	11300,3	2260,1	9040,3	2260,1	9040,3	2260,1	2260,1	174,0	9028,3	0,0
WATER	kg/hr	33,3	280,3	4,4	13585,6	191759,7	191759,7	15495,9	176252,9	14625,9	146,4	14759,8	191759,7	10,8	191759,7	280,3	280,3	15491,5	880,4	880,4	876,0	4,4	876,0	4,4	876,0	876,0	236,2	176999,8	13585,6
CO2	kg/hr	1265,7	10081,5	15,2	0,0	233,3	233,3	15,2	0,0	0,0	10061,2	20,2	233,3	218,1	233,3	10081,5	10081,5	0,0	15,2	15,2	0,0	15,2	0,0	15,2	0,0	0,0	8597,6	213,1	0,0
O2	kg/hr	403,7	403,9	0,0	0,0	0,0	0,0	0,0	0,0	0,0	403,8	0,0	0,0	0,0	0,0	403,9	403,9	0,0	0,0	0,0	0,0	0,0	0,0	0,0	0,0	0,0	0,1	0,0	0,0
NH3	kg/hr	0,5	1,1	20,7	0,0	20,9	20,9	20,7	0,0	0,0	0,0	1,1	20,9	0,2	20,9	1,1	1,1	0,0	20,7	20,7	0,0	20,7	0,0	20,7	0,0	0,0	0,3	19,8	0,0
AACID	kg/hr	0,0	0,0	0,0	7,7	2,7	2,7	0,1	2,6	0,0	0,0	0,0	2,7	0,0	2,7	0,0	0,0	0,1	0,0	0,0	0,0	0,0	0,0	0,0	0,0	0,0	0,0	2,7	7,7
H3O+	kg/hr	0,0	0,0	0,0	0,0	0,0	0,0	0,0	0,0	0,0	0,0	0,0	0,0	0,0	0,0	0,0	0,0	0,0	0,0	0,0	0,0	0,0	0,0	0,0	0,0	0,0	0,0	0,0	0,0
OH-	kg/hr	0,0	0,0	0,0	0,0	0,0	0,0	0,0	0,0	0,0	0,0	0,0	0,0	0,0	0,0	0,0	0,0	0,0	0,0	0,0	0,0	0,0	0,0	0,0	0,0	0,0	0,0	0,0	0,0
FURF	kg/hr	0,0	0,0	0,0	0,4	0,5	0,5	0,0	0,5	0,0	0,0	0,0	0,5	0,0	0,5	0,0	0,0	0,0	0,0	0,0	0,0	0,0	0,0	0,0	0,0	0,0	0,0	0,5	0,4
SODIU-01	kg/hr	0,0	0,0	0,0	0,0	134,3	134,3	0,0	134,3	0,0	0,0	0,0	134,3	0,0	134,3	0,0	0,0	0,0	0,0	0,0	0,0	0,0	0,0	0,0	0,0	0,0	0,0	134,3	0,0
KH2PO4	kg/hr	0,0	0,0	0,0	0,0	9,7	9,7	0,0	9,7	0,0	0,0	0,0	9,7	0,0	9,7	0,0	0,0	0,0	0,0	0,0	0,0	0,0	0,0	0,0	0,0	0,0	0,0	9,7	0,0
MGSO4-01	kg/hr	0,0	0,0	0,0	0,0	8,1	8,1	0,0	8,1	0,0	0,0	0,0	8,1	0,0	8,1	0,0	0,0	0,0	0,0	0,0	0,0	0,0	0,0	0,0	0,0	0,0	0,0	8,1	0,0
DIAMM-01	kg/hr	0,0	0,0	0,0	0,0	39,8	39,8	0,0	39,8	0,0	0,0	0,0	39,8	0,0	39,8	0,0	0,0	0,0	0,0	0,0	0,0	0,0	0,0	0,0	0,0	0,0	0,0	39,8	0,0
LIG	kg/hr	0,0	0,0	0,0	0,0	2805,0	2805,0	0,0	2805,0	0,0	0,0	0,0	2805,0	0,0	2805,0	0,0	0,0	0,0	0,0	0,0	0,0	0,0	0,0	0,0	0,0	0,0	0,0	2805,0	0,0

Heat

Stream Name	Q400H	QHT	QPH	S5	S8	S11
QCALC kW	20405,2	20405,2	-8188,9	9543,5	-11356,9	-11356,9
TBEGIN C			76,2	129,7		
TEND C			110,0	50,0		

Work

Stream Name	S13	W400T
POWER kW	273,80	273,80

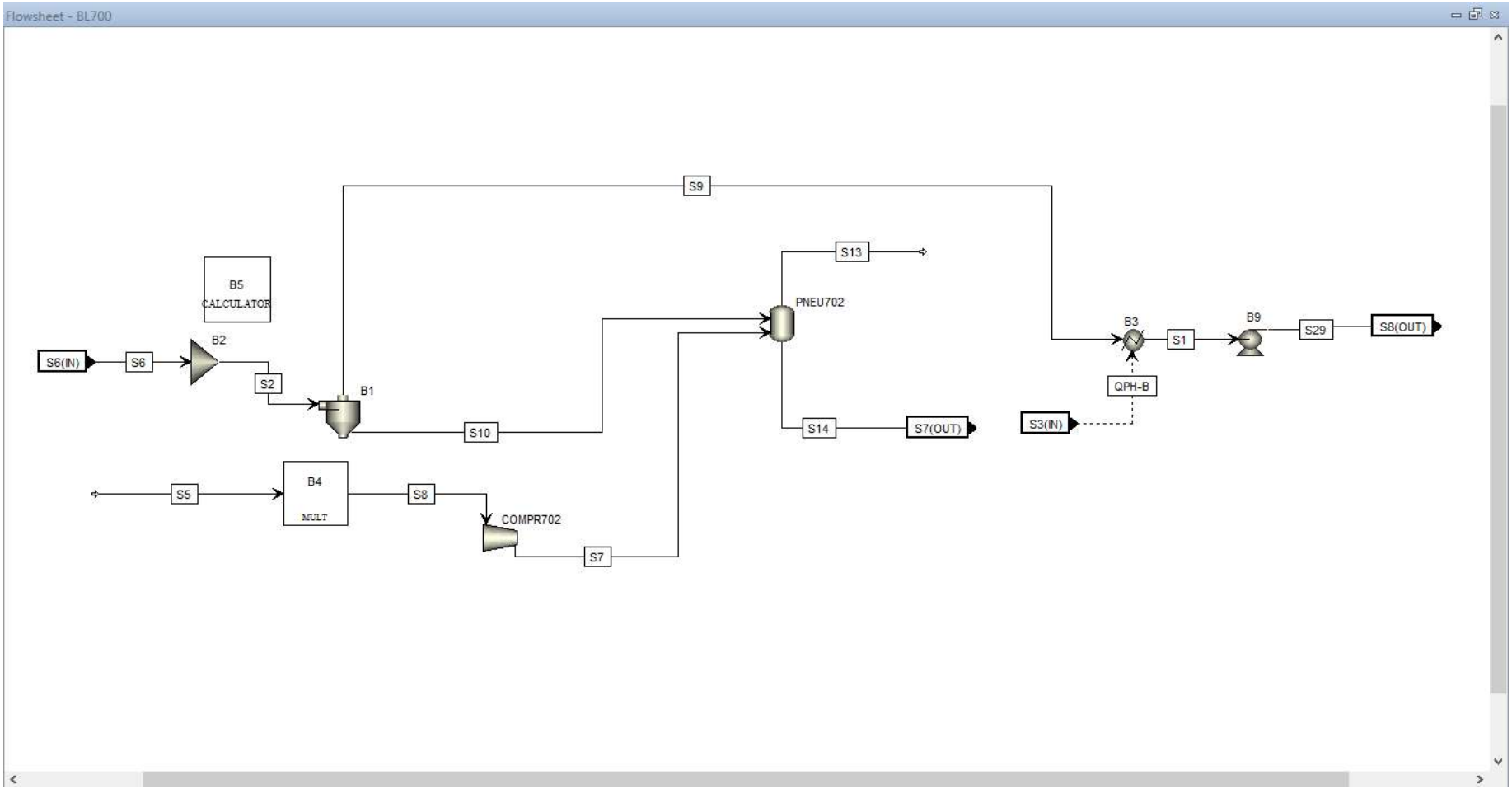

Fig C-6: Flowsheet for biosolids recovery plant (Pneumapress filtration system to remove water from lignin-rich distillery sludge from BL400) (BL700)

TABLE C.7.: Summary of mass and energy balance results around bio-solids (lignin) recovery plant (BL700)

Material

Stream Name	Units	S1	S2	S5	S6	S7	S8	S9	S10	S13	S14	S29
Description												
From		B3	B2			COMPR702	B4	B1	B1	PNEU702	PNEU702	B9
To		B9	B1	B4	B2	PNEU702	COMPR702	B3	PNEU702			
Stream Class		MIXCISLD	MIXCISLD	MIXCISLD	MIXCISLD	MIXCISLD	MIXCISLD	MIXCISLD	MIXCISLD	MIXCISLD	MIXCISLD	MIXCISLD
Total Stream												
Temperature	C	98,7	125,0	25,0	125,0	373,4	25,0	125,0	125,0	83,3	83,3	98,7
Pressure	atm	1,0	2,3	1,0	2,3	9,5	1,0	2,3	2,3	1,0	1,0	3,0
Molar Vapor Fraction		0,0	0,0	1,0	0,0	1,0	1,0	0,0	0,0	1,0	0,0	0,0
Molar Liquid Fraction		1,0	1,0	0,0	1,0	0,0	0,0	1,0	0,8	0,0	0,8	1,0
Molar Solid Fraction		0,0	0,0	0,0	0,0	0,0	0,0	0,0	0,2	0,0	0,2	0,0
Mass Vapor Fraction		0,0	0,0	1,0	0,0	1,0	1,0	0,0	0,0	1,0	0,0	0,0
Mass Liquid Fraction		1,0	0,9	0,0	1,0	0,0	0,0	1,0	0,5	0,0	0,5	1,0
Mass Solid Fraction		0,0	0,0	0,0	0,0	0,0	0,0	0,0	0,5	0,0	0,5	0,0
Molar Enthalpy	cal/mol	-6,77E+04	-6,80E+04	-1,63E+00	-6,80E+04	2,48E+03	-1,63E+00	-6,69E+04	-8,69E+04	-3,04E+04	-9,13E+04	-6,77E+04
Mass Enthalpy	kcal/kg	-3697,0	-3597,4	-0,1	-3597,4	86,1	-0,1	-3655,9	-2978,6	-1319,7	-2950,7	-3696,9
Molar Entropy	cal/mol-K	-36,7	-37,2	1,0	1,02E+27	2,0	1,0	-34,7	-79,2	-2,5	-89,5	-36,7
Mass Entropy	kcal/kg-K	-2,0	-2,0	0,0	5,41E+25	0,1	0,0	-1,9	-2,7	-0,1	-2,9	-2,0
Molar Density	mol/cc	0,1	0,0	0,0	0,0	0,0	0,0	0,0	0,0	0,0	0,0	0,1
Mass Density	gm/cc	1,0	0,0	0,0	0,9	0,0	0,0	0,0	0,1	0,0	1,2	1,0
Enthalpy Flow	kW	-736897,7	-784858,5	0,0	-784858,5	192,0	-0,1	-728708,7	-56149,8	-5052,2	-50905,6	-736884,4
Average MW		18,3	18,9	28,9	18,9	28,9	28,9	18,3	29,2	23,1	30,9	18,3
Mole Flows	kmol/hr	9364,9	9920,8	2,7	9920,8	66,4	66,4	9364,9	555,9	142,7	479,7	9364,9
Mass Flows	kg/hr	171386,8	187596,0	77,6	187596,0	1916,7	1916,7	171386,8	16209,2	3291,7	14834,3	171386,8
GLUCOSE	kg/hr	1264,4	1324,2	0,0	1324,2	0,0	0,0	1264,4	59,8	0,0	59,8	1264,4
CELLULOS	kg/hr	0,0	1566,2	0,0	1566,2	0,0	0,0	0,0	1566,2	0,0	1566,2	0,0
XYLOSE	kg/hr	961,5	1007,0	0,0	1007,0	0,0	0,0	961,5	45,5	0,0	45,5	961,5
XYLAN	kg/hr	0,0	606,5	0,0	606,5	0,0	0,0	0,0	606,5	0,0	606,5	0,0
BIOMASS	kg/hr	0,0	521,5	0,0	521,5	0,0	0,0	0,0	521,5	0,0	521,5	0,0
MICROORG	kg/hr	0,0	131,0	0,0	131,0	0,0	0,0	0,0	131,0	0,0	131,0	0,0
EXTRACT	kg/hr	205,1	214,8	0,0	214,8	0,0	0,0	205,1	9,7	0,0	9,7	205,1
ASH	kg/hr	0,0	2888,0	0,0	2888,0	0,0	0,0	0,0	2888,0	0,0	2888,0	0,0
ETHANOL	kg/hr	80,1	83,9	0,0	83,9	0,0	0,0	80,1	3,8	2,7	1,1	80,1
WATER	kg/hr	168294,6	176252,9	0,0	176252,9	0,0	0,0	168294,6	7958,4	1372,3	6586,1	168294,6
N2	kg/hr	0,0	0,0	59,5	0,0	1470,3	1470,3	0,0	0,0	1470,3	0,0	0,0
CO2	kg/hr	0,0	0,0	0,0	0,0	0,0	0,0	0,0	0,0	0,0	0,0	0,0
O2	kg/hr	0,0	0,0	18,1	0,0	446,4	446,4	0,0	0,0	446,4	0,0	0,0
NH3	kg/hr	0,0	0,0	0,0	0,0	0,0	0,0	0,0	0,0	0,0	0,0	0,0
AACID	kg/hr	2,5	2,6	0,0	2,6	0,0	0,0	2,5	0,1	0,0	0,1	2,5
H3O+	kg/hr	0,0	0,0	0,0	0,0	0,0	0,0	0,0	0,0	0,0	0,0	0,0
OH-	kg/hr	0,0	0,0	0,0	0,0	0,0	0,0	0,0	0,0	0,0	0,0	0,0
FURF	kg/hr	0,5	0,5	0,0	0,5	0,0	0,0	0,5	0,0	0,0	0,0	0,5
SODIU-01	kg/hr	128,2	134,3	0,0	134,3	0,0	0,0	128,2	6,1	0,0	6,1	128,2
KH2PO4	kg/hr	9,2	9,7	0,0	9,7	0,0	0,0	9,2	0,4	0,0	0,4	9,2
MGSO4-01	kg/hr	7,7	8,1	0,0	8,1	0,0	0,0	7,7	0,4	0,0	0,4	7,7
DIAMM-01	kg/hr	38,0	39,8	0,0	39,8	0,0	0,0	38,0	1,8	0,0	1,8	38,0
LIG	kg/hr	395,0	2805,0	0,0	2805,0	0,0	0,0	395,0	2410,0	0,0	2410,0	395,0

Heat

Stream Name	QPH-B
QCALC kW	-8188,9
TBEGIN C	76,2
TEND C	110,0

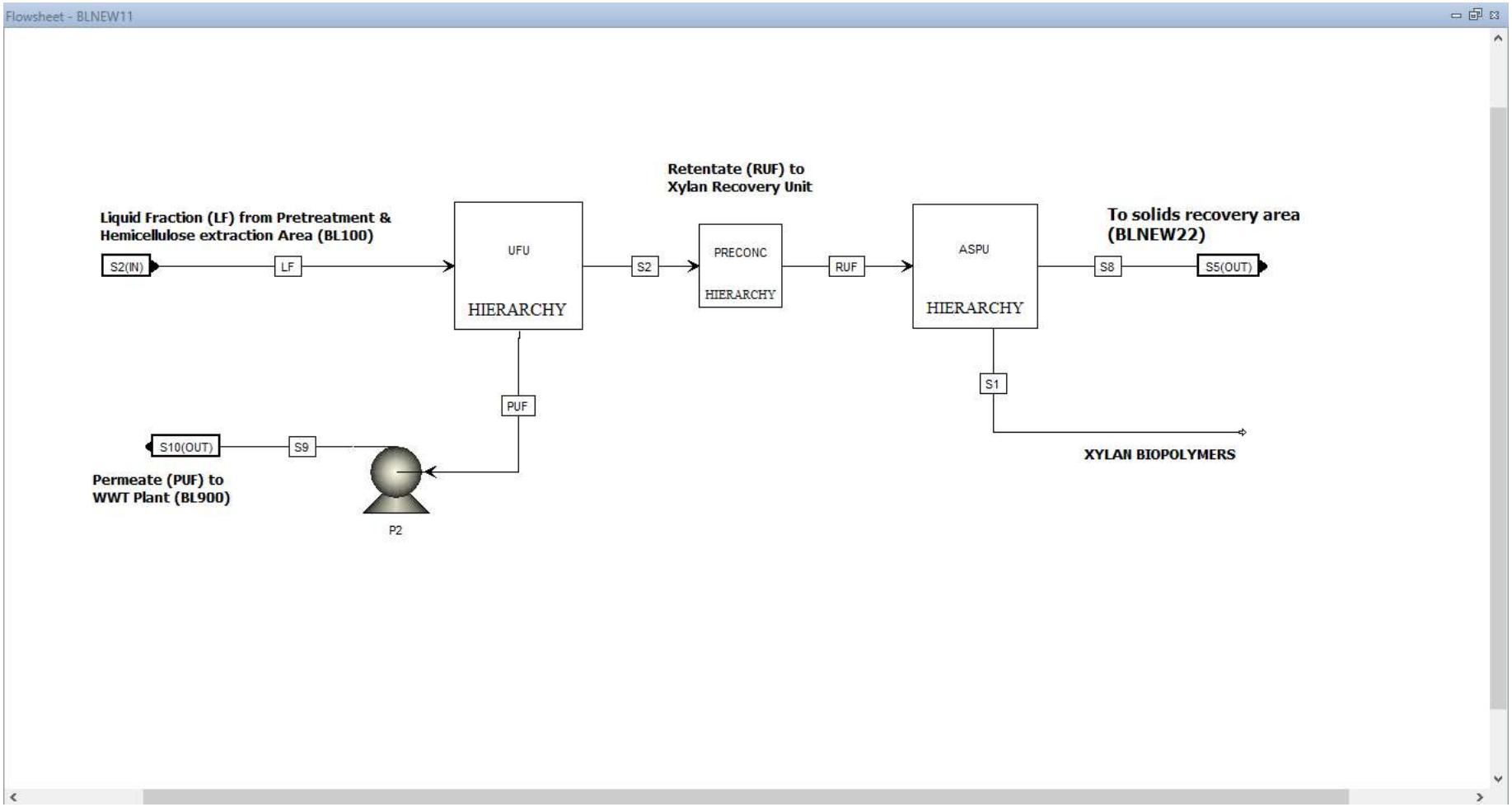

Fig C-7: Flowsheet for xylan recovery plant (BLNEW11)

TABLE C.8.: Summary of mass and energy balance results around xylan recovery plant (BLNEW11)

		Material						
Stream Name	Units	LF	PUF	RUF	S1	S2	S8	S9
Description								
From			UFU	PRECONC	ASPU	UFU	ASPU	P2
To		UFU	P2	ASPU		PRECONC		
Stream Class		MIXCISLD	MIXCISLD	MIXCISLD	MIXCISLD	MIXCISLD	MIXCISLD	MIXCISLD
Total Stream								
Temperature	C	76,5	55,0	49,5	84,8	57,3	90,5	55,0
Pressure	atm	1,0	6,0	0,1	1,1	6,0	1,0	3,0
Molar Vapor Fraction		0,0	0,0	0,0	0,0	0,0	0,0	0,0
Molar Liquid Fraction		1,0	1,0	1,0	0,2	1,0	0,9	1,0
Molar Solid Fraction		0,0	0,0	0,0	0,8	0,0	0,1	0,0
Mass Vapor Fraction		0,0	0,0	0,0	0,0	0,0	0,0	0,0
Mass Liquid Fraction		1,0	1,0	0,8	0,1	0,9	0,8	1,0
Mass Solid Fraction		0,0	0,0	0,2	0,9	0,1	0,2	0,0
Molar Enthalpy	cal/mol	-76094,3	-73406,4	-109162,8	-184199,1	-79763,2	-102157,6	-73407,4
Mass Enthalpy	kcal/kg	-3774,6	-3928,1	-3574,9	-1621,9	-3679,5	-3975,4	-3928,2
Molar Entropy	cal/mol-K	-62,3	-52,2	-177,9	-125,9	-77,5	-142,6	-52,1
Mass Entropy	kcal/kg-K	-3,1	-2,8	-5,8	-1,1	-3,6	-5,5	-2,8
Molar Density	mol/cc	0,1	0,1	0,0	0,0	0,0	0,0	0,1
Mass Density	gm/cc	1,0	1,0	1,1	1,3	1,0	1,0	1,0
Enthalpy Flow	kW	-571674,6	-280014,5	-118023,6	-10384,9	-294975,1	-99905,6	-280018,3
Average MW		20,2	18,7	30,5	113,6	21,7	25,7	18,7
Mole Flows	kmol/hr	6459,8	3279,9	929,6	48,5	3179,8	840,9	3279,9
Mass Flows	kg/hr	130225,6	61293,5	28387,3	5505,7	68932,1	21608,6	61293,5
GLUCOSE	kg/hr	426,7	218,2	208,6	10,2	208,6	198,3	218,2
CELLULOS	kg/hr	0,0	0,0	0,0	0,0	0,0	0,0	0,0
XYLOSE	kg/hr	5566,9	0,0	5566,9	0,0	5566,9	0,0	0,0
XYLAN	kg/hr	0,0	0,0	0,0	4898,9	0,0	0,0	0,0
CELLOB	kg/hr	405,4	207,3	198,1	9,7	198,1	188,4	207,3
EXTRACT	kg/hr	2825,2	1444,4	1380,8	67,8	1380,8	1313,0	1444,4
WATER	kg/hr	113752,6	58499,3	14718,6	93,2	55253,3	13822,5	58499,3
AACID	kg/hr	35,5	18,2	7,7	0,4	17,4	7,3	18,2
H3O+	kg/hr	0,0	0,0	0,0	0,0	0,0	0,0	0,0
OH-	kg/hr	0,0	0,0	0,0	0,0	0,0	0,0	0,0
FURF	kg/hr	6,6	3,4	2,7	0,1	3,2	2,6	3,4
SODIU-01	kg/hr	1765,7	902,8	863,0	42,4	863,0	820,6	902,8
LIG	kg/hr	5441,0	0,0	5441,0	267,2	5441,0	5173,8	0,0

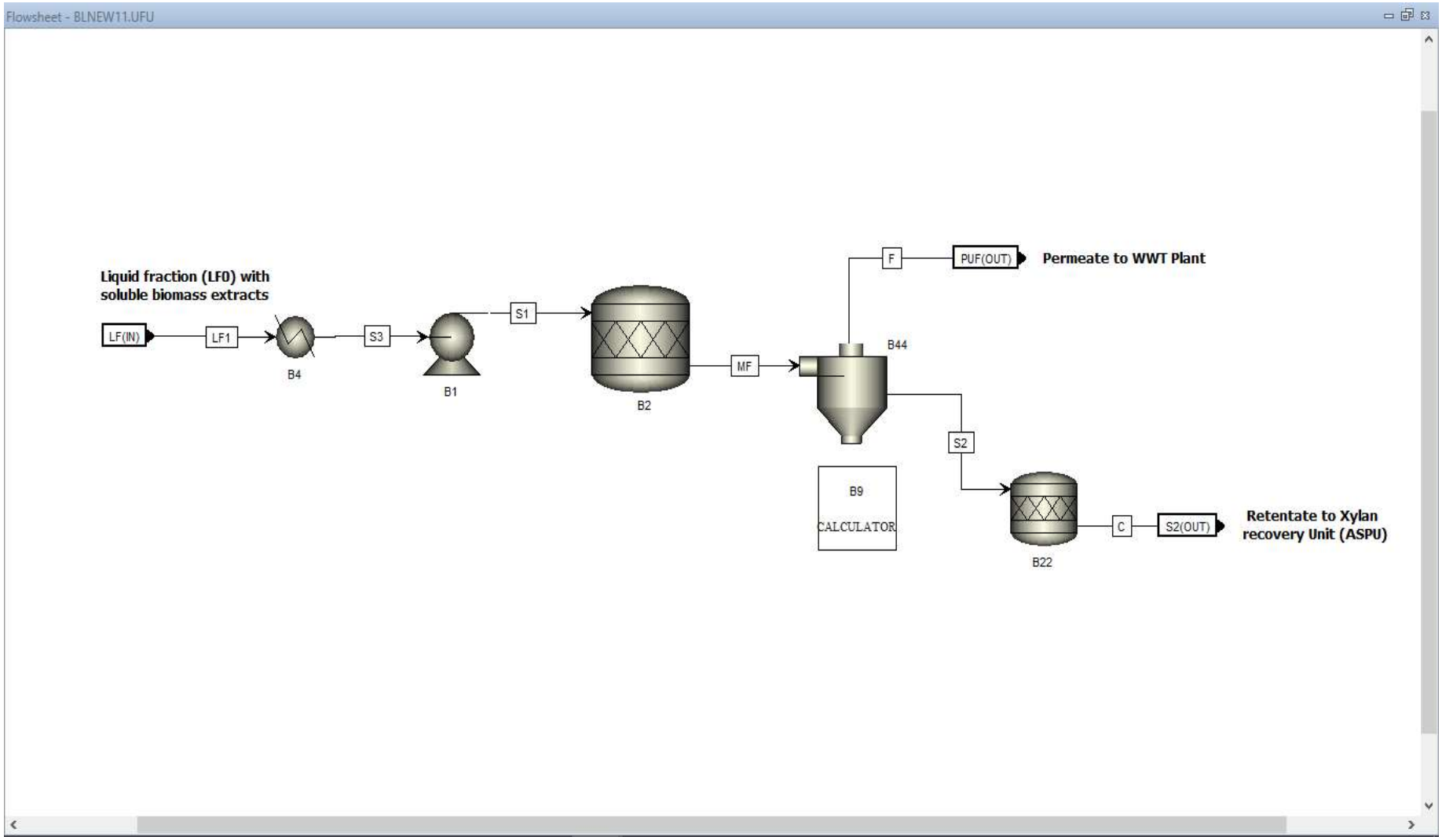

Fig C.7-1: Flowsheet for the ultrafiltration unit of xylan recovery plant (BLNEW11.UFU)

TABLE C.8-1.: Summary of mass and energy balance results around ultrafiltration unit of xylan recovery plant (BLNEW11.UFU)

		Material						
Stream Name	Units	C	F	LF1	MF	S1	S2	S3
Description								
From		B22	B44		B2	B1	B44	B4
To				B4	B44	B2	B22	B1
Stream Class		MIXCISLD	MIXCISLD	MIXCISLD	MIXCISLD	MIXCISLD	MIXCISLD	MIXCISLD
Total Stream								
Temperature	C	57,3	55,0	76,5	55,0	55,1	55,0	55,0
Pressure	atm	6,0	6,0	1,0	6,0	6,0	6,0	1,0
Molar Vapor Fraction		0,0	0,0	0,0	0,0	0,0	0,0	0,0
Molar Liquid Fraction		1,0	1,0	1,0	1,0	1,0	1,0	1,0
Molar Solid Fraction		0,0	0,0	0,0	0,0	0,0	0,0	0,0
Mass Vapor Fraction		0,0	0,0	0,0	0,0	0,0	0,0	0,0
Mass Liquid Fraction		0,9	1,0	1,0	0,9	1,0	0,9	1,0
Mass Solid Fraction		0,1	0,0	0,0	0,1	0,0	0,2	0,0
Molar Enthalpy	cal/mol	-79763,2	-73406,4	-76094,3	-76098,7	-76560,5	-78843,8	-76563,7
Mass Enthalpy	kcal/kg	-3679,5	-3928,1	-3774,6	-3796,5	-3797,7	-3679,5	-3797,9
Molar Entropy	cal/mol-K	-77,5	-52,2	-62,3	-60,3	-64,7	-68,7	-64,7
Mass Entropy	kcal/kg-K	-3,6	-2,8	-3,1	-3,0	-3,2	-3,2	-3,2
Molar Density	mol/cc	0,0	0,1	0,1	0,1	0,1	0,0	0,1
Mass Density	gm/cc	1,0	1,0	1,0	1,0	1,0	1,0	1,0
Enthalpy Flow	kW	-294975,1	-280014,5	-571674,6	-574989,5	-575177,3	-294975,1	-575201,2
Average MW		21,7	18,7	20,2	20,0	20,2	21,4	20,2
Mole Flows	kmol/hr	3179,8	3279,9	6459,8	6496,9	6459,8	3216,9	6459,8
Mass Flows	kg/hr	68932,1	61293,5	130225,6	130225,6	130225,6	68932,1	130225,6
GLUCOSE	kg/hr	208,6	218,2	426,7	426,7	426,7	208,6	426,7
CELLULOS	kg/hr	0,0	0,0	0,0	0,0	0,0	0,0	0,0
XYLOSE	kg/hr	5566,9	0,0	5566,9	0,0	5566,9	0,0	5566,9
XYLAN	kg/hr	0,0	0,0	0,0	4898,9	0,0	4898,9	0,0
CELLOB	kg/hr	198,1	207,3	405,4	405,4	405,4	198,1	405,4
EXTRACT	kg/hr	1380,8	1444,4	2825,2	2825,2	2825,2	1380,8	2825,2
WATER	kg/hr	55253,3	58499,3	113752,6	114420,6	113752,6	55921,3	113752,6
AACID	kg/hr	17,4	18,2	35,5	35,5	35,5	17,4	35,5
H3O+	kg/hr	0,0	0,0	0,0	0,0	0,0	0,0	0,0
OH-	kg/hr	0,0	0,0	0,0	0,0	0,0	0,0	0,0
FURF	kg/hr	3,2	3,4	6,6	6,6	6,6	3,2	6,6
SODIU-01	kg/hr	863,0	902,8	1765,7	1765,7	1765,7	863,0	1765,7
LIG	kg/hr	5441,0	0,0	5441,0	5441,0	5441,0	5441,0	5441,0

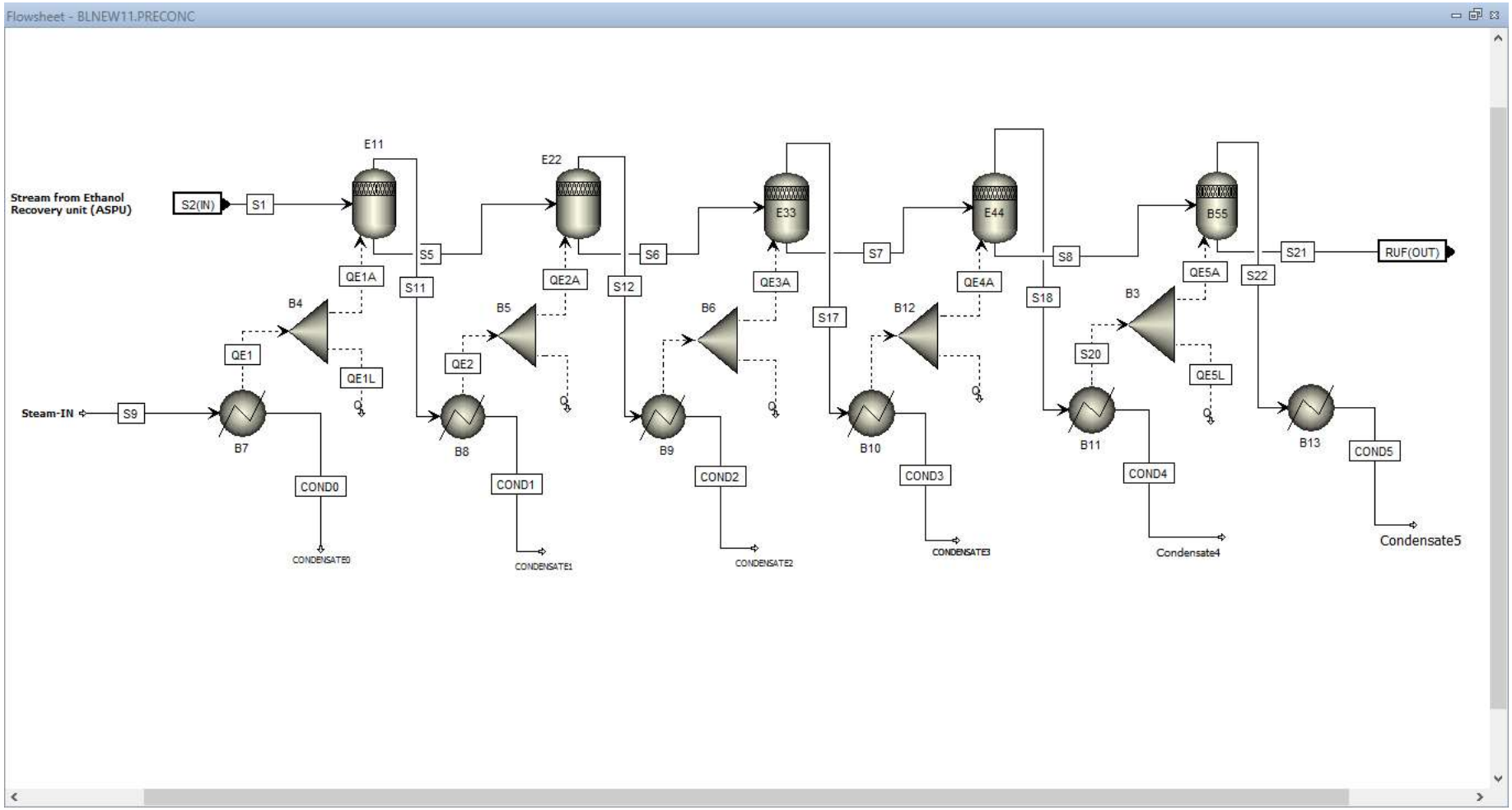

Fig C.7-2: Flowsheet for the evaporation (concentration) unit of the xylan recovery plant (BLNEW11.preconc)

TABLE C.8-2: Summary of mass and energy balance results around evaporation (concentration) unit of the xylan recovery plant (BLNEW11.preconc)

Material

Stream Name	Units	COND0	COND1	COND2	COND3	COND4	COND5	S1	S5	S6	S7	S8	S9	S11	S12	S17	S18	S21	S22
Description																			
From		B7	B8	B9	B10	B11	B13		E11	E22	E33	E44		E11	E22	E33	E44	B55	B55
To								E11	E22	E33	E44	B55	B7	B8	B9	B10	B11		B13
Stream Class		MIXCISLD	MIXCISLD	MIXCISLD	MIXCISLD	MIXCISLD	MIXCISLD	MIXCISLD	MIXCISLD	MIXCISLD	MIXCISLD	MIXCISLD	MIXCISLD	MIXCISLD	MIXCISLD	MIXCISLD	MIXCISLD	MIXCISLD	MIXCISLD
Total Stream																			
Temperature	C	111,0	98,1	91,5	83,1	71,3	49,5	57,3	98,1	91,5	83,1	71,3	111,0	98,1	91,5	83,1	71,3	49,5	49,5
Pressure	atm	1,5	0,9	0,7	0,5	0,3	0,1	6,0	0,9	0,7	0,5	0,3	1,5	0,9	0,7	0,5	0,3	0,1	0,1
Molar Vapor Fraction		0,0	0,0	0,0	0,0	0,0	0,0	0,0	0,0	0,0	0,0	0,0	1,0	1,0	1,0	1,0	1,0	0,0	1,0
Molar Liquid Fraction		1,0	1,0	1,0	1,0	1,0	1,0	1,0	1,0	1,0	1,0	1,0	0,0	0,0	0,0	0,0	0,0	1,0	0,0
Molar Solid Fraction		0,0	0,0	0,0	0,0	0,0	0,0	0,0	0,0	0,0	0,0	0,0	0,0	0,0	0,0	0,0	0,0	0,0	0,0
Mass Vapor Fraction		0,0	0,0	0,0	0,0	0,0	0,0	0,0	0,0	0,0	0,0	0,0	1,0	1,0	1,0	1,0	1,0	0,0	1,0
Mass Liquid Fraction		1,0	1,0	1,0	1,0	1,0	1,0	0,9	0,9	0,9	0,9	0,9	0,0	0,0	0,0	0,0	0,0	0,8	0,0
Mass Solid Fraction		0,0	0,0	0,0	0,0	0,0	0,0	0,1	0,1	0,1	0,1	0,1	0,0	0,0	0,0	0,0	0,0	0,2	0,0
Molar Enthalpy	cal/mol	-66759,6	-66996,0	-67116,3	-67268,6	-67481,9	-67875,5	-79763,2	-80366,3	-82753,3	-86460,9	-93079,7	-57122,7	-57223,6	-57275,3	-57341,2	-57434,6	-109162,8	-57608,9
Mass Enthalpy	kcal/kg	-3705,7	-3718,3	-3725,0	-3733,4	-3745,1	-3766,8	-3679,5	-3627,6	-3622,9	-3614,9	-3600,9	-3170,8	-3176,0	-3178,8	-3182,4	-3187,5	-3574,9	-3197,0
Molar Entropy	cal/mol-K	-34,4	-35,0	-35,3	-35,8	-36,4	-37,6	-77,5	-78,0	-85,9	-98,4	-121,1	-9,3	-8,7	-8,3	-7,8	-7,1	-177,9	-5,6
Mass Entropy	kcal/kg-K	-1,9	-1,9	-2,0	-2,0	-2,0	-2,1	-3,6	-3,5	-3,8	-4,1	-4,7	-0,5	-0,5	-0,5	-0,4	-0,4	-5,8	-0,3
Molar Density	mol/cc	0,1	0,1	0,1	0,1	0,1	0,1	0,0	0,0	0,0	0,0	0,0	0,0	0,0	0,0	0,0	0,0	0,0	0,0
Mass Density	gm/cc	0,9	1,0	1,0	1,0	1,0	1,0	1,0	1,0	1,0	1,1	1,1	0,0	0,0	0,0	0,0	0,0	1,1	0,0
Enthalpy Flow	kW	-53871,9	-28518,2	-31316,0	-34427,3	-38172,1	-43932,2	-294975,1	-262995,7	-232194,9	-198348,3	-160880,5	-46095,4	-24358,4	-26724,3	-29346,6	-32488,7	-118023,6	-37287,2
Average MW		18,0	18,0	18,0	18,0	18,0	18,0	21,7	22,2	22,8	23,9	25,8	18,0	18,0	18,0	18,0	18,0	30,5	18,0
Mole Flows	kmol/hr	693,9	366,0	401,2	440,1	486,4	556,5	3179,8	2813,8	2412,6	1972,6	1486,2	693,9	366,0	401,2	440,1	486,4	929,6	556,5
Mass Flows	kg/hr	12500,0	6594,7	7228,8	7929,1	8764,0	10028,4	68932,1	62337,5	55108,7	47179,6	38415,7	12500,0	6594,7	7228,8	7929,1	8764,0	28387,3	10028,4
GLUCOSE	kg/hr	0,0	0,0	0,0	0,0	0,0	0,0	208,6	208,6	208,6	208,6	208,6	0,0	0,0	0,0	0,0	0,0	208,6	0,0
CELLULOS	kg/hr	0,0	0,0	0,0	0,0	0,0	0,0	0,0	0,0	0,0	0,0	0,0	0,0	0,0	0,0	0,0	0,0	0,0	0,0
XYLOSE	kg/hr	0,0	0,0	0,0	0,0	0,0	0,0	5566,9	5566,9	5566,9	5566,9	5566,9	0,0	0,0	0,0	0,0	0,0	5566,9	0,0
XYLAN	kg/hr	0,0	0,0	0,0	0,0	0,0	0,0	0,0	0,0	0,0	0,0	0,0	0,0	0,0	0,0	0,0	0,0	0,0	0,0
CELLOB	kg/hr	0,0	0,0	0,0	0,0	0,0	0,0	198,1	198,1	198,1	198,1	198,1	0,0	0,0	0,0	0,0	0,0	198,1	0,0
EXTRACT	kg/hr	0,0	0,0	0,0	0,0	0,0	0,0	1380,8	1380,8	1380,8	1380,8	1380,8	0,0	0,0	0,0	0,0	0,0	1380,8	0,0
WATER	kg/hr	12500,0	6593,4	7227,2	7927,2	8761,7	10025,1	55253,3	48659,9	41432,7	33505,4	24743,7	12500,0	6593,4	7227,2	7927,2	8761,7	14718,6	10025,1
AACID	kg/hr	0,0	1,2	1,4	1,7	2,2	3,1	17,4	16,1	14,7	13,0	10,8	0,0	1,2	1,4	1,7	2,2	7,7	3,1
H3O+	kg/hr	0,0	0,0	0,0	0,0	0,0	0,0	0,0	0,0	0,0	0,0	0,0	0,0	0,0	0,0	0,0	0,0	0,0	0,0
OH-	kg/hr	0,0	0,0	0,0	0,0	0,0	0,0	0,0	0,0	0,0	0,0	0,0	0,0	0,0	0,0	0,0	0,0	0,0	0,0
FURF	kg/hr	0,0	0,1	0,1	0,1	0,1	0,2	3,2	3,2	3,1	3,0	2,9	0,0	0,1	0,1	0,1	0,1	2,7	0,2
SODIU-01	kg/hr	0,0	0,0	0,0	0,0	0,0	0,0	863,0	863,0	863,0	863,0	863,0	0,0	0,0	0,0	0,0	0,0	863,0	0,0
LIG	kg/hr	0,0	0,0	0,0	0,0	0,0	0,0	5441,0	5441,0	5441,0	5441,0	5441,0	0,0	0,0	0,0	0,0	0,0	5441,0	0,0

Heat

Stream Name	QE1	QE1A	QE1L	QE2	QE2A	QE2L	QE3	QE3A	QE3L	QE4A	QE4L	QE5A	QE5L	S19	S20
QCALC kW	7776,5	7621,0	155,5	4159,8	4076,6	83,2	4591,8	4499,9	91,8	4979,1	101,6	5569,7	113,7	5080,7	5683,4
TBEGIN C	111,0	111,0	111,0	98,1	98,1	98,1	91,5	91,5	91,5	83,1	83,1	71,3	71,3	83,1	71,3
TEND C	111,0	111,0	111,0	98,1	98,1	98,1	91,5	91,5	91,5	83,1	83,1	71,3	71,3	83,1	71,3

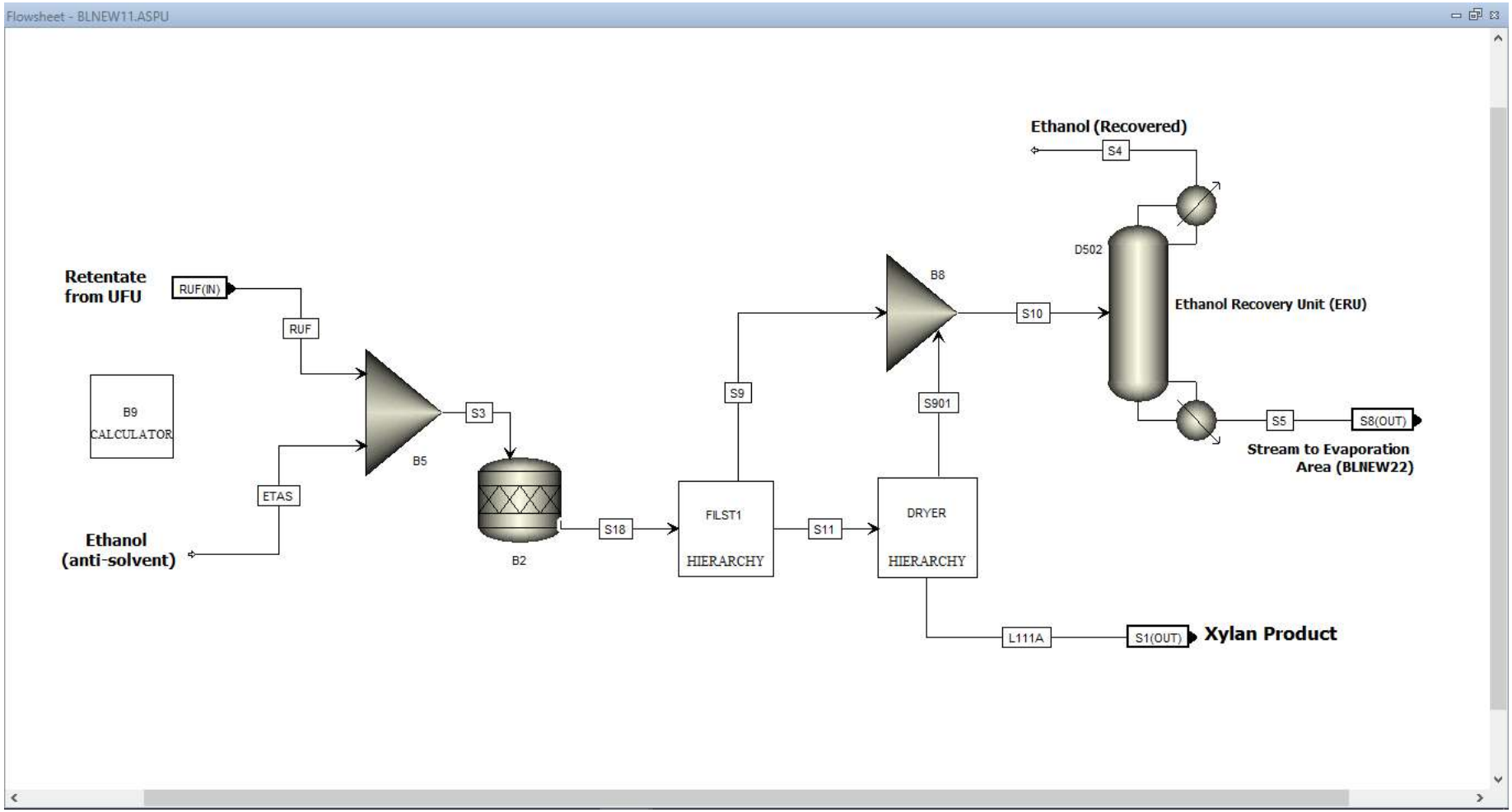

Fig C.7-3: Flowsheet for the anti-solvent precipitation unit (ASPU) of the xylan recovery plant (BLNEW11.ASPU)

TABLE C.8-3: Summary of mass and energy balance results around anti-solvent precipitation unit (ASPU) of the xylan recovery plant (BLNEW11.ASPU)

					Material							
Stream Name	Units	ETAS	L111A	RUF	S3	S4	S5	S9	S10	S11	S18	S901
Description			Retentate from the UF Unit									
From			DRYER		B5	D502	D502	FILST1	B8	FILST1	B2	DRYER
To		B5		B5	B2			B8	D502	DRYER	FILST1	B8
Stream Class		MIXCISLD	MIXCISLD	MIXCISLD	MIXCISLD	MIXCISLD	MIXCISLD	MIXCISLD	MIXCISLD	MIXCISLD	MIXCISLD	MIXCISLD
Total Stream												
Temperature	C	25,0	84,8	49,5	38,9	78,4	90,5	21,8	36,0	21,8	25,0	93,2
Pressure	atm	1,0	1,1	0,1	1,0	1,0	1,0	1,1	1,1	1,1	1,1	1,1
Molar Vapor Fraction		0,0	0,0	0,0	0,0	1,0	0,0	0,0	0,0	0,0	0,0	1,0
Molar Liquid Fraction		1,0	0,2	1,0	1,0	0,0	0,9	1,0	1,0	0,6	0,9	0,0
Molar Solid Fraction		0,0	0,8	0,0	0,0	0,0	0,1	0,0	0,0	0,4	0,1	0,0
Mass Vapor Fraction		0,0	0,0	0,0	0,0	1,0	0,0	0,0	0,0	0,0	0,0	1,0
Mass Liquid Fraction		1,0	0,1	0,8	0,9	0,0	0,8	0,9	0,9	0,3	0,8	0,0
Mass Solid Fraction		0,0	0,9	0,2	0,1	0,0	0,2	0,1	0,1	0,7	0,2	0,0
Molar Enthalpy	cal/mol	-66460,9	-184199,1	-109162,8	-95863,1	-55625,7	-102157,6	-91278,0	-89852,6	-123899,3	-93709,1	-56521,9
Mass Enthalpy	kcal/kg	-1450,7	-1621,9	-3574,9	-2716,2	-1348,5	-3975,4	-2882,6	-2854,1	-1830,3	-2728,0	-2079,1
Molar Entropy	cal/mol-K	-82,3	-125,9	-177,9	-148,8	-42,6	-142,6	-132,1	-125,4	-96,7	-129,5	-21,3
Mass Entropy	kcal/kg-K	-1,8	-1,1	-5,8	-4,2	-1,0	-5,5	-4,2	-4,0	-1,4	-3,8	-0,8
Molar Density	mol/cc	0,0	0,0	0,0	0,0	0,0	0,0	0,0	0,0	0,0	0,0	0,0
Mass Density	gm/cc	0,8	1,3	1,1	0,9	0,0	1,0	0,9	0,9	1,2	0,9	0,0
Enthalpy Flow	kW	-32502,9	-10384,9	-118023,6	-150526,5	-32208,0	-99905,6	-136288,4	-139897,7	-14897,0	-151185,4	-3609,3
Average MW		45,8	113,6	30,5	35,3	41,3	25,7	31,7	31,5	67,7	34,4	27,2
Mole Flows	kmol/hr	420,5	48,5	929,6	1350,1	497,9	840,9	1283,8	1338,8	103,4	1387,2	54,9
Mass Flows	kg/hr	19264,4	5505,7	28387,3	47651,7	20537,4	21608,6	40653,3	42146,0	6998,4	47651,7	1492,7
GLUCOSE	kg/hr	0,0	10,2	208,6	208,6	0,0	198,3	198,3	198,3	10,2	208,6	0,0
CELLULOS	kg/hr	0,0	0,0	0,0	0,0	0,0	0,0	0,0	0,0	0,0	0,0	0,0
XYLOSE	kg/hr	0,0	0,0	5566,9	5566,9	0,0	0,0	0,0	0,0	0,0	0,0	0,0
XYLAN	kg/hr	0,0	4898,9	0,0	0,0	0,0	0,0	0,0	0,0	4898,9	4898,9	0,0
CELLOB	kg/hr	0,0	9,7	198,1	198,1	0,0	188,4	188,4	188,4	9,7	198,1	0,0
EXTRACT	kg/hr	0,0	67,8	1380,8	1380,8	0,0	1313,0	1313,0	1313,0	67,8	1380,8	0,0
ETHANOL	kg/hr	19195,0	115,8	0,0	19195,0	18997,1	82,1	18252,4	19079,3	942,6	19195,0	826,9
WATER	kg/hr	69,4	93,2	14718,6	14788,0	1540,3	13822,5	14697,0	15362,8	759,0	15456,0	665,8
AACID	kg/hr	0,0	0,4	7,7	7,7	0,0	7,3	7,3	7,3	0,4	7,7	0,0
H3O+	kg/hr	0,0	0,0	0,0	0,0	0,0	0,0	0,0	0,0	0,0	0,0	0,0
OH-	kg/hr	0,0	0,0	0,0	0,0	0,0	0,0	0,0	0,0	0,0	0,0	0,0
FURF	kg/hr	0,0	0,1	2,7	2,7	0,0	2,6	2,6	2,6	0,1	2,7	0,0
SODIU-01	kg/hr	0,0	42,4	863,0	863,0	0,0	820,6	820,6	820,6	42,4	863,0	0,0
LIG	kg/hr	0,0	267,2	5441,0	5441,0	0,0	5173,8	5173,8	5173,8	267,2	5441,0	0,0

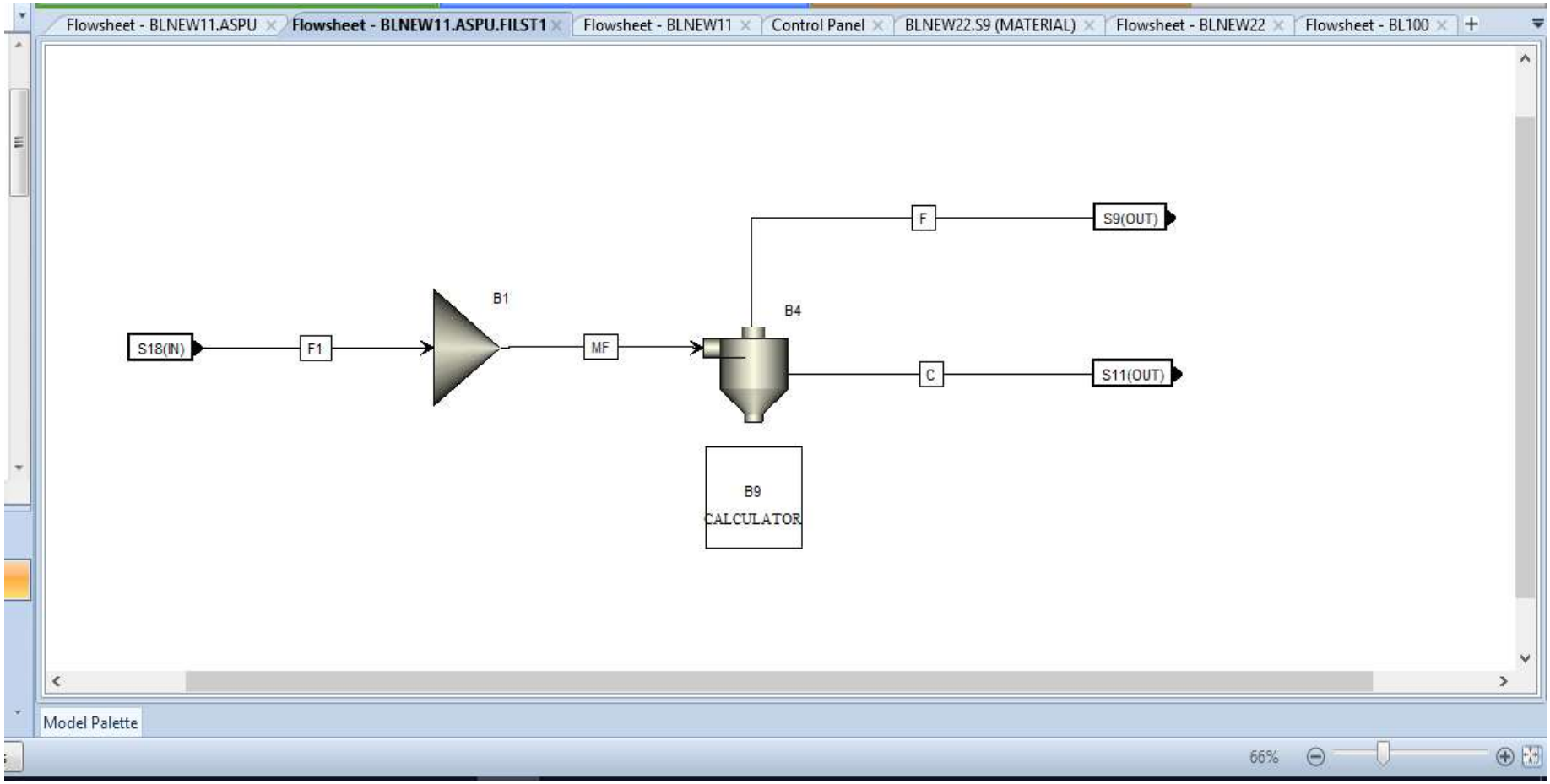

Fig C.7-3.a: Flowsheet for the separation sub-unit within the ASPU unit of the xylan recovery plant (BLNEW11.ASPU.FILST1)

TABLE C.8-3-a: Summary of mass and energy balance results around separation sub-unit within the ASPU unit of the xylan recovery plant (BLNEW11.ASPU.FILST1)

		Material			
Stream Name	Units	C	F	F1	MF
Description					
From		B4	B4		B1
To				B1	B4
Stream Class		MIXCISLD	MIXCISLD	MIXCISLD	MIXCISLD
Total Stream					
Temperature	C	21,8	21,8	25,0	21,8
Pressure	atm	1,1	1,1	1,1	1,1
Molar Vapor Fraction		0,0	0,0	0,0	0,0
Molar Liquid Fraction		0,6	1,0	0,9	0,9
Molar Solid Fraction		0,4	0,0	0,1	0,1
Mass Vapor Fraction		0,0	0,0	0,0	0,0
Mass Liquid Fraction		0,3	0,9	0,8	0,8
Mass Solid Fraction		0,7	0,1	0,2	0,2
Molar Enthalpy	cal/mol	-123899,3	-91278,0	-93709,1	-93709,1
Mass Enthalpy	kcal/kg	-1830,3	-2882,6	-2728,0	-2728,0
Molar Entropy	cal/mol-K	-96,7	-132,1	-129,5	-129,4
Mass Entropy	kcal/kg-K	-1,4	-4,2	-3,8	-3,8
Molar Density	mol/cc	0,0	0,0	0,0	0,0
Mass Density	gm/cc	1,2	0,9	0,9	0,9
Enthalpy Flow	kW	-14897,0	-136288,4	-151185,4	-151185,4
Average MW		67,7	31,7	34,4	34,4
Mole Flows	kmol/hr	103,4	1283,8	1387,2	1387,2
Mass Flows	kg/hr	6998,4	40653,3	47651,7	47651,7
GLUCOSE	kg/hr	10,2	198,3	208,6	208,6
CELLULOS	kg/hr	0,0	0,0	0,0	0,0
XYLOSE	kg/hr	0,0	0,0	0,0	0,0
XYLAN	kg/hr	4898,9	0,0	4898,9	4898,9
CELLOB	kg/hr	9,7	188,4	198,1	198,1
EXTRACT	kg/hr	67,8	1313,0	1380,8	1380,8
ETHANOL	kg/hr	942,6	18252,4	19195,0	19195,0
WATER	kg/hr	759,0	14697,0	15456,0	15456,0
AACID	kg/hr	0,4	7,3	7,7	7,7
H3O+	kg/hr	0,0	0,0	0,0	0,0
OH-	kg/hr	0,0	0,0	0,0	0,0
FURF	kg/hr	0,1	2,6	2,7	2,7
SODIU-01	kg/hr	42,4	820,6	863,0	863,0
LIG	kg/hr	267,2	5173,8	5441,0	5441,0

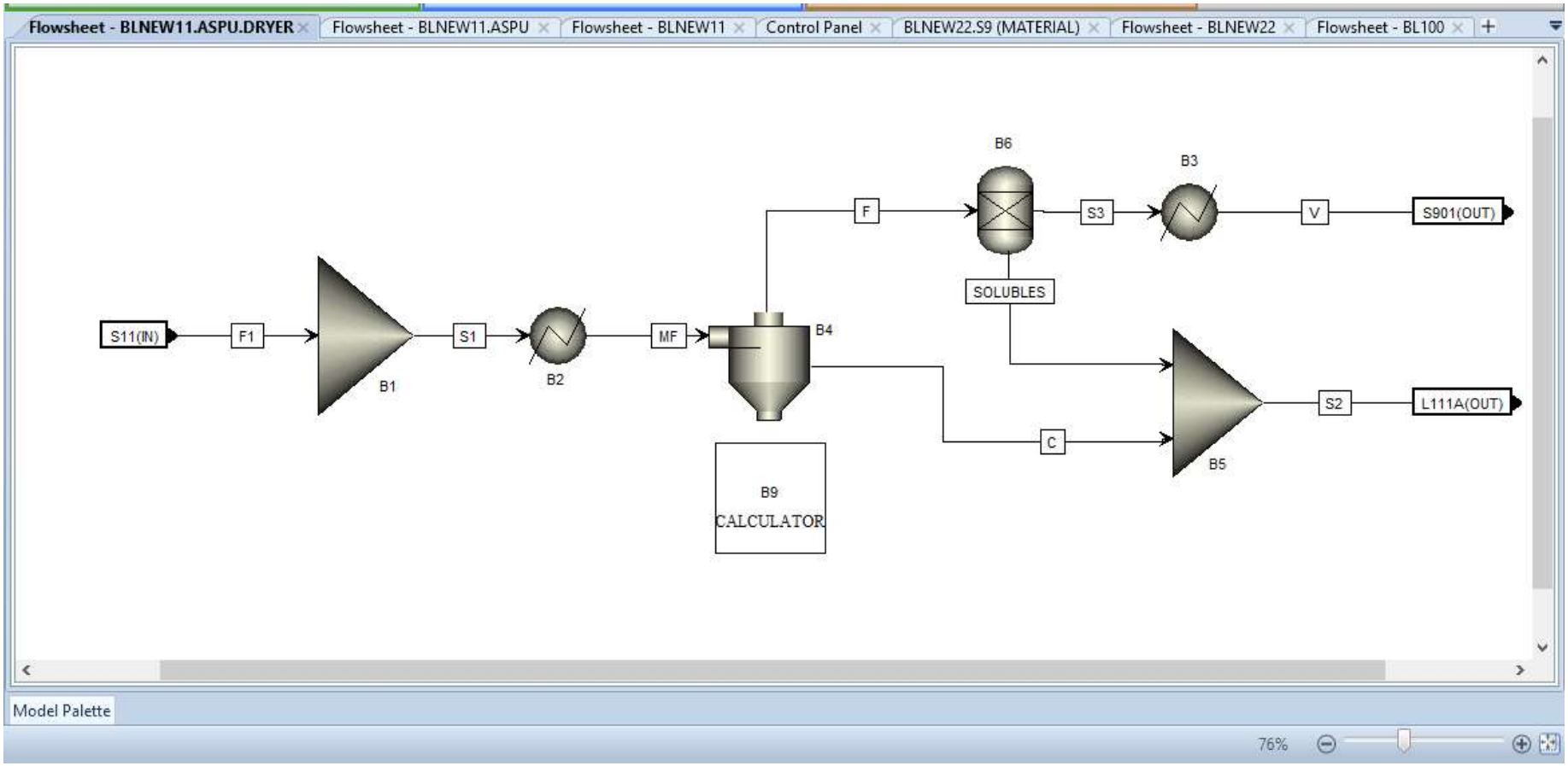

Fig C.7-3.b: Flowsheet for the drying sub-unit within the ASPU unit of the xylan recovery plant (BLNEW11.ASPU.DRYER)

TABLE C.8-3-b: Summary of mass and energy balance results around the drying sub-unit within the ASPU unit of the xylan recovery plant (BLNEW11.ASPU.DRYER)

		Material								
Stream Name	Units	C	F	F1	MF	S1	S2	S3	SOLUBLES	V
Description										
From		B4	B4		B2	B1	B5	B6	B6	B3
To		B5	B6	B1	B4	B2		B3	B5	
Stream Class		MIXCISLD	MIXCISLD	MIXCISLD	MIXCISLD	MIXCISLD	MIXCISLD	MIXCISLD	MIXCISLD	MIXCISLD
Total Stream										
Temperature	C	84,7	84,7	21,8	84,7	21,8	84,8	84,7	84,7	93,2
Pressure	atm	1,1	1,1	1,1	1,1	1,1	1,1	1,1	1,1	1,1
Molar Vapor Fraction		0,0	0,0	0,0	0,0	0,0	0,0	0,2	0,0	1,0
Molar Liquid Fraction		0,2	1,0	0,6	0,6	0,6	0,2	0,8	0,4	0,0
Molar Solid Fraction		0,8	0,0	0,4	0,4	0,4	0,8	0,0	0,6	0,0
Mass Vapor Fraction		0,0	0,0	0,0	0,0	0,0	0,0	0,2	0,0	1,0
Mass Liquid Fraction		0,0	0,9	0,3	0,3	0,3	0,1	0,8	0,3	0,0
Mass Solid Fraction		1,0	0,1	0,7	0,7	0,7	0,9	0,0	0,7	0,0
Molar Enthalpy	cal/mol	-163034,6	-89171,0	-123899,3	-121480,8	-123899,3	-184199,1	-64273,1	-478281,9	-56521,9
Mass Enthalpy	kcal/kg	-1429,8	-2816,1	-1830,3	-1794,6	-1830,3	-1621,9	-2364,2	-4460,1	-2079,1
Molar Entropy	cal/mol-K	-41,2	-118,0	-96,7	-84,4	-96,7	-125,9	-42,7	-1305,8	-21,3
Mass Entropy	kcal/kg-K	-0,4	-3,7	-1,4	-1,2	-1,4	-1,1	-1,6	-12,2	-0,8
Molar Density	mol/cc	0,0	0,0	0,0	0,0	0,0	0,0	0,0	0,0	0,0
Mass Density	gm/cc	1,3	0,5	1,2	0,9	1,2	1,3	0,0	1,2	0,0
Enthalpy Flow	kW	-8574,6	-6031,6	-14897,0	-14606,2	-14897,0	-10384,9	-4104,2	-1810,3	-3609,3
Average MW		114,0	31,7	67,7	67,7	67,7	113,6	27,2	107,2	27,2
Mole Flows	kmol/hr	45,2	58,2	103,4	103,4	103,4	48,5	54,9	3,3	54,9
Mass Flows	kg/hr	5156,7	1841,7	6998,4	6998,4	6998,4	5505,7	1492,7	349,0	1492,7
GLUCOSE	kg/hr	1,3	9,0	10,2	10,2	10,2	10,2	0,0	9,0	0,0
CELLULOS	kg/hr	0,0	0,0	0,0	0,0	0,0	0,0	0,0	0,0	0,0
XYLOSE	kg/hr	0,0	0,0	0,0	0,0	0,0	0,0	0,0	0,0	0,0
XYLAN	kg/hr	4898,9	0,0	4898,9	4898,9	4898,9	4898,9	0,0	0,0	0,0
CELLOB	kg/hr	1,2	8,5	9,7	9,7	9,7	9,7	0,0	8,5	0,0
EXTRACT	kg/hr	8,3	59,5	67,8	67,8	67,8	67,8	0,0	59,5	0,0
ETHANOL	kg/hr	115,8	826,9	942,6	942,6	942,6	115,8	826,9	0,0	826,9
WATER	kg/hr	93,2	665,8	759,0	759,0	759,0	93,2	665,8	0,0	665,8
AACID	kg/hr	0,0	0,3	0,4	0,4	0,4	0,4	0,0	0,3	0,0
H3O+	kg/hr	0,0	0,0	0,0	0,0	0,0	0,0	0,0	0,0	0,0
OH-	kg/hr	0,0	0,0	0,0	0,0	0,0	0,0	0,0	0,0	0,0
FURF	kg/hr	0,0	0,1	0,1	0,1	0,1	0,1	0,0	0,1	0,0
SODIU-01	kg/hr	5,2	37,2	42,4	42,4	42,4	42,4	0,0	37,2	0,0
LIG	kg/hr	32,8	234,4	267,2	267,2	267,2	267,2	0,0	234,4	0,0

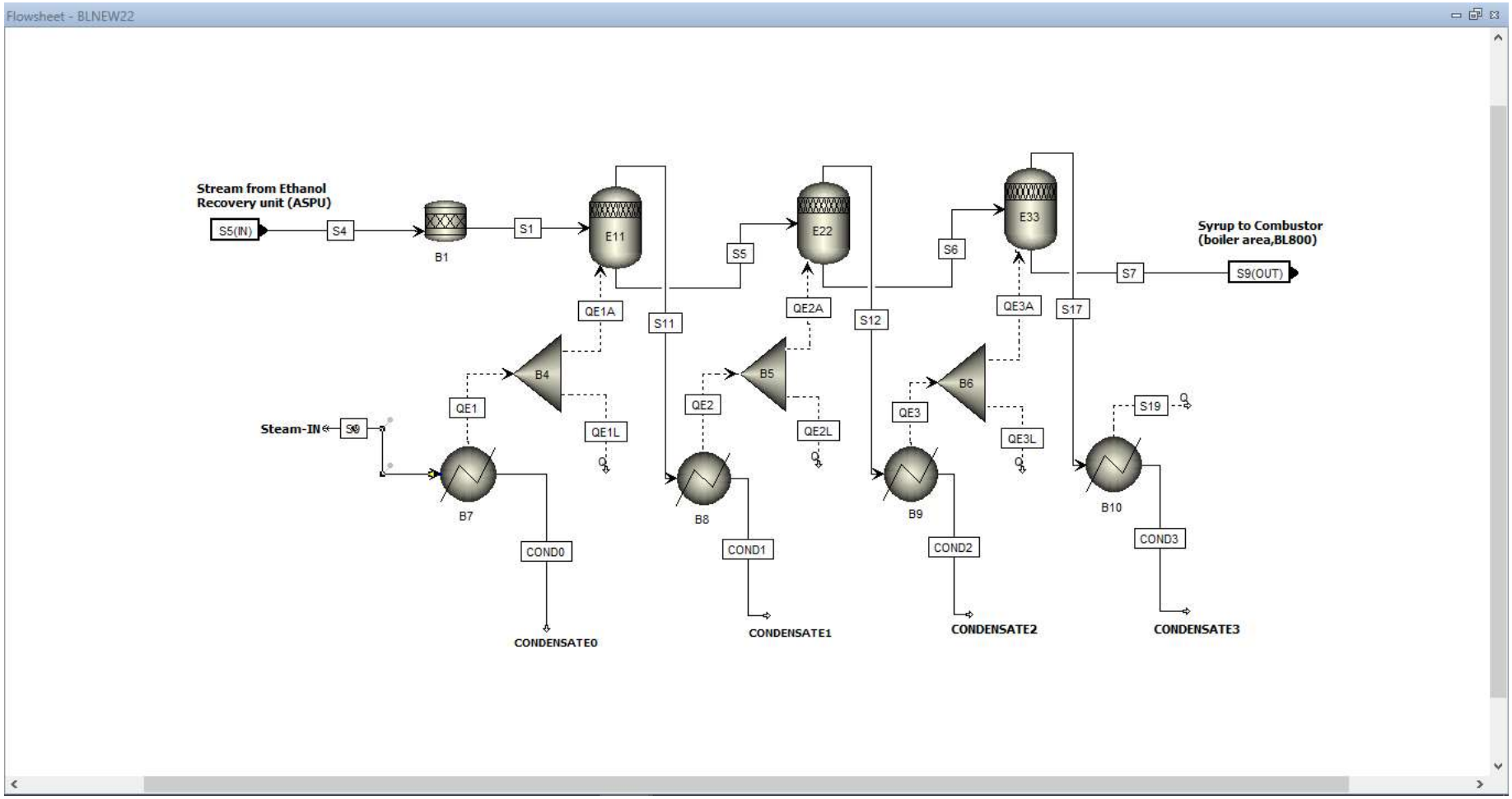

Fig C-8: the evaporation plant for recovery of biosolids (BLNEW22)

TABLE C.9: Summary of mass and energy balance results around the evaporation plant for recovery of biosolids (BLNEW22)

Material

Stream Name	Units	COND0	COND1	COND2	COND3	S1	S4	S5	S6	S7	S9	S11	S12	S17
Description														
From		B7	B8	B9	B10	B1		E11	E22	E33		E11	E22	E33
To						E11	B1	E22	E33		B7	B8	B9	B10
Stream Class		MIXCISLD	MIXCISLD	MIXCISLD	MIXCISLD	MIXCISLD	MIXCISLD	MIXCISLD	MIXCISLD	MIXCISLD	MIXCISLD	MIXCISLD	MIXCISLD	MIXCISLD
Total Stream														
Temperature	C	111,0	98,6	92,4	85,1	90,5	90,5	98,6	92,4	85,1	111,0	98,6	92,4	85,1
Pressure	atm	1,5	1,0	0,8	0,6	1,0	1,0	0,9	0,7	0,5	1,5	0,9	0,7	0,5
Molar Vapor Fraction		0,0	0,0	0,0	0,0	0,0	0,0	0,0	0,0	0,0	1,0	1,0	1,0	1,0
Molar Liquid Fraction		1,0	1,0	1,0	1,0	0,9	0,9	0,9	0,9	0,9	0,0	0,0	0,0	0,0
Molar Solid Fraction		0,0	0,0	0,0	0,0	0,1	0,1	0,1	0,1	0,1	0,0	0,0	0,0	0,0
Mass Vapor Fraction		0,0	0,0	0,0	0,0	0,0	0,0	0,0	0,0	0,0	1,0	1,0	1,0	1,0
Mass Liquid Fraction		1,0	1,0	1,0	1,0	0,8	0,8	0,7	0,7	0,6	0,0	0,0	0,0	0,0
Mass Solid Fraction		0,0	0,0	0,0	0,0	0,2	0,2	0,3	0,3	0,4	0,0	0,0	0,0	0,0
Molar Enthalpy	cal/mol	-66759,6	-66954,3	-67091,5	-67233,0	-102157,6	-102157,6	-110459,5	-126057,0	-161731,2	-57122,7	-57203,6	-57264,7	-57326,9
Mass Enthalpy	kcal/kg	-3705,7	-3670,7	-3710,4	-3728,0	-3975,4	-3975,4	-4013,1	-4085,3	-4198,2	-3170,8	-3136,1	-3166,9	-3178,7
Molar Entropy	cal/mol-K	-34,4	-35,2	-35,4	-35,7	-142,6	-142,6	-166,7	-215,3	-327,1	-9,3	-8,9	-8,3	-7,8
Mass Entropy	kcal/kg-K	-1,9	-1,9	-2,0	-2,0	-5,5	-5,5	-6,1	-7,0	-8,5	-0,5	-0,5	-0,5	-0,4
Molar Density	mol/cc	0,1	0,1	0,1	0,1	0,0	0,0	0,0	0,0	0,0	0,0	0,0	0,0	0,0
Mass Density	gm/cc	0,9	1,0	1,0	1,0	1,0	1,0	1,0	1,1	1,1	0,0	0,0	0,0	0,0
Enthalpy Flow	kW	-15084,1	-12889,7	-13742,2	-14608,7	-99905,6	-99905,6	-86759,3	-73190,3	-58761,5	-12906,7	-11012,6	-11729,4	-12456,3
Average MW		18,0	18,2	18,1	18,0	25,7	25,7	27,5	30,9	38,5	18,0	18,2	18,1	18,0
Mole Flows	kmol/hr	194,3	165,5	176,1	186,8	840,9	840,9	675,4	499,2	312,4	194,3	165,5	176,1	186,8
Mass Flows	kg/hr	3500,0	3019,3	3184,6	3369,5	21608,6	21608,6	18589,2	15404,6	12035,1	3500,0	3019,3	3184,6	3369,5
GLUCOSE	kg/hr	0,0	0,0	0,0	0,0	198,3	198,3	198,3	198,3	198,3	0,0	0,0	0,0	0,0
CELLULOS	kg/hr	0,0	0,0	0,0	0,0	0,0	0,0	0,0	0,0	0,0	0,0	0,0	0,0	0,0
XYLOSE	kg/hr	0,0	0,0	0,0	0,0	0,0	0,0	0,0	0,0	0,0	0,0	0,0	0,0	0,0
XYLAN	kg/hr	0,0	0,0	0,0	0,0	0,0	0,0	0,0	0,0	0,0	0,0	0,0	0,0	0,0
CELLOB	kg/hr	0,0	0,0	0,0	0,0	188,4	188,4	188,4	188,4	188,4	0,0	0,0	0,0	0,0
EXTRACT	kg/hr	0,0	0,0	0,0	0,0	1313,0	1313,0	1313,0	1313,0	1313,0	0,0	0,0	0,0	0,0
ETHANOL	kg/hr	0,0	59,9	17,8	3,9	82,1	82,1	22,3	4,4	0,6	0,0	59,9	17,8	3,9
WATER	kg/hr	3500,0	2958,4	3165,5	3363,8	13822,5	13822,5	10864,1	7698,6	4334,8	3500,0	2958,4	3165,5	3363,8
AACID	kg/hr	0,0	1,0	1,2	1,6	7,3	7,3	6,4	5,2	3,6	0,0	1,0	1,2	1,6
H3O+	kg/hr	0,0	0,0	0,0	0,0	0,0	0,0	0,0	0,0	0,0	0,0	0,0	0,0	0,0
OH-	kg/hr	0,0	0,0	0,0	0,0	0,0	0,0	0,0	0,0	0,0	0,0	0,0	0,0	0,0
FURF	kg/hr	0,0	0,1	0,1	0,2	2,6	2,6	2,5	2,3	2,1	0,0	0,1	0,1	0,2
SODIU-01	kg/hr	0,0	0,0	0,0	0,0	820,6	820,6	820,6	820,6	820,6	0,0	0,0	0,0	0,0
LIG	kg/hr	0,0	0,0	0,0	0,0	5173,8	5173,8	5173,8	5173,8	5173,8	0,0	0,0	0,0	0,0

Heat

Stream Name	QE1	QE1A	QE1L	QE2	QE2A	QE2L	QE3	QE3A	QE3L	S19
QCALC kW	2177,4	2133,9	43,5	1877,2	1839,6	37,5	2012,8	1972,5	40,3	2152,4
TBEGIN C	111,0	111,0	111,0	98,6	98,6	98,6	92,4	92,4	92,4	85,1
TEND C	111,0	111,0	111,0	98,6	98,6	98,6	92,4	92,4	92,4	85,1

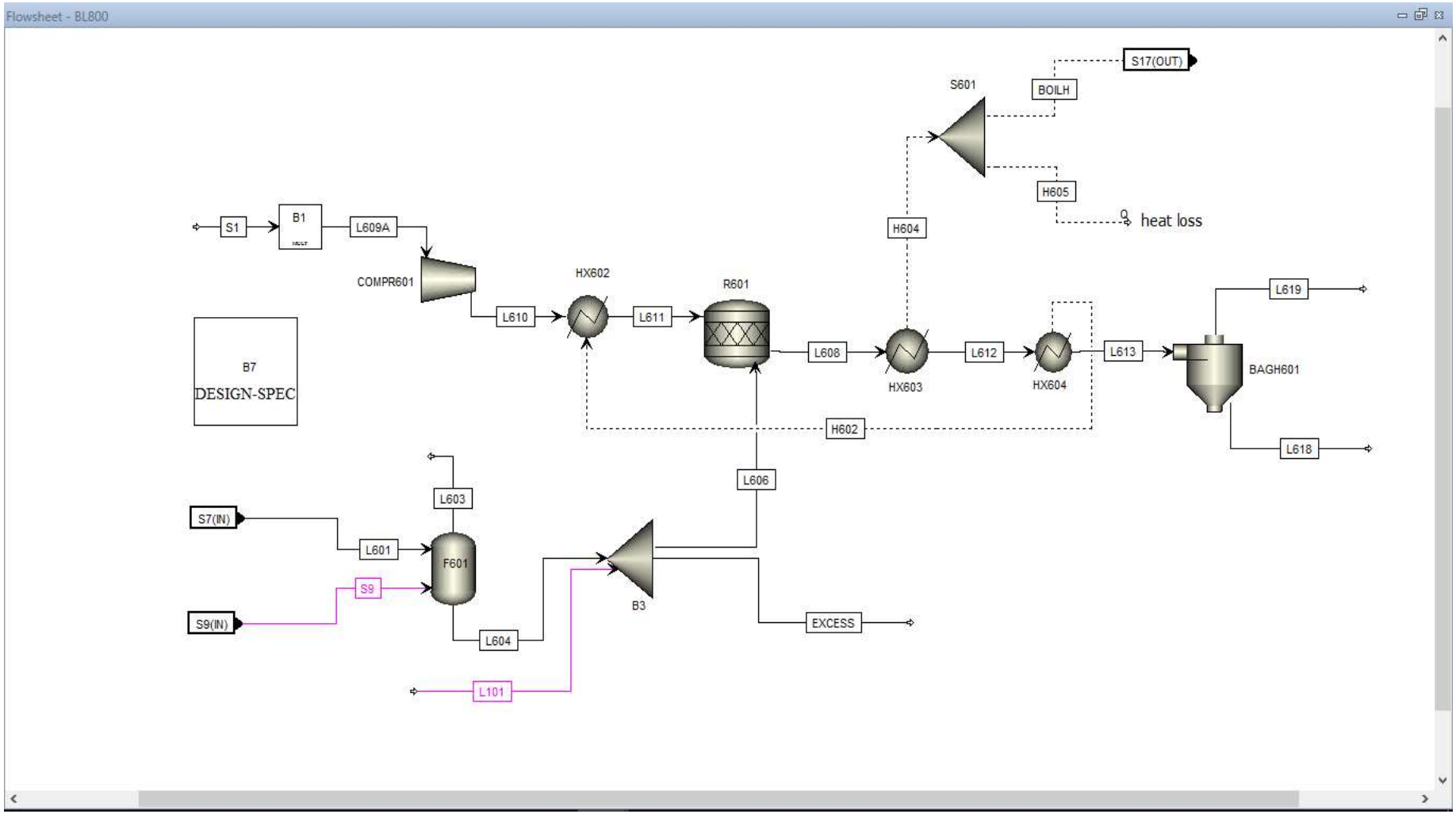

Fig C-9: Flowsheet for steam generation plant (BL800)

TABLE C.10: Summary of mass and energy balance results around the steam generation plant (BL800)

Material																	
Stream Name	Units	EXCESS	L101	L601	L603	L604	L606	L608	L609A	L610	L611	L612	L613	L618	L619	S1	S9
Description		Raw Biomass (Sugarcane Trash, SCT)															
From		B3			F601	F601	B3	R601	B1	COMPR601	HX602	HX603	HX604	BAGH601	BAGH601		
To			B3	F601		B3	R601	HX603	COMPR601	HX602	R601	HX604	BAGH601			B1	F601
Stream Class		MIXCISLD	MIXCISLD	MIXCISLD	MIXCISLD	MIXCISLD	MIXCISLD	MIXCISLD	MIXCISLD	MIXCISLD	MIXCISLD	MIXCISLD	MIXCISLD	MIXCISLD	MIXCISLD	MIXCISLD	MIXCISLD
Total Stream																	
Temperature	C		25,0	83,3		84,4	74,9	1052,3	25,0	26,6	235,1	278,3	149,0	149,0	149,0	25,0	85,1
Pressure	atm		1,0	1,0	1,0	1,0	1,0	1,0	1,0	1,0	1,0	1,0	1,0	1,0	1,0	1,0	0,5
Molar Vapor Fraction			0,0	0,0		0,0	0,0	1,0	1,0	1,0	1,0	1,0	1,0	1,0	0,0	1,0	0,0
Molar Liquid Fraction			0,9	0,8		0,8	0,8	0,0	0,0	0,0	0,0	0,0	0,0	0,0	0,0	0,0	0,9
Molar Solid Fraction			0,1	0,2		0,2	0,2	0,0	0,0	0,0	0,0	0,0	0,0	0,0	1,0	0,0	0,1
Mass Vapor Fraction			0,0	0,0		0,0	0,0	1,0	1,0	1,0	1,0	1,0	1,0	1,0	0,0	1,0	0,0
Mass Liquid Fraction			0,5	0,5		0,5	0,5	0,0	0,0	0,0	0,0	0,0	0,0	0,0	0,0	0,0	0,6
Mass Solid Fraction			0,5	0,5		0,5	0,5	0,0	0,0	0,0	0,0	0,0	0,0	0,0	1,0	0,0	0,4
Molar Enthalpy	cal/mol		-92407,8	-91254,4		-119051,8	-112905,2	-16997,6	-1195,5	-1184,5	291,9	-26000,4	-27182,9	-26101,1	-142445,9	-1195,5	-161731,2
Mass Enthalpy	kcal/kg		-2743,6	-2950,7		-3509,4	-3333,7	-605,1	-41,8	-41,4	10,2	-925,6	-967,7	-937,5	-2611,7	-41,8	-4198,2
Molar Entropy	cal/mol-K		-77,9	-89,5		-183,2	-160,1	11,6	1,0	1,0	4,7	0,7	-3,0	-2,6	-41,8	1,0	-327,1
Mass Entropy	kcal/kg-K		-2,3	-2,9		-5,4	-4,7	0,4	0,0	0,0	0,2	0,0	-0,1	-0,1	-0,8	0,0	-8,5
Molar Density	mol/cc		0,0	0,0		0,0	0,0	0,0	0,0	0,0	0,0	0,0	0,0	0,0	0,1	0,0	0,0
Mass Density	gm/cc		1,2	1,2		1,1	1,1	0,0	0,0	0,0	0,0	0,0	0,0	0,0	2,8	0,0	1,1
Enthalpy Flow	kW		-25526,4	-50905,6		-109667,1	-135193,5	-133359,2	-7512,2	-7443,1	1834,4	-203993,0	-213270,5	-202879,3	-10391,1	-115,6	-58761,5
Average MW			33,7	30,9		33,9	33,9	28,1	28,6	28,6	28,6	28,1	28,1	27,8	54,5	28,6	38,5
Mole Flows	kmol/hr	0	237,5	479,7	0,0	792,1	1029,6	6746,1	5402,9	5402,9	5402,9	6746,1	6746,1	6683,4	62,7	83,1	312,4
Mass Flows	kg/hr	0	8000,0	14834,3	0,0	26869,4	34869,4	189499,3	154629,9	154629,9	154629,9	189499,3	189499,3	186078,2	3421,0	2378,9	12035,1
GLUCOSE	kg/hr	0	0,0	59,8	0,0	258,1	258,1	2,6	0,0	0,0	0,0	2,6	2,6	2,6	0,0	0,0	198,3
CELLULOS	kg/hr	0	1740,0	1566,2	0,0	1566,2	3306,2	33,1	0,0	0,0	0,0	33,1	33,1	0,4	32,7	0,0	0,0
XYLOSE	kg/hr	0	0,0	45,5	0,0	45,5	45,5	0,5	0,0	0,0	0,0	0,5	0,5	0,5	0,0	0,0	0,0
XYLAN	kg/hr	0	1088,0	606,5	0,0	606,5	1694,5	16,9	0,0	0,0	0,0	16,9	16,9	0,2	16,7	0,0	0,0
BIOMASS	kg/hr	0	0,0	521,5	0,0	521,5	521,5	5,2	0,0	0,0	0,0	5,2	5,2	0,1	5,2	0,0	0,0
MICROORG	kg/hr	0	0,0	131,0	0,0	131,0	131,0	131,0	0,0	0,0	0,0	131,0	131,0	1,6	129,4	0,0	0,0
CELLOB	kg/hr	0	0,0	0,0	0,0	188,4	188,4	1,9	0,0	0,0	0,0	1,9	1,9	1,9	0,0	0,0	188,4
EXTRACT	kg/hr	0	320,0	9,7	0,0	1322,7	1642,7	32,9	0,0	0,0	0,0	32,9	32,9	32,9	0,0	0,0	1313,0
ASH	kg/hr	0	304,0	2888,0	0,0	2888,0	3192,0	3192,0	0,0	0,0	0,0	3192,0	3192,0	38,3	3153,7	0,0	0,0
ETHANOL	kg/hr	0	0,0	1,1	0,0	1,6	1,6	0,0	0,0	0,0	0,0	0,0	0,0	0,0	0,0	0,0	0,6
WATER	kg/hr	0	3680,0	6586,1	0,0	10920,9	14600,9	27279,1	2010,2	2010,2	2010,2	27279,1	27279,1	27279,1	0,0	30,9	4334,8
N2	kg/hr	0	0,0	0,0	0,0	0,0	0,0	117435,7	117364,1	117364,1	117364,1	117435,7	117435,7	117435,7	0,0	1805,6	0,0
CO2	kg/hr	0	0,0	0,0	0,0	0,0	0,0	36149,9	0,0	0,0	0,0	36149,9	36149,9	36149,9	0,0	0,0	0,0
O2	kg/hr	0	0,0	0,0	0,0	0,0	0,0	4281,2	35255,6	35255,6	35255,6	4281,2	4281,2	4281,2	0,0	542,4	0,0
NO2	kg/hr	0	0,0	0,0	0,0	0,0	0,0	0,0	0,0	0,0	0,0	0,0	0,0	0,0	0,0	0,0	0,0
NH3	kg/hr	0	0,0	0,0	0,0	0,0	0,0	0,0	0,0	0,0	0,0	0,0	0,0	0,0	0,0	0,0	0,0
AACID	kg/hr	0	0,0	0,1	0,0	3,7	3,7	0,0	0,0	0,0	0,0	0,0	0,0	0,0	0,0	0,0	3,6
SO2	kg/hr	0	0,0	0,0	0,0	0,0	0,0	5,0	0,0	0,0	0,0	5,0	5,0	5,0	0,0	0,0	0,0
CO	kg/hr	0	0,0	0,0	0,0	0,0	0,0	0,0	0,0	0,0	0,0	0,0	0,0	0,0	0,0	0,0	0,0
H3O+	kg/hr	0	0,0	0,0	0,0	0,0	0,0	0,0	0,0	0,0	0,0	0,0	0,0	0,0	0,0	0,0	0,0
OH-	kg/hr	0	0,0	0,0	0,0	0,0	0,0	0,0	0,0	0,0	0,0	0,0	0,0	0,0	0,0	0,0	0,0
FURF	kg/hr	0	0,0	0,0	0,0	2,2	2,2	0,0	0,0	0,0	0,0	0,0	0,0	0,0	0,0	0,0	2,1
SODIU-01	kg/hr	0	0,0	6,1	0,0	826,7	826,7	826,7	0,0	0,0	0,0	826,7	826,7	826,7	0,0	0,0	820,6
KH2PO4	kg/hr	0	0,0	0,4	0,0	0,4	0,4	0,4	0,0	0,0	0,0	0,4	0,4	0,4	0,0	0,0	0,0
MGSO4-01	kg/hr	0	0,0	0,4	0,0	0,4	0,4	0,4	0,0	0,0	0,0	0,4	0,4	0,4	0,0	0,0	0,0
DIAMM-01	kg/hr	0	0,0	1,8	0,0	1,8	1,8	1,8	0,0	0,0	0,0	1,8	1,8	1,8	0,0	0,0	0,0
LIG	kg/hr	0	868,0	2410,0	0,0	7583,8	8451,8	103,0	0,0	0,0	0,0	103,0	103,0	19,7	83,3	0,0	5173,8

Heat				
Stream Name	BOILH	H602	H604	H605
QCALC kW	67102,1	9277,5	70633,8	3531,7
TBEGIN C	1052,3	278,3	1052,3	1052,3
TEND C	278,3	149,0	278,3	278,3

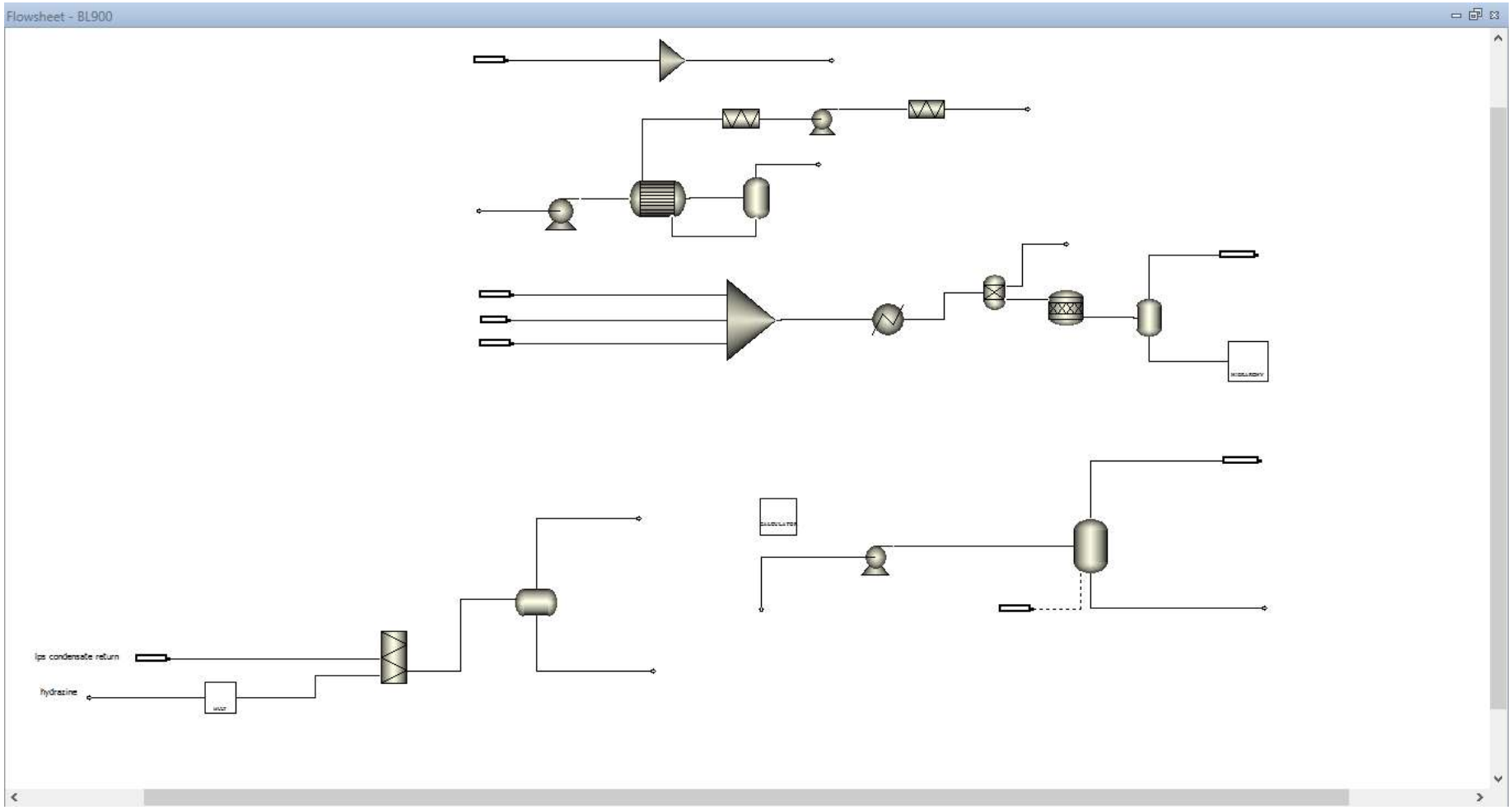

Fig C-10: Flowsheet for wastewater treatment plant (BL900)

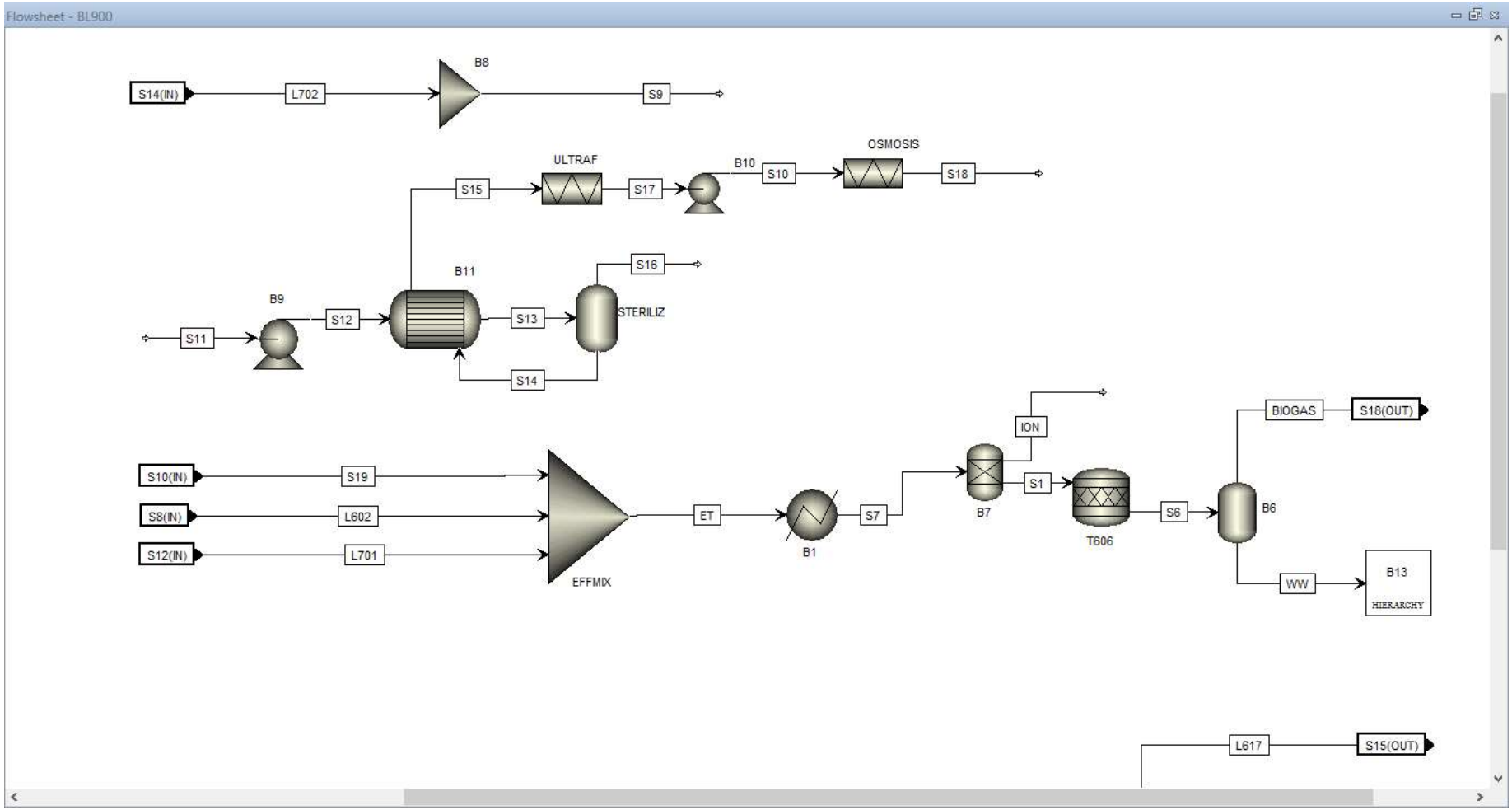

Fig C-10: Flowsheet for wastewater treatment plant (BL900)

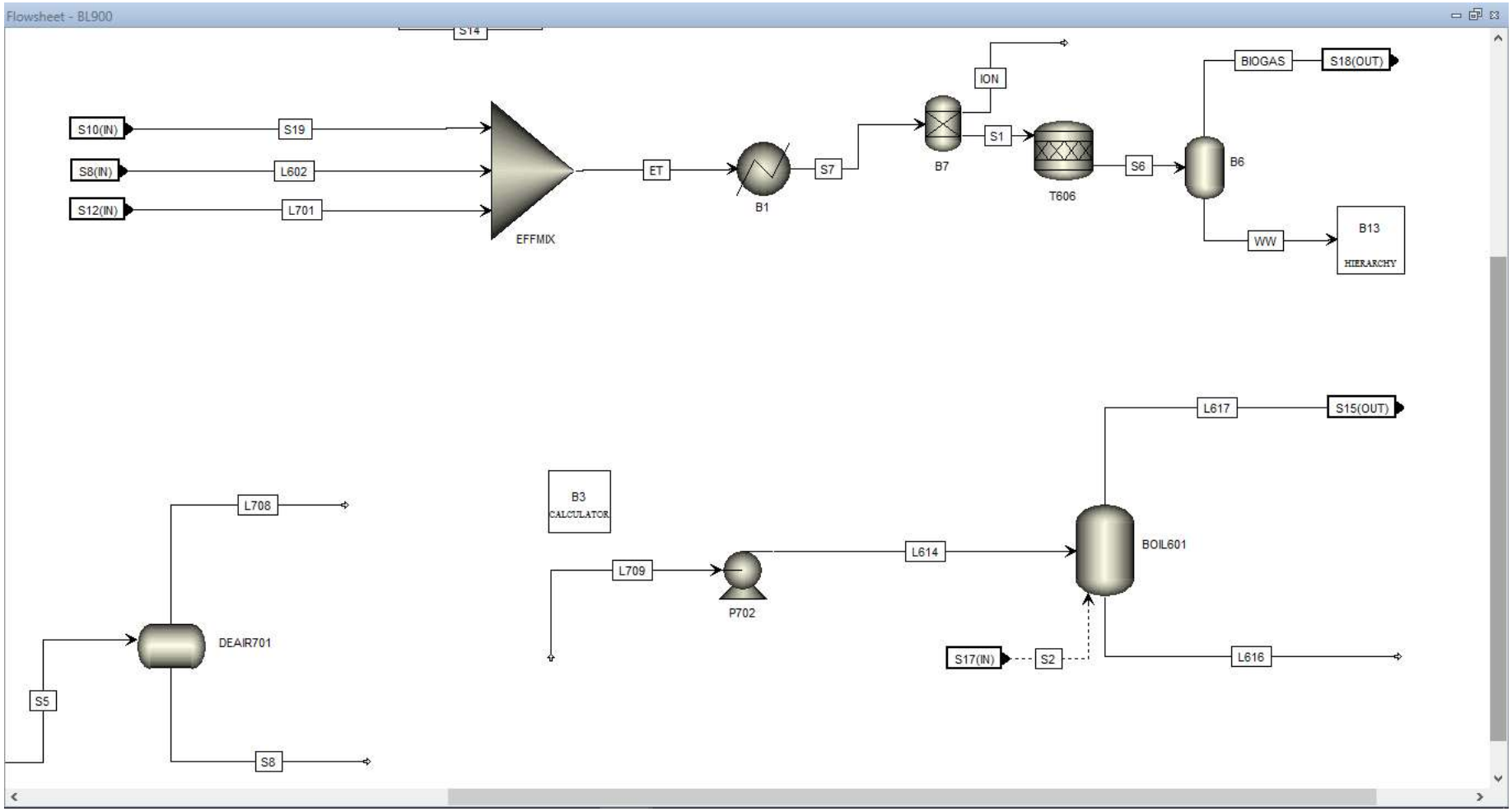

Fig C-10: Flowsheet for wastewater treatment plant (BL900)

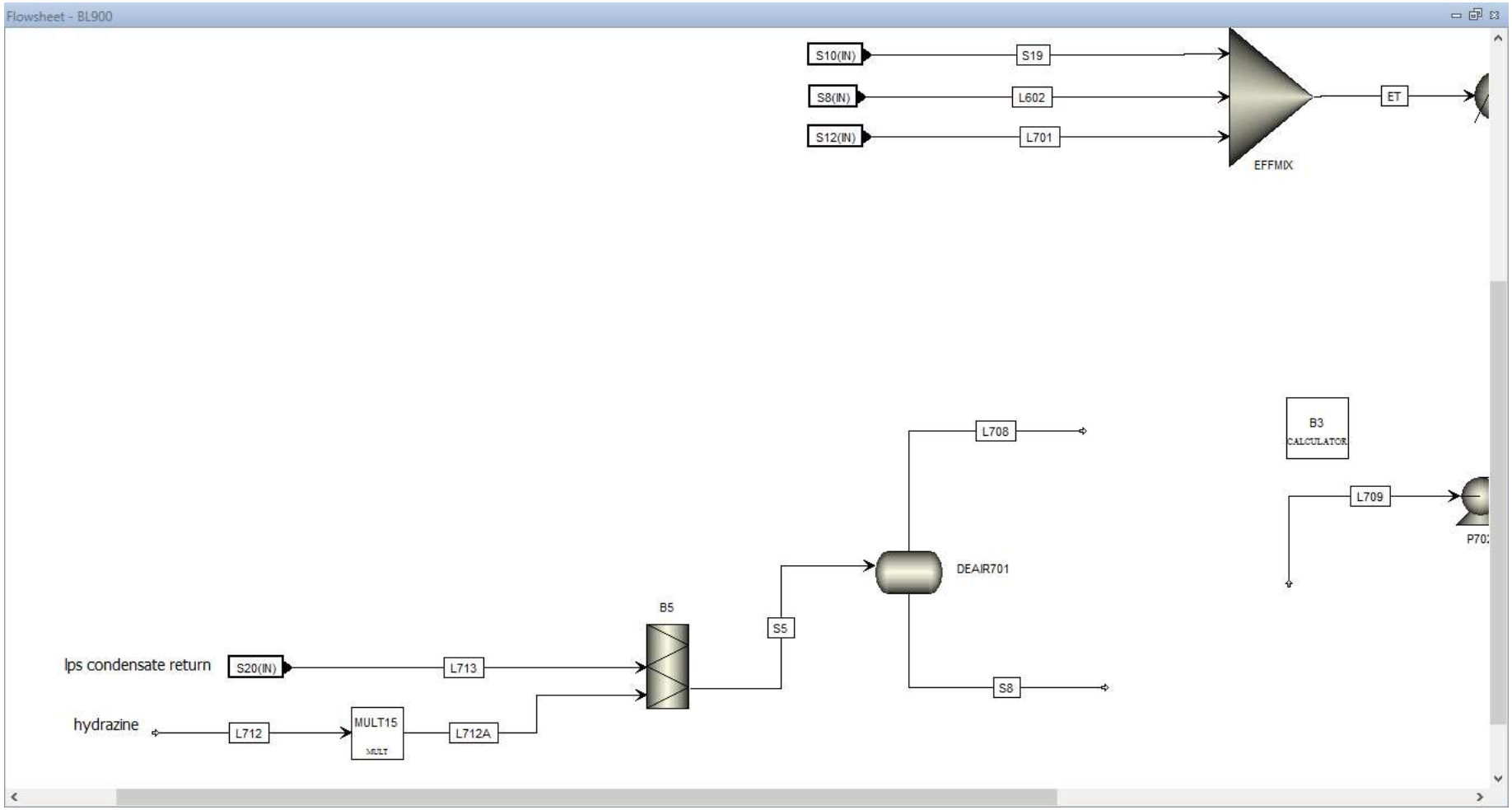

Fig C-10: Flowsheet for wastewater treatment plant (BL900)

TABLE C.11: Summary of mass and energy balance results around the wastewater treatment plant (BL900)

Material

Stream Name	Units	BIOGAS	ET	ION	L602	L614	L616	L617	L701	L702	L708	L709	L712	L712A	L713	S1	S5	S6	S7	S8	S9	S10	S11	S12	S13	S14	S15	S16	S17	S18	S19	WW
Description																																
From		B6	EFFMIX	B7		P702	BOIL601	BOIL601			DEAIR701			MULT15		B7	B5	T606	B1	DEAIR701	B8	B10		B9	B11	STERILIZ	B11	STERILIZ	ULTRAF	OSMOSIS		B6
To			B1		EFFMIX	BOIL601			EFFMIX	B8		P702	MULT15	B5	B5	T606	DEAIR701	B6	B7			OSMOSIS	B9	B11	STERILIZ	B11	ULTRAF		B10		EFFMIX	B13
Stream Class		MIXCISLD	MIXCISLD	MIXCISLD	MIXCISLD	MIXCISLD	MIXCISLD	MIXCISLD	MIXCISLD	MIXCISLD	MIXCISLD	MIXCISLD	MIXCISLD	MIXCISLD	MIXCISLD	MIXCISLD	MIXCISLD	MIXCISLD	MIXCISLD	MIXCISLD	MIXCISLD	MIXCISLD	MIXCISLD	MIXCISLD	MIXCISLD	MIXCISLD	MIXCISLD	MIXCISLD	MIXCISLD	MIXCISLD	MIXCISLD	MIXCISLD
Total Stream																																
Temperature	C	35,0	84,3	40,0	98,7	123,2		239,5	50,0	113,3	130,5	123,0	25,0	25,0	170,4	40,0	152,5	35,0	40,0	130,5	113,3	55,5	40,0	40,0	105,0	120,0	55,2		55,3	55,9	55,0	35,0
Pressure	atm	2,0	2,5	2,5	3,0	11,0	11,0	11,0	2,5	1,6	2,7	2,2	5,0	5,0	7,9	2,5	5,0	2,0	2,5	2,7	1,6	20,0	1,0	4,0	4,0	4,0	4,0	4,0	1,0	1,0	3,0	2,0
Molar Vapor Fraction		1,0	0,0	0,0	0,0	0,0		1,0	0,0	0,0	1,0	0,0	0,0	0,0	0,0	0,0	0,0	0,0	0,0	0,0	0,0	0,0	0,0	0,0	0,0	0,0	0,0		0,0	0,0	0,0	0,0
Molar Liquid Fraction		0,0	1,0	0,0	1,0	1,0		0,0	1,0	1,0	0,0	1,0	1,0	1,0	1,0	1,0	1,0	1,0	1,0	1,0	1,0	1,0	1,0	1,0	1,0	1,0	1,0		1,0	1,0	1,0	1,0
Molar Solid Fraction		0,0	0,0	1,0	0,0	0,0		0,0	0,0	0,0	0,0	0,0	0,0	0,0	0,0	0,0	0,0	0,0	0,0	0,0	0,0	0,0	0,0	0,0	0,0	0,0	0,0		0,0	0,0	0,0	0,0
Mass Vapor Fraction		1,0	0,0	0,0	0,0	0,0		1,0	0,0	0,0	1,0	0,0	0,0	0,0	0,0	0,0	0,0	0,0	0,0	0,0	0,0	0,0	0,0	0,0	0,0	0,0	0,0		0,0	0,0	0,0	0,0
Mass Liquid Fraction		0,0	1,0	0,0	1,0	1,0		0,0	1,0	1,0	0,0	1,0	1,0	1,0	1,0	1,0	1,0	1,0	1,0	1,0	1,0	1,0	1,0	1,0	1,0	1,0	1,0		1,0	1,0	1,0	1,0
Mass Solid Fraction		0,0	0,0	1,0	0,0	0,0		0,0	0,0	0,0	0,0	0,0	0,0	0,0	0,0	0,0	0,0	0,0	0,0	0,0	0,0	0,0	0,0	0,0	0,0	0,0	0,0		0,0	0,0	0,0	0,0
Molar Enthalpy	cal/mol	-54055,1	-69076,8	-379011,4	-67657,4	-66535,0		-56220,6	-67868,3	-66709,1	-56943,0	-66540,5	11013,0	11013,0	-65661,0	-69840,2	-65660,9	-69402,5	-69914,6	-66366,3	-66709,1	-67756,1	-68041,7	-68040,0	-66867,9	-66594,8	-67766,9		-67766,9	-67756,1	-73407,4	-69570,1
Mass Enthalpy	kcal/kg	-1864,7	-3758,3	-3094,2	-3696,9	-3693,3		-3120,7	-3765,7	-3691,6	-3160,8	-3693,6	343,7	343,7	-3644,7	-3805,0	-3644,7	-3815,3	-3803,9	-3683,9	-3691,6	-3761,0	-3776,9	-3776,8	-3711,7	-3696,6	-3761,6		-3761,6	-3761,0	-3928,2	-3849,4
Molar Entropy	cal/mol-K	-9,3	-40,1	-1271,3	-36,7	-33,8		-11,2	-37,5	-34,3	-10,1	-33,8	-82,3	-82,3	-31,7	-43,0	-31,7	-42,5	-43,3	-33,5	-34,3	-37,2	-38,1	-38,1	-34,7	-34,0	-37,2		-37,2	-37,2	-52,1	-42,9
Mass Entropy	kcal/kg-K	-0,3	-2,2	-10,4	-2,0	-1,9		-0,6	-2,1	-1,9	-0,6	-1,9	-2,6	-2,6	-1,8	-2,3	-1,8	-2,3	-2,4	-1,9	-1,9	-2,1	-2,1	-2,1	-1,9	-1,9	-2,1		-2,1	-2,1	-2,8	-2,4
Molar Density	mol/cc	0,0	0,1	0,0	0,1	0,1		0,0	0,1	0,1	0,0	0,1	0,0	0,0	0,0	0,1	0,0	0,0	0,1	0,0	0,1	0,1	0,1	0,1	0,1	0,1	0,1		0,1	0,1	0,1	0,1
Mass Density	gm/cc	0,0	1,0	1,0	1,0	0,9		0,0	1,0	0,9	0,0	0,9	1,0	1,0	0,9	1,0	0,1	0,1	1,0	0,9	0,9	1,0	1,0	1,0	1,0	0,9	1,0		1,0	1,0	1,0	1,0
Enthalpy Flow	kW	-9184,2	#########	-1421,5	-736884,4	-432854,5		-365752,3	-59533,5	-66845,2	-27732,6	-432889,9	0,0	0,1	-427168,3	########	-427168,2	########	-1089491,7	-399435,5	-66845,2	-1162234,8	-1167132,5	-1167103,6	-1146997,9	-1142313,3	-1162419,0		-1162419,0	-1162234,8	-280018,3	-1081867,0
Average MW		29,0	18,4	122,5	18,3	18,0		18,0	18,0	18,1	18,0	18,0	32,0	32,0	18,0	18,4	18,0	18,2	18,4	18,0	18,1	18,0	18,0	18,0	18,0	18,0	18,0		18,0	18,0	18,7	18,1
Mole Flows	kmol/hr	146,1	13399,1	3,2	9364,9	5593,9	0,0	5593,9	754,2	861,6	418,8	5593,9	0,0	0,0	5593,9	13395,9	5593,9	13517,3	13399,1	5175,1	861,6	14749,1	14749,1	14749,1	14749,1	14749,1	14749,1	0,0	14749,1	14749,1	3279,9	13371,2
Mass Flows	kg/hr	4235,0	246274,0	395,0	171386,8	100775,0	0,0	100775,0	13593,7	15569,4	7544,2	100775,0	0,0	0,3	100775,0	245879,0	100775,3	245889,9	246274,0	93231,1	15569,4	265709,2	265709,2	265709,2	265709,2	265709,2	265709,2	0,0	265709,2	265709,2	61293,5	241654,9
GLUCOSE	kg/hr	0,0	1482,6	0,0	1264,4	0,0	0,0	0,0	0,0	0,0	0,0	0,0	0,0	0,0	0,0	1482,6	0,0	0,0	1482,6	0,0	0,0	0,0	0,0	0,0	0,0	0,0	0,0	0,0	0,0	0,0	218,2	0,0
CELLULOS	kg/hr	0,0	0,0	0,0	0,0	0,0	0,0	0,0	0,0	0,0	0,0	0,0	0,0	0,0	0,0	0,0	0,0	0,0	0,0	0,0	0,0	0,0	0,0	0,0	0,0	0,0	0,0	0,0	0,0	0,0	0,0	0,0
XYLOSE	kg/hr	0,0	961,5	0,0	961,5	0,0	0,0	0,0	0,0	0,0	0,0	0,0	0,0	0,0	0,0	961,5	0,0	0,0	961,5	0,0	0,0	0,0	0,0	0,0	0,0	0,0	0,0	0,0	0,0	0,0	0,0	0,0
XYLAN	kg/hr	0,0	0,0	0,0	0,0	0,0	0,0	0,0	0,0	0,0	0,0	0,0	0,0	0,0	0,0	0,0	0,0	0,0	0,0	0,0	0,0	0,0	0,0	0,0	0,0	0,0	0,0	0,0	0,0	0,0	0,0	0,0
MICROORG	kg/hr	0,0	0,0	0,0	0,0	0,0	0,0	0,0	0,0	0,0	0,0	0,0	0,0	0,0	0,0	0,0	0,0	0,0	0,0	0,0	0,0	0,0	0,0	0,0	0,0	0,0	0,0	0,0	0,0	0,0	0,0	0,0
CELLOB	kg/hr	0,0	207,3	0,0	0,0	0,0	0,0	0,0	0,0	0,0	0,0	0,0	0,0	0,0	0,0	207,3	0,0	0,0	207,3	0,0	0,0	0,0	0,0	0,0	0,0	0,0	0,0	0,0	0,0	0,0	207,3	0,0
EXTRACT	kg/hr	0,0	1649,5	0,0	205,1	0,0	0,0	0,0	0,0	0,0	0,0	0,0	0,0	0,0	0,0	1649,5	0,0	0,0	1649,5	0,0	0,0	0,0	0,0	0,0	0,0	0,0	0,0	0,0	0,0	0,0	1444,4	0,0
ETHANOL	kg/hr	0,0	80,1	0,0	80,1	0,0	0,0	0,0	0,0	77,8	0,0	0,0	0,0	0,0	0,0	80,1	0,0	0,0	80,1	0,0	77,8	0,0	0,0	0,0	0,0	0,0	0,0	0,0	0,0	0,0	0,0	0,0
WATER	kg/hr	75,2	240379,5	0,0	168294,6	100775,0	0,0	100775,0	13585,6	15491,5	7544,2	100775,0	0,0	0,0	100775,0	240379,5	100775,0	240379,5	240379,5	93230,8	15491,5	265709,2	265709,2	265709,2	265709,2	265709,2	265709,2	0,0	265709,2	265709,2	58499,3	240304,3
CO2	kg/hr	2963,2	0,0	0,0	0,0	0,0	0,0	0,0	0,0	0,0	0,0	0,0	0,0	0,0	0,0	0,0	0,0	3218,9	0,0	0,0	0,0	0,0	0,0	0,0	0,0	0,0	0,0	0,0	0,0	0,0	0,0	255,7
O2	kg/hr	0,0	0,0	0,0	0,0	0,0	0,0	0,0	0,0	0,0	0,0	0,0	0,0	0,0	0,0	0,0	0,0	0,0	0,0	0,0	0,0	0,0	0,0	0,0	0,0	0,0	0,0	0,0	0,0	0,0	0,0	0,0
CH4	kg/hr	1196,6	0,0	0,0	0,0	0,0	0,0	0,0	0,0	0,0	0,0	0,0	0,0	0,0	0,0	0,0	0,0	1201,3	0,0	0,0	0,0	0,0	0,0	0,0	0,0	0,0	0,0	0,0	0,0	0,0	0,0	4,7
NH3	kg/hr	0,0	0,0	0,0	0,0	0,0	0,0	0,0	0,0	0,0	0,0	0,0	0,0	0,0	0,0	0,0	0,0	0,0	0,0	0,0	0,0	0,0	0,0	0,0	0,0	0,0	0,0	0,0	0,0	0,0	0,0	0,0
AACID	kg/hr	0,0	28,3	0,0	2,5	0,0	0,0	0,0	7,7	0,1	0,0	0,0	0,0	0,0	0,0	28,3	0,0	0,0	28,3	0,0	0,1	0,0	0,0	0,0	0,0	0,0	0,0	0,0	0,0	0,0	18,2	0,0
H3O+	kg/hr	0,0	0,0	0,0	0,0	0,0	0,0	0,0	0,0	0,0	0,0	0,0	0,0	0,0	0,0	0,0	0,0	0,0	0,0	0,0	0,0	0,0	0,0	0,0	0,0	0,0	0,0	0,0	0,0	0,0	0,0	0,0
OH-	kg/hr	0,0	0,0	0,0	0,0	0,0	0,0	0,0	0,0	0,0	0,0	0,0	0,0	0,0	0,0	0,0	0,0	0,0	0,0	0,0	0,0	0,0	0,0	0,0	0,0	0,0	0,0	0,0	0,0	0,0	0,0	0,0
FURF	kg/hr	0,0	4,3	0,0	0,5	0,0	0,0	0,0	0,4	0,0	0,0	0,0	0,0	0,0	0,0	4,3	0,0	4,3	4,3	0,0	0,0	0,0	0,0	0,0	0,0	0,0	0,0	0,0	0,0	0,0	3,4	4,3
SODIU-01	kg/hr	0,0	1031,0	0,0	128,2	0,0	0,0	0,0	0,0	0,0	0,0	0,0	0,0	0,0	0,0	1031,0	0,0	1031,0	1031,0	0,0	0,0	0,0	0,0	0,0	0,0	0,0	0,0	0,0	0,0	0,0	902,8	1031,0
KH2PO4	kg/hr	0,0	9,2	0,0	9,2	0,0	0,0	0,0	0,0	0,0	0,0	0,0	0,0	0,0	0,0	9,2	0,0	9,2	9,2	0,0	0,0	0,0	0,0	0,0	0,0	0,0	0,0	0,0	0,0	0,0	0,0	9,2
MGSO4-01	kg/hr	0,0	7,7	0,0	7,7	0,0	0,0	0,0	0,0	0,0	0,0	0,0	0,0	0,0	0,0	7,7	0,0	7,7	7,7	0,0	0,0	0,0	0,0	0,0	0,0	0,0	0,0	0,0	0,0	0,0	0,0	7,7
HYDRAZIN	kg/hr	0,0	0,0	0,0	0,0	0,0	0,0	0,0	0,0	0,0	0,0	0,0	0,3	0,0	0,0	0,0	0,3	0,0	0,0	0,3	0,0	0,0	0,0	0,0	0,0	0,0	0,0	0,0	0,0	0,0	0,0	0,0
DIAMM-01	kg/hr	0,0	38,0	0,0	38,0	0,0	0,0	0,0	0,0	0,0	0,0	0,0	0,0	0,0	0,0	38,0	0,0	38,0	38,0	0,0	0,0	0,0	0,0	0,0	0,0	0,0	0,0	0,0	0,0	0,0	0,0	38,0
LIG	kg/hr	0,0	395,0	395,0	395,0	0,0	0,0	0,0	0,0	0,0	0,0	0,0	0,0	0,0	0,0	0,0	0,0	0,0	395,0	0,0	0,0	0,0	0,0	0,0	0,0	0,0	0,0	0,0	0,0	0,0	0,0	0,0

Heat	
Stream Name	S2
QCALC kW	67102,1
TBEGIN C	1052,3
TEND C	278,3

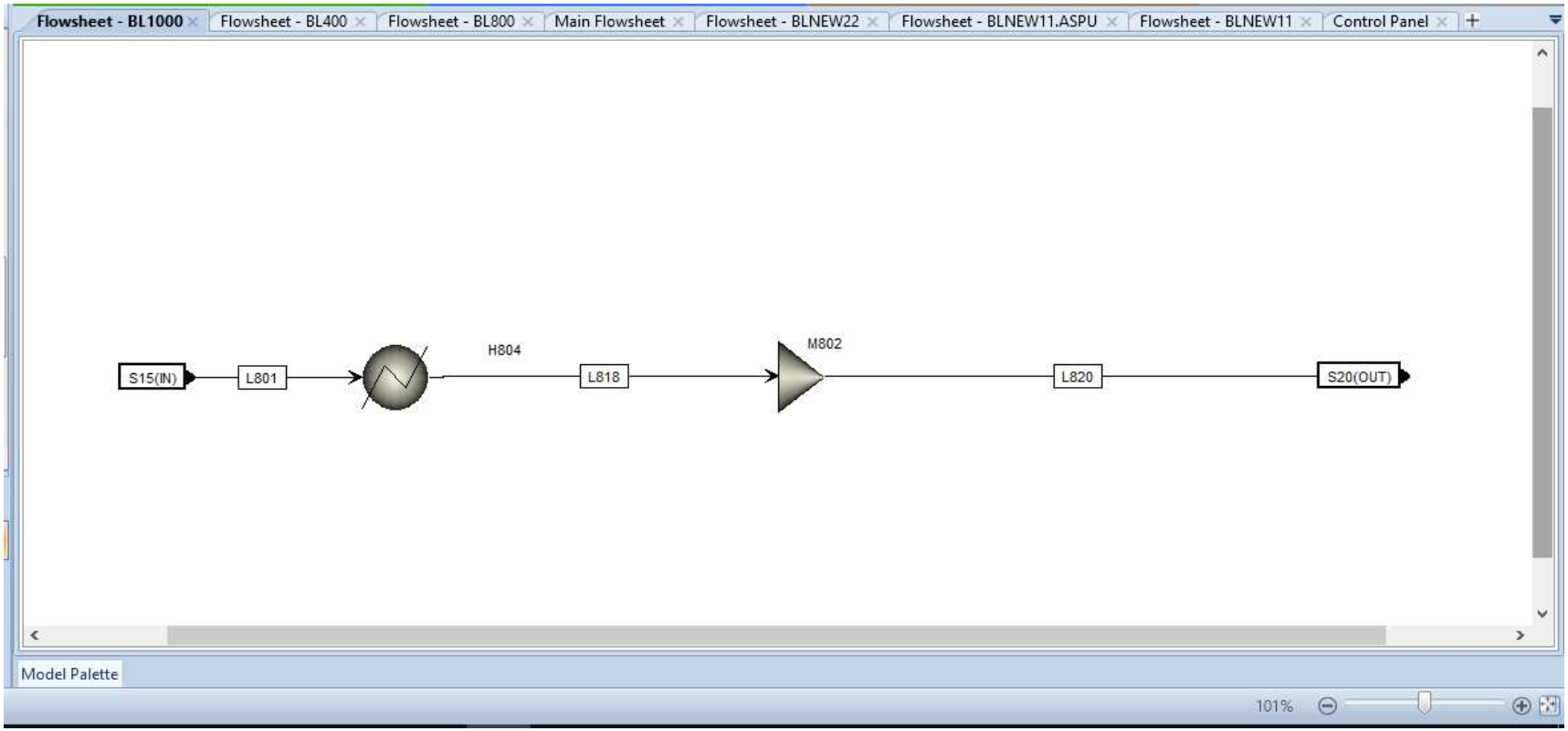

Fig C-11: Flowsheet for condensing steam extraction plant (BL1000)

TABLE C.12: Summary of mass and energy balance results around condensing steam extraction plant (BL1000)

Material				
Stream Name	Units	L801	L818	L820
Description				
From			H804	M802
To		H804	M802	
Stream Class		MIXCISLD	MIXCISLD	MIXCISLD
Total Stream				
Temperature	C	239,5	170,4	170,4
Pressure	atm	11,0	7,9	7,9
Molar Vapor Fraction		1,0	0,0	0,0
Molar Liquid Fraction		0,0	1,0	1,0
Molar Solid Fraction		0,0	0,0	0,0
Mass Vapor Fraction		1,0	0,0	0,0
Mass Liquid Fraction		0,0	1,0	1,0
Mass Solid Fraction		0,0	0,0	0,0
Molar Enthalpy	cal/mol	-56220,6	-65661,0	-65661,0
Mass Enthalpy	kcal/kg	-3120,7	-3644,7	-3644,7
Molar Entropy	cal/mol-K	-11,2	-31,7	-31,7
Mass Entropy	kcal/kg-K	-0,6	-1,8	-1,8
Molar Density	mol/cc	0,0	0,0	0,0
Mass Density	gm/cc	0,0	0,9	0,9
Enthalpy Flow	kW	-365752,3	-427168,3	-427168,3
Average MW		18,0	18,0	18,0
Mole Flows	kmol/hr	5593,9	5593,9	5593,9
Mass Flows	kg/hr	100775,0	100775,0	100775,0
WATER	kg/hr	100775,0	100775,0	100775,0

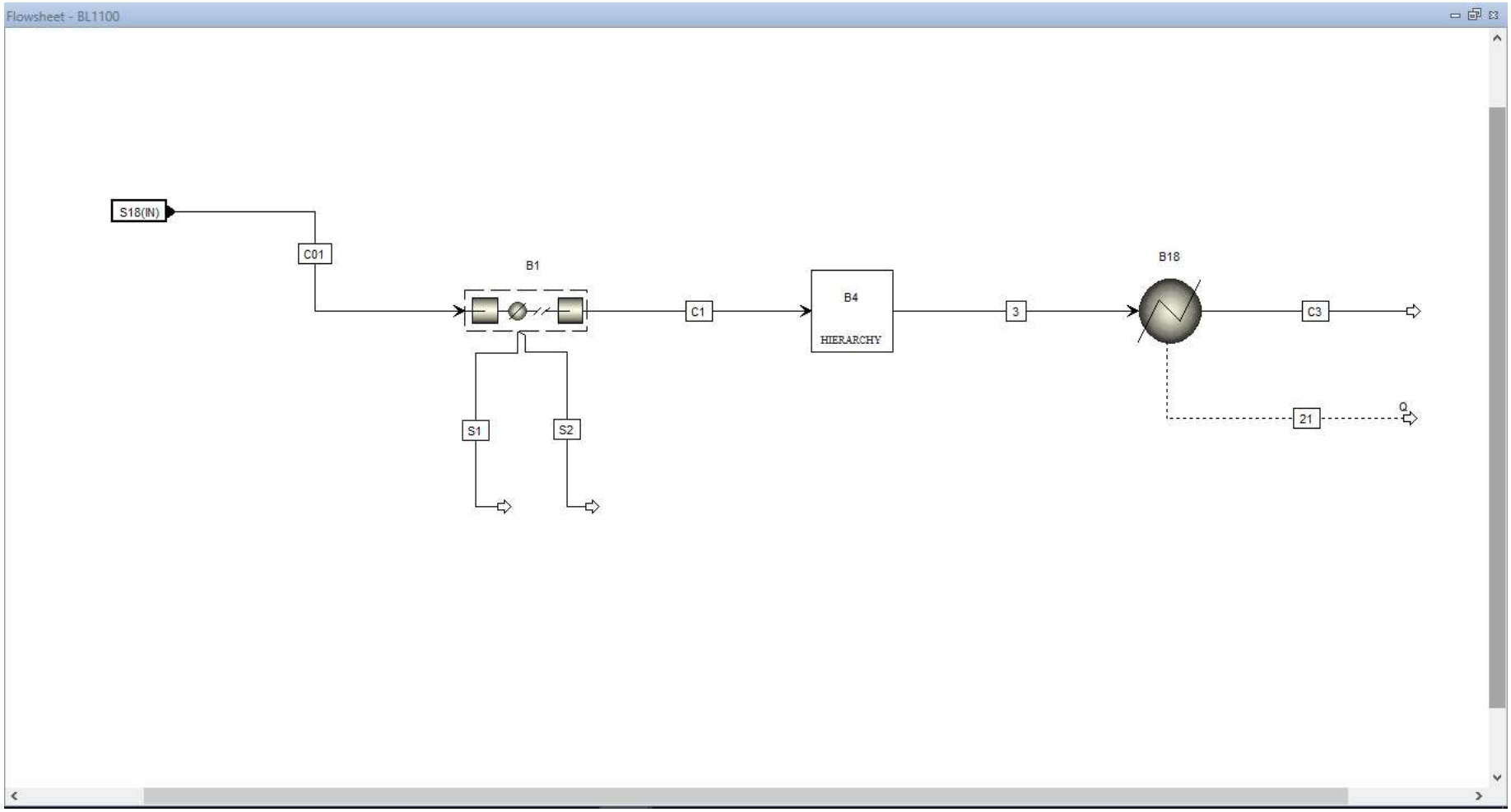

Fig C-12 Flowsheet for bio-power generation plant (BL1100)

TABLE C.13: Summary of mass and energy balance results around the bio-power generation plant (BL1100)

Material							
Stream Name	Units	3	C1	C01	C3	S1	S2
Description							
From		B4	B1		B18	B1	B1
To		B18	B4	B1			
Stream Class		MIXCISLD	MIXCISLD	MIXCISLD	MIXCISLD	MIXCISLD	MIXCISLD
Total Stream							
Temperature	C	652,9	60,0	35,0	140,0		60,0
Pressure	atm	1,1	15,0	2,0	1,1		7,7
Molar Vapor Fraction		1,0	1,0	1,0	1,0		0,0
Molar Liquid Fraction		0,0	0,0	0,0	0,0		1,0
Molar Solid Fraction		0,0	0,0	0,0	0,0		0,0
Mass Vapor Fraction		1,0	1,0	1,0	1,0		0,0
Mass Liquid Fraction		0,0	0,0	0,0	0,0		1,0
Mass Solid Fraction		0,0	0,0	0,0	0,0		0,0
Molar Enthalpy	cal/mol	-7078,6	-54019,5	-54055,1	-11099,0		-67706,6
Mass Enthalpy	kcal/kg	-244,9	-1862,6	-1864,7	-384,1		-3752,8
Molar Entropy	cal/mol-K	9,5	-13,1	-9,3	3,2		-36,9
Mass Entropy	kcal/kg-K	0,3	-0,5	-0,3	0,1		-2,0
Molar Density	mol/cc	0,0	0,0	0,0	0,0		0,1
Mass Density	gm/cc	0,0	0,0	0,0	0,0		1,0
Enthalpy Flow	kW	-15278,1	-9167,0	-9184,2	-23955,6		-14,0
Average MW		28,9	29,0	29,0	28,9		18,0
Mole Flows	kmol/hr	1855,9	145,9	146,1	1855,9	0,0	0,2
Mass Flows	kg/hr	53632,9	4231,8	4235,0	53632,9	0,0	3,2
WATER	kg/hr	2759,4	72,0	75,2	2759,4	0,0	3,2
N2	kg/hr	37329,2	0,0	0,0	37329,2	0,0	0,0
CO2	kg/hr	6245,7	2963,2	2963,2	6245,7	0,0	0,0
O2	kg/hr	7224,6	0,0	0,0	7224,6	0,0	0,0
CH4	kg/hr	0,0	1196,6	1196,6	0,0	0,0	0,0
NO	kg/hr	72,7	0,0	0,0	72,7	0,0	0,0
NO2	kg/hr	1,3	0,0	0,0	1,3	0,0	0,0
NH3	kg/hr	0,0	0,0	0,0	0,0	0,0	0,0
CO	kg/hr	0,0	0,0	0,0	0,0	0,0	0,0
FURF	kg/hr	0,0	0,0	0,0	0,0	0,0	0,0
SODIU-01	kg/hr	0,0	0,0	0,0	0,0	0,0	0,0
KH2PO4	kg/hr	0,0	0,0	0,0	0,0	0,0	0,0
MGSO4-01	kg/hr	0,0	0,0	0,0	0,0	0,0	0,0
DIAMM-01	kg/hr	0,0	0,0	0,0	0,0	0,0	0,0

Heat	
Stream Name	21
QCALC kW	8677,5
TBEGIN C	652,9
TEND C	140,0

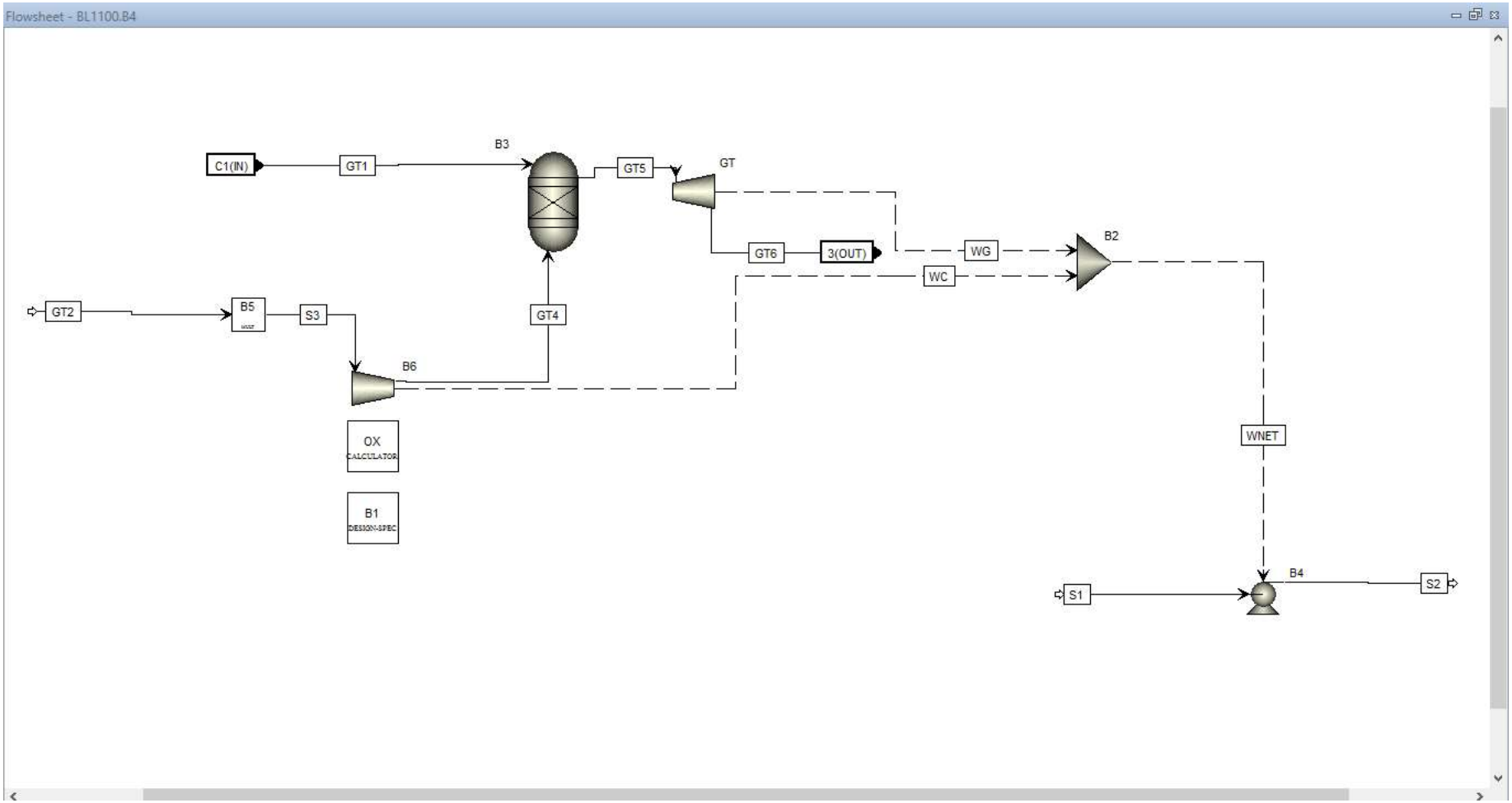

Fig C-12-1 Flowsheet for the biogas-combustion and power generation unit (BL1100.B4)

TABLE C.14: Summary of mass and energy balance results around the biogas-combustion and power generation unit (BL1100.B4)

		Material							
Stream Name	Units	GT1	GT2	GT4	GT5	GT6	S1	S2	S3
Description									
From				B6	B3	GT		B4	B5
To		B3	B5	B3	GT		B4		B6
Stream Class		MIXCISLD	MIXCISLD	MIXCISLD	MIXCISLD	MIXCISLD	MIXCISLD	MIXCISLD	MIXCISLD
Total Stream									
Temperature	C	60,0	25,0	431,6	1291,9	652,9	25,0	25,1	25,0
Pressure	atm	15,0	1,0	14,8	14,8	1,1	1,0	17,8	1,0
Molar Vapor Fraction		1,0	1,0	1,0	1,0	1,0	0,0	0,0	1,0
Molar Liquid Fraction		0,0	0,0	0,0	0,0	0,0	1,0	1,0	0,0
Molar Solid Fraction		0,0	0,0	0,0	0,0	0,0	0,0	0,0	0,0
Mass Vapor Fraction		1,0	1,0	1,0	1,0	1,0	0,0	0,0	1,0
Mass Liquid Fraction		0,0	0,0	0,0	0,0	0,0	1,0	1,0	0,0
Mass Solid Fraction		0,0	0,0	0,0	0,0	0,0	0,0	0,0	0,0
Molar Enthalpy	cal/mol	-54019,5	-1,6	2920,1	-1556,7	-7078,6	-68311,3	-68302,7	-1,6
Mass Enthalpy	kcal/kg	-1862,6	-0,1	101,1	-53,9	-244,9	-3791,9	-3791,4	-0,1
Molar Entropy	cal/mol-K	-13,1	1,0	1,8	8,8	9,5	-39,0	-39,0	1,0
Mass Entropy	kcal/kg-K	-0,5	0,0	0,1	0,3	0,3	-2,2	-2,2	0,0
Molar Density	mol/cc	0,0	0,0	0,0	0,0	0,0	0,1	0,1	0,0
Mass Density	gm/cc	0,0	0,0	0,0	0,0	0,0	1,0	1,0	0,0
Enthalpy Flow	kW	-9167,0	-1,3	5807,1	-3359,9	-15278,1	-4,41E+07	-4,41E+07	-3,2
Average MW		29,0	28,9	28,9	28,9	28,9	18,0	18,0	28,9
Mole Flows	kmol/hr	145,9	678,1	1710,0	1855,9	1855,9	5,55E+05	5,55E+05	1710,0
Mass Flows	kg/hr	4231,8	19589,6	49401,2	53632,9	53632,9	1,00E+07	1,00E+07	49401,2
WATER	kg/hr	72,0	0,0	0,0	2759,4	2759,4	1,00E+07	1,00E+07	0,0
N2	kg/hr	0,0	14816,1	37363,5	37329,2	37329,2	0,0	0,0	37363,5
CO2	kg/hr	2963,2	0,0	0,0	6245,7	6245,7	0,0	0,0	0,0
O2	kg/hr	0,0	4773,4	12037,7	7224,6	7224,6	0,0	0,0	12037,7
CH4	kg/hr	1196,6	0,0	0,0	0,0	0,0	0,0	0,0	0,0
NO	kg/hr	0,0	0,0	0,0	72,7	72,7	0,0	0,0	0,0
NO2	kg/hr	0,0	0,0	0,0	1,3	1,3	0,0	0,0	0,0
NH3	kg/hr	0,0	0,0	0,0	0,0	0,0	0,0	0,0	0,0
CO	kg/hr	0,0	0,0	0,0	0,0	0,0	0,0	0,0	0,0
FURF	kg/hr	0,0	0,0	0,0	0,0	0,0	0,0	0,0	0,0
SODIU-01	kg/hr	0,0	0,0	0,0	0,0	0,0	0,0	0,0	0,0
KH2PO4	kg/hr	0,0	0,0	0,0	0,0	0,0	0,0	0,0	0,0
MGSO4-01	kg/hr	0,0	0,0	0,0	0,0	0,0	0,0	0,0	0,0
DIAMM-01	kg/hr	0,0	0,0	0,0	0,0	0,0	0,0	0,0	0,0

	Work		
Stream Name	WC	WG	WNET
POWER kW	6049,9	-11584,6	-5534,6

Table C-15: Non-Biomass Inputs extracted from material balances

Process Block (BL)	Input Description		Amount IN	
	Input Type	Stream code	Unit	Amt
BL100	Sodium hydroxide (NaOH)	S1	[kg/hr]	1 900
	Water with Biomass In	S5	[kg/hr]	34 960
	Water of Dilution for SF	L113	[kg/hr]	64 990
	Water for solids washing	S11	[kg/hr]	114 570
	Steam for Presteaming	LS102B	[kg/hr]	3 040
	Steam for Pretreatment	S4	[kg/hr]	13 300
BL200	DAP (Diammonium Phosphate)	LDAP	[kg/hr]	40
	Ammonia (NH3)	L204A	[kg/hr]	15
	KH2PO4 (Di-Potassium Phosphate)	[""]	[kg/hr]	10
	MgSO4 (Magnesium phosphate)	[""]	[kg/hr]	8
	Micro-organisms	L202A	[kg/hr]	0,00038
	Glucose	L203B	[kg/hr]	678
	Oxygen	L205B	[kg/hr]	1 330
BL300	Water (added to fermentation unit)	W	[kg/hr]	76 148
	Ammonia (NH3)	L306A	[kg/hr]	24
BL400	No material inputs, but energy in the form of heat and work			
BL700	Air for pneumapress filtration unit	S5	[kg/hr]	78
	Nitrogen (N2)	S5	[kg/hr]	60
	Oxygen (O2)	S5	[kg/hr]	18
BL800	Air for solids combustion	S1	[kg/hr]	154 630
	Nitrogen (N2)	S1	[kg/hr]	117 364
	Oxygen (O2)	S1	[kg/hr]	35 256
	Water	S1	[kg/hr]	2 010
BL900	Hydrazine	L712A	[kg/hr]	0
	Boiler feed water	L709	[kg/hr]	100 775
BL1000	None but steam generated at boiler	L801	[kg/hr]	100 775
BL1100	Air for biogas combustion	S3	[kg/hr]	49 401
	Nitrogen (N2)	S3	[kg/hr]	37 363
	Oxygen (O2)	S3	[kg/hr]	12 038
BLNEW11	Steam for MEE-Preconcentration unit	S9	[kg/hr]	12 500
	Anti-solvent (Ethanol): gross	ETAS	[kg/hr]	19 264
	Ethanol	[""]	[kg/hr]	19 195
	Water	[""]	[kg/hr]	69
BLNEW22	Steam for MEE-concentration unit	S9	[kg/hr]	3 500

(II) Simulation Results by model type:

Table C-16: ASPENPLUS simulation results (raw data) from which are extracted utilities requirement (thermal/heat duty; electrical/work duty by block type) for major thermal and electrically-driven units modelled and presented as blocks in the respective aspen flowsheets

Heaters (Heating, cooling and chilling units)

	Heater																															
Name	BL100.B5	BL100.B6	BL100.B44	BL300.B4	BL300.COOLER	BL400.B1	BL400.B2	BL400.B3	BL400.B5	BL400.B6	BL400.B10	BL400.B15	BL700.B3	BL800.HX602	iL800.HX60	L800.HX60	BL900.B1	iL1000.H80	BL1100.B1	BLNEW11.ASPU.DRYER.B2	BLNEW11.ASPU.DRYER.B3	BLNEW11.PRECONC.B7	BLNEW11.PRECONC.B8	BLNEW11.PRECONC.B9	BLNEW11.PRECONC.B10	BLNEW11.PRECONC.B11	BLNEW11.PRECONC.B13	BLNEW11.UFU.B4	BLNEW22.B7	BLNEW22.B8	BLNEW22.B9	BLNEW22.B10
Property method	ELECNRTL	ELECNRTL	ELECNRTL	ELECNRTL	ELECNRTL	ELECNRTL	ELECNRTL	ELECNRTL	ELECNRTL	ELECNRTL	ELECNRTL	ELECNRTL	ELECNRTL	ELECNRTL	ELECNRTL	ELECNRTL	ELECNRTL	STEAM-TA	PENG-ROB	ELECNRTL	ELECNRTL	ELECNRTL	ELECNRTL	ELECNRTL	ELECNRTL	ELECNRTL	ELECNRTL	ELECNRTL	ELECNRTL	ELECNRTL	ELECNRTL	ELECNRTL
Henry's component list ID	HC	HC	HC	HC	HC	HC	HC	HC	HC	HC	HC	HC	HC	HC	HC	HC	HC	HC		HC	HC	HC	HC	HC	HC	HC	HC	HC	HC	HC	HC	HC
Electrolyte chemistry ID																																
Use true species approach for electrolytes	YES	YES	YES	YES	YES	YES	YES	YES	YES	YES	YES	YES	YES	YES	YES	YES	YES	YES	YES	YES	YES	YES	YES	YES	YES	YES	YES	YES	YES	YES	YES	YES
Free-water phase properties method	STEAM-TA	STEAM-TA	STEAM-TA	STEAM-TA	STEAM-TA	STEAM-TA	STEAM-TA	STEAM-TA	STEAM-TA	STEAM-TA	STEAM-TA	STEAM-TA	STEAM-TA	STEAM-TA	STEAM-TA	STEAM-TA	STEAM-TA	STEAM-TA	STEAM-TA	STEAM-TA	STEAM-TA	STEAM-TA	STEAM-TA	STEAM-TA	STEAM-TA	STEAM-TA	STEAM-TA	STEAM-TA	STEAM-TA	STEAM-TA	STEAM-TA	STEAM-TA
Water solubility method	3	3	3	3	3	3	3	3	3	3	3	3	3	3	3	3	3	3	3	3	3	3	3	3	3	3	3	3	3	3	3	3
Specified pressure [bar]	10	10	1	1	1	1	1,36	0	0	0	1,5	0	1	0	0	0	0	8	0	1,11	0							1				
Specified temperature [C]			40	50	31	35	120	50	35		35	110	90		278,3	149	40	171	140			111	0	0	0	0	0	55	111	0	0	0
Specified vapor fraction	1	1																0		0,001	1	0	0	0	0	0	0		0	0	0	0
Specified heat duty [kW]			0																													
EO Model components																																
Calculated pressure [atm]	9,87	9,87	1,00	1,00	1,00	1,00	1,36	2,50	2,50	4,00	1,50	4,00	1,00	1,01	0,97	0,97	2,50	7,90	1,07	1,11	1,11	1,46	0,93	0,73	0,53	0,33	0,12	1,00	1,46	1,02	0,78	0,58
Calculated temperature [C]	180,14	180,14	40,00	50,00	31,00	35,00	120,00	50,00	35,00	76,21	35,00	110,00	98,66	235,10	278,30	149,00	40,00	170,41	140,00	84,72	93,24	111,00	98,12	91,49	83,08	71,28	49,47	55,00	111,00	98,56	92,44	85,11
Calculated vapor fraction	1,00	1,00	0,00	0,00	0,00	0,00	1,00	0,00	0,96	0,00	0,00	0,00	0,00	1,00	1,00	1,00	0,00	0,00	1,00	0,00	1,00	0,00	0,00	0,00	0,00	0,00	0,00	0,00	0,00	0,00	0,00	0,00
Calculated heat duty [kW]	2060,41	9014,00	1066,25	1323,37	-2582,24	-2546,73	174,36	-9543,50	-387,79	9543,50	-1277,64	8188,94	-8188,94	9277,46	-70633,84	-9277,46	-13055,44	-61415,95	-8677,45	290,78	494,96	-7776,50	-4159,79	-4591,76	-5080,69	-5683,39	-6645,02	-3526,56	-2177,42	-1877,17	-2012,78	-2152,44
Temperature change [K]																		-10,00				0,00	0,00	0,00	0,00	0,00	0,00		0,00	0,00	0,00	0,00
Degrees of superheating [K]																																
Degrees of subcooling [K]																																
Pressure-drop correlation parameter																																
Net duty [kW]	2060,41	9014,00	1066,25	1323,37	-2582,24	-2546,73	174,36	-9543,50	-387,79	0,00	-1277,64	8188,94	0,00	0,00	-70633,84	-9277,46	-13055,44	-61415,95	-8677,45	290,78	494,96	-7776,50	-4159,79	-4591,76	-5080,69	-5683,39	-6645,02	-3526,56	-2177,42	-1877,17	-2012,78	-2152,44
First liquid / total liquid			1,00	1,00	1,00	1,00		1,00	1,00	1,00	1,00	1,00	1,00		1,00	1,00	1,00	1,00		1,00		1,00	1,00	1,00	1,00	1,00	1,00	1,00	1,00	1,00	1,00	1,00
Total feed stream CO2e flow [kg/hr]	0,00	0,00	0,00	0,00	0,00	15,16	15,16	0,00	10081,47	233,29	0,00	233,29	0,00	0,00	36149,91	36149,91	0,00	0,00	6245,71	0,00	0,00	0,00	0,00	0,00	0,00	0,00	0,00	0,00	0,00	0,00	0,00	0,00
Total product stream CO2e flow [kg/hr]	0,00	0,00	0,00	0,00	0,00	15,16	15,16	0,00	10081,47	233,29	0,00	233,29	0,00	0,00	36149,91	36149,91	0,00	0,00	6245,71	0,00	0,00	0,00	0,00	0,00	0,00	0,00	0,00	0,00	0,00	0,00	0,00	0,00
Net stream CO2e production [kg/hr]	0,00	0,00	0,00	0,00	0,00	0,00	0,00	0,00	0,00	0,00	0,00	0,00	0,00	0,00	0,00	0,00	0,00	0,00	0,00	0,00	0,00	0,00	0,00	0,00	0,00	0,00	0,00	0,00	0,00	0,00	0,00	0,00
Utility CO2e production [kg/hr]	487,72	2133,71	0,00	0,00	0,00	0,00	41,27	0,00	0,00	0,00	0,00	0,00	0,00	0,00	0,00	0,00	0,00	0,00	0,00	68,83	117,16	0,00	0,00	0,00	0,00	0,00	0,00	0,00	0,00	0,00	0,00	0,00
Total CO2e production [kg/hr]	487,72	2133,71	0,00	0,00	0,00	0,00	41,27	0,00	0,00	0,00	0,00	0,00	0,00	0,00	0,00	0,00	0,00	0,00	0,00	68,83	117,16	0,00	0,00	0,00	0,00	0,00	0,00	0,00	0,00	0,00	0,00	0,00
Utility usage [kg/hr]	3398,52	14868,06			2582,24	2546,73	287,59		387,79		1277,64						13055,44	########		479,63	816,41					5683,39	6645,02	3526,56				2152,44
Utility cost [$/hr]	14,09	61,66			0,00	0,00	1,19		0,00		0,00						0,00			1,99	3,39					0,00	0,00	0,00				0,00
Utility ID	LPU	LPU			CHILLW	COOLW	LPU		COOLW		COOLW						COOLW	STEAMGEN		LPU	LPU					COOLW	COOLW	COOLW				COOLW

Model Type: Heatx (Heat Exchangers)

HeatX		
Name	BL400.B11	BL900.B11
Hot side property method	ELECNRTL	ELECNRTL
Hot side Henry's component list ID	HC	HC
Hot side electrolyte chemistry ID		
Hot side use true species approach for elect	YES	YES
Hot side free-water phase properties methc	STEAM-TA	STEAM-TA
Hot side water solubility method	3	3
Cold side property method	ELECNRTL	ELECNRTL
Cold side Henry's component list ID	HC	HC
Cold side electrolyte chemistry ID		
Cold side use true species approach for elec	YES	YES
Cold side free-water phase properties meth	STEAM-TA	STEAM-TA
Cold side water solubility method	3	3
Exchanger specification	71	105
Units of exchanger specification	C	C
Exchanger area [sqm]		
Constant UA [cal/sec-K]		
Minimum temperature approach [K]	1	1
Hot side outlet pressure [atm]	0	0
Cold side outlet pressure [atm]	0	0
EO Model components		
Hot side EO Model components		
Cold side EO Model components		
Inlet hot stream temperature [C]	120	120
Inlet hot stream pressure [atm]	1,36	4
Inlet hot stream vapor fraction	1	0
Outlet hot stream temperature [C]	93,58	55,22
Outlet hot stream pressure [atm]	1,36	4
Outlet hot stream vapor fraction	1	0
Inlet cold stream temperature [C]	35	40,03
Inlet cold stream pressure [atm]	1,5	4
Inlet cold stream vapor fraction	0	0
Outlet cold stream temperature [C]	71	105
Outlet cold stream pressure [atm]	1,5	4
Outlet cold stream vapor fraction	0	0
Heat duty [kW]	114,21	20105,67
Calculated heat duty [kW]	114,21	20105,67
Required exchanger area [sqm]	2,50	1567,11
Actual exchanger area [sqm]	2,50	1567,11
Average U (Dirty) [cal/sec-sqcm-K]	0,02	0,02
Average U (Clean)		
UA [cal/sec-K]	508,47	318152,42
LMTD (Corrected) [K]	53,65	15,09
LMTD correction factor	1	1
Thermal effectiveness		
Number of transfer units		
Number of shells in series	1	1
Number of shells in parallel		
Total feed stream CO2e flow [kg/hr]	15,16	0
Total product stream CO2e flow [kg/hr]	15,16	0
Net stream CO2e production [kg/hr]	0	0
Utility CO2e production [kg/hr]	0	0
Total CO2e production [kg/hr]	0	0

Model Type: Flash2 (flash separator with 2 effluent streams)

Flash2

Name	BL100.F101	BL100.F102	BL200.F201	BL300.F301	BL700.PNEU702	BL800.F601	BL900.B6	BL900.BOIL601	BL900.DEAIR701	BL900.STERILIZ	BL900.B13.B1	BLNEW11.PRECONC.B55	BLNEW11.PRECONC.E11	BLNEW11.PRECONC.E22	BLNEW11.PRECONC.E33	BLNEW11.PRECONC.E44	BLNEW22.E11	BLNEW22.E22	BLNEW22.E33
Property method	ELECNRTL	ELECNRTL	ELECNRTL	ELECNRTL	ELECNRTL	ELECNRTL	ELECNRTL	IAPWS-95	NRTL	ELECNRTL	ELECNRTL	ELECNRTL	ELECNRTL	ELECNRTL	ELECNRTL	ELECNRTL	ELECNRTL	ELECNRTL	ELECNRTL
Henry's component list ID		HC	HC	HC	HC	HC	HC	HC	HC	HC	HC	HC	HC	HC	HC	HC	HC	HC	HC
Electrolyte chemistry ID	GLOBAL																		
Use true species approach for electrolytes	YES	YES	YES	YES	YES	YES	YES	YES	YES	YES	YES	YES	YES	YES	YES	YES	YES	YES	YES
Free-water phase properties method	STEAM-TA	STEAM-TA	STEAM-TA	STEAM-TA	STEAM-TA	STEAM-TA	STEAM-TA	STEAM-TA	STEAM-TA	STEAM-TA	STEAM-TA	STEAM-TA	STEAM-TA	STEAM-TA	STEAM-TA	STEAM-TA	STEAM-TA	STEAM-TA	STEAM-TA
Water solubility method	3	3	3	3	3	3	3	3	3	3	3	3	3	3	3	3	3	3	3
Temperature [C]			30						108	120	40								
Pressure [atm]	0	4,7	1	0	1	1	0	0	2,7	0	1	0,11	0,91	0,71	0,51	0,31	0,91	0,71	0,51
Specified vapor fraction		0,07																	
Specified heat duty [kW]	0	0	0	0	0	0	0		0										
EO Model components																			
Outlet temperature [C]	129,72	61,53	30,00	36,95	83,31	84,44	35,00	239,47	130,54	120,00	40,00	49,47	98,12	91,49	83,08	71,28	98,56	92,44	85,11
Outlet pressure [atm]	2,50	4,70	1,00	1,00	1,00	1,00	2,00	11,00	2,70	4,00	1,00	0,11	0,91	0,71	0,51	0,31	0,91	0,71	0,51
Vapor fraction	0,26	0,00	0,08	0,02	0,28	0,00	0,01	1,00	0,07	0,00	0,00	0,39	0,12	0,14	0,19	0,25	0,21	0,28	0,41
Heat duty [kW]	0,00	0,00	0,00	0,00	0,00	0,00	0,00	67102,15	0,00	4684,60	1430,44	5569,72	7620,97	4076,60	4499,92	4979,08	2133,87	1839,63	1972,52
Net duty [kW]	0,00	0,00	0,00	0,00	0,00	0,00	0,00	0,00	0,00	4684,60	1430,44	0,00	0,00	0,00	0,00	0,00	0,00	0,00	0,00
First liquid / total liquid	1,00	1,00	1,00	1,00	1,00	1,00	1,00		1,00	1,00	1,00	1,00	1,00	1,00	1,00	1,00	1,00	1,00	1,00
Total feed stream CO2e flow [kg/hr]	0,00	0,00	1273,81	8810,69	0,00	0,00	33251,13	0,00	0,00	0,00	373,18	0,00	0,00	0,00	0,00	0,00	0,00	0,00	0,00
Total product stream CO2e flow [kg/hr]	0,00	0,00	1273,81	8810,69	0,00	0,00	33251,13	0,00	0,00	0,00	373,18	0,00	0,00	0,00	0,00	0,00	0,00	0,00	0,00
Net stream CO2e production [kg/hr]	0,00	0,00	0,00	0,00	0,00	0,00	0,00	0,00	0,00	0,00	0,00	0,00	0,00	0,00	0,00	0,00	0,00	0,00	0,00
Utility CO2e production [kg/hr]	0,00	0,00	0,00	0,00	0,00	0,00	0,00	0,00	0,00	1108,89	0,00	0,00	1803,96	0,00	0,00	0,00	505,11	0,00	0,00
Total CO2e production [kg/hr]	0,00	0,00	0,00	0,00	0,00	0,00	0,00	0,00	0,00	1108,89	0,00	0,00	1803,96	0,00	0,00	0,00	505,11	0,00	0,00
Utility usage [kg/hr]									0,00	7726,97			12570,34				3519,69		
Utility cost [$/hr]									0,00	32,04			52,13				14,60		
Utility ID									LPU	LPU			LPU				LPU		

Model Type: Separators

Sep			
Name	BL400.B8	BL900.B7	BLNEW11.ASPU.DRYER.B6
Property method	ELECNRTL	ELECNRTL	ELECNRTL
Henry's component list ID	HC	HC	HC
Electrolyte chemistry ID			
Use true species approach for electrolytes	YES	YES	YES
Free-water phase properties method	STEAM-TA	STEAM-TA	STEAM-TA
Water solubility method	3	3	3
Inlet flash pressure [atm]	0	0	0
First outlet flash temperature			
First outlet flash pressure			
First outlet flash temperature change			
First outlet flash vapor fraction			
First outlet flash temperature estimate			
First outlet flash pressure estimate			
Second outlet flash temperature			
Second outlet flash pressure			
Second outlet flash temperature change			
Second outlet flash vapor fraction			
Second outlet flash temperature estimate			
Second outlet flash pressure estimate			
EO Model components			
Heat duty [kW]	-0,06	-0,03	117,08
Total feed stream CO2e flow [kg/hr]	15,16	0,00	0,00
Total product stream CO2e flow [kg/hr]	15,16	0,00	0,00
Net stream CO2e production [kg/hr]	0,00	0,00	0,00
Utility CO2e production [kg/hr]	0,00	0,00	0,00
Total CO2e production [kg/hr]	0,00	0,00	0,00
Utility usage			
Utility cost			
Utility ID			

Model Type: Pump

	Pump												
Name	BL100.P102	BL200.P201	BL200.P202	BL300.P301	BL400.B14	BL400.P401	BL700.B9	BL900.B9	BL900.B10	BL900.P702	BL1100.B4.B4	BLNEW11.P2	BLNEW11.UFU.B1
Property method	ELECNRTL	ELECNRTL	ELECNRTL	ELECNRTL	ELECNRTL	ELECNRTL	ELECNRTL	ELECNRTL	ELECNRTL	ELECNRTL	ELECNRTL	ELECNRTL	ELECNRTL
Henry's component list ID	HC	HC	HC	HC	HC	HC	HC	HC	HC	HC	HC	HC	HC
Electrolyte chemistry ID													
Use true species approach for electrolytes	YES	YES	YES	YES	YES	YES	YES	YES	YES	YES	YES	YES	YES
Free-water phase properties method	STEAM-TA	STEAM-TA	STEAM-TA	STEAM-TA	STEAM-TA	STEAM-TA	STEAM-TA	STEAM-TA	STEAM-TA	STEAM-TA	STEAM-TA	STEAM-TA	STEAM-TA
Water solubility method	3	3	3	3	3	3	3	3	3	3	3	3	3
Model Type													
Specified discharge pressure [atm]	3	3	3	2	3	4	3	4	20	11		3	6
Specified pressure increase [atm]													
Specified pressure ratio													
Specified power required [kW]													
Pump efficiencies				0,7	0,75					0,75		0,75	0,75
Driver efficiencies													
Suction area [sqm]													
Hydraulic static head [m-kgf/kg]													
Number of curves													
Operating shaft speed [rpm]													
Impeller diameter [meter]													
EO Model components													
Fluid power [kW]	3,67	0,52	0,54	2,96	0,17	16,90	9,95	22,61	144,17	26,54	4756,32	-5,14	17,88
Calculated brake power [kW]	5,57	1,26	1,30	4,23	0,22	22,13	13,25	28,90	184,14	35,39	5534,61	-3,86	23,84
Electricity [kW]	5,57	1,26	1,30	4,23	0,22	22,13	13,25	28,90	184,14	35,39	5534,61	-3,86	23,84
Volumetric flow rate [l/min]	1086,24	152,50	158,71	1754,13	66,51	3449,82	2946,38	4462,86	4493,31	1786,02	167140,12	1014,93	2117,45
Calculated discharge pressure [atm]	3,00	3,00	3,00	2,00	3,00	4,00	3,00	4,00	20,00	11,00	17,84	3,00	6,00
Calculated pressure change [atm]	2,00	2,00	2,00	1,00	1,50	2,90	2,00	3,00	19,00	8,80	16,85	-3,00	5,00
Calculated pressure ratio													
NPSH available [m-kgf/kg]	10,03	8,48	0,00	7,81	10,54	0,99	0,52	9,65	8,83	0,59	9,90	60,02	8,53
NPSH required													
Head developed [m-kgf/kg]	20,72	17,70	20,10	8,88	19,72	30,34	21,32	31,24	199,19	96,69		-30,80	50,40
Pump efficiency used	0,66	0,41	0,41	0,70	0,75	0,76	0,75	0,78	0,78	0,75	0,86	0,75	0,75
Net work required [kW]	5,57	1,26	1,30	4,23	0,22	22,13	13,25	28,90	184,14	35,39	0,00	-3,86	23,84
Specific speed, operating													
Suction sp. speed, operating													
Head coefficient													
Flow coefficient													
Total feed stream CO2e flow [kg/hr]	0,00	0,00	8,10	0,00	0,00	233,29	0,00	0,00	0,00	0,00	0,00	0,00	0,00
Total product stream CO2e flow [kg/hr]	0,00	0,00	8,10	0,00	0,00	233,29	0,00	0,00	0,00	0,00	0,00	0,00	0,00
Net stream CO2e production [kg/hr]	0,00	0,00	0,00	0,00	0,00	0,00	0,00	0,00	0,00	0,00	0,00	0,00	0,00
Utility CO2e production [kg/hr]	1,93	0,44	0,00	1,47	0,00	7,68	4,60	10,02	63,88	12,28	1919,97	1,34	8,27
Total CO2e production [kg/hr]	1,93	0,44	0,00	1,47	0,00	7,68	4,60	10,02	63,88	12,28	1919,97	1,34	8,27
Utility usage [kW]	5,57	1,26		4,23		22,13	13,25	28,90	184,14	35,39	5534,61	3,86	23,84
Utility cost [$/hr]	0,43	0,10		0,33		1,71	1,03	2,24	14,27	2,74	428,93	0,30	1,85
Utility ID	ELECTUSE	ELECTUSE		ELECTUSE		ELECTUSE	ELECTUSE	ELECTUSE	ELECTUSE	ELECTUSE	ELECGEN	ELECTUSE	ELECTUSE

Model Type: Compr (=> Compressors, turbine)

	Compr						
Name	BL100.B8	BL400.C401	BL700.COMPR702	BL800.COMPR601	BL900.B13.COMPR702	BL1100.B4.B6	BL1100.B4.GT
Property method	ELECNRTL	ELECNRTL	ELECNRTL	ELECNRTL	ELECNRTL	PENG-ROB	RKS-BM
Henry's component list ID	HC	HC	HC	HC	HC		
Electrolyte chemistry ID							
Use true species approach for electrolytes	YES	YES	YES	YES	YES	YES	YES
Free-water phase properties method	STEAM-TA	STEAM-TA	STEAM-TA	STEAM-TA	STEAM-TA	STEAM-TA	STEAM-TA
Water solubility method	3	3	3	3	3	3	3
Model Type	ISENTROPIC	ISENTROPIC	ISENTROPIC	ISENTROPIC	ISENTROPIC	ME-POLYTR(	ISENTROPIC
Specified discharge pressure [bar]	16,5	2,5	9,5	1,014	9,5	15	1,07911125
Specified pressure increase [atm]							
Specified pressure ratio							
Specified power required [kW]							
Isentropic efficiency		0,75	0,75	0,75	0,75	0,85	0,8977
Mechanical efficiency						0,9604	0,972
Polytropic efficiency						0,87	
EO Model components							
Indicated horsepower [kW]	544,99	251,67	192,12	69,06	86,75	5810,36	-11918,26
Calculated brake horsepower [kW]	544,99	251,67	192,12	69,06	86,75	6049,94	-11584,55
Net work required [kW]	544,99	251,67	192,12	69,06	86,75	6049,94	-11584,55
Power loss [kW]	0,00	0,00	0,00	0,00	0,00	239,58	333,71
Efficiency (polytropic / isentropic) used	0,72	0,75	0,75	0,75	0,75	0,87	0,90
Calculated discharge pressure [atm]	16,28	2,50	9,50	1,01	9,50	14,80	1,07
Calculated pressure change [atm]	6,42	1,50	8,50	0,01	8,50	13,80	13,74
Calculated pressure ratio	1,65	2,50	9,50	1,01	9,50	14,80	0,07
Outlet temperature [C]	259,23	125,21	373,42	26,57	373,42	431,63	652,90
Isentropic outlet temperature [C]	239,33	104,03	288,51	26,18	288,51	360,65	576,70
Vapor fraction	1	1	1	1	1	1	1
Displacement							
Volumetric efficiency							
Head developed [m-kgf/kg]	10830,62	6315,96	27596,33	122,96	27596,33	37563,58	-90872,40
Isentropic power requirement [kW]	392,39	188,75	144,09	51,80	65,06	4759,56	-13276,44
Inlet heat capacity ratio	1,36	1,29	1,40	1,40	1,40	1,40	1,29
Inlet volumetric flow rate [l/min]	44370,11	110341,24	27076,87	2201724,28	12226,80	696961,81	269126,61
Outlet volumetric flow rate [l/min]	31494,07	56719,90	6199,60	2182782,43	2799,49	111861,83	2207713,91
Inlet compressibility factor	0,96	1,00	1,00	1,00	1,00	1,00	1,00
Outlet compressibility factor	0,95	0,99	1,00	1,00	1,00	1,00	1,00
Compressor percent above surge							
Percent below stonewall							
Surge volume flow rate							
Stonewall volume flow rate							
Shaft speed							
Specific speed							
Inlet Mach number							
Total feed stream CO2e flow [kg/hr]	0,00	10081,47	0,00	0,00	0,00	0,00	6245,71
Total product stream CO2e flow [kg/hr]	0,00	10081,47	0,00	0,00	0,00	0,00	6245,71
Net stream CO2e production [kg/hr]	0,00	0,00	0,00	0,00	0,00	0,00	0,00
Utility CO2e production [kg/hr]	189,06	87,31	66,65	23,96	30,09	0,00	0,00
Total CO2e production [kg/hr]	189,06	87,31	66,65	23,96	30,09	0,00	0,00
Utility usage [kW]	544,99	251,67	192,12	69,06	86,75		
Utility cost [$/hr]	42,24	19,50	14,89	5,35	6,72		
Utility ID	ELECTUSE	ELECTUSE	ELECTUSE	ELECTUSE	ELECTUSE		

Model type: Mcompr (=> Multistage Compressor)

MCompr	
Name	BL1100.B1
Property method	**ELECNRTL**
Henry's component list ID	**HC**
Electrolyte chemistry ID	
Use true species approach for electrolytes	**YES**
Free-water phase properties method	**STEAM-TA**
Water solubility method	**3**
Number of stages	**3**
Fix discharge pressure from last stage [atm]	**15**
Feed stream stage	
Product stream stage	
No. of performance maps	
Number of curves	
Outlet pressure [atm]	15,00
Total work [kW]	326,13
Total cooling duty [kW]	-322,92
Net work required [kW]	326,13
Net cooling duty [kW]	-322,92
Total feed stream CO2e flow [kg/hr]	32877,95
Total product stream CO2e flow [kg/hr]	32877,95
Net stream CO2e production [kg/hr]	0
Utility CO2e production [kg/hr]	113,13
Total CO2e production [kg/hr]	113,13

Design Specs

Name	BL800.B7	BL1100.B4.B1
Specification	**O2F*100**	**TEX-650-273**
Specification target	**2**	**0**
Specification tolerance	**0,1**	**5**
Lower bound	**1000**	**1**
Upper bound	**100000**	**20**

Model Type: Valve

Valve	
Name	BL100.V101
Property method	**NRTL**
Henry's component list ID	**HC**
Electrolyte chemistry ID	
Use true species approach for electrolytes	**YES**
Free-water phase properties method	**STEAM-TA**
Water solubility method	**3**
Specified outlet pressure [atm]	**2,5**
Specified pressure drop [atm]	**0**
Valve operating specification: % operating	
Valve operating specification: flow coef	
Cv at 100% opening	
Valve pressure drop ratio factor	
Valve pressure recovery factor	
Valve inlet diameter [meter]	
Calculation type	**ADIAB-FLASH**
Valve pressure specification (design mode)	**P-OUT**
EO Model components	
Valve pressure specification (rating mode)	**VAL-POSN**
Calculated outlet pressure [atm]	2,5
Calculated pressure drop [atm]	13,7842339
Calculated valve % operating	
Checked outlet pressure	
Cavitation index	
Pressure drop ratio factor	
Pressure recovery factor	
Piping geometry factor	1
Total feed stream CO2e flow [kg/hr]	0
Total product stream CO2e flow [kg/hr]	0
Net stream CO2e production [kg/hr]	0

Model Type: RadFrac (multi-stage separation columns: distillation and rectification units)

RadFrac				
Name	BL400.C403	BL400.D501	BL400.D502	BLNEW11.A SPU.D502
Property method	NRTL-HOC	NRTL	ELECNRTL	ELECNRTL
Henry's component list ID	HC	HC	HC	HC
Electrolyte chemistry ID				
Use true species approach for electrolytes	YES	YES	YES	YES
Free-water phase properties method	STEAM-TA	STEAM-TA	STEAM-TA	STEAM-TA
Water solubility method	3	3	3	3
Number of stages	4	23	45	45
Condenser	NONE	PARTIAL-V	PARTIAL-V	PARTIAL-V
Reboiler	NONE	KETTLE	KETTLE	KETTLE
Number of phases	2	2	2	2
Free-water	NO	NO	NO	NO
Top stage pressure [atm]	1,02	2,04137892	1,6	1,6
Specified reflux ratio		3	1	0,1
Specified bottoms rate [kmol/hr]				
Specified boilup rate [kmol/hr]				
Specified distillate rate [kmol/hr]		280		
EO Model components				
Calculated molar reflux ratio	3,26	3,00	3,57	1,97
Calculated bottoms rate [kmol/hr]	824,25	9920,82	861,60	798,65
Calculated boilup rate [kmol/hr]	251,55	1624,17	218,36	1613,86
Calculated distillate rate [kmol/hr]	249,36	6,23	295,72	497,86
Condenser / top stage temperature [C]	25,46	62,35	90,56	78,35
Condenser / top stage pressure [atm]	1,02	2,04	1,60	1,00
Condenser / top stage heat duty [kW]	0,00	-229,32	-11127,61	-10649,73
Condenser / top stage subcooled duty				
Condenser / top stage reflux rate [kmol/hr]	812,60	18,68	1056,04	981,88
Condenser / top stage free water reflux ratio				
Reboiler pressure [atm]	1,02	2,28	1,60	1,00
Reboiler temperature [C]	27,22	124,96	113,25	100,53
Reboiler heat duty [kW]	0,00	17954,01	2451,15	18433,74
Total feed stream CO2e flow [kg/hr]	10081,47	233,29	15,16	0,00
Total product stream CO2e flow [kg/hr]	10081,47	233,29	15,16	0,00
Net stream CO2e production [kg/hr]	0,00	0,00	0,00	0,00
Utility CO2e production [kg/hr]	0,00	4249,90	580,21	4363,46
Total CO2e production [kg/hr]	0,00	4249,90	580,21	4363,46
Condenser utility usage [kW]		229,32	11127,61	10649,73
Condenser utility cost [$/hr]		0,00	0,00	0,00
Condenser utility ID		COOLW	COOLW	COOLW
Reboiler utility usage [kg/hr]		29614,09	4043,02	30405,37
Reboiler utility cost [$/hr]		122,81	16,77	126,09
Reboiler utility ID		LPU	LPU	LPU
Basis for specified distillate to feed ratio	MOLE	MOLE	MOLE	MOLE
Specified distillate to feed ratio				
Basis for specified bottoms to feed ratio	MOLE	MOLE	MASS	MASS
Specified bottoms to feed ratio			0,1	0,1
Basis for specified boilup ratio	MOLE	MOLE	MOLE	MOLE
Specified boilup ratio				
Calculated molar boilup ratio		0,16	0,25	2,02
Calculated mass boilup ratio	0,71	0,15	0,26	1,83

Model Type: Rstoic (stochiometric reactor setup)

RStoic										
Name	BL100.R101	BL200.R201	BL300.B1	BL300.R302 222	BL800.R601	BL900.T606	BLNEW11. ASPU.B2	BLNEW11 .UFU.B2	BLNEW11. UFU.B22	BLNEW22 .B1
Property method	ELECNRTL	ELECNRTL	ELECNRTL	ELECNRTL	ELECNRTL	ELECNRTL	ELECNRTL	ELECNRTL	ELECNRTL	ELECNRTL
Henry's component list ID		HC	HC		HC	HC	HC	HC	HC	HC
Electrolyte chemistry ID	GLOBAL			GLOBAL						
Use true species approach for electrolytes	YES	YES	YES	YES	YES	YES	YES	YES	YES	YES
Free-water phase properties method	STEAM-TA	STEAM-TA	STEAM-TA	STEAM-TA	STEAM-TA	STEAM-TA	STEAM-TA	STEAM-TA	STEAM-TA	STEAM-TA
Water solubility method	3	3	3	3	3	3	3	3	3	3
Specified pressure [bar]	16,5	1	1	0	-0,034	2	1,1	6	0	0
Specified temperature [C]	204	30	50	30	870	35	25	55	20	
Specified vapor fraction				0						
Specified heat duty [kW]	0	0		0	0		0	0	0	0
EO Model components										
Outlet temperature [C]	204,00	30,00	50,00	37,79	1052,32	35,00	25,00	55,00	57,34	90,50
Outlet pressure [atm]	16,28	1,00	1,00	1,00	0,97	2,00	1,10	6,00	6,00	1,00
Calculated heat duty [kW]	6483,92	-3338,25	-57,91	0,00	0,00	-2932,61	-658,92	187,80	0,00	0,00
Net heat duty [kW]	6483,92	-3338,25	-57,91	0,00	0,00	-2932,61	-658,92	187,80	0,00	0,00
Calculated vapor fraction	0,00	0,08	0,00	0,00	1,00	0,01	0,00	0,00	0,00	0,00
First liquid / total liquid	1,00	1,00	1,00	1,00		1,00	0,35	0,01	1,00	1,00
Total feed stream CO2e flow [kg/hr]	0,00	0,00	0,00	8,10	0,00	0,00	0,00	0,00	0,00	0,00
Total product stream CO2e flow [kg/hr]	0,00	1273,81	0,00	8810,69	36149,91	33251,13	0,00	0,00	0,00	0,00
Net stream CO2e production [kg/hr]	0,00	1273,81	0,00	8802,59	36149,91	33251,13	0,00	0,00	0,00	0,00
Utility CO2e production [kg/hr]	0,00	0,00	0,00	0,00	0,00	0,00	0,00	0,00	0,00	0,00
Total CO2e production [kg/hr]	0,00	1273,81	0,00	8802,59	36149,91	33251,13	0,00	0,00	0,00	0,00
Utility usage [kW]		3338,25								
Utility cost [$/hr]		0,00								
Utility ID		CHILLW								

Model type: Rgibbs (Gibbs reactor)

RGibbs	
Name	BL1100.B4.B3
Property method	**RKS-BM**
Henry's component list ID	
Electrolyte chemistry ID	
Use true species approach for electrolytes	**YES**
Free-water phase properties method	**STEAM-TA**
Water solubility method	**3**
Specified pressure [bar]	**15**
Specified temperature [C]	
Specified heat duty [kW]	**0**
EO Model components	
Outlet temperature [C]	1291,92
Outlet pressure [atm]	14,80
Calculated heat duty [kW]	0,00
Net heat duty [kW]	0,00
Vapor fraction	1,00
Number of fluid phases	1,00
Maximum number of pure solids	0,00
Total feed stream CO2e flow [kg/hr]	32877,94
Total product stream CO2e flow [kg/hr]	6245,71
Net stream CO2e production [kg/hr]	-26632,23
Utility CO2e production [kg/hr]	0,00
Total CO2e production [kg/hr]	-26632,23
Utility usage	
Utility cost	
Utility ID	

Model Type: Mixers

	Mixer																								
Name	BL100.ALKIMP	BL100.B2	BL100.B41	BL100.FILST1.B1	BL100.FILST2.B1	BL200.B1	BL200.T202	BL400.B4	BL400.B9	BL400.B12	BL400.B13	BL400.M401	BL700.B2	BL900.B5	BL900.B8	BL900.EFFMIX	BL900.OSMOSIS	BL900.ULTRAF	BL1000.M802	BL1100.B4.B2	BLNEW11.ASPU.B5	BLNEW11.ASPU.B8	BLNEW11.ASPU.DRYER.B1	BLNEW11.ASPU.DRYER.B5	BLNEW11.ASPU.FILST1.B1
Property method	ELECNRTL	ELECNRTL	ELECNRTL	ELECNRTL	ELECNRTL	ELECNRTL	ELECNRTL	ELECNRTL	ELECNRTL	ELECNRTL	ELECNRTL	ELECNRTL	ELECNRTL	ELECNRTL	ELECNRTL	ELECNRTL	ELECNRTL	ELECNRTL	ELECNRTL	ELECNRTL	ELECNRTL	ELECNRTL	ELECNRTL	ELECNRTL	ELECNRTL
Henry's component list ID	HC	HC	HC	HC	HC	HC	HC	HC	HC	HC	HC	HC	HC	HC	HC	HC	HC	HC	HC	HC	HC	HC	HC	HC	HC
Electrolyte chemistry ID																									
Use true species approach for electrolytes	YES	YES	YES	YES	YES	YES	YES	YES	YES	YES	YES	YES	YES	YES	YES	YES	YES	YES	YES	YES	YES	YES	YES	YES	YES
Free-water phase properties method	STEAM-TA	STEAM-TA	STEAM-TA	STEAM-TA	STEAM-TA	STEAM-TA	STEAM-TA	STEAM-TA	STEAM-TA	STEAM-TA	STEAM-TA	STEAM-TA	STEAM-TA	STEAM-TA	STEAM-TA	STEAM-TA	STEAM-TA	STEAM-TA	STEAM-TA	STEAM-TA	STEAM-TA	STEAM-TA	STEAM-TA	STEAM-TA	STEAM-TA
Water solubility method	3	3	3	3	3	3	3	3	3	3	3	3	3	3	3	3	3	3	3	3	3	3	3	3	3
Specified pressure [atm]	1	0	0	0	0	0	0	0	0	0	0	1,1	0	0	0	0	1	1	0	0	1	0	0	0	0
Temperature estimate [C]	75																				20				
EO Model components																									
Outlet temperature [C]	51,73	31,92	25,03	76,47	41,05	28,05	29,61	36,56				36,32	124,97	#####	113,25	84,34	55,88	55,28	170,41		38,90	36,00	21,77	84,85	21,77
Calculated outlet pressure [atm]	1,00	1,00	3,00	1,00	1,00	1,00	1,00	1,00				1,10	2,28	5,00	1,60	2,50	1,00	1,00	7,90		1,00	1,10	1,10	1,11	1,10
Vapor fraction	0,00	0,00	0,00	0,00	0,00	0,08	0,00	1,00				0,00	0,03	0,04	0,00	0,00	0,00	0,00	0,00		0,00	0,00	0,00	0,00	0,00
First liquid /Total liquid	1,00	1,00	1,00	1,00	1,00	1,00	1,00	1,00				1,00	1,00	1,00	1,00	1,00	1,00	1,00	1,00		1,00	1,00	1,00	1,00	1,00
Total feed stream CO2e flow [kg/hr]	0,00	0,00	0,00	0,00	0,00	0,00	0,00	10081,47	0,00	0,00	0,00	233,29	0,00	0,00	0,00	0,00	0,00	0,00	0,00	0,00	0,00	0,00	0,00	0,00	0,00
Total product stream CO2e flow [kg/hr]	0,00	0,00	0,00	0,00	0,00	0,00	0,00	10081,47	0,00	0,00	0,00	233,29	0,00	0,00	0,00	0,00	0,00	0,00	0,00	0,00	0,00	0,00	0,00	0,00	0,00
Net stream CO2e production [kg/hr]	0,00	0,00	0,00	0,00	0,00	0,00	0,00	0,00	0,00	0,00	0,00	0,00	0,00	0,00	0,00	0,00	0,00	0,00	0,00	0,00	0,00	0,00	0,00	0,00	0,00

Model Type: Feed Splitters

	FSplit										
Name	BL300.B3	BL800.B3	BL800.S601	BLNEW11.PRECONC.B3	BLNEW11.PRECONC.B4	BLNEW11.PRECONC.B5	BLNEW11.PRECONC.B6	BLNEW11.PRECONC.B12	BLNEW22.B4	BLNEW22.B5	BLNEW22.B6
Property method	ELECNRTL	ELECNRTL	ELECNRTL	ELECNRTL	ELECNRTL	ELECNRTL	ELECNRTL	ELECNRTL	ELECNRTL	ELECNRTL	ELECNRTL
Henry's component list ID	HC	HC	HC	HC	HC	HC	HC	HC	HC	HC	HC
Electrolyte chemistry ID											
Use true species approach for electrolytes	YES	YES	YES	YES	YES	YES	YES	YES	YES	YES	YES
Free-water phase properties method	STEAM-TA	STEAM-TA	STEAM-TA	STEAM-TA	STEAM-TA	STEAM-TA	STEAM-TA	STEAM-TA	STEAM-TA	STEAM-TA	STEAM-TA
Water solubility method	3	3	3	3	3	3	3	3	3	3	3
First outlet stream			0,05		0,02	0,02	0,02	0,02	0,02	0,02	0,02
First specified split fraction			0,05		0,02	0,02	0,02	0,02	0,02	0,02	0,02
First calculated split fraction	0,95	1	0,05	0,98	0,02	0,02	0,02	0,02	0,02	0,02	0,02
First actual volume flow [l/min]											
First limit flow [kmol/hr]											
First volume limit flow [l/min]											
First cum limit flow [kmol/hr]											
First cum volume limit flow [l/min]											
First residual fraction											
Second outlet stream	0,05	0		0,02							
Second specified split fraction	0,05	0		0,02							
EO Model components											
Second calculated split fraction	0,05	0	0,95	0,02	0,98	0,98	0,98	0,98	0,98	0,98	0,98
Second actual volume flow [l/min]											
Second limit flow [kmol/hr]											
Second volume limit flow [l/min]											
Second cum limit flow [kmol/hr]											
Second cum volume limit flow [l/min]											
Second residual fraction											
Total feed stream CO2e flow [kg/hr]	0	0	0	0	0	0	0	0	0	0	0
Total product stream CO2e flow [kg/hr]	0	0	0	0	0	0	0	0	0	0	0
Net stream CO2e production [kg/hr]	0	0	0	0	0	0	0	0	0	0	0

Model Type: Stream splitter

SSplit							
Name	BL100.FILST1.B4	BL100.FILST2.B4	BL700.B1	BL800.BAGH601	BLNEW11.ASPU.DRYER.B4	BLNEW11.ASPU.FILST1.B4	BLNEW11.UFU.B44
Property method	ELECNRTL	ELECNRTL	ELECNRTL	ELECNRTL	ELECNRTL	ELECNRTL	ELECNRTL
Henry's component list ID	HC	HC	HC	HC	HC	HC	HC
Electrolyte chemistry ID							
Use true species approach for electrolytes	YES	YES	YES	YES	YES	YES	YES
Free-water phase properties method	STEAM-TA	STEAM-TA	STEAM-TA	STEAM-TA	STEAM-TA	STEAM-TA	STEAM-TA
Water solubility method	3	3	3	3	3	3	3
First outlet stream							
First specified split fraction				1			
First flow [kg/hr]							
First calculated split fraction	0,77	0,75	0,95	1,00	0,88	0,95	0,51
Second outlet stream							
Second specified split fraction							
Second flow [kg/hr]	1000,00	1000,00	15000,00		1000,00	1000,00	50,00
Second calculated split fraction	0,23	0,25	0,05	0,00	0,12	0,05	0,49
Total feed stream CO2e flow [kg/hr]	0,00	0,00	0,00	36149,91	0,00	0,00	0,00
Total product stream CO2e flow [kg/hr]	0,00	0,00	0,00	36149,91	0,00	0,00	0,00
Net stream CO2e production [kg/hr]	0,00	0,00	0,00	0,00	0,00	0,00	0,00

Utilities

Name	CHILLW	COOLA	COOLW	ELECGEN	ELECTUSE	HPU	LPU	STEAMGEN
Utility type	**ELECTRICITY**	**GENERAL**	**ELECTRICITY**	**ELECTRICITY**	**ELECTRICITY**	**STEAM**	**STEAM**	**GENERAL**
Specified price [$/kg]								
Specified cooling value [kcal/kg]		**-5**						**0**
Specified inlet degrees subcooled [K]								
Specified outlet degrees subcooled [K]								
Specified inlet degrees superheated [K]								
Specified outlet degrees superheated [K]								
Specified electricity price [$/kWhr]	**0,00**		**0,00**	**0,08**	**0,08**			
Specified energy price [$/kJ]	**0,00**	**0,00**	**0,00**			**0,00**	**0,00**	**0,00**
Specified inlet pressure [atm]	**1,00**		**1,00**			**13,00**	**9,50**	
Specified outlet pressure [atm]	**1,00**		**1,00**			**13,00**	**8,00**	
Specified inlet temperature [C]	**4,00**	**30,00**	**28,00**			**266,00**	**233,00**	
Specified outlet temperature [C]	**15,00**	**35,00**	**37,00**			**192,00**		
Specified inlet vapor fraction								
Specified outlet vapor fraction							**0,00**	
Specified CO2 emission factor [kg/cal]				0,00	0,00	0,00	0,00	
Specified CO2 energy source efficiency factor	**1,00**	**1,00**	**1,00**	**0,58**	**0,58**	**0,85**	**0,85**	**1,00**
Calculated heating/cooling value [kcal/kg]		-1,19				513,74	521,29	0,00
Calculated mass price								
Calculated inlet enthalpy [kcal/kg]						-3108,18	-3122,87	
Calculated outlet enthalpy [kcal/kg]						-3621,92	-3644,17	
Calculated inlet pressure [atm]						13,00	9,50	
Calculated outlet pressure [atm]						13,00	8,00	
Calculated inlet temperature [C]		30,00				266,00	233,00	
Calculated outlet temperature [C]		35,00				192,00	170,96	
Calculated inlet vapor fraction						1,00	1,00	
Calculated outlet vapor fraction						0,00	0,00	
Calculated purchase price [$/kWhr]	0,00		0,00	0,08	0,08		0,00	
Calculated total cost [$/hr]	0,00	0,00	0,00	428,93	138,98	0,00	446,74	0,00
Calculated total usage rate [kg/hr]		0,00				0,00	107729,69	1,13E+277
Calculated total Electric usage [kW]	5920,49		57466,14	5534,61	1793,28			
Calculated CO2 emission factor [kg/cal]				0,00	0,00	0,00	0,00	
Calculated CO2 emission rate [kg/hr]				1919,97	622,10		15460,22	